Interactive Influences of Crosslinking, Counterface Roughness and Kinematics on the Wear of Crosslinked UHMWPE.

Alison Louise Galvin (BMedSc).

Submitted in accordance with the requirements for the degree of

Doctor of Philosophy.

University of Leeds.

Department of Mechanical Engineering,

July 2003.

The candidate confirms that the work submitted is her own and that appropriate credit has been given where reference has been made to the work of others.

Acknowledgements.

I would like to thank Professor John Fisher and Professor Eileen Ingham for all their help and support. I would also like to thank Dr Joanne Tipper for all her help with wear debris digestion and counting.

Thanks to EPSRC and DePuy for funding the work.

Thanks to Devon Darby, Alan Heald, Lee Wetherill, Jane Cardie and John Harrington for all their help and technical assistance.

Lastly I would like to thank my family, friends and Richard for all their support over the last 4 years.

Abstract.

Ultra high molecular weight polyethylene (UHMWPE) wear debris has been shown to be a major cause of long term failure of total joint replacements. *In vitro* studies have shown that not only is the size and shape of the particles important for cellular response but also the volumetric concentration of the particles. Recently, crosslinking has been extensively introduced to reduce the wear of UHMWPE. In this study the wear and wear debris of non-crosslinked and crosslinked UHMWPE were compared.

The materials examined were UHMWPE GUR 1050, non crosslinked, moderately crosslinked – 5MRad and highly crosslinked – 10MRad. The wear was examined on a multidirectional pin on plate rig. The first test looked at the wear of the UHMWPE's with different serum concentrations. The effect of counterface roughness with high multidirectionality against different counterfaces was then examined. The second test examined the effect of different counterface surfaces at lower multidirectionality. The debris produced was then analysed.

The wear results from the first pin on plate study showed that serum concentration had a significant effect on the wear rate of non-crosslinked UHMWPE. The high serum concentration resulted in a much higher wear rate than the lower serum concentration for the non-crosslinked UHMWPE. The crosslinked UHMWPE's did not show any significant difference in wear rate with serum concentration. The results from the different counterface conditions showed that highly crosslinked UHMWPE significantly reduced wear against smooth and scratched counterfaces.

The second pin on plate study showed that all the UHMWPE's had lower wear rates than the previous study because of reduced cross shear frictional energy. As with the previous study the highly crosslinked UHMWPE had significantly lower wear rates against all the counterfaces, and there was no significant difference between the 0MRad and 5MRad UHMWPE. The reduction in wear rate found with the highly crosslinked UHMWPE was dependent on kinematics with less reduction with lower levels of cross shear frictional energy.

The wear debris from the high multidirectional study on smooth and highly scratched plates was analysed. The use of field emission gun SEM revealed nanometre sized particles for the first time in all three materials under both counterface conditions. No significant difference was found in the percentage number and percentage area of the particles from any of the materials against any of the counterfaces although more larger wear particles were observed from the scratched counterface debris. The actual volumes of the particles showed that the highly crosslinked UHMWPE had a significantly lower volume in the 0.1-1.0μm size range. This was an important observation as this is the most biologically active size range. The specific biological activity did not show any significant difference between the materials. The functional biological activity which takes into account the wear volume showed that the highly crosslinked UHMWPE had a lower FBA for debris from both the smooth and scratched counterfaces. The debris from the scratched tests had a higher FBA for all the materials because of the increased wear rates with the scratched counterface.

Table of Contents.

List of Figures.

List of Tables.

Nomenclature.

A	Total two-dimensional area of particles (μm^2).
ANOVA	Analysis of variance.
A_r	Total two-dimensional area of particle in size range r (μm^2).
A_s	Surface area of each pore size filter membrane.
$\overline{a}_r$	Mean two-dimensional surface area of particles in a size range r (μm^2) .
B(r)	Biological activity as a function of particle size.
C	Carbon.
C(r)	Volumetric concentration as a function of particle size.
d_{max}	Maximum diameter.
d_{min}	Minimum diameter.
ECD	Equivalent circle diameter.
F	Frictional force.
FEGSEM	Field emission gun scanning electron microscope.
FBA	Functional biological activity.
FWHM	Full width half maximum.
FL	Length.
FW	Width.
H	Hydrogen.
HMWPE	High molecular weight polyethylene.
i	Number of SEM's.
k	Wear factor.
IL-6	Interleukin 6.
IL-1β	Interleukin 1β.
MSD	Minimum significant difference.
N	Total number of particles.
N_r	Number of wear particles in size range r.
n_r	Number of particles per unit area in size range r
$n_{r,i}$	Number of particles in size range r on a micrograph i.
$\overline{n}_r$	Mean number of particles per unit area in the size range r.

P	Applied load.
p	Perimeter.
PE	Polyethylene.
Q_i	Area of region that was analysed using computer image analysis (μm^2).
Ra	Average surface roughness.
Rp	Maximum height of profile above mean line.
Rpm	Revolution per minute.
Rv	The depth of the valleys.
SBA	Specific biological activity.
SEM	Scanning electron microscope..
SD	Standard deviation.
THR	Total hip replacement.
TNF-α	Tissue necrosis factor.
UHMWPE	Ultra high molecular weight polyethylene.
V	Volume.
V/v	Volume per volume.
W/v	Weight per volume.
x	Sliding distance.
95%CL	95% confidence limits.
μm	Micron.

Chapter 1.

1. Background and Literature Review.

1.1. General Introduction.

Every year thousands of artificial joints are implanted worldwide. Many of the joints in the body can be replaced but the joint most commonly replaced is the hip (Figure 1.1). In the UK alone over 50,000 replacement hip joints are implanted every year (Fisher *et al.*, 1991). Hip replacement operations are one of the most successful surgical procedures of our time, less than 10 percent fail within the first ten years of implantation. However as more and more young people are needing joint replacements, the durability and lifetime of the joints needs to be extended. The current limitations are related to the wear of the components. The wear releases debris particles into the surrounding tissue and this can cause aseptic loosening of the femoral or acetabular components. The particles activate macrophages, which causes the activation of osteoclasts, which results in bone resorption. The size of the particles produced is important in their biological activity, with phagocytosible particles being most reactive. Larger particles stimulate the formation of giant cells and so are less reactive.

Ultra high molecular weight polyethylene (UHMWPE) is the chosen polymer in artificial joints because its high molecular weight and molecular structure produce a very high strain energy to failure and a much greater wear resistance than other polymers. This thesis addresses the wear of UHMWPE and wear debris generated in artificial hip joints and investigates the effect of different kinematic conditions with various levels of crosslinking.

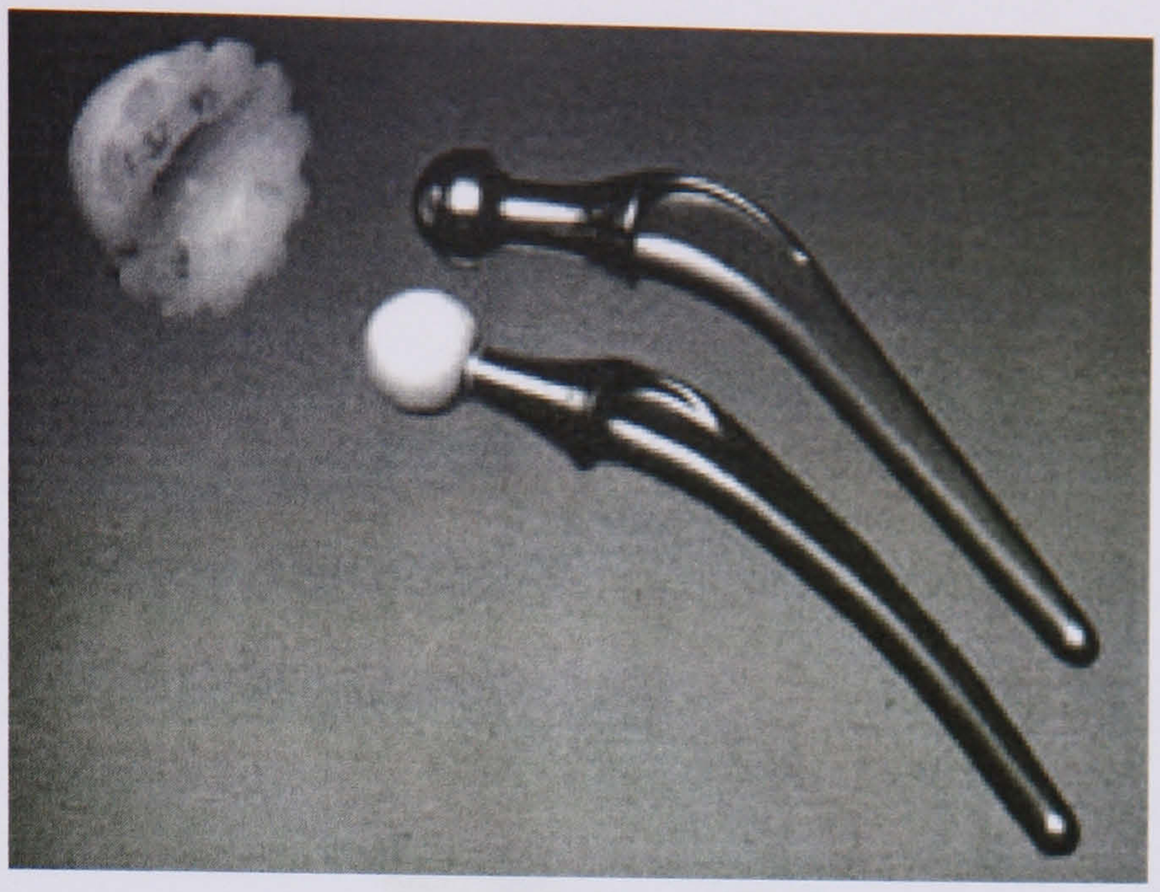

Figure 1.1 Femoral (bottom; ceramic, top; metal) and UHMWPE acetabular cup components of a typical artificial hip joint.

1.2. The Natural Hip.

1.2.1. Anatomy.

The hip joint is a ball and socket joint. This allows the joint to undergo a wide range of movement. The joint consists of a femoral head (the ball) and an acetabular cup (the socket) and is extremely stable. The stability is determined by the shape of the articular surfaces (the acetabular cup holds the femoral head securely), the strength of the articular capsule and also the ligaments and muscles surrounding the joints (Figure 1.2). The hip is also a synovial joint, which means that the joint is lubricated by synovial fluid contained inside a fibrous articular capsule. The hip joint is involved with the transmission of weight and must be able to support the whole weight of the body on one leg. It must also be able to transfer the weight in a stable manner during walking and running.

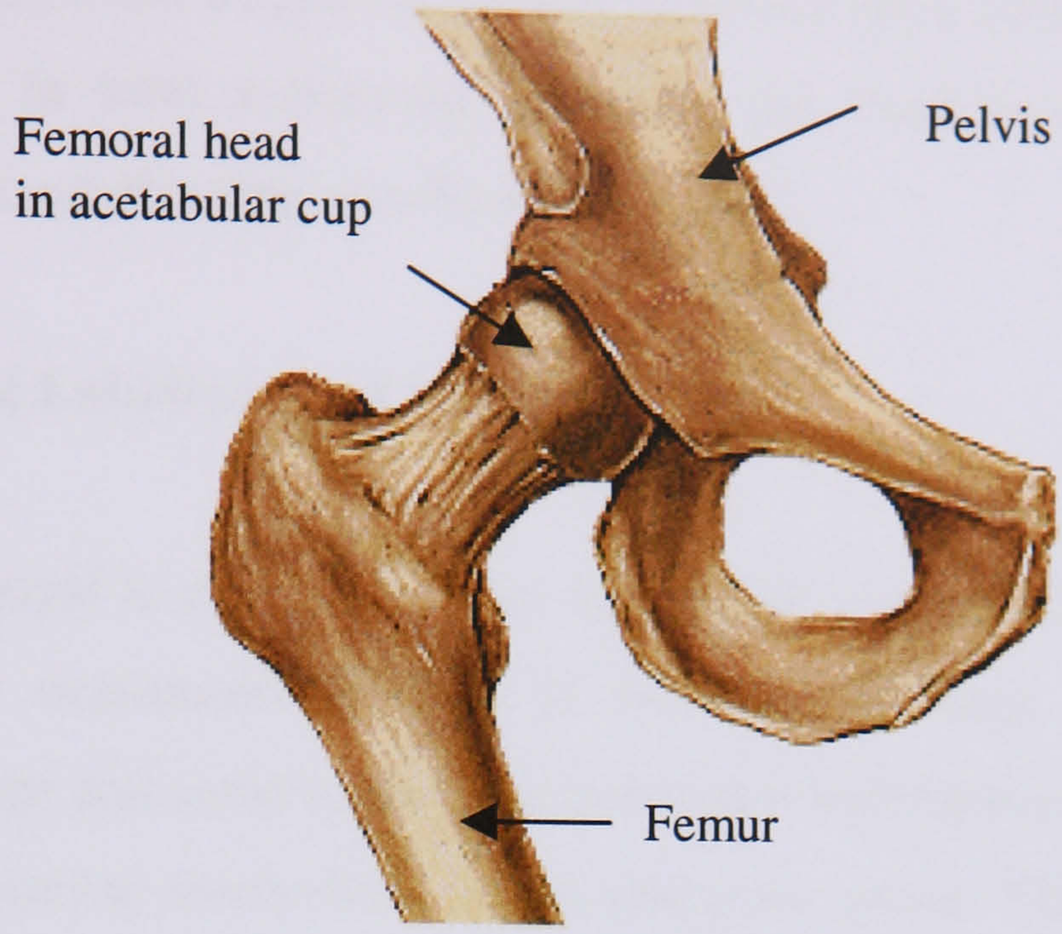

Figure 1.2 Natural hip joint. (Adapted from www.strykereurope.com)

Synovial joints have a space called a synovial cavity between the articulating bones. The structure of these joints allows the bones to move freely. The bones of a synovial joint are covered by articular cartilage. The cartilage provides a smooth, slippery surface for the articulating bones, but it does not bind them together. Articular cartilage reduces friction between bones of the joint during movement and helps to absorb shock.

The articular capsule is composed of two layers, an outer fibrous capsule and an inner synovial membrane. The outer layer, the fibrous capsule, usually consists of dense, irregular connective tissue that attaches to the periosteum of the articulating bones. The inner layer of the articular capsule, the synovial membrane, is composed of areolar connective tissue with elastic fibres.

The synovial membrane secretes synovial fluid, which forms a thin film over the surfaces within the articular capsule. Synovial fluid consists of hyaluronic acid secreted by fibroblast-like cells in the synovial membrane, and interstitial fluid filtered from blood plasma. Its several functions include reducing friction by lubricating the joint, and supplying nutrients to, and removing metabolic wastes from the chondrocytes within the articular cartilage. Synovial fluid also contains phagocytic cells that remove microbes and the debris that results from normal wear

and tear in the joint. When a synovial joint is immobile for a time, the fluid becomes quite viscous but as joint movement increases, the fluid becomes less viscous. Effectively it is a shear thinning non-Newtonian fluid.

1.2.2. Friction and Lubrication of Natural Joints.

One of the first people to investigate joint lubrication was MacConail *et al.* (1932). He compared the anatomical features of the hip and knee joints to those of engineering bearings and came to the conclusion that hydrodynamic lubrication was the principal lubrication mechanism in hip and knee joints. This theory was later changed, because, for hydrodynamic lubrication to occur, high speed relative movement is needed between the two opposing surfaces to provide a substantial load carrying pressure, but this is not the case in synovial joints.

It is thought that there are a number of mechanisms involved in hip joint lubrication. One of these is fluid film lubrication.

Fluid film lubrication is only thought to play a part during active walking and running, when there are conditions of cyclic loading and high relative sliding velocity. Jin *et al.* (1992) predicted that after 0.5 seconds of loading the thickness of the lubricating film is between 0.6-2μm. When relative sliding of the surfaces occurs the entraining action can produce a film of between 0.5-1.8μm for normal walking (Jin *et al.*, 1993).

Boosted lubrication is another mechanism that is thought to occur. During this mechanism a viscous gel of high molecular weight protein is formed from the synovial fluid. This occurs when the lubricating films start to become very thin. High molecular weight proteins are left behind as the water in the synovial fluid enters the cartilage. This results in the formation of a highly viscous lubricating layer.

Biphasic lubrication can maintain low friction under extreme loading conditions. The load is carried in the fluid phase of the articular cartilage for long periods of

time. Another method of lubrication is boundary lubrication. This involves the use of glycoprotein complexes or phospholipids to form boundary layers. These have been shown to reduce friction in articular cartilage contacts.

1.2.3. Motion of the Hip.

The main motion of the hip joint is the walking cycle. The main movements involved are:

- Flexion and extension.
- Abduction and adduction.
- Internal and external rotation.

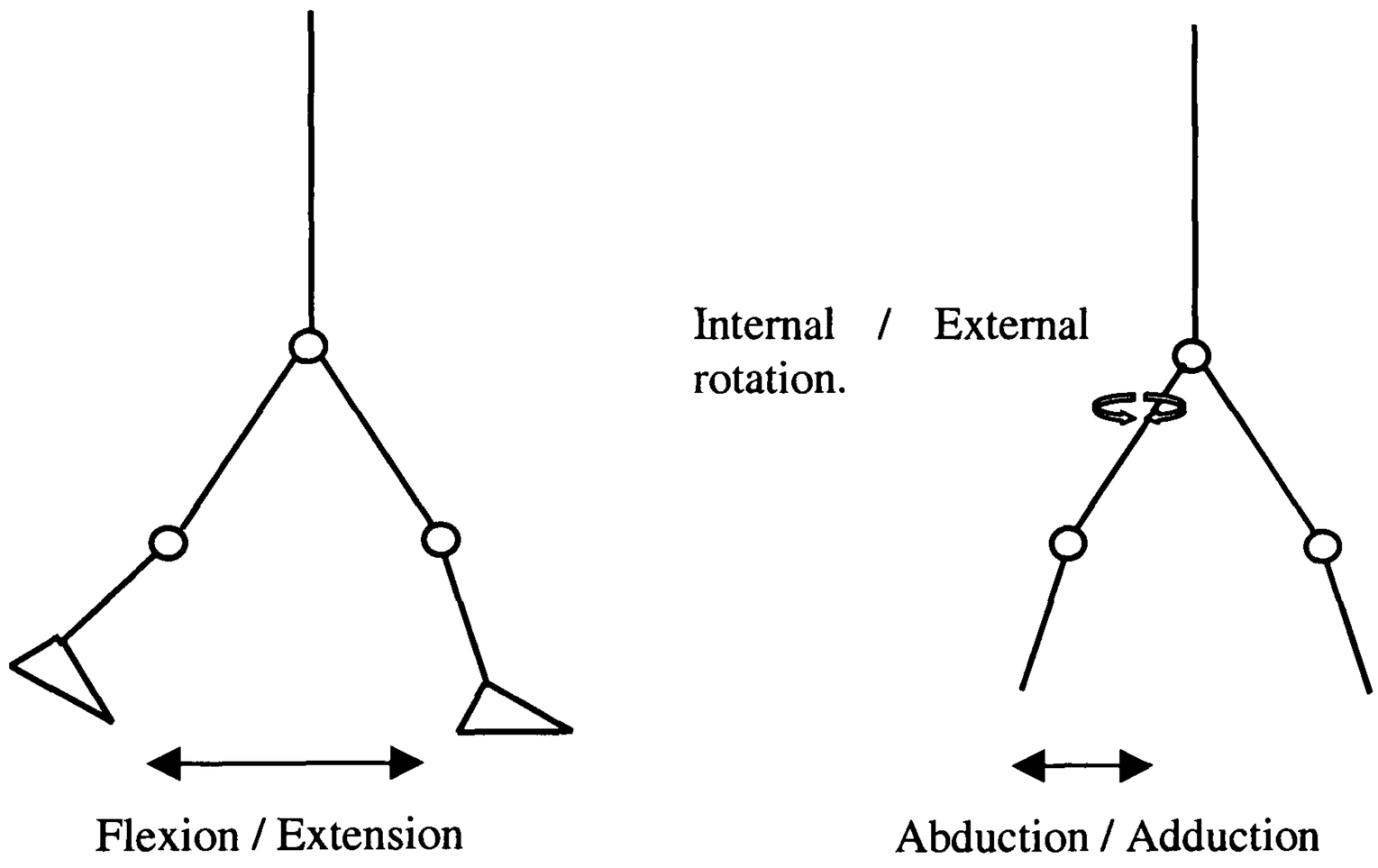

Figure 1.3 Hip Kinematics.

The main action is in the flexion and extension direction. The hip can flex up to 145° but extension is limited to about 30°. The total range of abduction and adduction, and internal and external rotation is 90° for each combination (Pastalanga *et al.*, 2002).

During the walking cycle there are two main phases. These are the swing phase and the stance phase. During the stance phase of walking, the hip has two load peaks, one at heel strike and one at toe-off. During these periods loads can reach up to four times body weight. In between these two peaks the load drops to about two times

body weight. Stance phase takes about two thirds of the walking cycle. During the swing phase the loads are much less and are generally said to be about 10 percent of body weight (Paul, 1967).

1.2.4. Disease of the Natural Hip.

Arthritis is one of the major diseases which makes a hip replacement operation necessary. Arthritis means an inflammation of the joint but is generally used to describe any condition in which there is damage to the cartilage. In the early stages of arthritis the pain comes mainly from the inflammation, but in the later stages, when most of the cartilage has worn away, the pain comes from the friction of the two bone ends rubbing together. There are two types of arthritis, osteoarthritis and rheumatoid arthritis.

Osteoarthritis mainly damages the joint cartilage and is usually caused by wear and tear. It is a degenerative disorder that results from a combination of ageing, irritation of the joints, wear and abrasion. It is characterised by the deterioration of articular cartilage and by the formation of new bone. The cartilage slowly degenerates, and as the bone ends become exposed, spurs (small bumps) of new osseous tissue are deposited on them. These spurs decrease the space of the joint cavity and restrict joint movement.

Rheumatoid arthritis starts in the synovium and is an autoimmune disease. The body's immune system starts to attack its own tissues, in a hip this is the cartilage and joint linings. It causes swelling, pain and loss of function and eventually destroys the joint cartilage. The bone next to the cartilage is also damaged which makes it very soft. Rheumatoid arthritis affects about 1.5 million people in the UK and starts usually between the ages of 35-55.

A major distinction between osteoarthritis and rheumatoid arthritis is that osteoarthritis strikes the larger joints (knees, hips) first whereas rheumatoid arthritis strikes smaller joints first. At the end stage of both of these diseases, the patient is in a lot of pain, it is then that a hip joint replacement becomes necessary.

1.3. Hip Replacements.

1.3.1. Introduction.

Hip replacements have been carried out for over a hundred years. During this time there have been many material combinations tried, each with varying degrees of success.

1.3.2. History of Total Hip Replacements.

Gluck attempted the first total hip replacement in 1890. He used ivory to replace a femoral head and an acetabular cup. The prosthesis was held in place using glue. In 1919 a rubber component was used but these early attempts were unsuccessful

Another approach to joint replacements was the interpositional arthroplasty (Figure 1.3). In 1923, Smith Peterson attempted this using glass. The principle was to stimulate cartilage regeneration on both sides of the glass and then remove the glass once the cartilage had been restored. However the glass was too fragile and fractured. He tried again using Pyrex, Bakelite and finally vitallium (cobalt chrome alloy). The vitallium was the most successful of the materials tested.

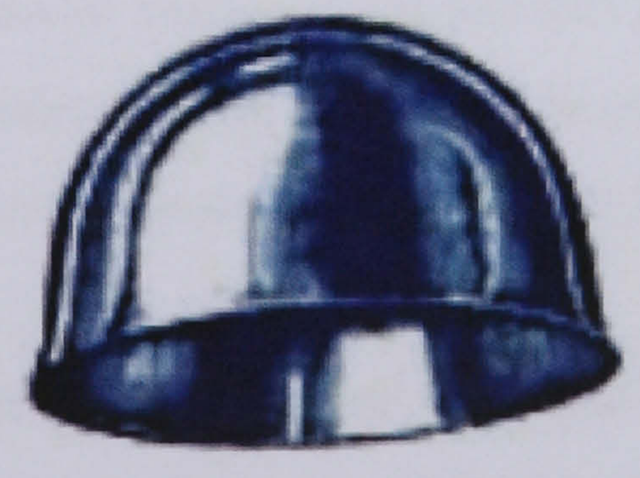

Figure 1.4 Glass interpositional arthroplasty, (www.geocities.com).

In 1938, Mr Philip Wiles first used stainless steel. He used it to replace the femoral and acetabular parts of the joint. It was fixed in place using screws but failed due to loosening.

Prosthesis design continued to advance and in 1946 the Judet brothers designed the first short stemmed prosthesis (Figure 1.4). It was made from polymethylmethacrylate with a head that was a two-thirds sphere attached to a short stem. The prosthesis failed due to the creation of wear debris. The inflammatory reaction to the debris resulted in loosening. Later versions were made of vitallium but these were only partially successful.

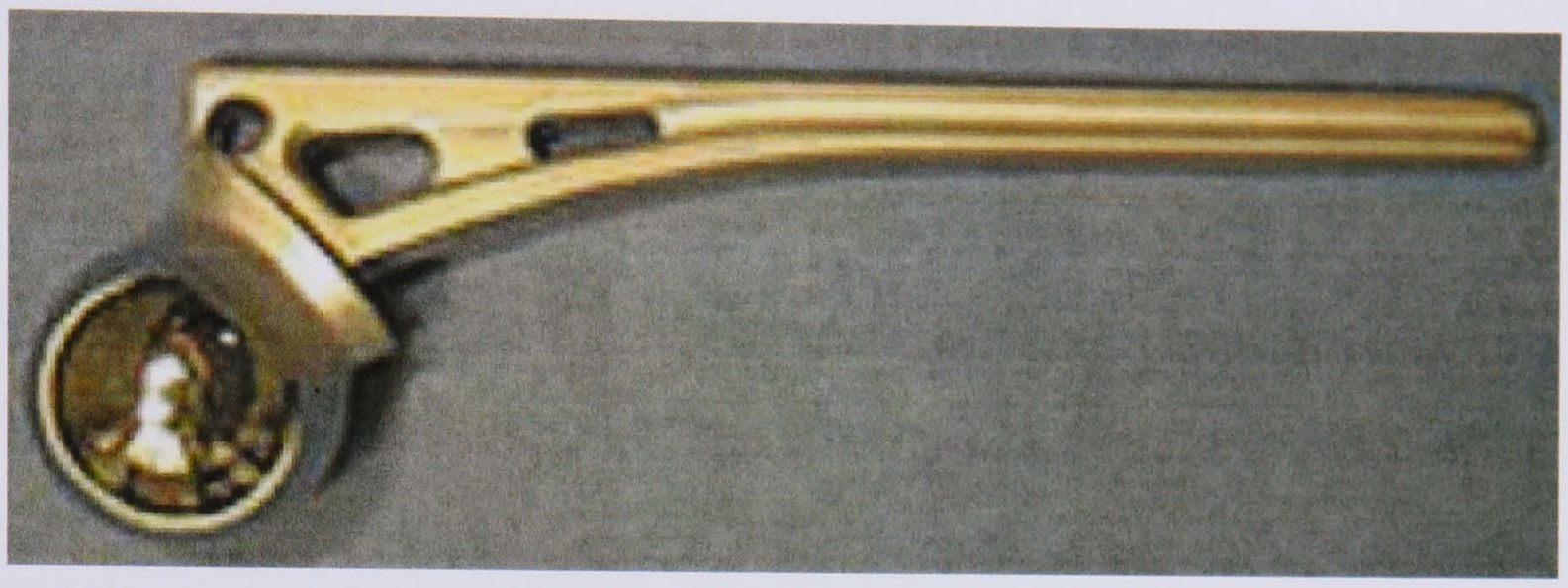

Figure 1.5 Judet hip replacement, (www.geocities.com).

In the 1950's Mr McKee, Mr Watson-Farrar and also Sir John Charnley began to devise their hip replacements. The McKee-Farrar total hip was a metal on metal joint. Later versions included a cement fixed version and this was the first widely used and successful total hip replacement.

Sir John Charnley developed the concept of the low friction arthroplasty. He was convinced that the high frictional torque in the McKee-Farrar metal on metal joint was unsatisfactory. His first attempt used Teflon shells on the surface of the femoral and acetabular components. Unfortunately the Teflon on Teflon bearings wore out.

The next design was a small diameter metal head that articulated against a thick walled Teflon shell. However this also failed quickly due to poor wear characteristics and a massive inflammatory reaction, which caused osteolysis and loosening in the surrounding bone. Charnley abandoned Teflon in 1961.

Charnleys third attempt involved using a socket made of high molecular weight polyethylene (HMWPE). Its wear properties were much better than that of Teflon. The socket articulated with a highly polished stainless steel ball. This remains the

basis of the majority of total hip replacements (THR) today.

For a THR to be considered successful there are several criteria it must meet. It must have:

1. A low wear rate, resistance to third body damage and a low coefficient of friction.
2. A rapid and viable way of fixing the prosthesis to the host.
3. It should be replaceable if the need for revision surgery ever arose.
4. Any wear generated should be of a small volume and the body should have a low reaction to such debris.
5. It must be dimensionally stable and durable for up to 20 years.
6. Bring relief from pain and restore mobility.
7. Not cause any tissue irritation or rejection.
8. Be resistant to mechanical failure and loosening.

Hip replacements can be either cemented or cementless. Cemented stems are usually fixed in place using acrylic bone cement. There are however problems associated with this. Over time the cement can crack and become fragmented, which results in particles being released from the bone cement. This causes scratching of the counterfaces of the joint replacement, which increases the wear of the polyethylene and increases the chance of an osteolytic reaction. The cracks that form can also result in loosening. Another problem is the reaction of the body to the cement particles. In the process of trying to remove the particles the bone can be structurally weakened. This has led to the development of cementless systems. These have a porous or hydroxyapatite coating over part or all of the stem. This provides a rough surface for the bone to grow into and creates a strong bond between the tissue and the implant.

1.3.3. Wear of Hip Replacements.

With the advances in prosthesis design and engineering, the wear of UHMWPE is the main concern in long term failure of total hip replacements. The wear and surface degradation of UHMWPE bearing surfaces in orthopaedic implants is of leading clinical concern. Wear has several detrimental effects including the

deterioration of articular performance. On clinically retrieved hip implants three wear mechanisms have been observed. These are abrasive wear, adhesive wear and fatigue wear.

Abrasive and adhesive wear are associated with surface characteristics of the PE-metal interface. Abrasive wear occurs by cutting and scratching of the UHMWPE surface. This usually happens when loose third body particles are trapped between the articulating surfaces. Adhesive wear occurs by the shearing of microscopic asperities from the polymer surface. Fatigue wear is the initiation and propagation of surface or subsurface cracks under cyclic loading conditions. In hips this usually takes the form of surface microcracking. Subsurface delamination is rarely seen in the hip replacements but has been frequently observed in the knee replacements.

McKellop *et al.* (1995) showed that the surface of a retrieved total hip replacement appeared smoother than the original machined PE. This was responsible for the release of submicron sized wear particles. This wear mechanism otherwise referred to as asperity wear interaction was responsible for the bulk of polymer wear. It is difficult to classify this in the conventional sense of abrasive, adhesive and fatigue wear. As the microscopic asperities of the metal interact with the polymer surface there are both adhesive and deformation forces applied to the polymer. Equally there may be many asperity interactions with a single molecule before a wear particle is generated. Set in this context, the burnishing or polishing wear on smooth metal heads is a mixed mode of wear potentially involving abrasion, adhesion and fatigue. If metal femoral heads become scratched or roughened then more abrasive mechanisms predominate.

Historically, one major cause of failure of total hip replacements was oxidative degradation, which was a result of irradiation used for sterilisation. During sterilisation using gamma irradiation, chain scission occurs, which produces both crosslinks and free radicals in the UHMWPE. If the irradiation is carried out in the presence of oxygen, the free radicals initiate a series of long term oxidation reactions that result in further chain scission. Oxidation of the UHMWPE causes deterioration in some of the important mechanical properties such as tensile strength, impact strength, fatigue strength, density and Young's modulus. A study by Besong *et al.*

(1997) showed that as the age of the material after irradiation in air increased, the wear rate increased significantly when compared to non irradiated UHMWPE. After ten years the wear rate for the irradiated UHMWPE was thirty times greater than for the non-irradiated. When the tests were carried out on a rough surface the wear rate of the ten year shelf aged irradiated material was two hundred times greater than the wear of non irradiated UHMWPE on a smooth surface. The wear particles produced were also found to be smaller for irradiated material suggesting that irradiated material could produce a more severe biological reaction. Since then, different methods of sterilisation have been adopted, such as irradiation in an inert atmosphere, which greatly reduces oxidation. The other mechanisms of wear are now of more concern. These surface wear mechanisms produce wear on a much smaller scale and they also produce smaller wear debris.

1.4. Ultra High Molecular Weight Polyethylene.

1.4.1. Introduction.

A UHMWPE molecule consists of repeating units of ethylene monomers. It has a backbone structure based on C-C covalent bonds (Figure 1.5). The polymer chains have very few branches. UHMWPE has a molecular weight of over a million. It can be distinguished from other polymers by its extremely long and highly entangled molecular chains. It is this property that makes UHMWPE extremely wear resistant.

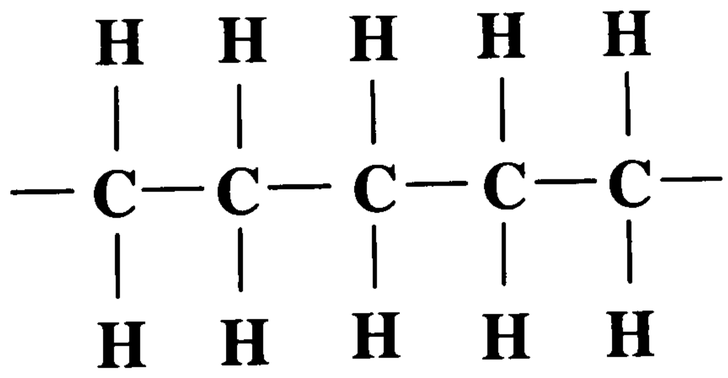

Figure 1.6 Polyethylene chains consist of carbon and hydrogen only.

When UHMWPE is in a solid state the molecules are arranged in ordered and disordered regions also known as crystalline and amorphous regions. In the

crystalline regions the chains are folded with the C-C axis which is oriented perpendicularly to the chain fold interface. There is no regular chain folding in the amorphous regions. In this region, adjacent chains are interconnected through random mechanical entanglements, and also occasionally crosslinks. Tie molecules connect the amorphous and crystalline regions together.

The mechanical properties of UHMWPE are determined by:

1. The crystallinity i.e. the balance between the amorphous and the crystalline regions.
2. The number of tie molecules connecting the crystalline regions.
3. The amount of entanglement and crosslinks between the crystalline regions.
4. The presence or orientation of the crystallites (Morrey *et al.*, 1991).

It was Pooley *et al.* (1972) who first suggested that PE might draw itself into a preferred orientation, which is in the direction of sliding. They found that after sliding had commenced, the friction between the PE and its counterface reduced. This happened as the molecular chains became oriented parallel to the direction of sliding. Wang *et al.* (1998) also showed how important molecular orientation was in UHMWPE. These authors suggested that a fibrillar structure is easily formed even on worn surfaces by surface traction forces, even if there is no third body wear. It was found that this structure was stronger in the orientation direction but weaker in the direction perpendicular to orientation. Under multidirectional motion they found that it was this orientation softening phenomenon that was predominately responsible for the detachment of fibrous wear debris from worn surfaces. It is not clear if similar orientational hardening occurs in the presence of more abrasive wear conditions.

The production of UHMWPE wear particles activates processes in the body that can lead to bone resorption. The wear particles are engulfed by macrophages, which are part of the mononuclear phagocyte system. Their primary role in the immune system is to organise the processes of inflammation and repair sites in the body that have been damaged, or invaded by a foreign particle. Macrophages initiate osteoclastic bone resorption and also stimulate the formation of a granuloma along the bone implant interface. This can lead to aseptic loosening of the prosthesis.

1.4.2. Wear of UHMWPE.

UHMWPE is thought to wear by one of three different mechanisms. The three mechanisms are wear caused by microscopic counterface asperities, wear caused by macroscopic polymer asperities and also structural failure. In microscopic counterface asperity wear (Figure 1.6), it is assumed that the polymer surface is smooth and the counterface has asperities of up to 0.1μm. During sliding, small cyclic stresses are produced at, or near the polymer surface. During motion the asperities on the counterface repeatedly deform the polymer, and the polymer eventually fails due to surface fatigue failure and wear particles are produced. If the counterface has larger asperities wear may change to a more abrasive action. This wear mechanism is based on the assumption that the polymer has a very flat surface but this is not usually the case.

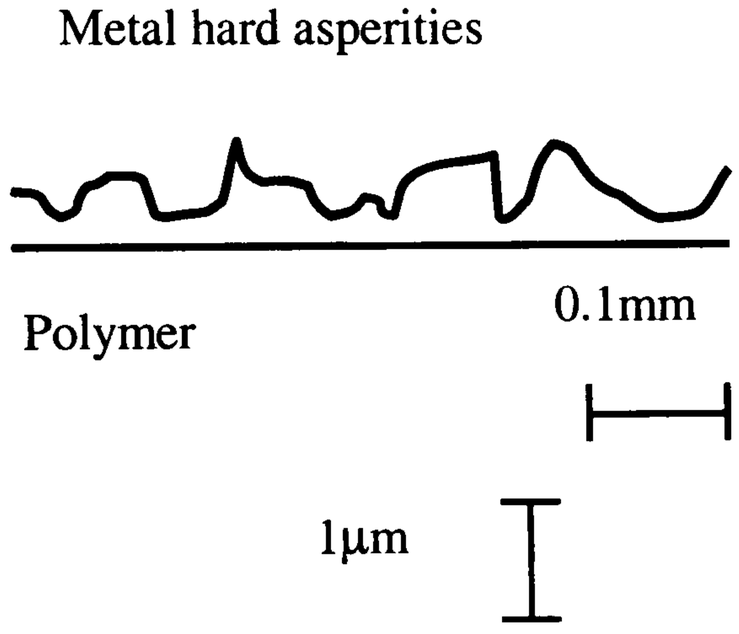

Figure 1.7 Diagram representing microscopic counterface asperity wear (Fisher, 1994).

Wear is also likely to be caused by macroscopic asperities on the polymer surface (Figure 1.7). When a load is applied to the polymer it causes the asperities on the polymer surface to deform. Initially this deformation is elastic but after a few cycles it becomes plastic. Local stress concentrations build up in the polymer asperity and under a constant load the polymer asperities may fail by rupture. However under a cyclic load the cyclic deformation can produce crack propagation and surface fatigue within about 10μm of the polymer surface underneath the asperity (Fisher, 1994).

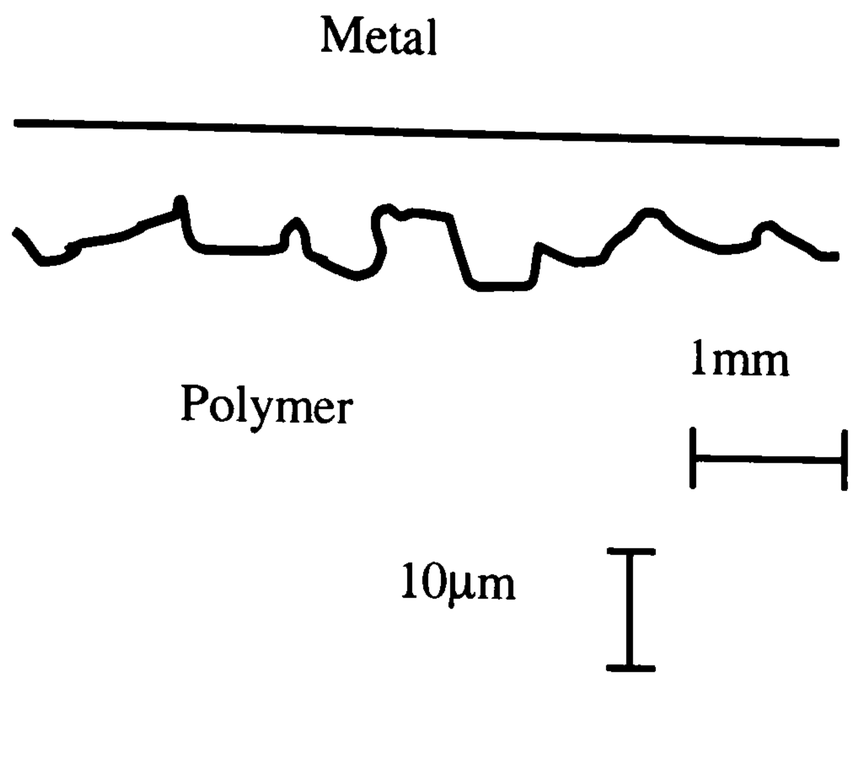

Figure 1.8 Diagram representing macroscopic counterface asperity wear (Fisher, 1994).

The third wear mechanism that is also known as delamination does not occur on the surface of the polymer, but occurs beneath the surface (Figure 1.8). It is caused when loads above the yield stress of the polymer are applied and results in a structural stress field that varies with time according to the amount of load at any particular time. The geometry of the contact, the load, and the elastic modulus of the material determine the size of this stress field. In most prostheses the joints are designed so that the yield stress is never exceeded, however, in knee replacements, the yield stress can often be exceeded because of their less conforming nature, resulting in structural fatigue of the polymer and failure after a very low number of loading cycles. This wear process rarely causes problems in hip prostheses because these are more conforming. In addition, delamination is rarely seen in more conforming knee prostheses. This wear mode releases the most wear particles although recently most problems of delamination have been overcome by better design of the knee components and using thicker UHMWPE for the tibial component. In the long term the first and second wear mechanisms are more likely to cause wear in hip replacements.

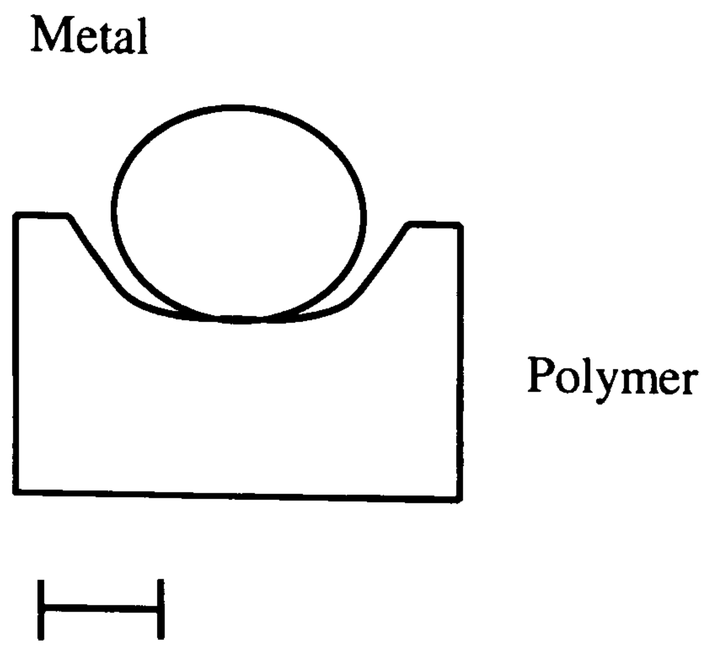

Figure 1.9 Diagram representing structural failure (Fisher, 1994).

Multidirectional motion is very important in producing clinically relevant wear rates and wear debris. In unidirectional tests the molecules in the material are stretched along the direction of sliding. This results in the material becoming stronger in this direction but weaker perpendicular to it. The process is known as orientational hardening. In the knee joint the motions are much more unidirectional than in the hip joint. The hip undergoes much more multidirectional motion. In the hip joint the main movement is the flexion and extension direction. The molecules align themselves in this principal direction. However there is also other movements happening simultaneously. In the hip this is adduction and abduction. In this direction the material is much weaker and rupture occurs between the oriented molecules, which results in the formation of wear particles. Barbour *et al.* (1999) showed how important the shape of the wear path was on wear. They tested two different motions in a hip joint simulator. The more open multidirectional path caused a significant increase in the wear rate compared to the more unidirectional path. This study showed how important the direction of motion is in producing clinically relevant wear rates. A study by Bennett *et al.* (2002) examined the motions of the hip, in hip replacement patients. They showed that there was a large variation in the shape and size of the wear paths in different patients. They found that those with more multidirectional motion had greater wear than those with more unidirectional motion.

Under linear motion the tensile surface stresses and shear stresses in the polymer are parallel to the aligned molecules. The diameter of the instantaneous asperity contact

spot is of the order of a micron or less (Wang *et al.*, 1996). This is much less than the length of the molecules, and as the shear force applied to the asperity is usually less than that required to cause an instantaneous rupture of the molecules, in order to produce wear, the molecules must be broken. At microscopic levels it is the fibres that must be broken to generate wear particles. Therefore, it is the strength of the fibres rather than the strength between the fibres that determines the wear resistance. The strength of individual fibres depends on the molecular orientation within the fibre and the number of molecules per cross-sectional area. The degree of molecular alignment depends on the mobility of molecules at the wear surface (Wang *et al.*, 1996).

Gamma irradiation of UHMWPE produces crosslinking of the molecular chains and this reduces the mobility of the molecules resulting in less molecular alignment. As a result the strength of fibres in non-irradiated UHMWPE should be greater than those in irradiated UHMWPE. Consequently, the wear resistance should be greater for non-irradiated UHMWPE than for irradiated UHMWPE under mainly unidirectional motion. Crosslinking is described more fully in section 1.5.4. In the hip where there is mainly multidirectional motion, the use of crosslinked PE has been shown to reduce wear rates when femoral heads remain smooth, (Marrs *et al.*, 1999; McKellop *et al.*, 1999; Muratoglu *et al.*, 2000). This reduction in wear was lost when rougher counterfaces were used. This encouraged the use of scratch resistant ceramic femoral heads. In the knee, in which the degree of multidirectionality is lower, the advantages of crosslinked PE are less clear, indeed the ability of the material to be fractionally orientated (as in non crosslinked material) may be an advantage. Furthermore in the knee the majority of femoral components are metallic, and are therefore susceptible to third body damage and abrasive wear. This indicates that an optimum solution found in the hip may not be an optimum configuration or material in the knee (Wang *et al.*, 1996).

The UHMWPE wear debris produced usually shows a large variation in the size and shape of each particle. It is generally colourless and is strongly birefringent under polarised light. Submicrometre sized UHMWPE is reported to appear round or granular. Particles in the 1-5μm size range are usually described as small fragments,

filamentous, round or needle like. In the 5-25μm size range the debris is reported to resemble fibres and flakes, splinters or spears and needles. Larger particles up to 200μm resemble flakes and shards, or appear as shredded fibres several hundred microns in length (Savio *et al.*, 1994). Tipper *et al.* (2000) examined debris from Charnley explants. They found that the size and shape of the wear debris varied widely. They found large platelet type particles and fibrils and also small round granules.

Table 1.1 Summary of wear mechanisms

Wear Mechanism	Type of surface		Surface appearance	Particle appearance
Adhesive wear	Smooth surfaces	Shearing of microscopic asperities on the polymer surface (Fisher *et al.*, 1994).	Smooth polished appearance (McKellop *et al.*, 1995) Rippled effect (Jasty *et al.*, 1997) Back transfer of PE particles onto surface. (Endo *et al.*, 2001)	Granules, small round particles (Tipper *et al.*, 2000).
Fatigue wear	Smooth surfaces	Initiation and propagation of surface cracks under cyclic loading conditions (Dally *et al.*, 1990)	Smooth with visible cracks	Granules (Tipper *et al.*, 2000).
Abrasive wear	Scratched surfaces.	Cutting of smooth surfaces by large asperities on the harder counterface. (Marrs *et al.*, 1999). Microscopic counterface asperity wear when counterface asperities are higher (Fisher *et al.*, 1994).	Scratches on surface Signs of roughness or damage. (Atkinson *et al.*, 1985)	Flakes and Shards (Savio *et al.*, 1994). Fibrils (Tipper *et al.*, 2000).

1.4.3. Biological Reactions to UHMWPE Wear Particles.

Willert *et al.* (1977) first examined the effect of polyethylene particles in tissues retrieved at revision. They found that after a joint was implanted a new capsule forms around the joint, to replace the original capsule. They found that the particles generally induced a foreign body reaction and that the foreign body granulation tissue showed a tendency towards fibrosis. These were some of the very first observations of how polyethylene particles reacted in the body.

More recent studies by Wang *et al.* (1996) showed that PE particles alone were sufficient to induce osteolysis, and that it was not metal or cement particles which initiated the reaction. They also observed that in many cases only submicrometre sized particles were present suggesting that it was these particles rather than micrometre sized particles, which caused osteolysis. If there were enough submicrometre sized particles present, the macrophages were activated. The macrophages then released factors, which stimulated bone resorption.

Studies carried out by Campbell *et al.* (1995) of digested explant tissue examined under a scanning electron microscope showed that the vast majority of wear particles are submicron in size with some larger particles and large shreds of debris. It has often been suggested that submicrometre sized particles are the most biologically active. Wear debris induced osteolysis is dependent on the amount of submicrometre wear particles and is therefore accelerated by the production of greater numbers of submicrometre particles.

Macrophages attempt to degrade and break down a foreign body in a process called phagocytosis (Figure 1.9). During this process macrophages adhere to and engulf a foreign particle, by extending their pseuodopodia around the particle and then internalising it into a phagocytic vacuole. This process causes the macrophages to become activated and they can then release an array of cytokines and low molecular weight mediators which may play a role in osteolysis (Ingham *et al.*, 2000). Cytokines are the principle method of communication between cells. They are soluble low molecular weight glycoproteins which are released from a variety of cells and can modulate the activity of other cells (Green *et al.*, 1998). The vacuoles

contain cationic proteins, proteolytic and hydrolytic enzymes which can breakdown micro-organisms. However the PE particles can not be degraded and a foreign body granuloma is formed.

Granulomatous tissue forms to store the wear particles. The granulomatous tissue forms within the capsule and has specific characteristics for each type of foreign material. Granulomas may develop areas of central necrosis. Large bag like crypts, which are filled with debris may develop in the capsular tissue. This promotes continued development and leads to the production of even more granulomatous tissue. The greater the amount of tissue the greater the tendency towards necrosis. The formation of granulomas is an attempt by mononuclear phagocytes to isolate the particle and protect surrounding tissues from a potentially damaging foreign body.

The tissue that has formed also has a tendency to form scar tissue during which more and more collagen fibres are differentiated. The thickly scarred and callous capsule that can result, tends to reduce the mobility of the artificial joint (Willert *et al.*, 1977).

It was found by Green *et al.* (2000) that the volume and size of particles were critical factors in macrophage activation, with particles in the size range of 0.1-10μm being the most biologically active. The small particles (0.2μm) stimulated macrophages at a concentration of $10\mu m^3$ particles per macrophage. At higher volumetric concentrations the particles appeared to be inactive. This was probably due to a negative feedback mechanism to the macrophages due to overstimulation in a closed culture system. Large particles may not activate the macrophages as they are too large to be phagocytosed. When particles are too large, multinucleated giant cells are formed (Amstutz *et al.*, 1992).

Green *et al.* (1998) also showed that PE particles could stimulate primary macrophages to produce elevated levels of osteolytic cytokines, IL-6, IL-1β and TNF-α *in vitro*. Parry *et al.* (1995) showed that IL-6 stimulates osteoclast formation and bone resorption. Kontinnen *et al.* (1997) showed that IL-1β is involved in stimulating the proliferation and maturation of progenitor cells into osteoblasts,

which stimulated the osteoclasts to mature into multinucleated bone resorbing cells. They also showed that TNF-α caused the proliferation of osteoclast progenitors, and through osteoblasts, activate multinucleated osteoclasts to resorb bone. A study by Ingham *et al.* (1999) suggests that TNFα maybe one of the principle cytokines produced in wear particle induced osteolysis.

A study by Matthews *et al.* (2000) investigated the biological activity function of wear debris particles. It was carried out by determining the biological activity function of sterile, endotoxin free, polyethylene wear debris which was generated *in vitro*, as a function of particle size. TNFα was used as the marker for biological activity as this has previously been shown to correlate with bone resorption (Ingham *et al.* 1999). Three size ranges were examined. These were 0.1-1.0μm, 1.0-10μm and 10-100μm. It was found that the 0.1-1.0μm size range was the most reactive. Fisher *et al.* (2001) normalised this as a value of one. The bigger size ranges were normalised with respect to the smallest size range.

The volume and morphology of debris are important factors in determining the nature of the cellular reactions that are stimulated. The smallest UHMWPE particles may be transported and eliminated by the lymphatic system. The macrophages can only deal with small volumes of particles. If large amounts of particles are being produced, the system becomes overloaded and the wear particles accumulate in the synovium. This produces a chronic inflammatory response which can eventually lead to bone resorption (Cooper *et al.*, 1993; Dowson *et al.*, 1991).

In an *in vivo* study carried out by Goodman *et al.* (1995) phagocytosable particles of PE were associated with decreased net bone formation in a bone harvest chamber at two and three weeks. The decreased amount of bone could have been due to increased resorption. The decrease in bone formation was associated with a foreign body reaction, a chronic inflammatory response, and extensive formation of fibrous tissue. On the basis of this study Goodman *et al.* (1995) concluded that an excessive amount of PE debris may inhibit the ingrowth of bone into porous coated joint components

In a study carried out by Revel *et al.* (1997) it was shown that between osteolysis positive and osteolysis negative cases there was a significant difference in the number of particles present but no difference in the size ranges of the particles. This study suggested that a certain volume of particles were needed before osteolytic reactions were stimulated. The critical number was found to be $1x10^{10}$ particles/gram of tissue. In this study almost all particles were less than 5μm in size with the majority being less than 1μm.

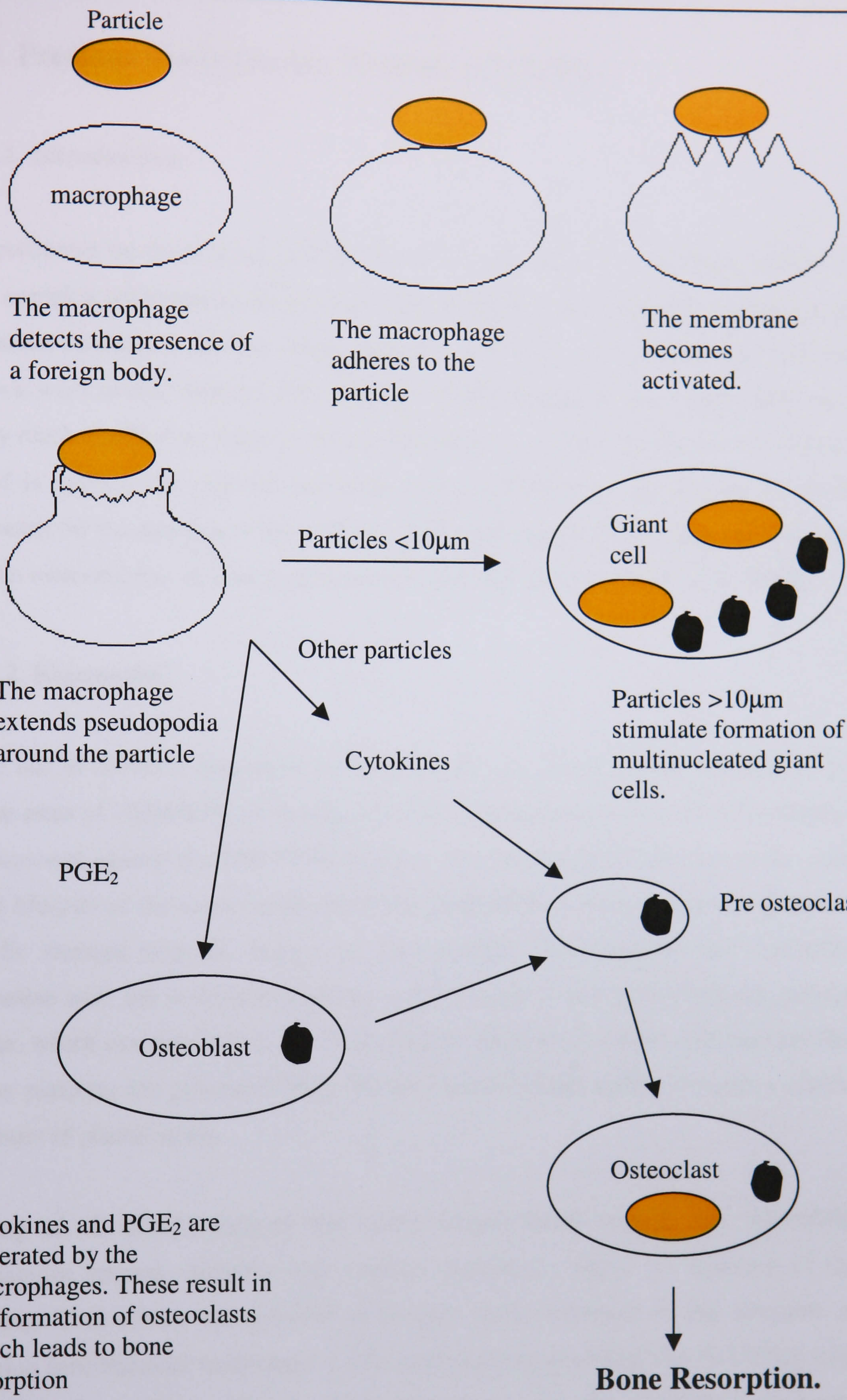

Figure 1.10 Phagocytosis of a wear debris particle.

1.5. Previous Studies on the Wear of UHMWPE:

1.5.1. Introduction.

Experiments on the wear of UHMWPE can be quite difficult to perform because of the complex behaviour of the polymer. One problem is that when PE is placed in an aqueous medium it absorbs water making it difficult to calculate weight loss and hence wear of the material. Pre-soaking UHMWPE pins in de-ionised water until they reach equilibrium helps to reduce this problem. Another problem is that when a load is applied the material undergoes creep deformation. The amount of creep depends on the structure of the polymer. Differentiating between creep and wear can make measurement of wear by geometrical methods difficult (Rose *et al.*, 1984).

1.5.2. Kinematics.

The use of different kinematics in wear studies has shown a large variation in the wear rates of UHMWPE. In the hip joint, the multidirectional motion of the metallic component against the UHMWPE component, plays an important role in the wear and lifespan of the replacement joint. The UHMWPE components are subjected to cyclic stresses near the surface of the material. This orientates the crystalline lamellae near the articulating surface and produces a plastically induced damage layer, which can then lead to debris generation. Kurtz *et al.* (1999) hypothesised that wear particles are generated when the deformation at the surface exceeds a critical amount of plastic strain.

Wang *et al.* (1997) showed that under unidirectional motion, the UHMWPE molecules become stretched and orientate themselves along the direction of the sliding. This allows the material to become strain hardened in the direction of motion (orientational hardening). Under multidirectional sliding like that in hip joint simulators and natural hip joints, the orientation of molecules in one direction means that the other directions perpendicular to sliding are much weaker. This leads to strain softening and a weaker wear surface (orientational softening). This means that multidirectional motion will have a higher wear rate than unidirectional motion.

Orientational hardening results in a high wear resistance and low wear rates under unidirectional motion

Studies carried out by Marrs *et al.* (1999) and Wang *et al.* (1997) have shown that the wear rates under multidirectional motions were far greater than those under unidirectional motion. It was assumed that orientational hardening and softening occurred under both motions and that the difference in wear rates was due to the difference in frictional force. Under unidirectional motion, the frictional force is in a constant direction which is the same direction that the molecules are orientated, resulting in very low wear rates. Under multidirectional motion however, the frictional force constantly changes direction, which results in an increased wear rate. In a crosslinked material, the crosslinks prevent some degree of orientational hardening from taking place, but also act to strengthen the material in the perpendicular direction. This reduces the wear of crosslinked material in multidirectional tests.

Besong *et al.* (1999) found that PE tested under multidirectional motion on a smooth stainless steel counterface wore at a significantly higher rate, compared to unidirectional sliding on the same counterface. Different particle morphologies were observed for multidirectional and unidirectional sliding and approximately 75% of the mass of wear debris was less than 10μm in size in multidirectional tests, compared to 33% in unidirectional tests. It was also found that the total number of particles generated, and the number of particles per unit volume, in the multidirectional model was significantly greater than in the unidirectional model. These authors concluded that as the motion approached unidirectional motion, the number of particles in the biologically active range was reduced.

1.5.3. Counterface Conditions.

It has been reported that there are two different wear mechanisms involved in wear on rough and smooth surfaces. Smooth surfaces are more likely to undergo adhesive, deformation wear, microfatigue wear and also polishing, while rough surfaces produce a more abrasive wear mechanism. Adhesive and deformation wear involves

the harder counterface asperities removing small particles of polymer after many interactions. Abrasive wear involves cutting of the softer surface by the large surface asperities on the harder material. A low cycle fatigue or abrasive action removes the polymer (Marrs *et al.*, 1999).

Marrs *et al.* (1999) performed experiments with crosslinked and non-crosslinked material on rough (Ra~0.09μm) and smooth (Ra~0.01μm) surfaces. It was found that the rougher counterface increased the wear rate of both materials between 30 and 410 times. The multidirectional rough tests had the highest wear volumes with little difference between the two types of material. In the unidirectional rough tests, the crosslinked material had a significantly higher wear rate than in unidirectional smooth tests. Against a more abrasive counterface, less molecular orientation is produced as the surface molecules are removed by a single interaction by the rough asperity. This helps to account for the higher wear rates seen with the rough surfaces.

In a unidirectional study carried out by Hailey *et al.* (1996) it was found that an increase in counterface roughness, by a factor of 4, caused an increase in wear by a factor of 30. The size of the particles was also found to decrease by an order of magnitude, therefore, causing a dramatic increase in the total number of particles produced. These studies indicated that third body wear can cause huge increases in wear rates *in vivo*, and that a single scratch on the surface of an implant could dramatically increase the wear rate over time. It should be noted that this effect is greater in unidirectional studies. Equally as there are differences in particle morphology between unidirectional and multidirectional studies (Besong *et al.* 1999) the effect of surface roughness on particle morphology may be different in multidirectional studies.

It was shown by Dowson *et al.* (1987) that UHMWPE wears more quickly *in vivo* than in laboratory tests. This is due to the generation of fine scratches on the surface of the implant and also to third body wear. An indentation in the material, which produces no piled up material around the edges of the indent, does not cause a noticeable increase in the wear rate. If there is piled up material around an indent

removing this material restores it back to the wear characteristic of unblemished material. These experiments were in agreement with the work of Hailey *et al.* (1996)

Dowson (1987) also noted that the increase in wear rate with transverse scratches was strongly dependent on the depth of the scratch, for depths up to 10μm, but after this the wear factor is only slightly influenced by the scratch depth.

1.5.4. Crosslinked UHMWPE.

Crosslinking of PE can be carried out using several different methods, including using ionising radiation, peroxide chemistry or silane chemistry. All ionising radiation leads to the formation of free radicals in polymeric materials through homolytic chain cleavage. In UHMWPE, some of the free radicals recombine to form crosslinks while others remain as highly reactive free radicals. UHMWPE becomes highly crosslinked after an absorbed dose of 50kGy. To achieve a highly crosslinked UHMWPE using peroxide chemistry, a peroxide concentration of 0.1-0.2% by weight is necessary (Kurtz *et al.*, 1999).

The addition of crosslinks to UHMWPE by peroxide irradiation chemistry makes wear mechanisms even more complex. Independent studies have shown, substantial improvements in wear rates in crosslinked UHMWPE, in *in vitro* hip simulators (Edidin *et al.*, 1998; Jasty *et al.*, 1997; Wang *et al.*, 1997). However, Edidin *et al.* (1998) still found evidence of a plastically induced damage layer near the surface of the cups, although it was at a substantially reduced depth.

The first studies to be published on the effects of peroxide crosslinking were carried out by Shen *et al.* (1996). They found evidence of improved wear resistance, but questions have since been asked about its long-term stability to oxidative degradation. Accelerated oxidation studies carried out by Muratoglu *et al.* (1997) showed oxidation and embrittlement of the polymer when it was crosslinked using peroxide chemistry.

Atkinson *et al.* (1980) first proposed the use of PE crosslinked by silane chemistry in total hip arthroplasty, when they studied the contribution of creep to the

penetration of the socket by the ball using *in vitro* testing methods. During the first few years it was found that creep rather than wear played the major role in penetration and they suggested that silane crosslinking could reduce this initial creep. A slightly improved creep resistance and wear resistance was seen at high sliding velocities in unidirectional testing, when compared with uncrosslinked material (Kurtz *et al.*, 1999).

Crosslinking reduces the ability of the molecules to orientate and reorientate, and as a result reduces wear. The level of crosslinking controlling the wear behaviour of the UHMWPE overcomes any reduction in mechanical and physical material properties that may result from the crosslinking. Muratoglu *et al.* (1999) concluded that it was the molecular weight between crosslinks that defined the wear behaviour of crosslinked UHMWPE. However, under abrasive conditions the loss of toughness and durability may dominate the molecular mechanisms, and therefore accelerate wear. (Kurtz *et al.*, 1999). Marrs *et al.* (1999) showed that crosslinking did not significantly reduce wear against rough counterfaces.

Wang *et al.* (1999) concluded that crosslinking reduced the wear rate under multidirectional motion e.g. hip joints, since crosslinking reduced the extent of molecular orientation. It was the molecular orientation that decreased the strength of the material. Crosslinking slows down molecular mobility, however, the same is not true in knees which have a more unidirectional motion .

A study carried out by Kurtz *et al.* (1999) showed that crosslinking increased the ultimate strength and decreased the ductility of UHMWPE. It was also shown to increase the ultimate hardening behaviour and promote orientation of crystalline lamellae. This study supports the theory that crosslinking promotes strain hardening, during multiaxial loading, because of increased resistance to molecular mobility at large deformations.

The efficiency of crosslinking can be improved by the use of a sensitising atmosphere, such as acetylene, which leads to a higher ratio of crosslinking to chain scission, compared to irradiation in air or an inert atmosphere. (Kurtz *et al.*, 1999).

Marrs *et al.* (1999) concluded that additional crosslinks in the material could reduce wear in both multidirectional and unidirectional tests, because the crosslinks provide resistance to both deformation and adhesive fatigue wear processes. However, it can also be said that it could increase the wear rate in unidirectional tests, because the crosslinks reduce the amount of orientational hardening that takes place.

The latest crosslinked UHMWPE has been stabilised to inhibit oxidation, and highly crosslinked to reduce wear. It has been suggested that thermal treatment of irradiated UHMWPE can reduce the concentration of free radicals, resulting in a polymer that is resistant to long term oxidative degradation. An oxidative stabilised UHMWPE known as Duration has been shown to exhibit a 32% reduction in volumetric wear compared to an air irradiated control UHMWPE (Essner *et al.*, 1997). Further research by Wang *et al.* (1997, 1998) has shown that doses of up to 100kGy can reduce wear of stabilised GUR 1450 HP in a hip simulator, however, in a knee simulator the wear produced was insensitive to radiation crosslinking. Wang *et al.* (1997) concluded that although crosslinking may improve wear rates under multidirectional motion as in the hip, it does not necessarily improve wear resistance in the more linear motion seen in the knee.

Although crosslinked materials have been shown to reduce wear under multidirectional smooth conditions, relatively few studies have been carried out to investigate the effects of reduced multidirectionality and the effect of surface roughness on UHMWPE with different levels of crosslinking.

These conditions are particularly important in knee prostheses when the kinematics, although multidirectional, are more unidirectional than in the hip, and where the metal femoral condyles can become damaged or roughened.

Furthermore, the effect of crosslinking on the morphology of wear particles has not been studied. Endo *et al.* (2001) have shown that low levels of irradiation can reduce the size of the wear particles and make them more reactive. Besong *et al.* (1998) have shown oxidation can reduce the wear particle size and increase its biological activity. More recently Ingram *et al.* (2002) have shown that an increase in

molecular weight can increase the percentage of smaller particles and hence the reactivity of the debris.

At the beginning of this study in 1999, although it was known that crosslinked polyethylene could reduce the wear rate, it was not known what effect crosslinking would have on the size of the UHMWPE particles, and hence the biological activity.

1.6. Aims and Objectives.

1.6.1. Overall Aim.

To investigate the effect of serum concentration, kinematic conditions and surface roughness on the wear rate of UHMWPE under different levels of crosslinking, and the morphology of the resulting debris.

In a hip joint it has been shown that crosslinked UHMWPE can lower the wear rate as long as the surfaces are smooth and not damaged. Crosslinking the UHMWPE increases the yield stress of the material and decreases the strain to failure. Due to the network of crosslinks more force is needed to allow the chains to untangle and slide. It is this reduction in the relative movement between the crosslinks that lowers the strain to failure. Under more unidirectional kinematics e.g. the knee, it is thought that crosslinked UHMWPE may have a detrimental effect on the wear properties, because the crosslinks in the material reduce the amount of orientation hardening, which normally occurs in a unidirectional test. This means that the material can wear more easily, increasing the wear rates. The greater the level of crosslinking in the material, the greater effect this could have on the wear properties. The surface roughness may also affect the relative wear rate of crosslinked and non-crosslinked UHMWPE.

The aim of this project therefore, was to investigate the wear and wear particles of UHMWPE with different levels of crosslinking, and varying degrees of surface roughness and multidirectionality. Three different levels of crosslinking will be investigated under three different surface roughnesses and two different degrees of multidirectional motion.

1.6.2. Objectives.

- Crosslinked UHMWPE: To investigate the effect of crosslinking on the wear rate of UHMWPE. Three levels will be analysed, 5MRad because this material is already in clinical use in hip replacements. 10MRad will be used to represent a highly crosslinked material, as this material has been shown to have a lower wear rates. 0MRad UHMWPE will be used as a standard to compare the wear rates of the two crosslinked material against.

- Counterface roughness: To investigate how the roughness of the counterface affects the wear rate. Three different levels will be investigated. These are a smooth surface to represent a new unscratched joint replacement. Severe scratches to represent the most severe conditions the implant would have to operate under, and medium scratches which are more likely to occur *in vivo*.

- Kinematics: To investigate how different kinematics affect the wear rate of UHMWPE as it moves from a highly multidirectional motion such as that seen in the hip to a more unidirectional motion such as that in the knee. The rotations used will be 20° and 60°.

- Wear particles: These will be analysed to investigate the size and the shape of the wear particle changes under different wear conditions. Crosslinked UHMWPE has been shown to produce less wear volume under highly multidirectional motion. However the particles produced have not been analysed and hence their biological activity is not known.

1.7. Structure of Thesis.

- Chapter 2 gives details of the materials and methods used throughout the project. It describes in detail the wear testing methods and the debris isolation method used.

- Chapters 3 and 4 give the results from the pin on plate tests. Chapter 3 describes the results from ±60° rotation and Chapter 4 describes the results from ±20° rotation. Chapter 4 also has a discussion of the two different kinematic conditions.

- Chapter 5 describes the results of the wear debris analysis.

- Chapter 6 contains the final discussion and conclusions.

Chapter 2.

2. Materials and Methods.

2.1. Introduction.

This chapter outlines the general experimental procedures and materials used during the research studies.

2.2. Materials.

2.2.1. Pins.

The materials used during the investigations were Ultra High Molecular Weight Polyethylene (UHMWPE) GUR 1050 and high nitrogen stainless steel. The polyethylene representing the material used in a acetabular cup and the high nitrogen stainless steel representing the femoral head material.

The UHMWPE was irradiated to two different levels to create different levels of crosslinking. The levels of radiation were 5MRad which gave a medium crosslinked material and 10MRad which resulted in a highly crosslinked material. Crosslinking was achieved using gamma irradiation in nitrogen followed by annealing at a temperature above 150°C. The UHMWPE bars were first sealed in pouches under partial vacuum and subsequently exposed to either 5 or 10 MRad of gamma irradiation. Following irradiation the bars were annealed at 155°C for 24 hours in a nitrogen purged oven. This final step was undertaken to extinguish the free radicals and to help stabilise against long term oxidation. The bars were then cooled slowly and subsequently machined into pins. The irradiation was carried out by DePuy International.

The UHMWPE pins were all machined from a single block of material for each radiation level. They were taken from the centre of the block, with the pins oriented

along the length of the block, to form a truncated cone with a flat surface of 8mm diameter, which was the contact face (Figure 2.1). The wear surfaces of the pins were microtomed to remove any material that was damaged by the machining process. This was carried out using a sharp blade in a sledge microtome. Microtoming removed approximately 40μm of the pin wear surface to leave behind smooth undamaged material. Although machining marks can be clearly seen in the unworn surface of an acetabular cup they were much smoother than the machining marks seen on the pin surfaces. In a simulator study these marks are removed after one million cycles, but as a pin on plate test is much shorter it is started with a smooth surface.

Before wear testing, the wear pins were marked so they could be easily identified. They were then put into de-ionised water for a minimum of four weeks in order for them to absorb water and to stabilise their water content. Immediately before testing they were cleaned in soapy water and then put into an ultrasonic cleaner in iso-propanol for ten minutes to remove any debris or grease.

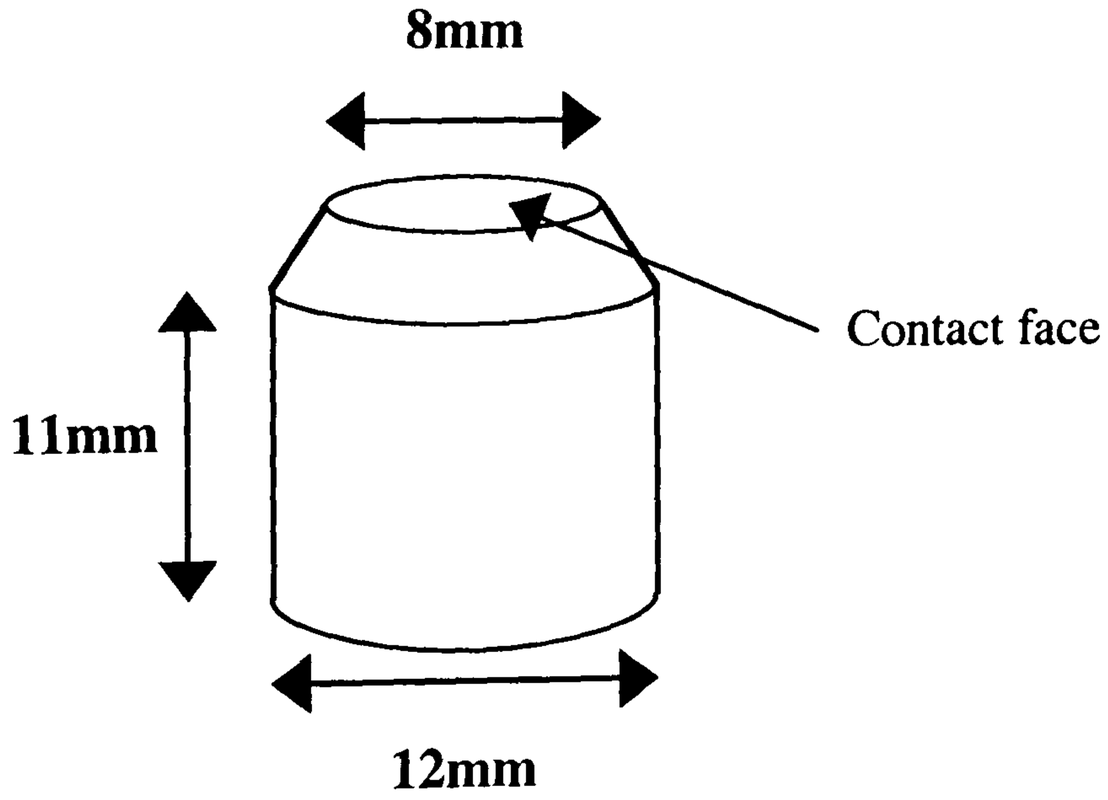

Figure 2.1 Dimensions of pin.

2.2.2. Plates.

The plates used during testing were high nitrogen stainless steel plates. High nitrogen stainless steel has improved fatigue and corrosion resistance compared to 316 stainless steel. The dimensions of the plate are shown in Figure 2.2.

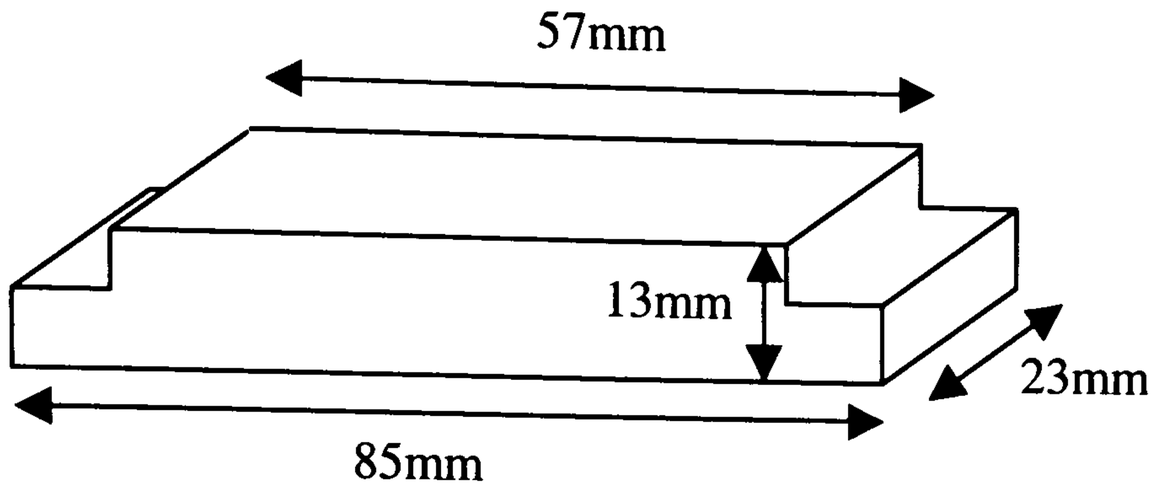

Figure 2.2 Dimensions of plate.

The plates were polished and lapped until they had a smooth surface finish with an average surface roughness Ra ~ 0.01. Scratched surfaces were achieved by producing discrete scratches perpendicular to the direction of sliding, on the surfaces, using a diamond stylus. A plate was secured into a pin on plate friction machine and a conical diamond with a diameter at its widest point of 100μm was put into a holder on the friction rig. The diamond was lowered onto the plate and a load was applied. The load applied varied according to the scratch height to be obtained. For the high scratches a load of 2.8N was used and for the medium scratches, 1.5N. A thin layer of petroleum jelly was applied to the surface of the plate to help prevent the diamond juddering across the surface and to help achieve a smooth scratch profile. The stylus was then driven across the surface. High scratches with an average peak height of 1.8μm and medium scratches with an average peak height of 0.8μm were generated. It was assumed that the diamond point did not change shape during scratching. After scratching, the plates were cleaned to ensure that no debris was left on the plates. The position and spacing of the scratches is shown in Figure 2.3.

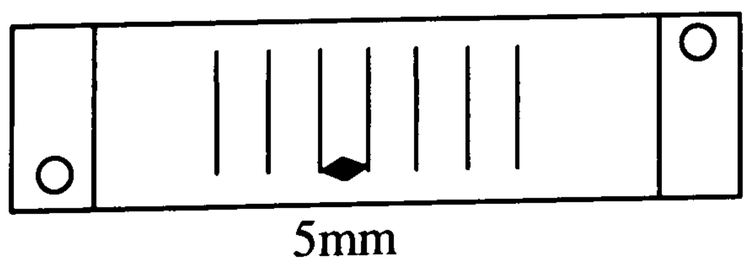

Figure 2.3 Position and spacing of scratches.

The scratches were measured using a Rank Taylor Hobson Form Talysurf surface measuring machine. This gives data on surface roughness and topography. The

machine measures surface roughness by drawing a stylus across the surface and measuring how much it moved from a set origin. A filter was used for smooth plate measurements and a cut off length of 0.8mm was used. For the scratched plates no filter was used.

The following parameters were used to identify the scratch geometries:

- Ra- arithmetical mean deviation of the assessed profile (ISO 4287), measure of the average deviation from a mean line. It gives an indication of the surface roughness but not any indication about the form of the roughness. For the smooth plates the Ra measurement was determined and the smoothest plates were selected, the rest were then scratched.
- Rp- maximum profile peak height (ISO 4287), the amount of material displaced above the surface of the plate.
- Rv- maximum profile valley depth (ISO 4287), the depth of the valleys.
- FWHM- full width half maximum, the full width at half the maximum height (h/2) or depth (d/2).

The parameters are shown in Figure 2.4.

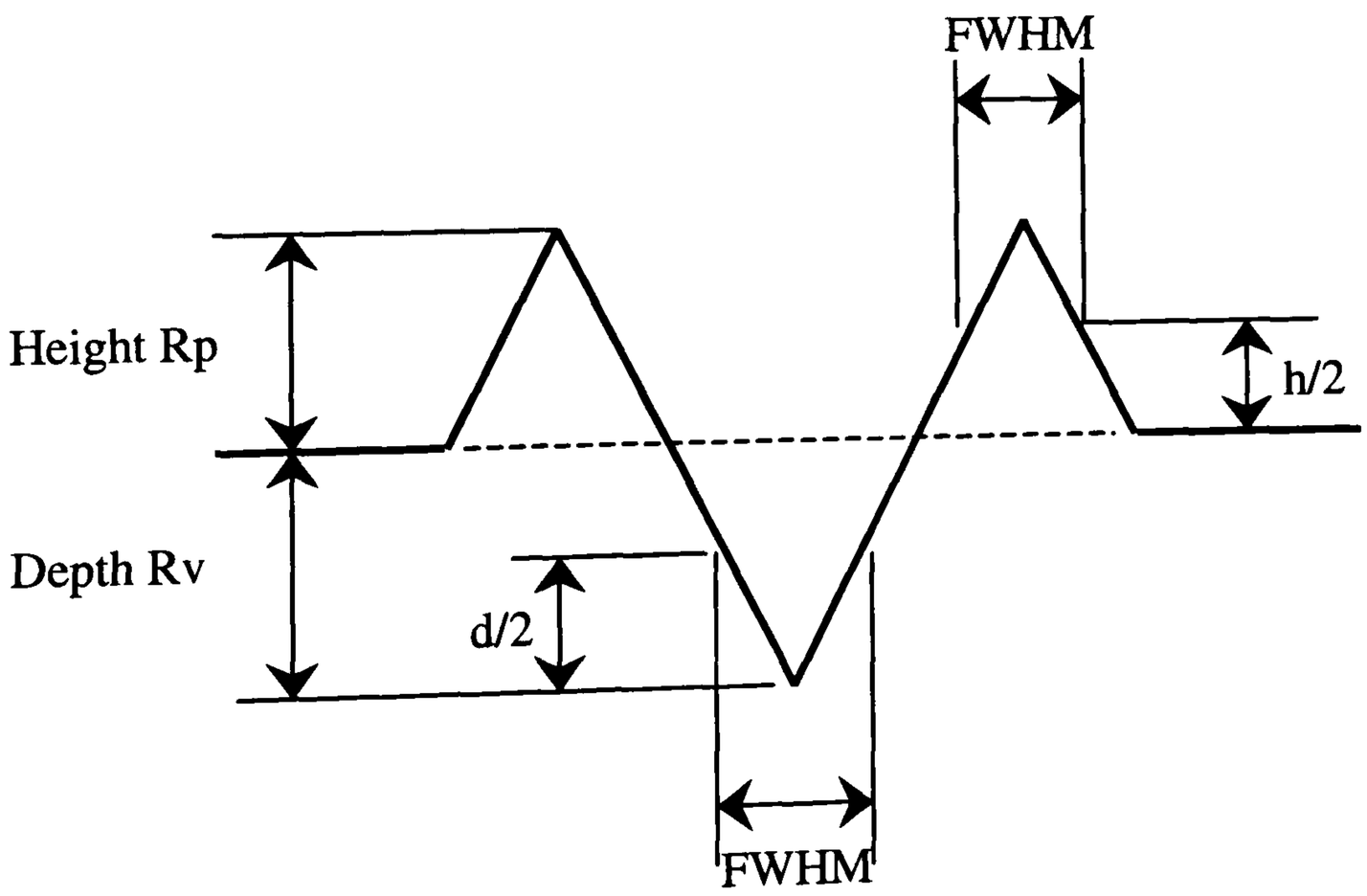

Figure 2.4 Scratch geometry as seen on a profilometer.

2.3. Experimental Procedure for Pin on Plate Experiments.

2.3.1. Pin on Plate Rig.

For the experiments described in Chapters 3 and 4 a multidirectional pin on plate rig was used as shown in Figure 2.5. The pin on plate rig allowed variables such as amount of rotation, stroke length, frequency, load, contact area, counterface surface roughness, and test materials to be easily changed so that many different combinations of physiological conditions could be tested. For the experiments in Chapters 3 and 4, variations in the amount of rotation, stroke length, counterface surface roughness and test materials were all investigated.

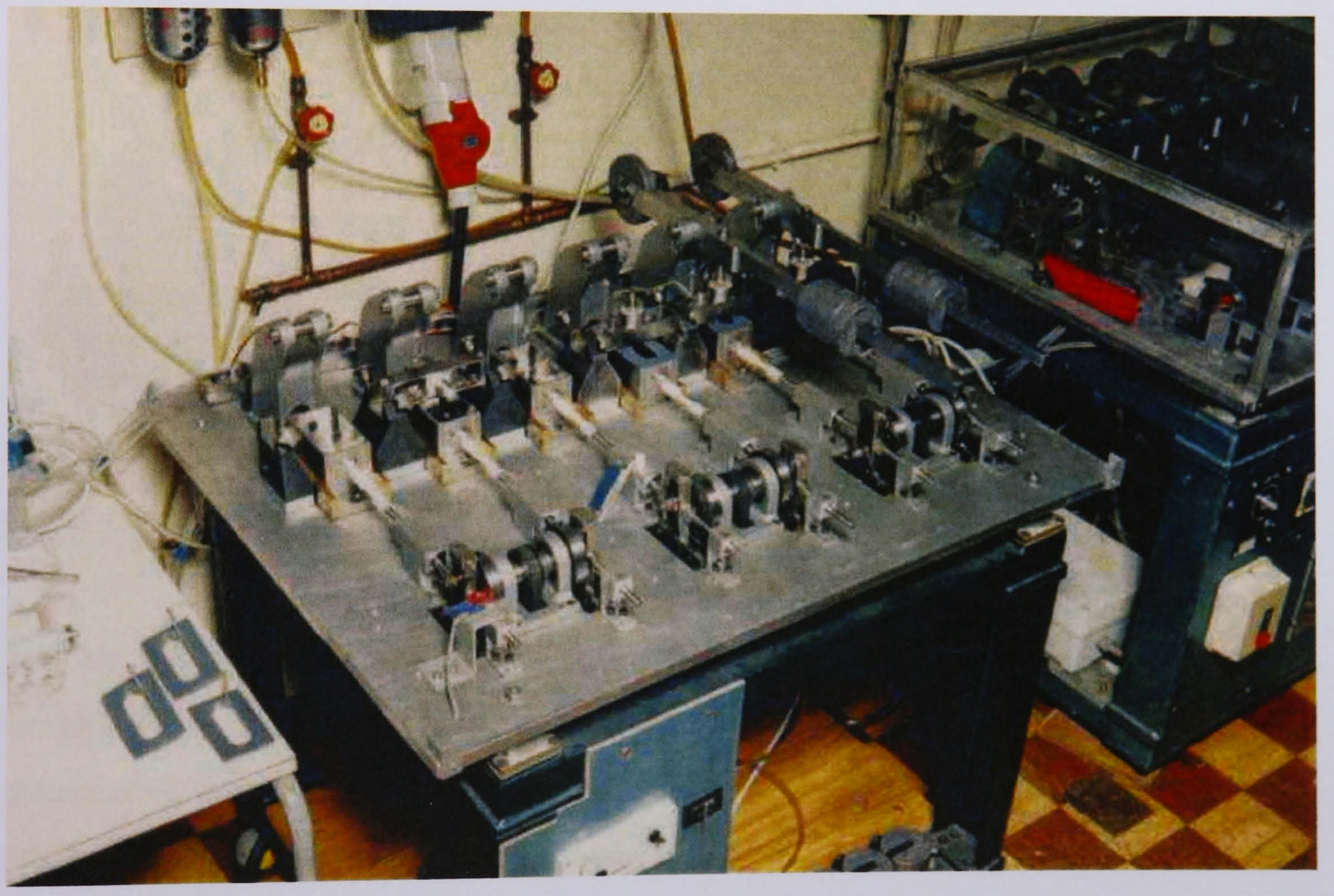

Figure 2.5 Six station pin on plate reciprocating rig.

The reciprocating pin on plate rig comprised of 6 identical test stations. A schematic diagram of a station from a pin on plate rig is shown in Figure 2.6. The carriages were each supported by an air bearing to help maintain smooth motion. The air bearing assisted in the production of low friction and reduced the wear on the mechanism. The carriage was constrained by the air bearings so that it could only move in the desired direction. Inside the carriage was a securely held stainless steel

lubricating bath, which contained the plate and the serum lubricant. The plate was firmly fastened inside the bath. The lubricant was maintained at a level, which kept the surface of the plate constantly covered and was topped up by a 0.1% (w/v) sodium azide solution made up in distilled water, which was added via a motorised syringe mechanism.

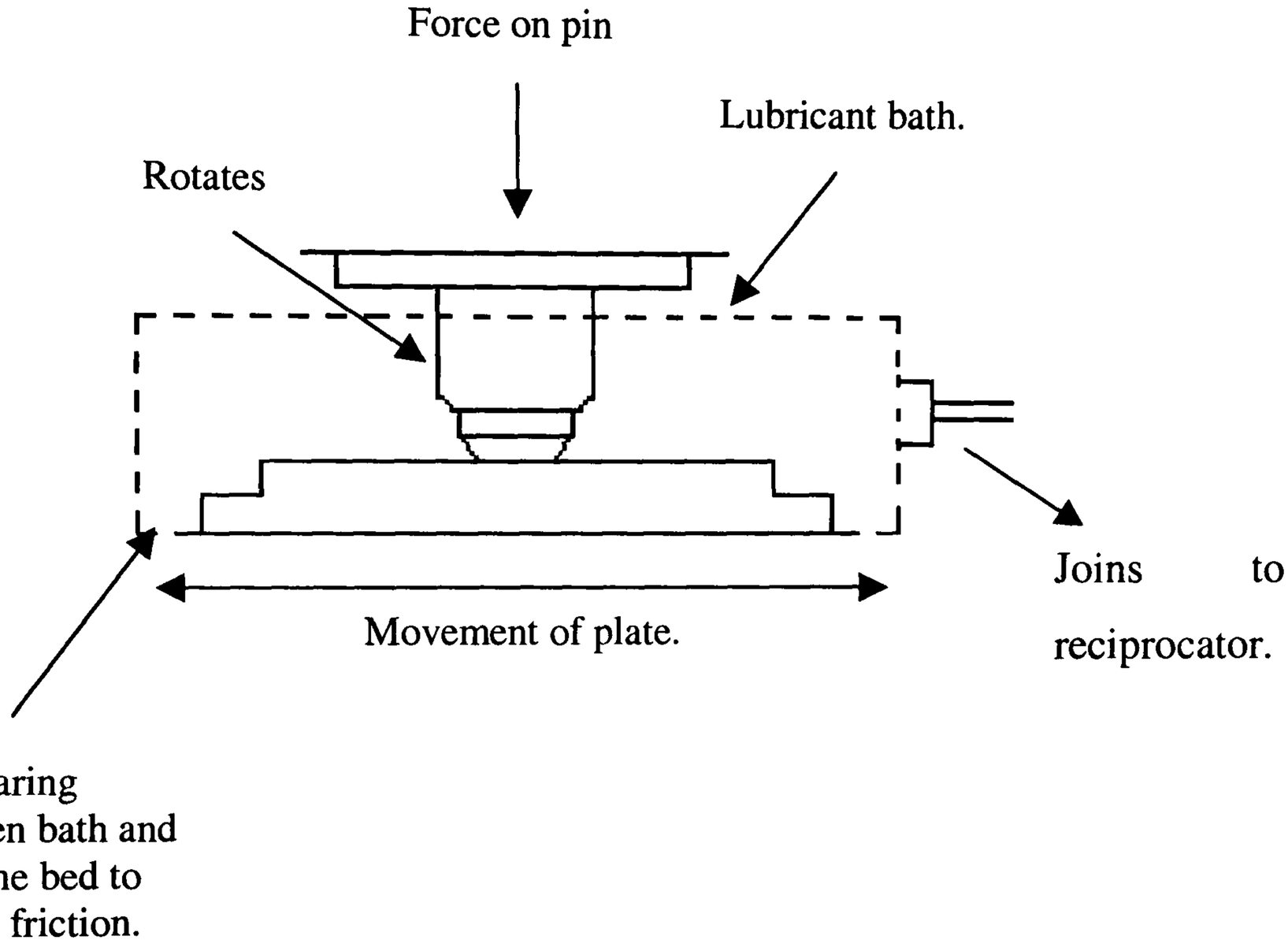

Figure 2.6 Schematic diagram of a station from the pin on plate rig.

The pin on plate machine loaded the pin under a constant force and the plate was reciprocated underneath. Rotation was achieved by a rack and pinion which was attached to the side of the bath and by a cogwheel which was placed on the pin holder. These are shown in Figure 2.7.

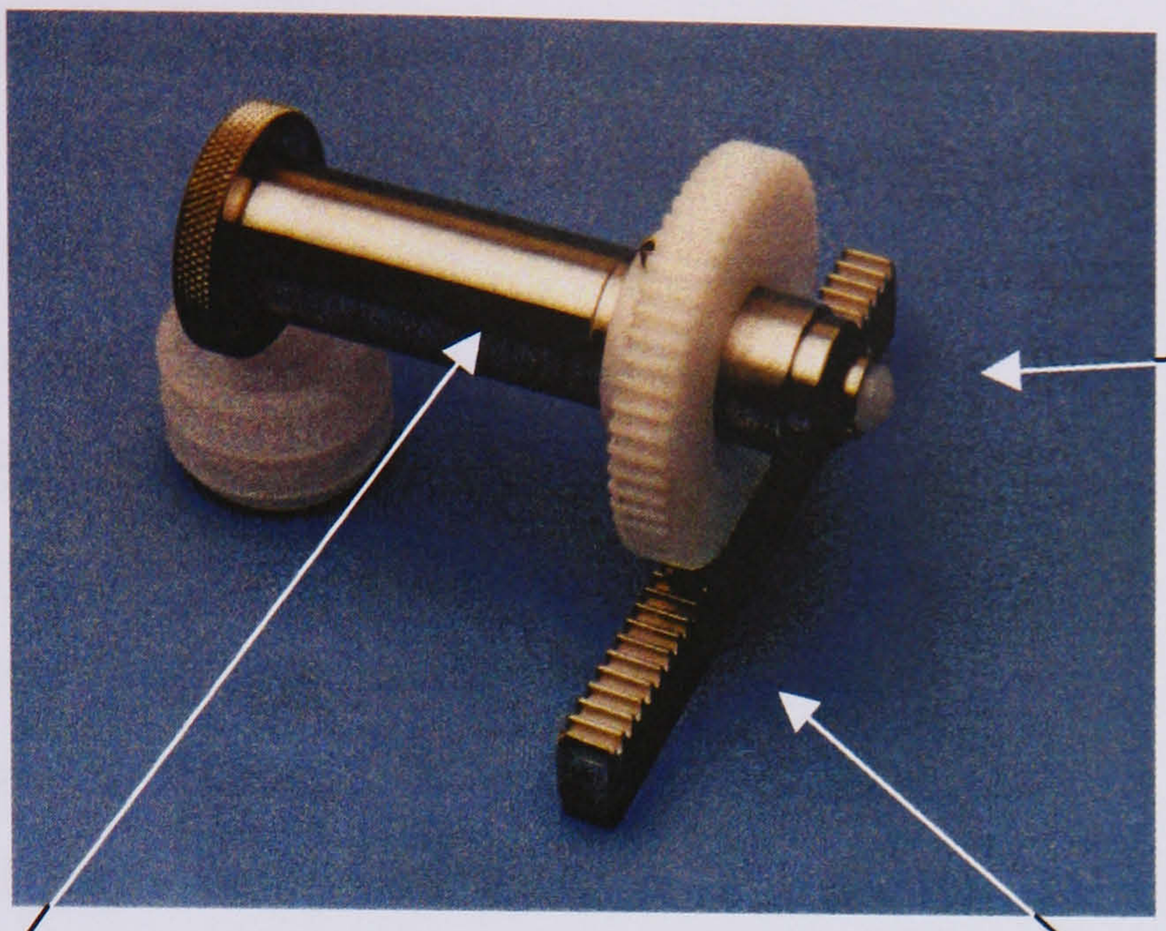

Figure 2.7 Picture of the cog wheel and rack and pinion.

The pin was placed in a pin holder and held in a bridge above the plate. The pin holder was allowed to move up and down so it remained in contact with the counterface surface no matter how much material had been lost from the pin surface. The pin holder was loaded via a cantilever mechanism, which allowed loads of between 80-240N to be applied.

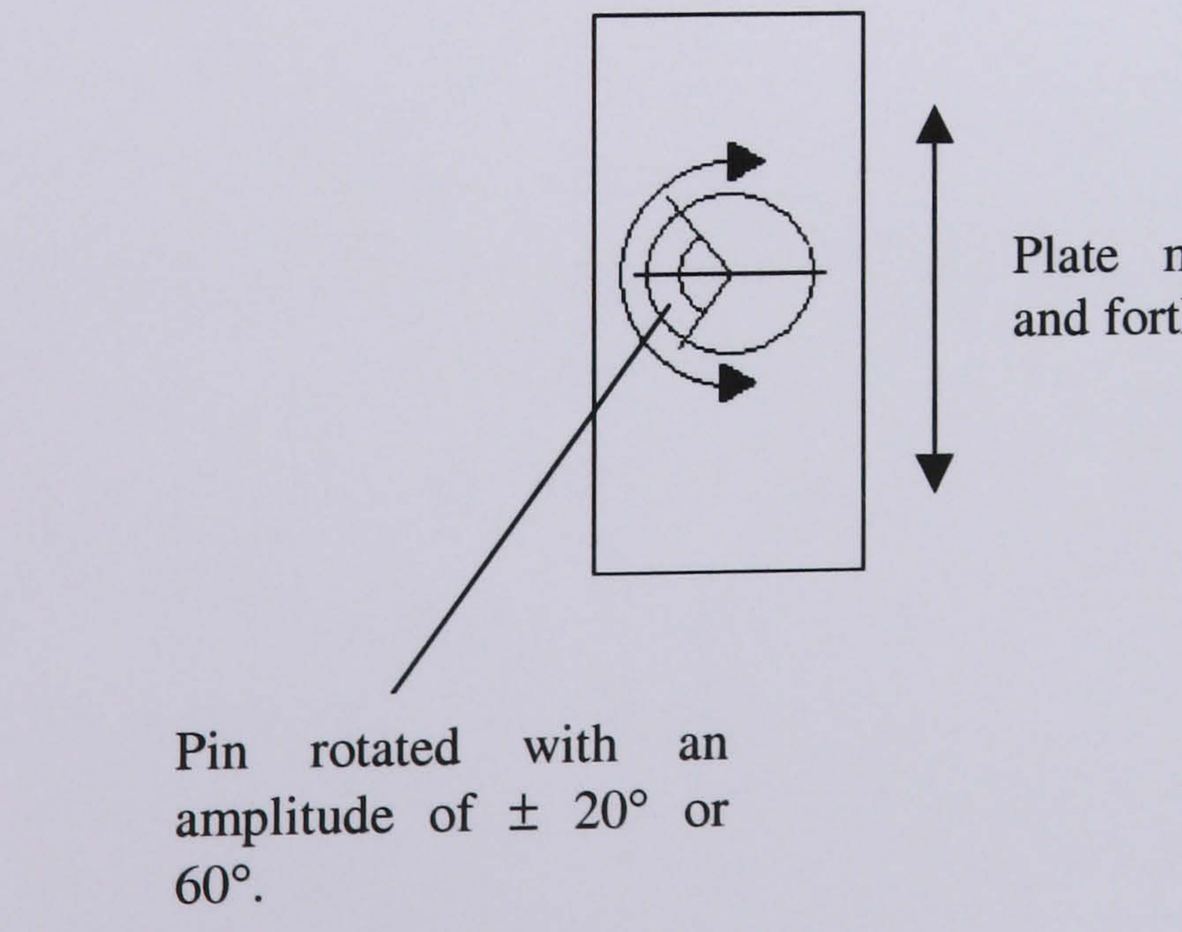

Figure 2.8 Plan view of multidirectional pin on plate test.

2.3.2. Variation in Frictional Force with Multidirectional Motion.

During the multidirectional tests the wear pin was constantly rotated. This resulted in a frictional force *F* that constantly changed direction as the pin rotated. This force had components that acted both in the original sliding direction and at 90° to the sliding direction. In the unidirectional tests the friction force was always in one direction. A pin wear face can be split into elements as shown in Figure 2.9 (a). As the pin rotated, the forces on the element resembled those in Figure 2.9 (b) and (c). The frictional force was assumed not to change significantly with respect to the plate, as this moved in a unidirectional motion, although it did change direction with respect to the pin, which rotated. If the frictional force *F*, is resolved along the fixed x and y axes of the element, and the variation in the components of the friction force against rotation is plotted, a sinusoidal relationship can be seen Figure 2.9. (d). This showed that there was a great deal of variation in the frictional force along the *x* and *y* axes of the pin (Marrs *et al.*, 1999).

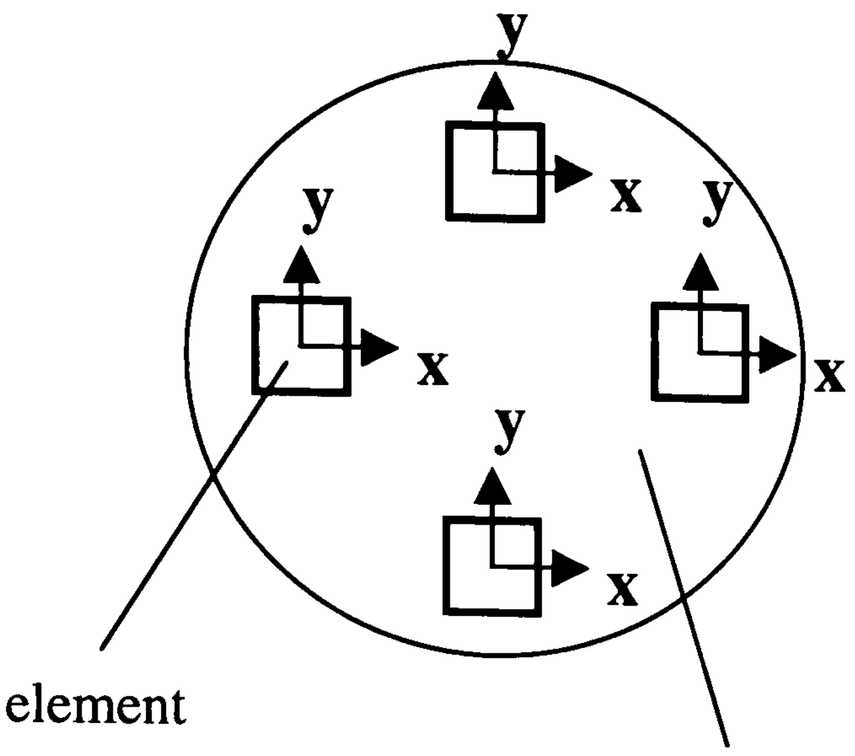

(a) Elements on wear surface of pin.

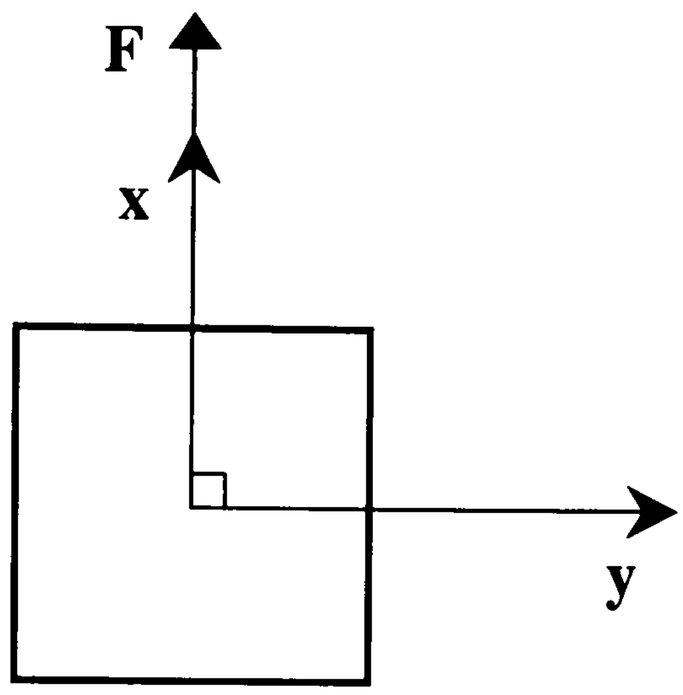

(b) Translational frictional force *F* along the principal axes *x* and *y* of an element on the pin wear surface for zero pin rotation *F* in the direction of sliding motion.

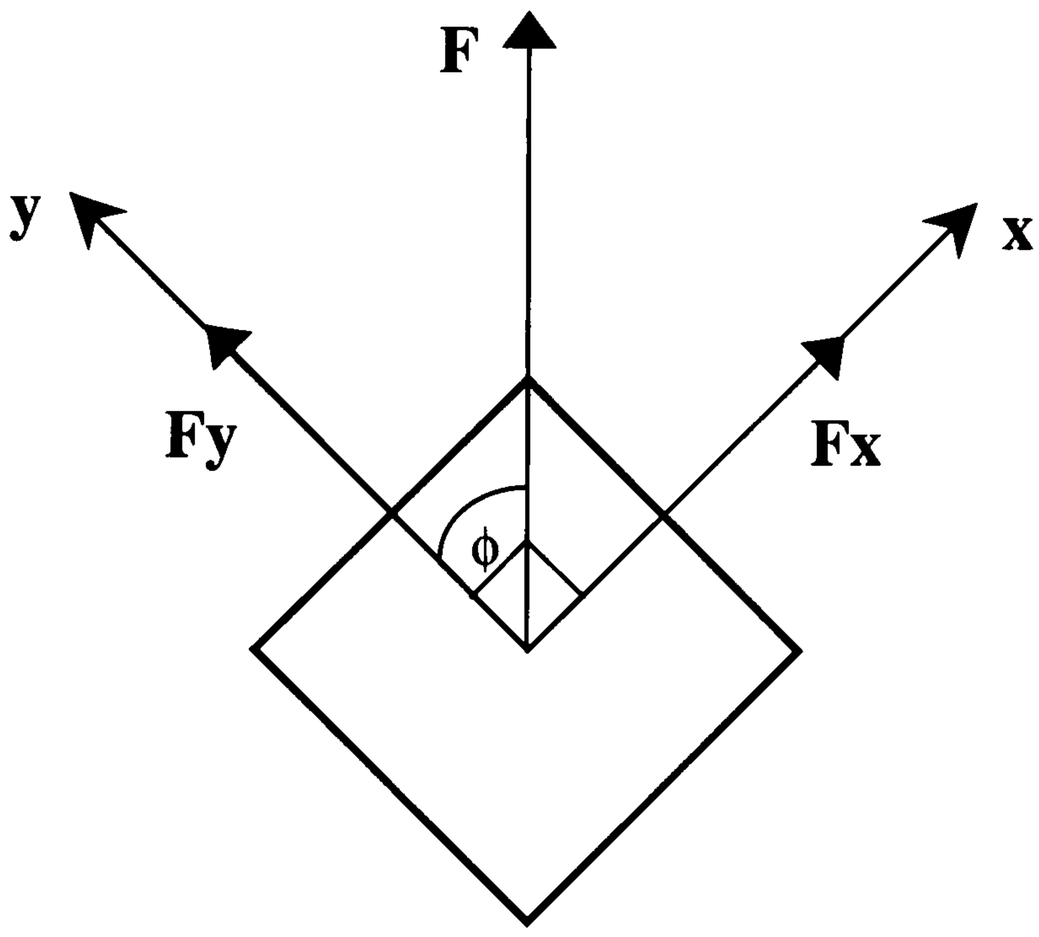

(c) Translational frictional force components *Fx, Fy* along the principal axes *x* and *y* after pin has rotated through an angle ϕ.

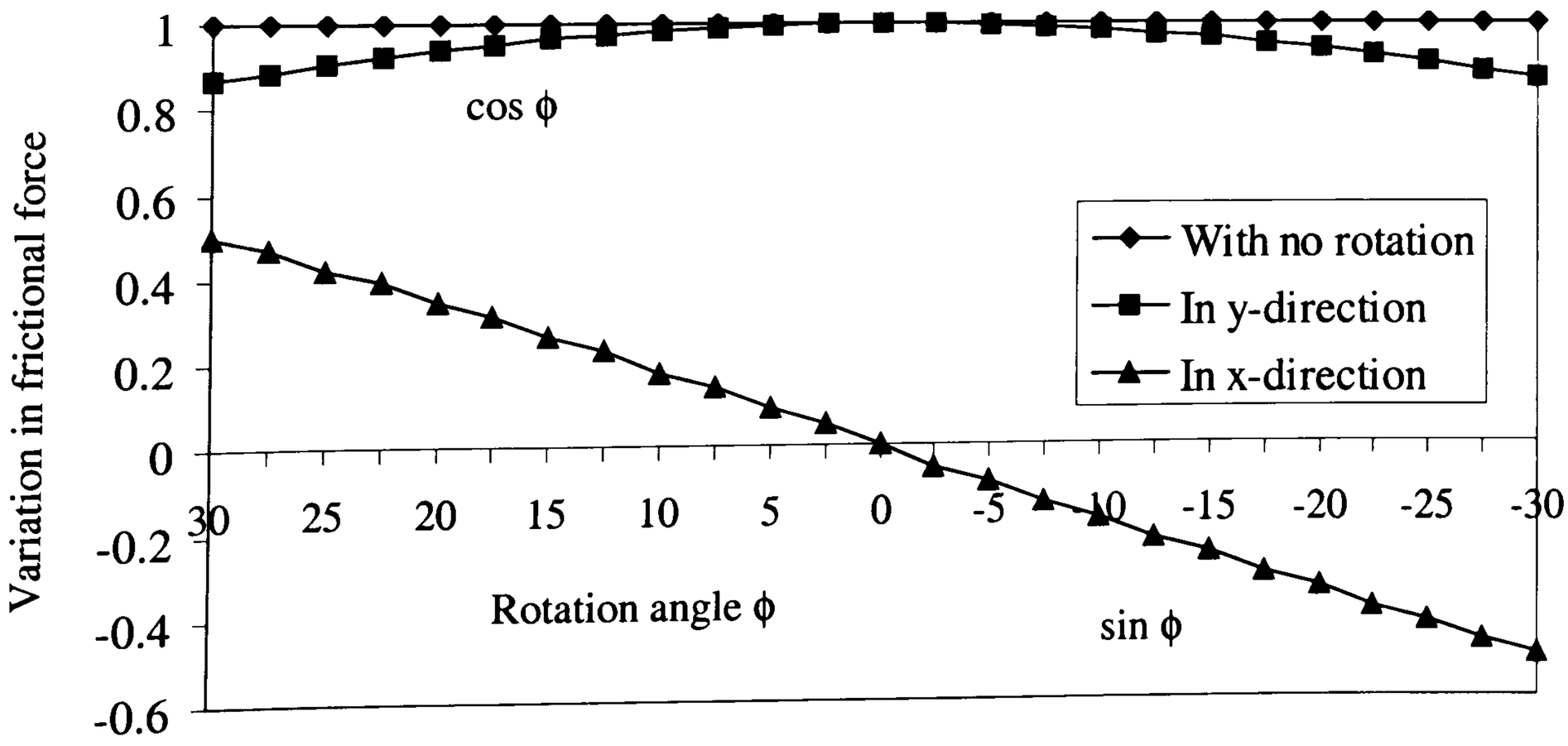

(d) Variation in the frictional force *Fx* and *Fy* along the principal axes (*x* and *y*) of an element on a pin wear face per half cycle.

Figure 2.9 Frictional force. Adapted from Marrs *et al.* (1999).

During rotation the amount of frictional energy changed with the change in frictional force. A diagram of the frictional energy is shown in Figure 2.10. The calculations for the frictional energy in the principal direction and transverse to this direction are also shown. When these values were known the cross shear energy could be calculated.

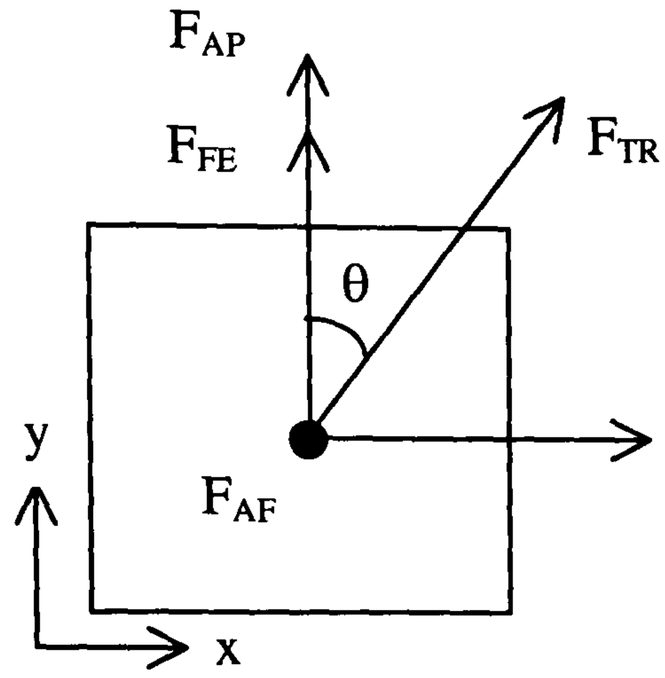

Figure 2.10 Frictional energy.

Consider FE as principal direction of motion and only incorporate rotation.

(a) Energy due to friction force in principal direction of motion (y axis):

$$\text{Energy}\ \tfrac{1}{2}\ \text{cycle}\ \alpha \int_{o}^{\theta} \cos\theta = [\sin\theta]_{o}^{\theta}$$

θ = rotational angle

α = proportional to

(b) Energy due to friction force transverse to principal direction of motion (x axis):

$$\text{Energy}\ \tfrac{1}{2}\ \text{cycle}\ \alpha \int_{o}^{\theta} \sin\theta = [-\cos\theta]_{o}^{\theta}$$

(c) Cross shear ratio:

$$\text{Cross shear} = \frac{[-\cos\theta]_{o}^{\theta}}{[\sin\theta]_{o}^{\theta}}$$

The cross shear energy for the 20° rotation was 0.087 and for the 60° rotation it was 0.268.

Studies undertaken clinically and using simulators have shown the different levels of cross shear frictional energy that can be observed. In a study by Barbour *et al.* (1999) they showed that the shape of the wear path can have a significant effect on the wear of acetabular cups. They tested this using a simulator and by changing the conditions part way through the test to give a different shaped wear path. This change resulted in different levels of cross shear frictional energy occurring. They showed that greater wear occurred when more cross shear frictional energy was present. A study by Bennett *et al.* (2002) looked at the different wear paths that are found clinically. They found a wide range in the shape and length of wear paths ranging from thin which would give a lower cross shear frictional energy, up to wide open paths which would have a high level of cross shear frictional energy. The thin paths resembled wear paths produced under more unidirectional motions whereas the open paths where more like multidirectional wear paths. These studies show the importance of cross shear frictional energy on the wear rates produced by UHMWPE and show that clinically a wide range of frictional energy can be found.

2.3.3. Lubricants.

Testing was carried out using a lubricant. In natural joints the lubricant is synovial fluid. Synovial fluid has similar constituents to blood plasma but does not contain clotting agents, has less proteins and higher levels of hyaluronic acid. Synovial fluid has two main functions. The first is to supply the cartilage with all the nutrients it needs to survive and the other is to lubricate the joint surfaces. After a joint has been replaced a form of pseudosynovial fluid is generated. This fluid no longer has to supply nutrients to the cartilage and typically contains lower levels of hyaluronic acid and so is less viscous than healthy synovial fluid. The regenerated synovial fluid is unable to provide full fluid lubrication, because of the increased surface roughness and stiffness of the polymer insert when compared to cartilage. The surface of the polymer can be up to ten times rougher than cartilage. Tests carried out *in vitro* using water as a lubricant all resulted in the formation of a polymer

transfer film onto the surface of the counterface. This was a result of the lack of proteins and produced false results as it protected the surfaces from wear (Cooper *et al.*, 1993). In order to reduce the possibility of transfer film a lubricant that contains proteins is necessary. As synovial fluid was hard to obtain in large enough quantities, bovine serum was used instead. Bovine serum was obtained from Seralab.

The levels of protein in the bovine serum lubricant have been shown to have a significant effect on the wear rates of UHMWPE. It has been shown that high levels of protein in serum can reduce the wear rates of UHMWPE (Wang *et al.*, 1999). To obtain clinically relevant wear rates the protein levels in the lubricant need to contain between 5mg/ml – 25mg/ml of proteins. Regular bovine serum contains a higher concentration of proteins so it needs to be diluted by at least 50% before use (Wang *et al.*, 1999). Bell *et al.* (2000) showed that bovine serum also produced clinically relevant wear debris particles.

Bovine serum was used as the lubricant with sodium azide added as an antimicrobial agent. Sodium azide reduces the microbial growth in the lubricant which helps to prevent large scale contamination and also prevents the micro-organisms becoming a health hazard.

2.3.4. Test Protocols.

In any one test, two pins of UHMWPE at each radiation level (0MRad, 5MRad, and 10MRad) were tested. Control pins were also used and were kept in lubricant for the duration of the test. They were left inside the test rig so that they were subjected to the same conditions of temperature as the test pins. Before testing the pins were cleaned as described before and then left for 48hrs in an atmosphere of controlled temperature and humidity to stabilise the polymer before weighing. The pins were weighed using a Sartorius 2405 balance which was sensitive to 1μg and accurate to ±2μg. Each pin was weighed until four measurements within a 10μg range had been obtained. During measuring, the zero was constantly checked and adjusted if it drifted.

At the end of each week the rig was taken apart and cleaned using a detergent and then iso-propanol to kill any microbial contamination from the lubricant. The lubricant was collected, frozen and stored in preparation for wear debris digestion.

The wear was determined by measuring the weight of each pin weekly during the test. The mean of the four measurements was calculated and subtracted from the previous results to determine the weight loss. The weight change of the control pins was calculated in the same way and the result was either added or subtracted from the test pins depending on whether they had lost or gained weight. The net weight changes of the test pins were then converted to a volume change using the density of the UHMWPE.

The mass loss was converted to volume loss using the density of the polymer. The wear factor k was obtained by combining the volume with the load and sliding distance to determine;-

$$k = \frac{V}{PX} \quad (2.1)$$

where:

k is the wear factor (mm^3/Nm)

V is the volume (mm^3)

P is the applied load (N)

and x is the sliding distance (m).

(Dowson *et al.*, 1987).

A six station test was replicated for each set of conditions giving four replicates or pins for each material.

2.4. Analysis of Pin Surface.

The surface of one pin from each experimental condition was analysed after testing had been completed. A visual examination of the pin surface was carried out and a 3D image of the surface was taken. The 3D image was obtained using a contact

profilometer (Form Talysurf, Rank Taylor Hobson, Leicester, UK). A typical image is shown in Figure 2.11. The pins were also examined under a scanning electron microscope. The pins were mounted onto stubs and coated with platinum. Images were then taken up to 50000x magnification.

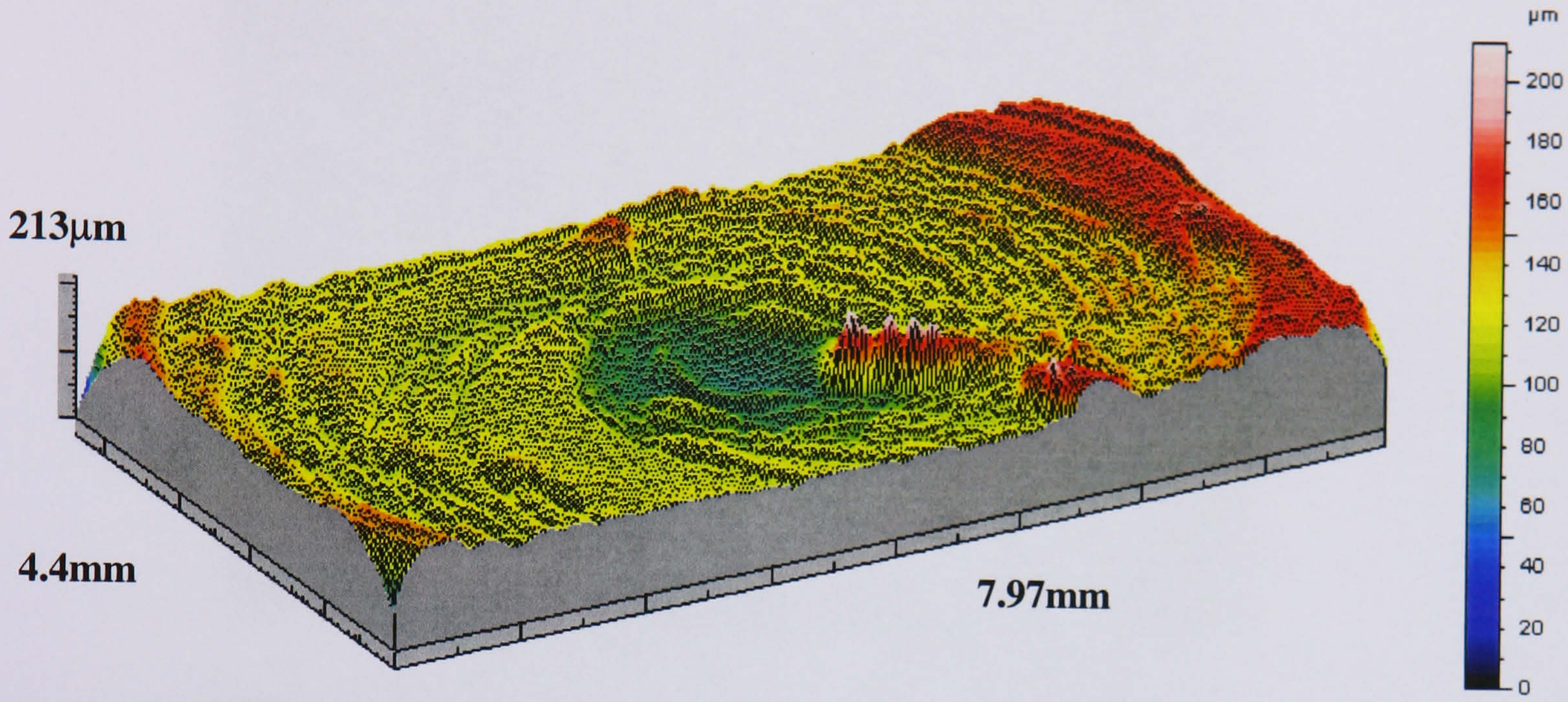

Figure 2.11 3D surface image of pin.

2.4.1. Scanning Electron Microscope.

Scanning electron microscopy (SEM) was carried out on a Leo 1500 series field emission gun scanning electron microscope (FEGSEM). The field emission gun consists of an extremely sharp tungsten-zirconium tip cathode which is biased up to a large negative voltage with respect to two anodes. The tip is so sharp that the field is enhanced causing field emission of electrons. The electrons are then controlled by anodes. The vacuum in the gun needs to be very good to prevent the tip from degrading due to oxidation. Once the electrons are formed they then pass through a condenser lens. This controls the amount of current in the beam and eliminates any high angle electrons from the beam. A second condenser forms the electrons into a tight coherent beam. A set of coils scans the beam in a grid fashion across the surface according to the scan speed. The final lens focuses the scanning beam onto the part required. The image is made by collecting secondary, backscattered and auger electrons that are released from the sample. The secondary electrons are detected by a scintillation material that produces flashes of light from the electrons.

These light flashes are detected and multiplied by a photomultiplier tube. For this study low voltages between 1-3KV at high resolutions were used. A typical SEM micrograph is shown in figure 2.12.

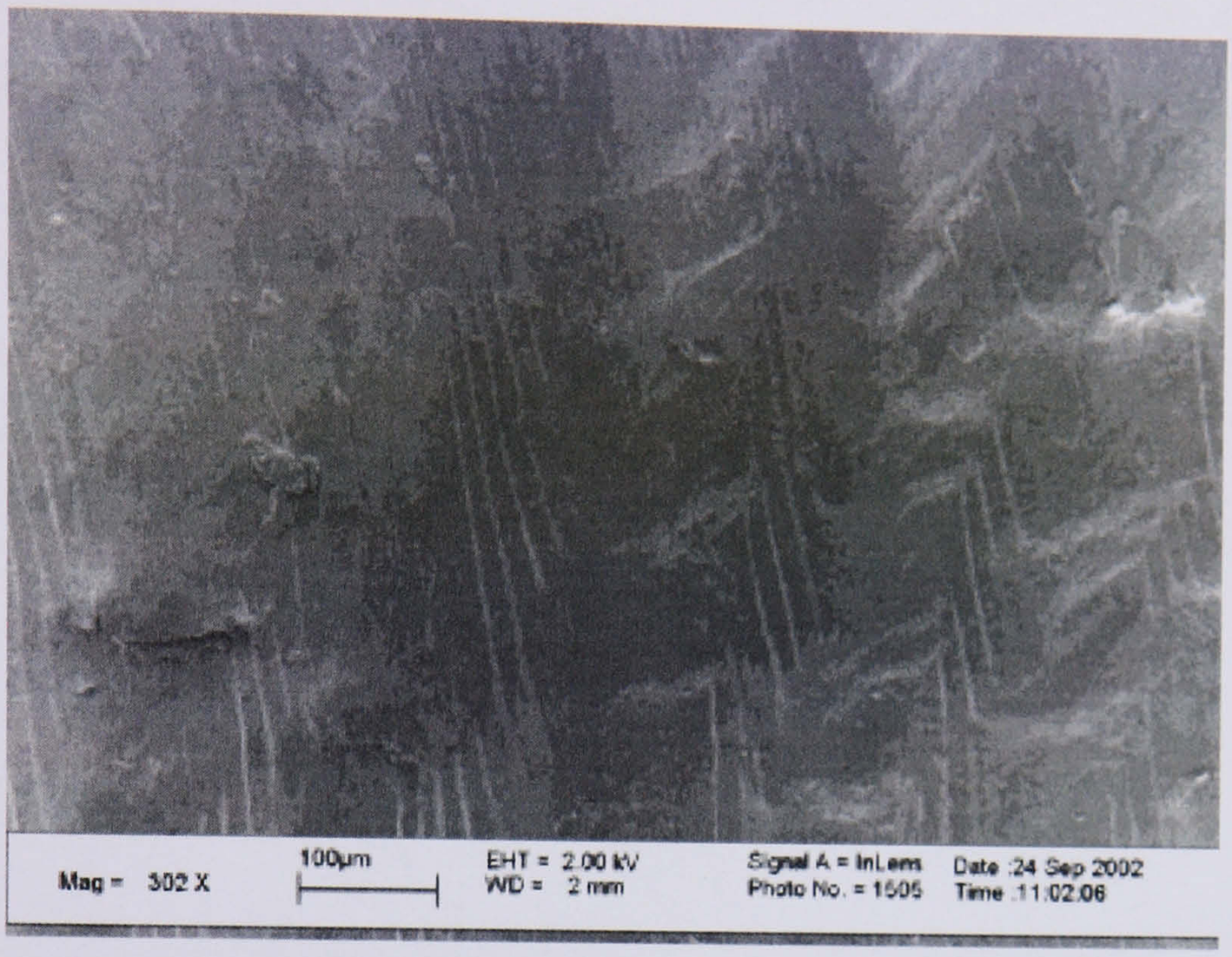

Figure 2.12 SEM image of the surface of a pin.

2.5. Experimental Procedure for Wear Debris Isolation.

The wear particles were isolated from the lubricant using a multistage digestion procedure described by Tipper *et al*. (2000). Approximately 80ml of lubricant was allowed to thaw and placed into clean glass Universal containers. Each Universal contained 10ml of serum. Three grams of potassium hydroxide were added to give a 5M solution. The Universals were left in a water bath at 60°C for 48 hours, until the proteins in the lubricant were digested. They were then cooled to 4°C in a freezer for a minimum of 30 minutes and chloroform/methanol in a 2:1 ratio was added. This was incubated for 24 hours at room temperature in a fume cupboard. After this, the samples were centrifuged for 10 minutes at 2000rpm to remove residual proteins and lipids from the sample. The top layer, the supernatant, was carefully removed and put into a clean glass Universal and chloroform/methanol was again added. This procedure was repeated three more times. Absolute ethanol was placed at -20°C until ice cold. The supernatant was then added to double the volume of ethanol. Ultrapure water was added until the solution became clear and a stirrer bar was

placed in the solution. The solutions were put onto a stirrer platform at 4°C for approximately 24 hours to precipitate any remaining proteins. The supernatant was decanted into plastic Universals and centrifuged for 2 hours at 3000rpm. This was later altered after filters were found to be contaminated and the supernatant was centrifuged at 10,000rpm for 30 minutes. The supernatant was decanted into a bottle and 400ml of ultrapure water was added to every 100ml of solution. The solution was then filtered through a 1μm and then a 0.1μm filter. The filters were left under an infrared lamp for at least 4 hours to thoroughly dry. Three small random sections from each filter paper were taken from halfway between the centre and the edge of the filter paper, and placed onto a stub and then platinum coated for SEM analysis.

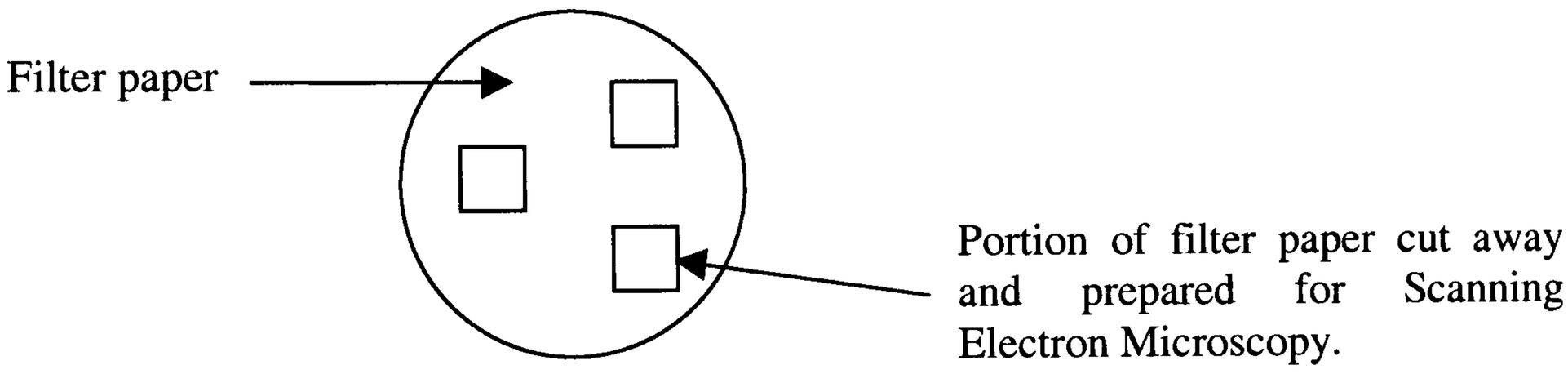

Figure 2.13 Section which is cut from filter paper and prepared from SEM.

The microscope used was described previously for the pin surface analysis. The images obtained from the SEM were stored on a computer for analysis. The micrograph images were analysed using an images analysis package, Image Pro Plus (Media Cybernetics. Version 3. 1993-97).

The area of the micrograph being analysed was obtained and the particles inside the area were drawn around and the following measurements were obtained:

- The 2-dimensional surface area *A*,
- Maximum diameter d_{max},
- Minimum diameter d_{min},
- Perimeter *p*,
- Length FL and
- Width FW.

A spreadsheet was produced in Microsoft Excel to process the raw data. The aspect ratios, roundness, elongation, equivalent circle diameters, and form factors of the particles were calculated according to the ASTM F1877 standards.

- Aspect ratio = d_{max} / d_{min}
- Roundness = $(4A)/(\pi d_{max}^2)$
- Elongation = FL/FW
- Equivalent circle diameter = $(4*A/\pi)^{1/2}$
- Form Factor = $4\pi A/p^2$

The aspect ratio is a measure of shape. The roundness tells how closely a particles resembles a circle. A perfect circle has a value of one. The elongation is similar to aspect ratio but is used more for longer particles in which the major axis line does not stay inside the particle. The equivalent circle diameter is a measure of size and the form factor is another measurement of how close to a circle the particle is. The form factor is more sensitive to variations in the roughness of a particle.

The results were then sorted into size ranges. The size ranges used were 0.01-0.1μm, 0.1-1.0μm, 1.0-10.0μm and >10μm. This allowed the percentage number of particles per size range to be calculated and also the percentage area of particles in each size range. This was carried out using the following calculations:

The number of particles per unit area of the filter (concentration of particles) $n_{r,i}$, in each size range '*r*', was calculated for each of the SEM images i,

$$\text{where } n_{r,i} = \frac{n_r}{Q_i} \qquad (2.2)$$

Q_i = area of micrograph.

n_r = number of particles per unit area in size range *r*

The mean number of particles in a size range '*r*', $\overline{n}_r$ was then calculated by summing the number of particles in that size range '*r*' and dividing it by the number of SEM's 'i'.

$$\overline{n}_r = \frac{\sum_{j=1}^{i} n_{r,i}}{i} \quad (2.3)$$

The total number of particles in each size range '*r*' N_r on each pore size filter was estimated by calculating the mean no of particles per unit area in the size range 'r' $\overline{n}_r$ and multiplying by the surface area of each pore size filter membrane A_s.

$$N_r = \overline{n}_r \, x \, A_s \quad (2.4)$$

The percentage area with respect to size range 'r' was then calculated.

The mean 2-dimensional surface area $\overline{a}_r$, of particles in each size range '*r*' was calculated.

The total 2-dimensional surface area A_r of particles in each size range was estimated as follows

$$A_r = \overline{a_r} \, x \, N_r \quad (2.5)$$

The estimated total area of particles A was calculated summing all the mean areas of wear particles of each size range. The percentage area was plotted with respect to particle size range.

2.6 Statistical Analysis.

For the experiments in Chapters 3 and 4 the mean and standard deviation were calculated for each material under each condition. Once these had been obtained the 95% confidence limits were calculated and the results analysed using ANOVA's.

The results of the ANOVA's were examined for any statistically significant differences. This was done by calculating the minimum significant difference (MSD) using the T method and comparing the value obtained to the averages in the ANOVA table. If the difference in averages was greater than the MSD they were judged to be statistically significantly different.

For the results in Chapter 5 the data had to be transformed before any analysis could be done as the results were percentages. Once the data was transformed, means, standard deviations and then 95% confidence limits were calculated. One way ANOVA was also carried out on the transformed data. Statistical significance was judged using the MSD method. The data was back transformed into percentages for the graphs.

Chapter 3.

3. Pin on Plate Wear Studies with 60° Rotation under Three Different Counterface Conditions for Three Different Levels of Crosslinking.

3.1. Introduction.

UHMWPE wear particles are considered a major factor in osteolysis and loosening of implants. Crosslinked UHMWPE has been shown to produce lower wear rates compared to non-crosslinked polyethylene in various studies (Endo *et al.*, 2000; Marrs *et al.*, 1999). In this study two different levels of crosslinked material and one non-crosslinked material were compared in order to determine if crosslinking affected the wear rate. The experiments were completed on a pin on plate rig. Pin on plate rigs provide a simple method to investigate the wear properties of materials. They are usually used as the initial test to determine how a material performs and are generally viewed as exclusion tests. If a material gives high wear rates in a pin on plate test it can usually be disregarded for further testing. However a low wear rate does not necessarily mean that the material will perform well in a replacement joint situation, but it could mean that further investigation, such as a simulator study may be useful.

In this study, a pin on plate rig was used to compare the wear rates of an UHMWPE which had been irradiated at three different radiation levels. High multidirectionality was used so that the kinematics in the rig were comparable to those seen in a hip joint. Multidirectional tests have been shown to be important in reproducing conditions, that are similar to those seen in the body. Unidirectional wear tests give much lower wear rates than would be seen *in vivo* due to the orientational hardening of the UHMWPE.

Crosslinking has been introduced to reduce the wear of UHMWPE in artificial joints. McKellop *et al.* (1999) have shown 5MRad crosslinked UHMWPE to reduce

wear by 83% in their hip joint simulator. Muratoglu *et al.* (2000) showed an 85% reduction in wear with 10MRad material. These studies both used high concentrations (90 – 100%) of serum proteins in the lubricant. When lower serum concentrations (25%) were used in a study by Endo *et al.* (2000), smaller reductions in wear with crosslinking were seen. Additionally Endo *et al.* (2000) also used damaged counterfaces and found smaller reductions in wear rates with crosslinking. Although there is a general consensus that crosslinking reduces wear, there remains considerable variation in the percentage reduction in wear reported by different centres, partly due to different levels of crosslinking. As many factors such as protein concentration, and counterface roughness can control the wear mechanisms of polyethylene, it is thought they may also play an important role in the reduction of wear, induced by crosslinking of polyethylene. The aim of this study was to compare the effect of changes in serum concentration, and counterface condition for three different levels of crosslinking.

3.2. Materials and Methods.

3.2.1. Materials.

The material studied was UHMWPE GUR 1050, which had been irradiated at three different levels as described in Chapter 2. The three materials were non-crosslinked – 0MRad, medium crosslinked – 5MRad and highly crosslinked – 10MRad. The pins were machined to have a wear surface with a diameter of 8mm and were soaked in de-ionised water for at least four weeks before testing. The counterface surface was high nitrogen stainless steel. Three counterfaces were used during testing. These were a smooth surface, and two scratched surfaces. The height and FWHM were compared with scratches seen on explants by Barbour *et al.* (1999).

3.2.2. Method for Pin on Plate Tests.

The experiments were all carried out on a multidirectional pin on plate machine which has previously been described in Chapter 2. For the first test the effects of serum concentration on the wear rates of the UHMWPE were investigated. This was

carried out using 25% (v/v) and 95% (v/v) serum concentrations. The serum was diluted using a 0.1% (w/v) solution of sodium azide. During testing two pins of each radiation level were run in 25% (v/v) serum, for three weeks, against smooth counterfaces and then wear tests were repeated for a further three weeks with different pins. Four pins of each material were tested in total. The experiment was then carried out in 95% (v/v) serum for two weeks.

The second test investigated the effect that the counterface roughness had on the wear rates. Scratches were achieved as described in Chapter 2. For the tests, two different scratch heights were used. These were a medium scratch with an average Rp of 0.8μm and a high scratch with an average Rp of 1.8μm. Different loads were used to obtain the two scratch heights. The smooth plates had an average Ra of 0.01. The average surface roughness and peak height of the scratches on the plates before testing are shown in Table 3.1.

Plate surface	**Plate number.**					
	1	**2**	**3**	**4**	**5**	**6**
Average surface roughness Ra of smooth plates (μm)	0.01	0.01	0.01	0.01	0.01	0.01
Average peak height of medium scratches (μm)	0.46	0.82	0.69	0.94	1.02	0.72
Average peak height of high scratches. (μm)	1.93	1.68	1.95	1.57	1.91	1.76

Table 3.1 Average surface roughness and scratch height before testing.

Two pins of each radiation level were run on medium scratches for three weeks and then wear tests were repeated for a further three weeks with new pins. The whole method was then repeated with different pins against the higher scratches. During testing the pins were rotated across the plates to reduce the plate variability from affecting the overall wear factors. For these experiments a 25% (v/v) serum concentration was used. The serum was diluted using 0.1% (w/v) sodium azide. For all the tests a stroke length of 28mm and a load of 160N was applied. Control pins

from each radiation level were placed in the same lubricant as the wear pins in order to monitor moisture uptake during the test. The weight of the control pins was subtracted or added depending on absorption or loss. Wear factors were calculated and data analysed using one way ANOVA followed by calculation of the minimum significant difference using the T-method.

The results already obtained in the previous experiments with 25% (v/v) serum concentrations on smooth plates were then compared with the results from six weeks on high scratched plates and six weeks on medium scratched plates. A summary of the test conditions are shown Table 3.2.

	SERUM CONCENTRATION		**COUNTERFACE ROUGHNESS**		
	25%	**95%**	**Smooth Ra~0.007μm**	**Medium Rp~0.8μm**	**High Rp~1.8μm**
First study	✔	✔	■		
Second study	■		✔	✔	✔
✔ = variable ■ = constant					

Table 3.2 Summary of test conditions.

At the end of each test the serum was collected and frozen for subsequent digestion and isolation of the wear particles.

3.3. Results.

The results of the peak height, and FWHM of the scratches on the counterface were compared to scratches seen on explants by Barbour *et al.* (1999). The results are shown in Figure 3.1. They showed that the peak height and FWHM of the scratches were comparable to those seen on explants. The high scratches resembled the severe scratches seen on explants while the medium scratches were similar to the moderate scratches observed *ex-vivo*.

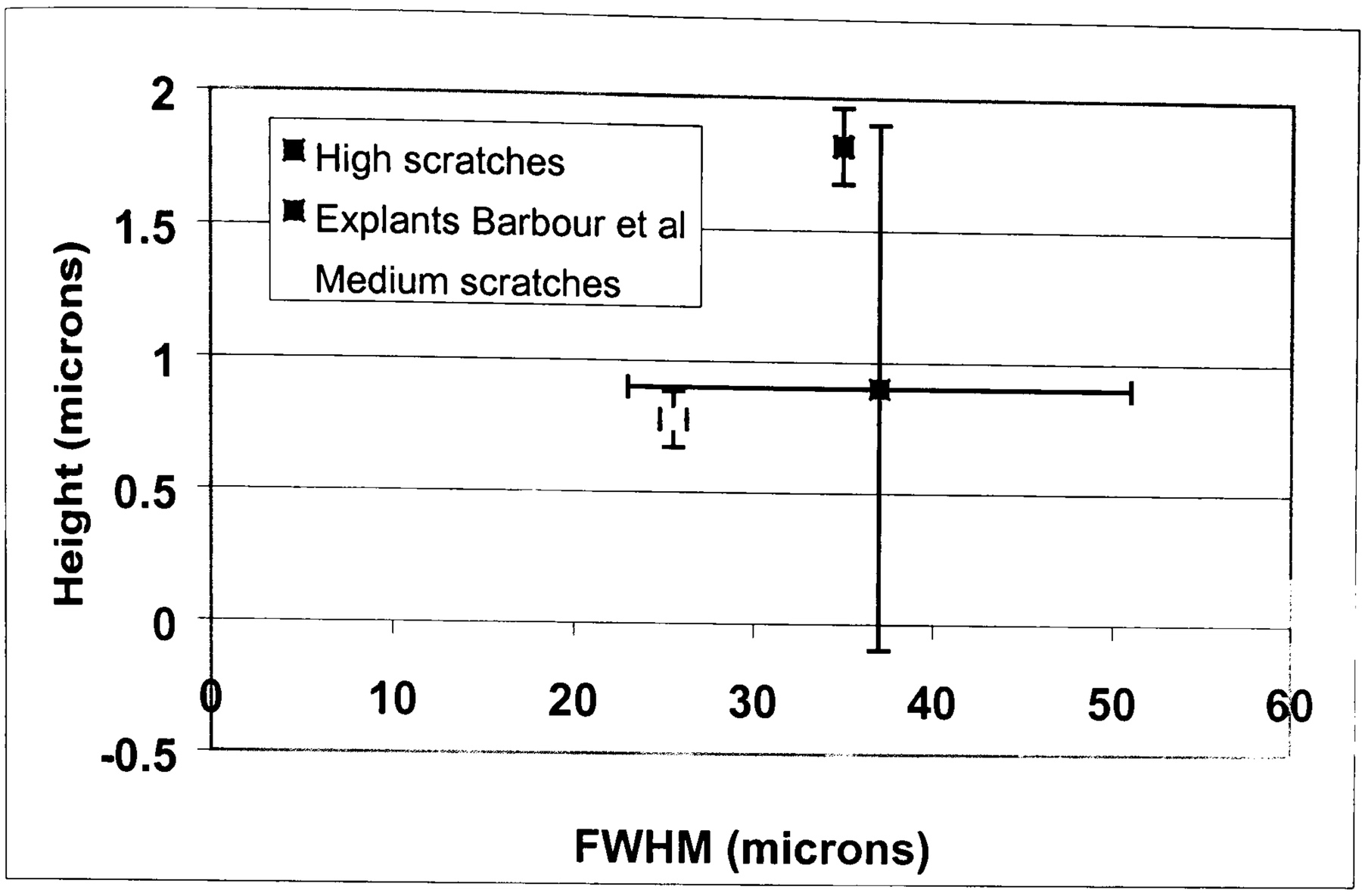

Figure 3.1 Comparison of FWHM against peak height for high and medium scratches with explants.

The average surface roughness and peak height after testing was completed are shown in Table 3.3. In all tests the plates had no significant change in there surface roughness and a smaller peak height after testing.

Plate surface	**Plate number**					
	1	**2**	**3**	**4**	**5**	**6**
Average surface roughness Ra of smooth plates (μm)	0.01	0.01	0.01	0.01	0.01	0.01
Average peak height of medium scratches (μm)	0.42	0.70	0.61	0.86	0.73	0.7
Average peak height of high scratches. (μm)	1.46	1.23	1.32	1.51	1.67	1.66

Table 3.3 Average surface roughness and scratch height after testing.

3.3.1. Effect of Serum Concentration on the Wear of UHMWPE in Pin on Plate Tests against a smooth counterface.

The wear rates of the three different polyethylenes tested at two different serum concentrations are shown in Table 3.4 and Figure 3.2. With both serum concentrations there was a reduction in wear as crosslinking levels increased. For 95% (v/v) serum concentrations there was a 94% reduction in wear rate between 0MRad and 10MRad UHMWPE. For the 25% (v/v) serum concentrations the reduction was 73%. For the 5MRad and 10MRad UHMWPE there was no statistically significant difference in the wear rates between the two serum concentrations. The difference in wear rates for 0MRad UHMWPE at the two serum concentrations was statistically significantly different ($p<0.05$). These results showed that the serum concentration had a major effect when comparing wear rates.

Radiation level.	**Wear factor (mean ± 95% Confidence intervals ($x10^{-7}$ mm^3/Nm))**	
	25% serum concentration.	**95% serum concentration.**
0 MRad	2.16±0.43	5.13±1.07
5 MRad	1.8±0.3	1.87±0.49
10 MRad	0.58±0.21	0.3±0.75

Table 3.4 Average wear factors with different serum concentrations ±95% confidence limits.

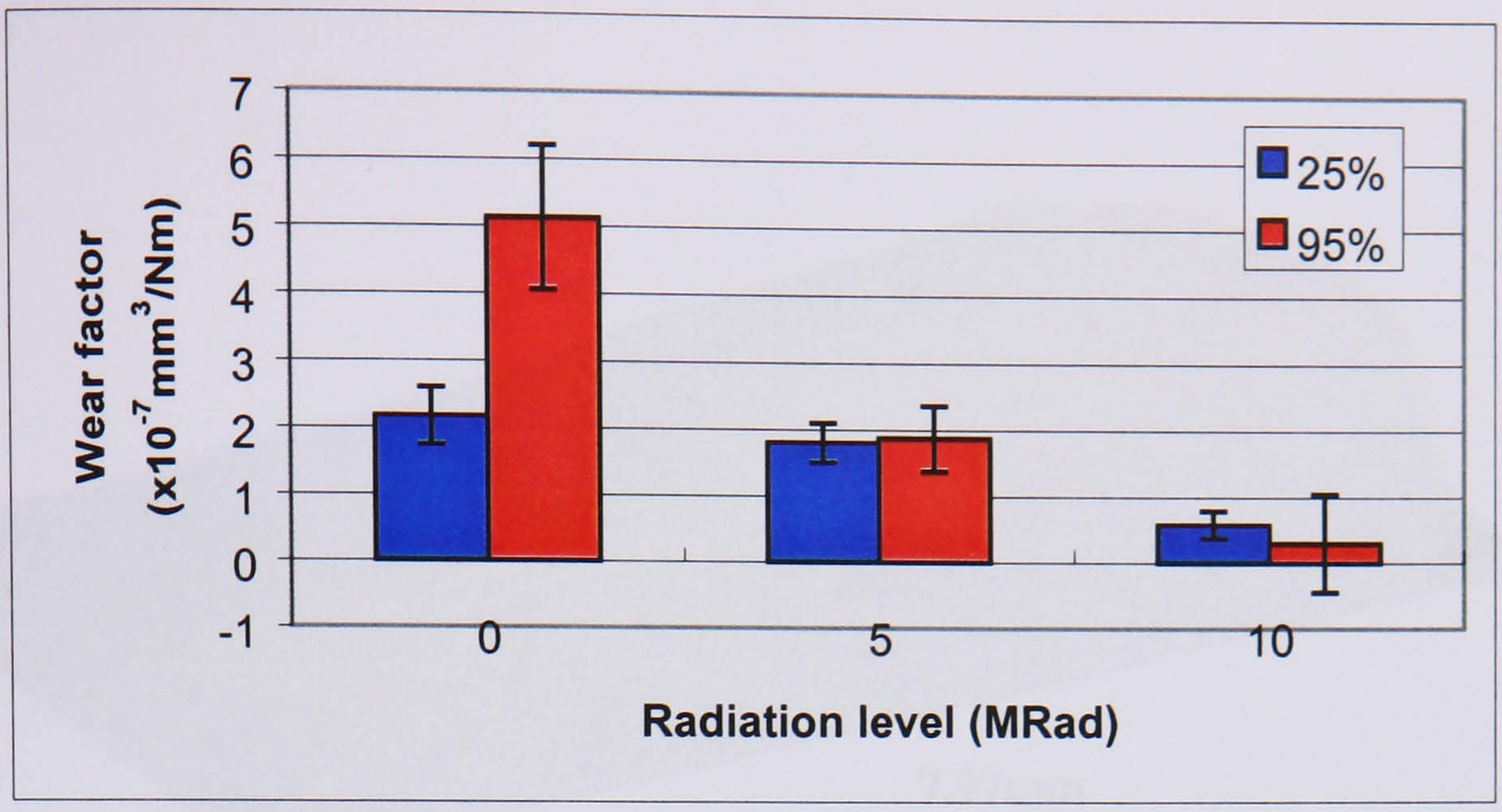

Figure 3.2 Average wear factors from serum concentration experiments ± 95% confidence limits.

3D talysurf images of the pins were obtained after wear testing. A 5MRad UHMWPE pin which had been tested in 25% (v/v) serum is shown in Figure 3.3. This image and all other images were taken from the centre of the pin. On the surface of this pin several raised areas were observed. The pin also sloped across its surface.

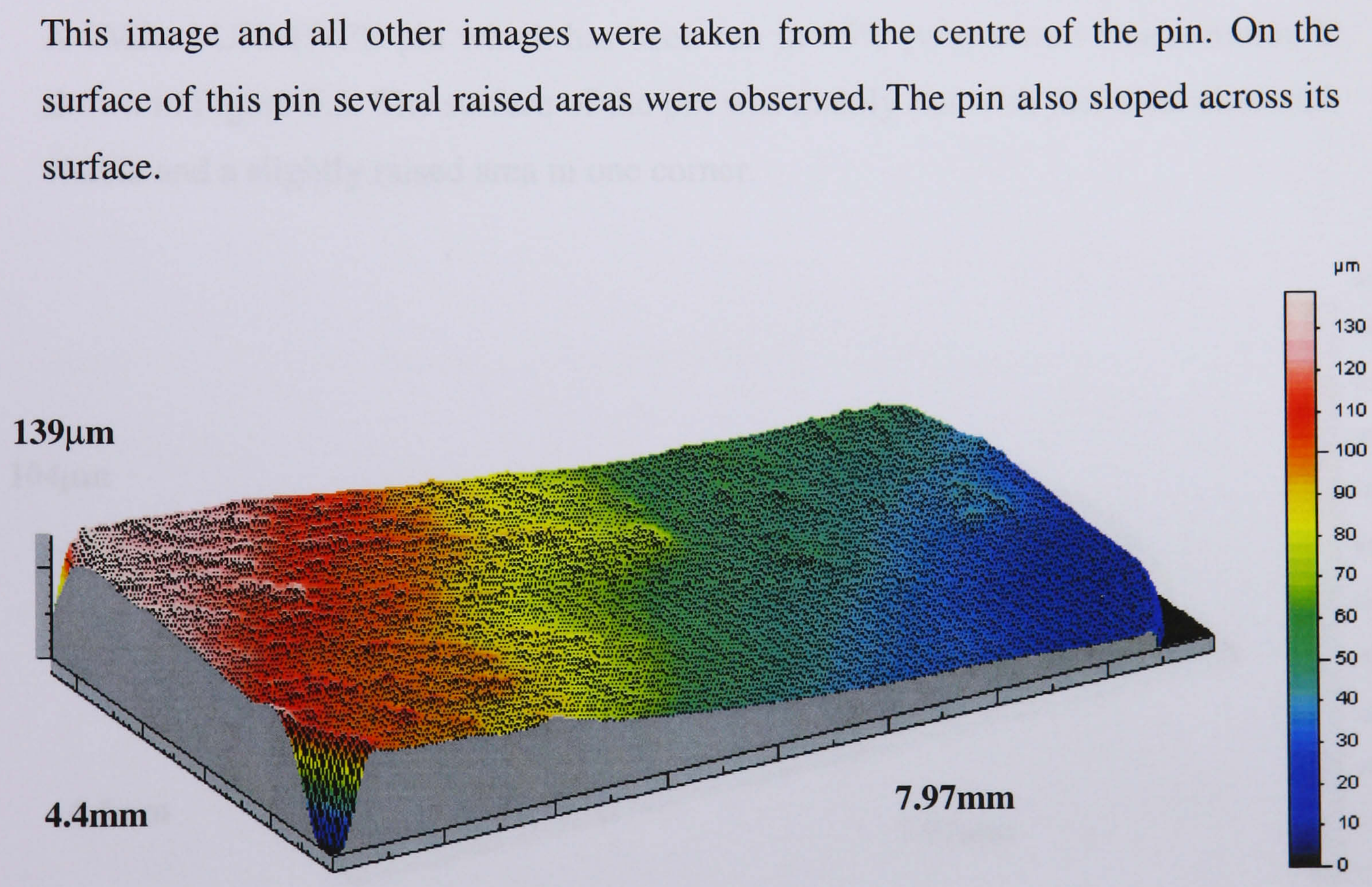

Figure 3.3 3D talysurf image of a 5MRad UHMWPE pin run in 25% (v/v) serum concentration.

A 10MRad UHMWPE pin surface which had also been run in a 25% (v/v) serum concentration is shown in Figure 3.4. This pin did not have any raised areas on the surface but again it had a slope across the surface of the pin.

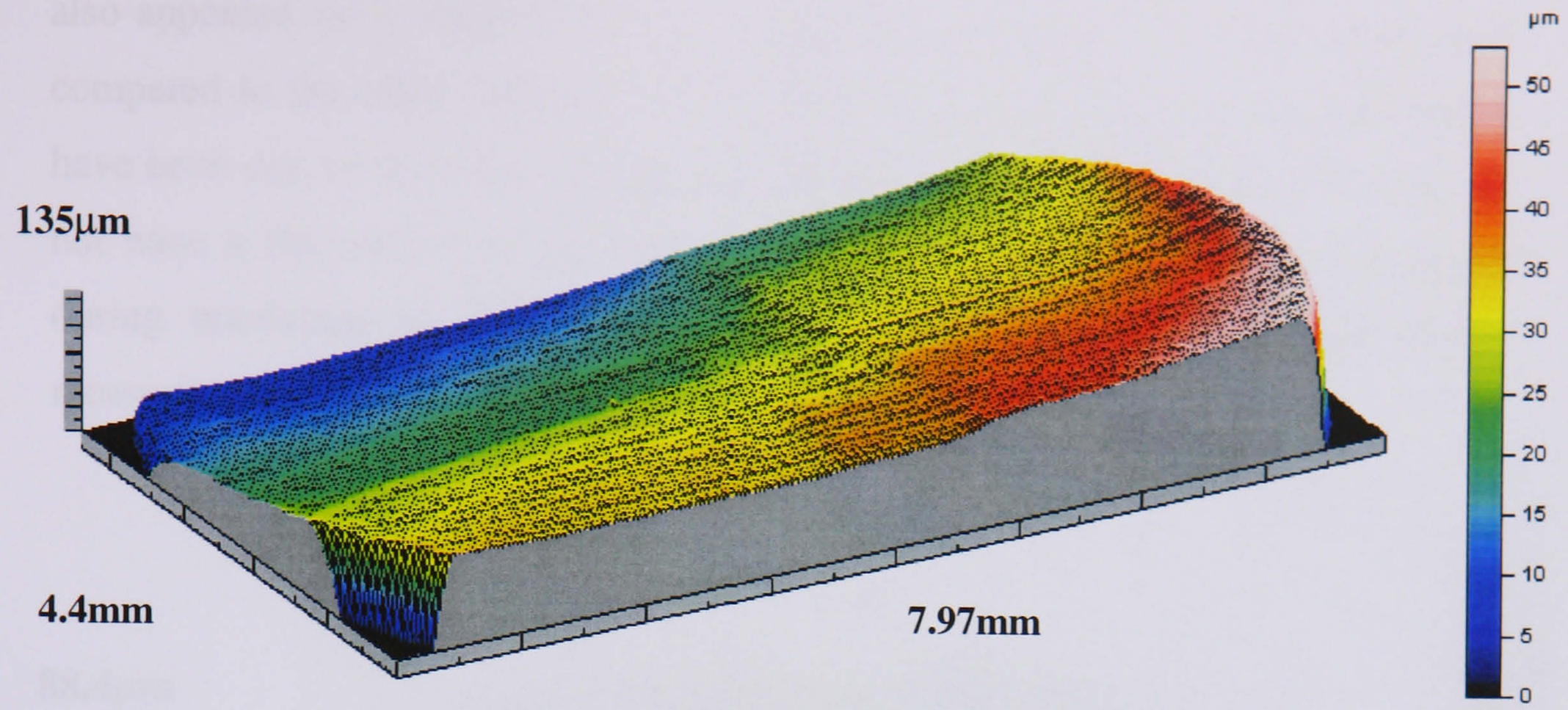

Figure 3.4 3D talysurf image of a 10MRad UHMWPE pin run in 25% (v/v) serum concentration.

A 0MRad UHMWPE pin which has been run in 95% (v/v) serum concentration is shown in Figure 3.5. The surface of the pin was mainly flat with just a small scratch visible and a slightly raised area in one corner.

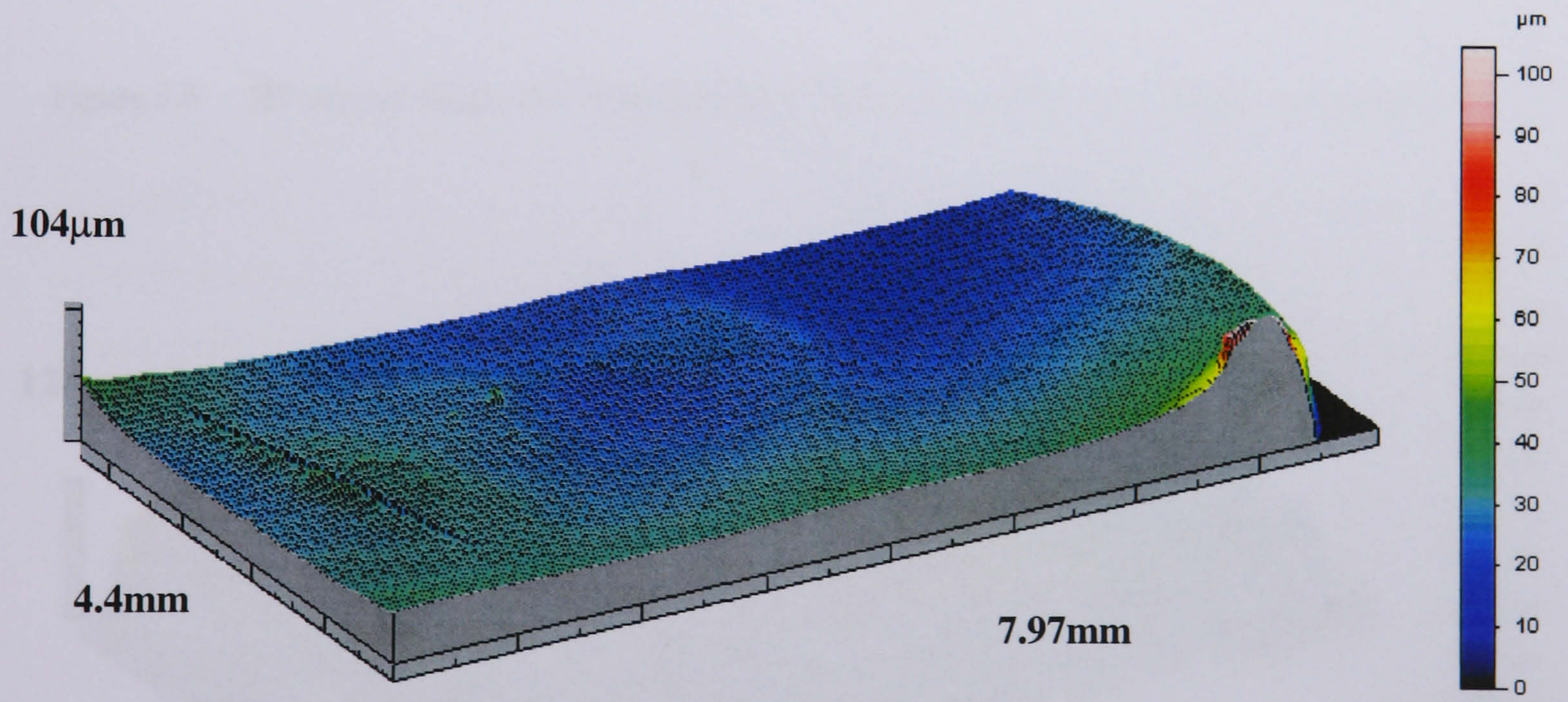

Figure 3.5 3D talysurf image of a 0MRad UHMWPE pin run in 95% (v/v) serum concentration.

A 3D talysurf image of a 5MRad UHMWPE pin which was also tested in 95% (v/v) serum is shown in Figure 3.6. The surface of this pin appeared to be less flat although the overall difference in heights across the surface was smaller than seen in the previous pins. There were no signs of scratches or other obvious damage. A 10MRad UHMWPE pin from the same conditions is shown in Figure 3.7. This pin

also appeared fairly smooth with no obvious damage but had a bigger slope on it compared to the other two pins. The slopes across the surfaces of the pins could have been due to them not wearing flat. This could have been because the pins did not have a flat surface at the start of the wear tests, which could have occurred during machining or microtoming. It could also have just been part of the measurement.

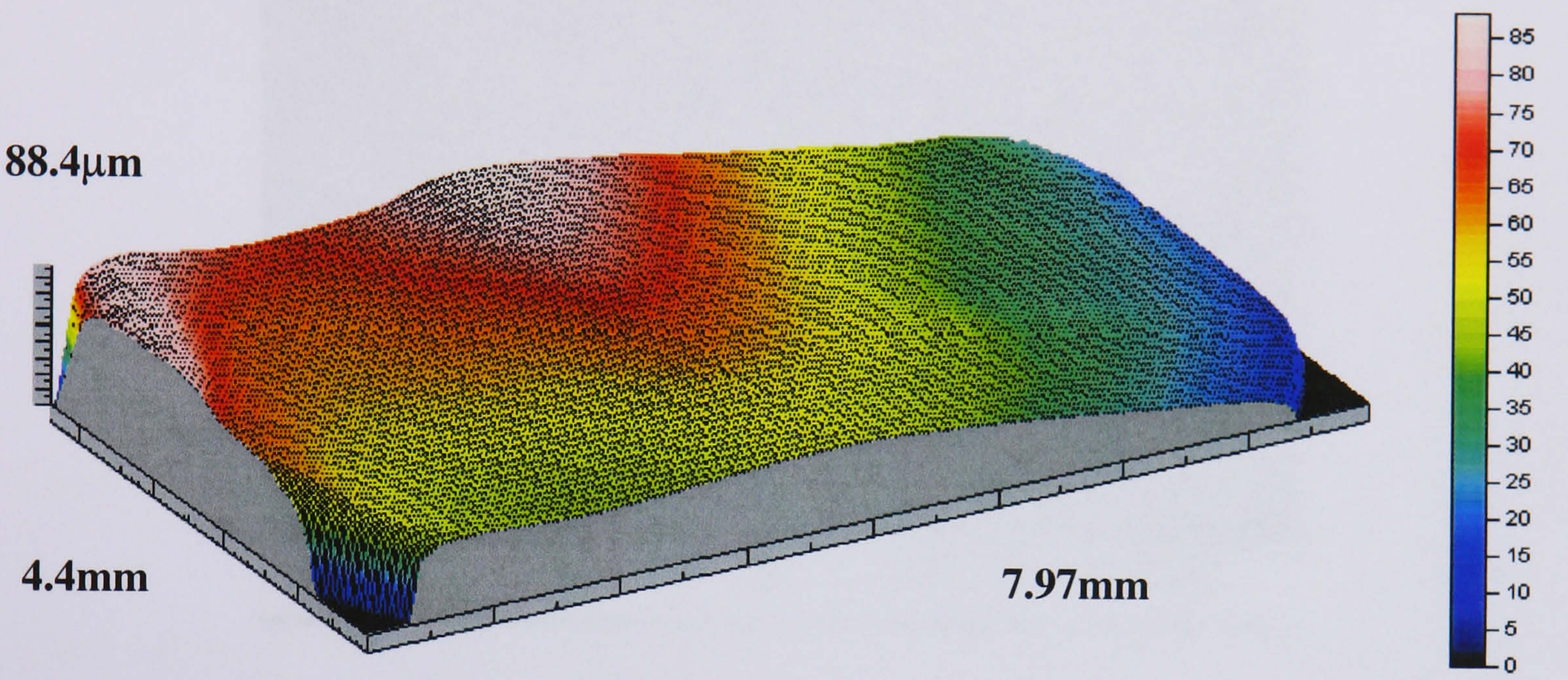

Figure 3.6 3D talysurf image of a 5MRad UHMWPE pin run in 95% (v/v) serum concentration.

Figure 3.7 3D talysurf image of a 10MRad UHMWPE pin run in 95% (v/v) serum concentrations.

SEM micrographs were also taken of the surfaces of the UHMWPE pins that had been tested under the different conditions. A SEM image of the 5MRad UHMWPE pin run in 25% (v/v) serum concentrations is shown in Figure 3.8. The surface showed signs of pulls which are associated with adhesive wear.

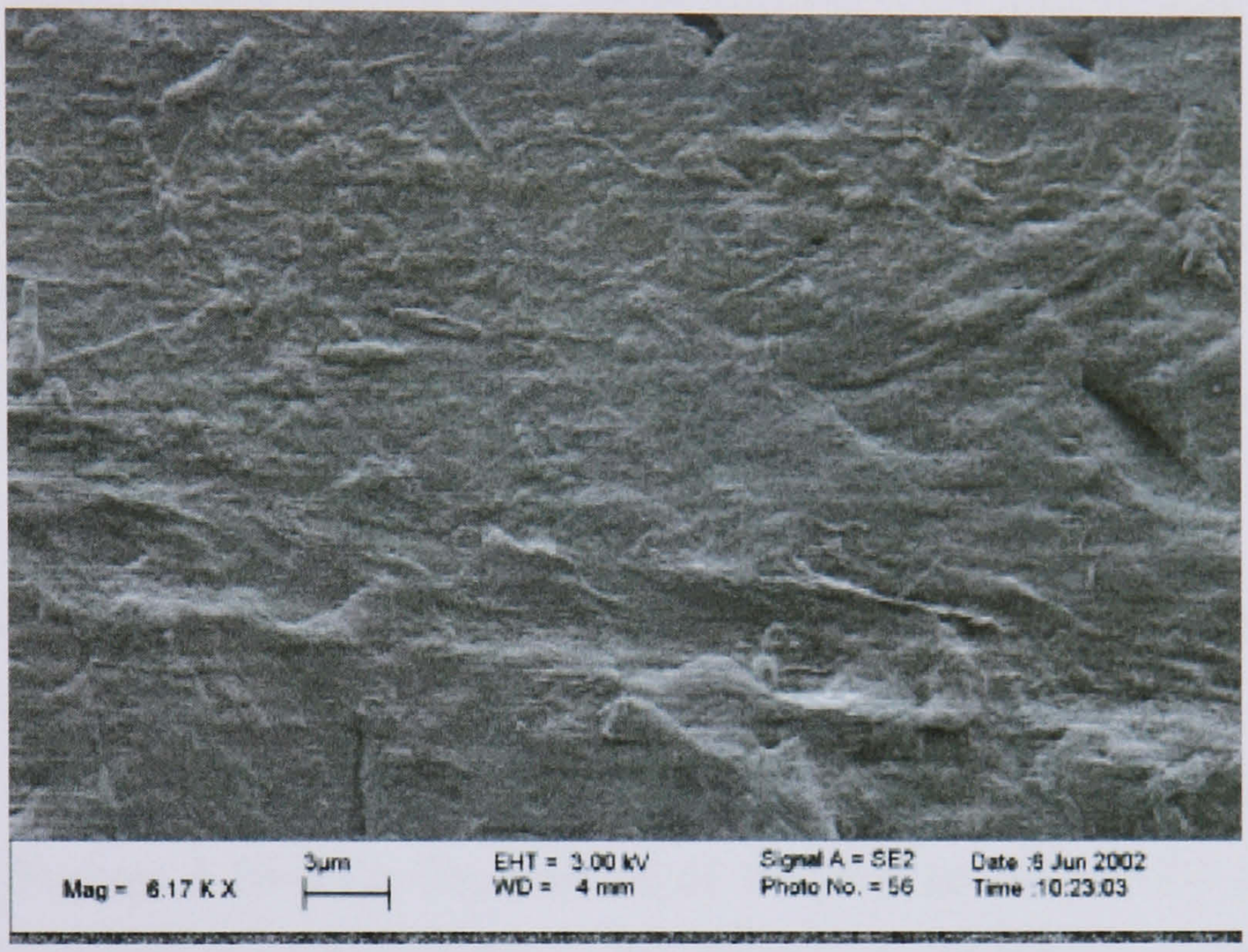

Figure 3.8 SEM micrograph of a 5MRad UHMWPE pin run in 25% (v/v) serum concentration.

A SEM micrograph of a 10MRad UHMWPE pin run in 25% (v/v) serum concentration is shown in Figure 3.9. The surface of this pin appeared much smoother, although it did have a crack across it, than the 5MRad UHMWPE pin. There were still signs of an adhesive wear process. There was a gross difference in the appearance of the wear surfaces from the different levels of crosslinking.

A 0MRad UHMWPE pin is not shown as none were saved from this test.

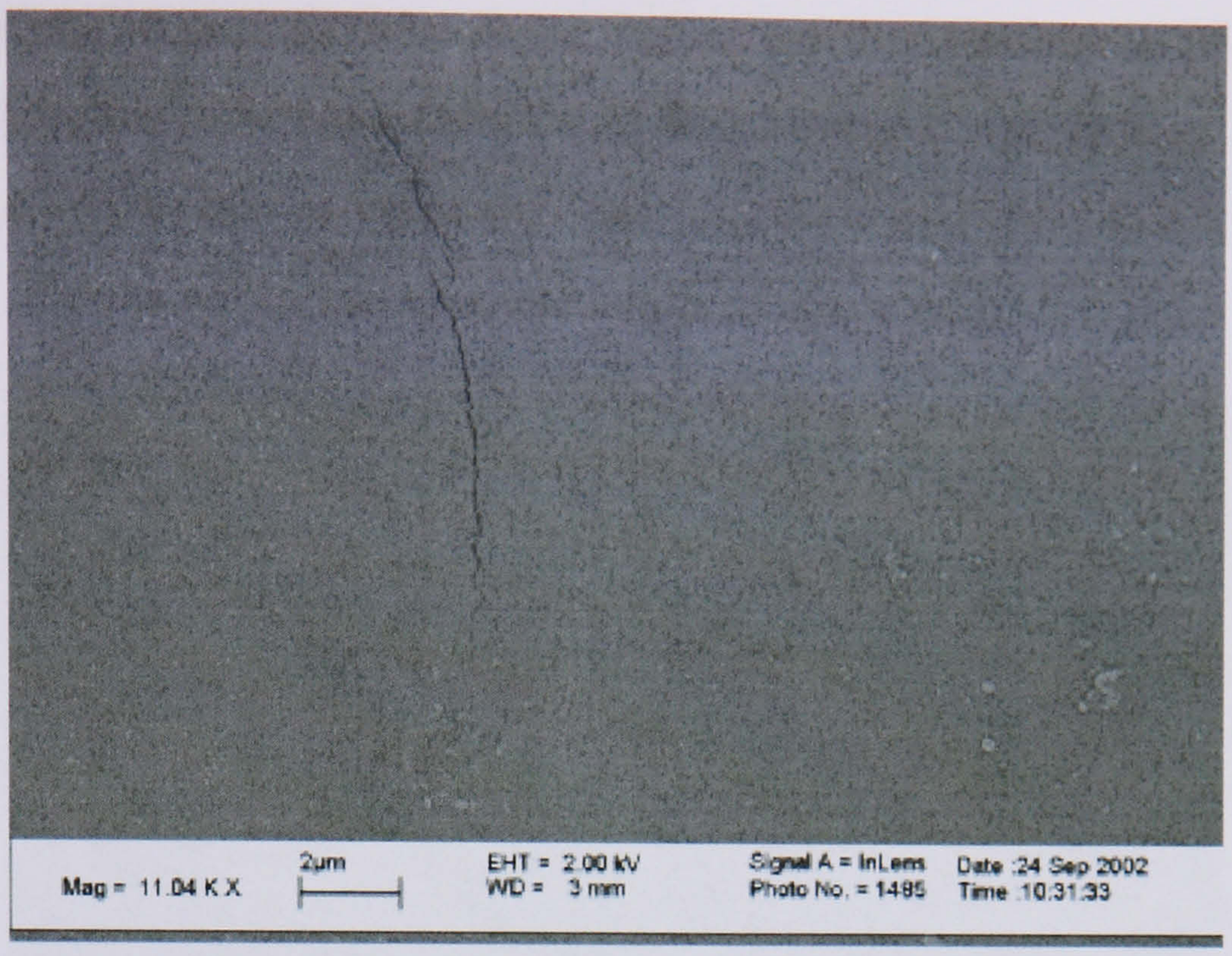

Figure 3.9 SEM micrograph of a 10MRad UHMWPE pin run in 25% (v/v) serum concentration.

SEM images of UHMWPE pins which were run in 95% (v/v) serum concentrations are shown in Figures 3.10-3.12. The surface of the 0MRad UHMWPE pin showed many ripples and also particles on the surface which could have been PE particles breaking loose or reattachment of the PE particles onto the surface.

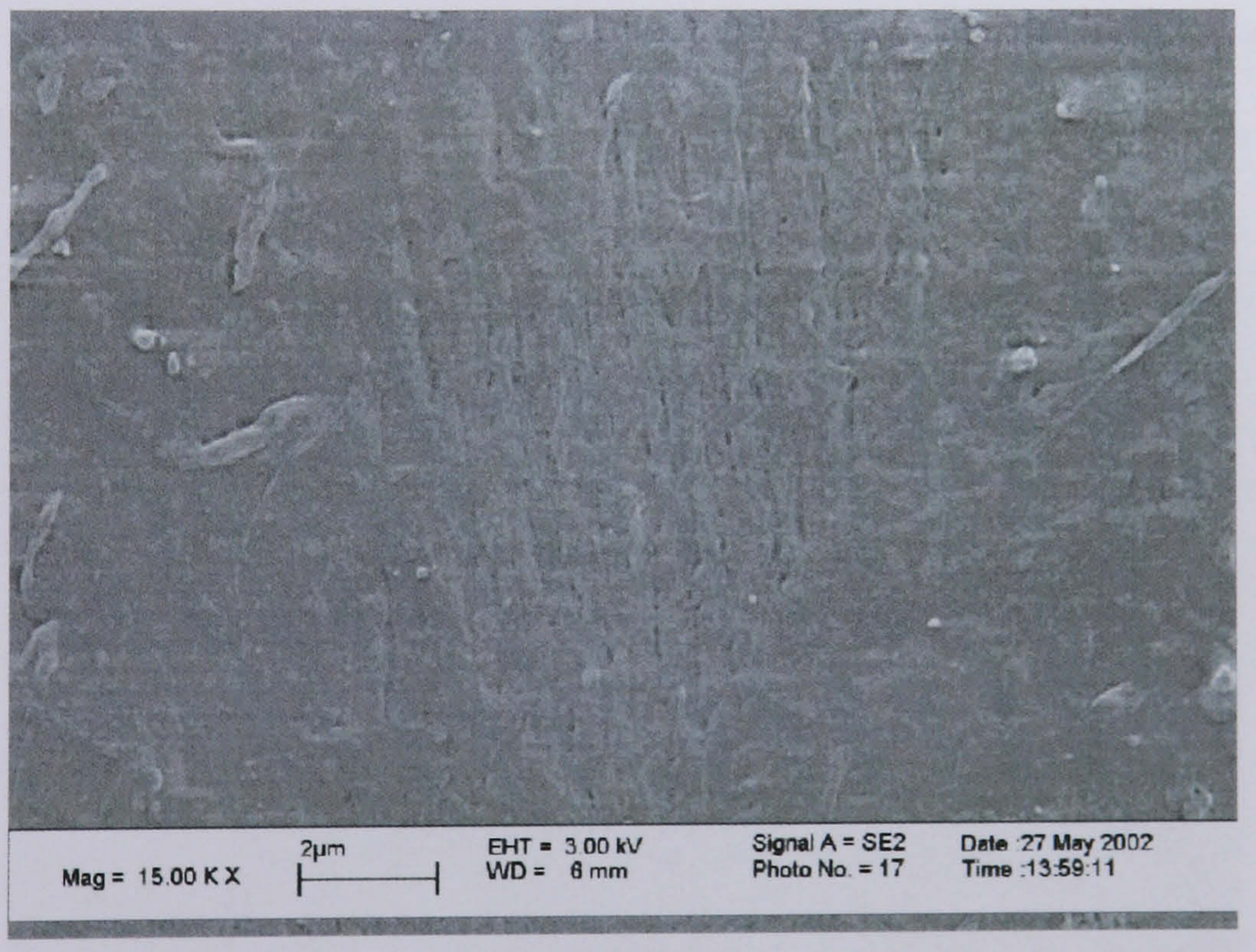

Figure 3.10 SEM micrograph of a 0MRad UHMWPE pin run in 95% (v/v) serum concentration.

The surface of the 5MRad UHMWPE pin (Figure 3.11) appeared smoother than the 0MRad pin although there were signs of small scratches in the surface. There were no signs of the ripples seen in the 0MRad pin.

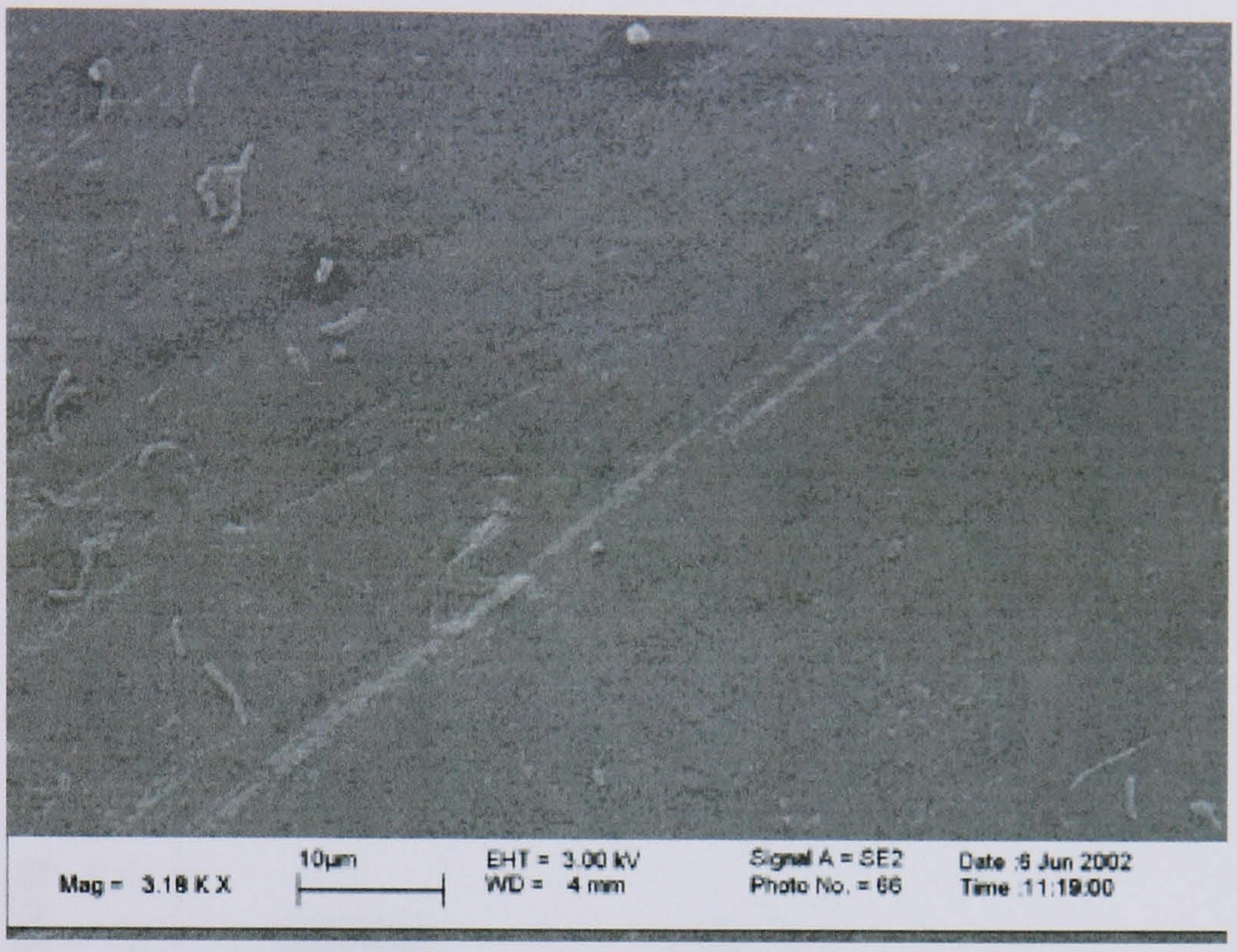

Figure 3.11 SEM micrograph of a 5MRad UHMWPE pin run in 95% (v/v) serum concentration.

The surface of the 10MRad UHMWPE pin had many ripples which are characteristic of an adhesive wear mechanism taking place. There was also a crack in the surface (Figure 3.12).

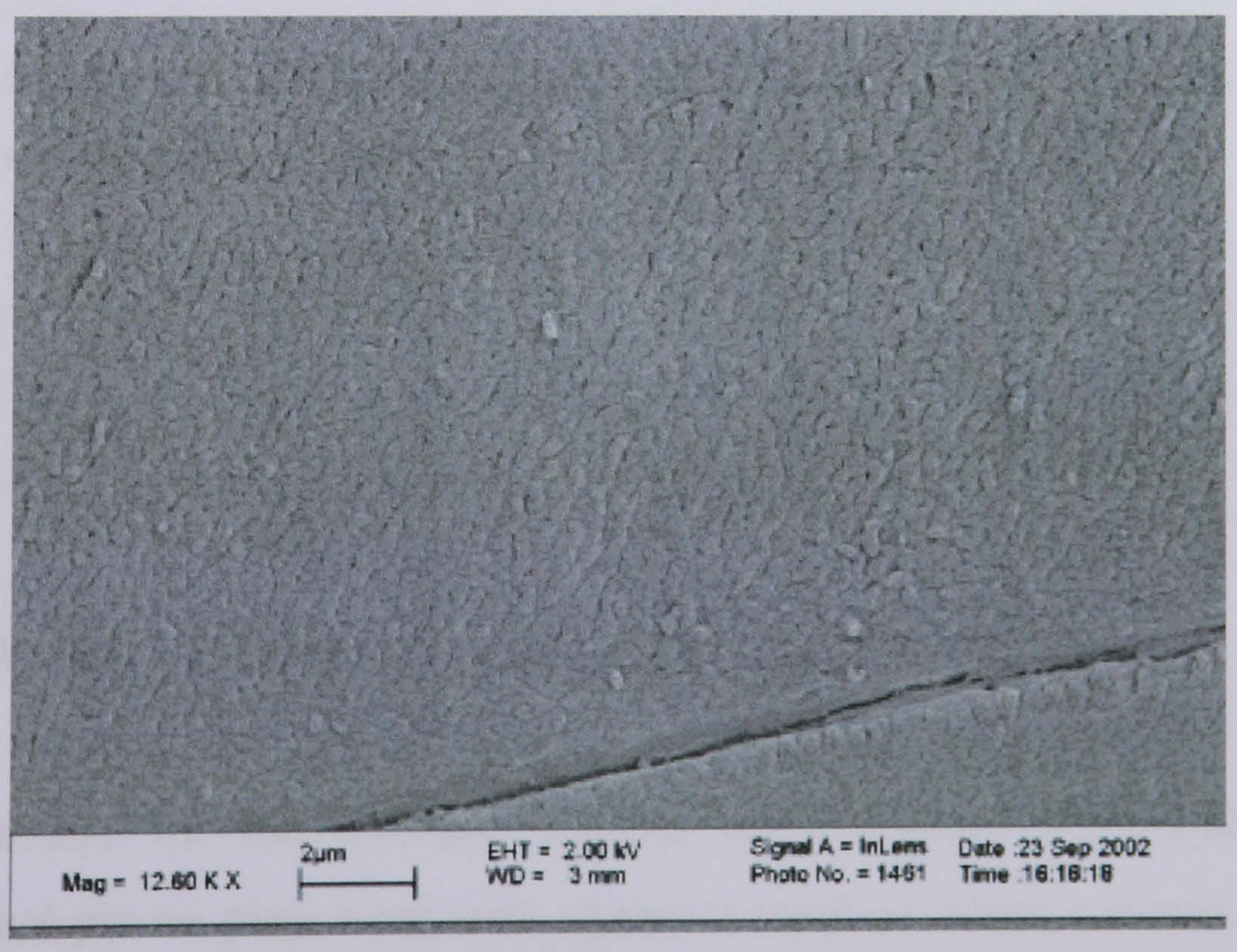

Figure 3.12 SEM micrograph of a 10MRad UHMWPE pin run in 95% (v/v) serum concentration.

3.3.2. Multidirectional Smooth Pin on Plate Wear Test.

The wear factors for the 0MRad, 5MRad and 10MRad UHMWPE pins in multidirectional pin on plate tests against a smooth counterface are shown in Table 3.5 and Figure 3.13. The results showed that the highest wear factor was for the 0MRad non-crosslinked material with the wear factor decreasing with increased crosslinking. There was no statistically significant difference between wear factors for the 0MRad and 5MRad materials, however the wear factor for the 10MRad material was found to be significantly lower ($p<0.05$; ANOVA) than for the other materials. These results showed that for a smooth surface which represents an undamaged counterface, the highly crosslinked material had the greatest wear resistance.

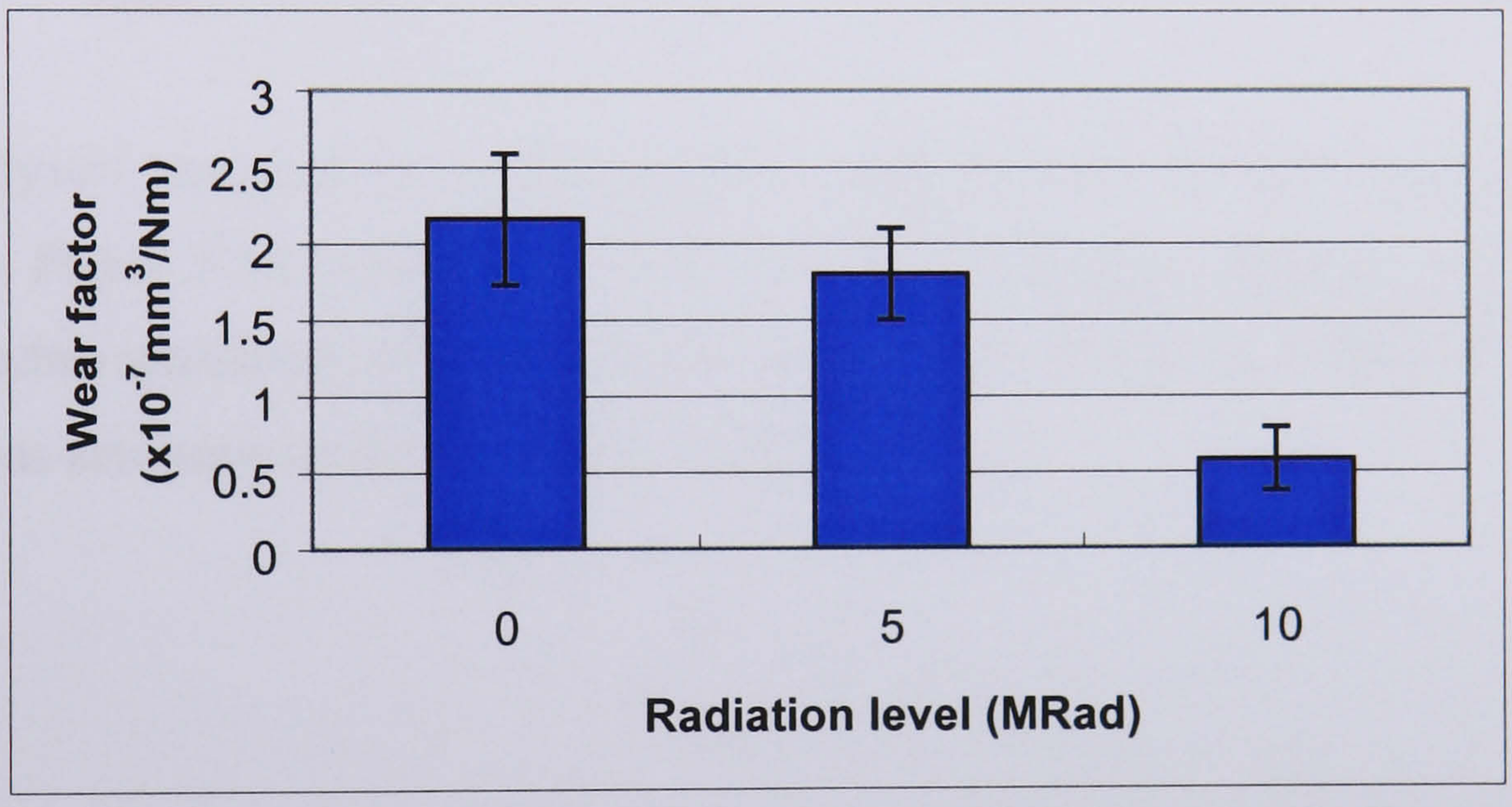

Figure 3.13 Average wear factors after six weeks on smooth plates ± 95% confidence limits (25% (v/v) serum concentration).

The 3D talysurf and SEM micrographs of the surface of the pins were shown in the last section. They showed that the mechanism involved was mainly an adhesive wear mechanism for the three different materials.

3.3.3. Multidirectional Medium Scratched Pin on Plate Wear Tests.

The wear factors for the 0MRad, 5MRad and 10MRad UHMWPE pins in multidirectional pin on plate wear tests against a medium scratched counterface are shown in Figure 3.14 and Table 3.5. The highest wear factor for this test was for the 5MRad crosslinked material. However there was no significant difference between

the 0MRad and 5MRad UHMWPE. The 10MRad crosslinked material again had a significantly lower wear factor then the other two materials ($p<0.05$; ANOVA).

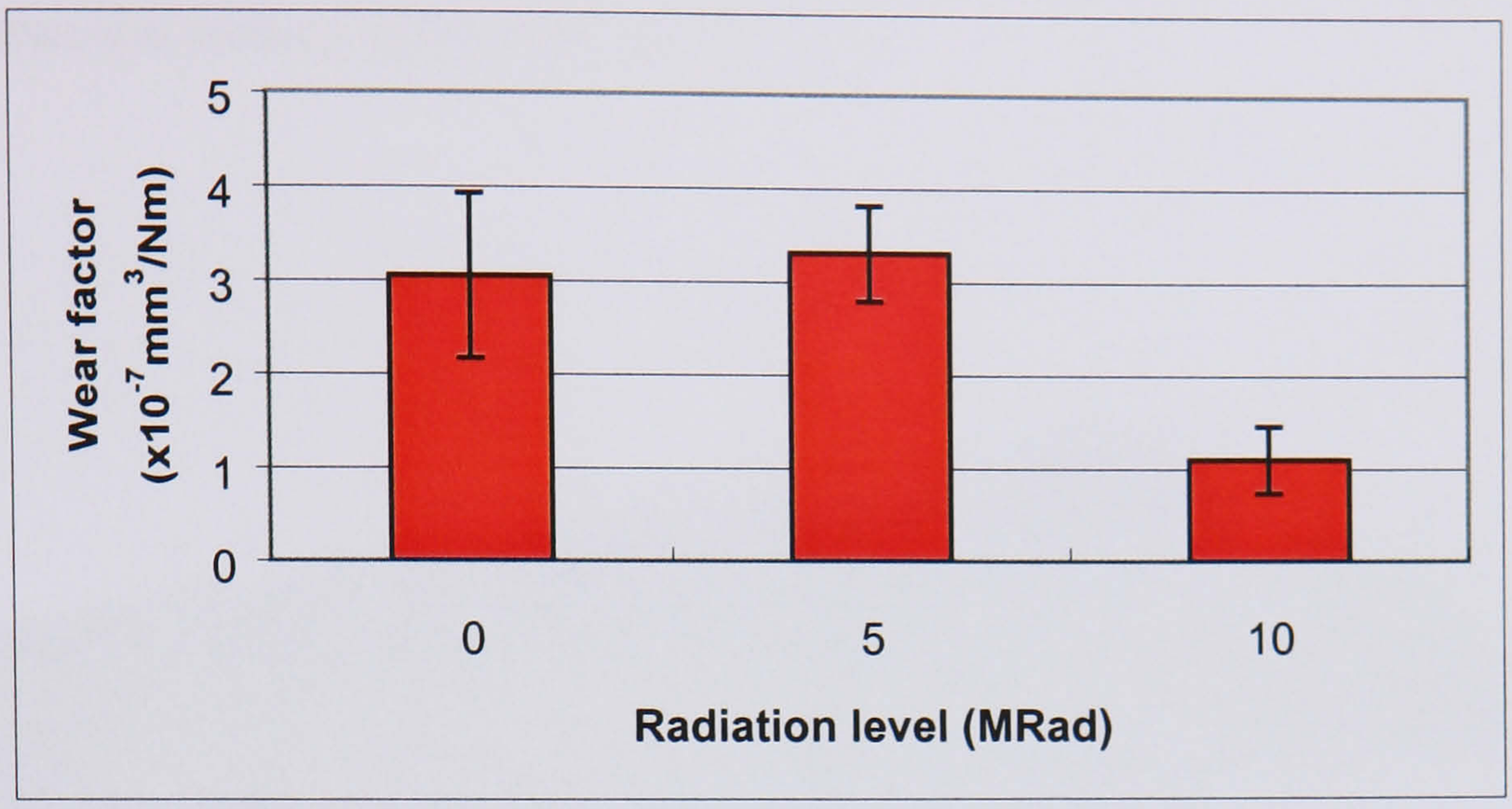

Figure 3.14 Average wear factors from six weeks on medium scratched plates ± 95% confidence limits.

A 3D talysurf image of the surface of one of the 0MRad pins which was tested is shown in Figure 3.15. Scratches could be seen in the surface of the pin with some of the scratches appearing quite deep. There was a slope across the surface of the pin which was also seen on the other pins tested.

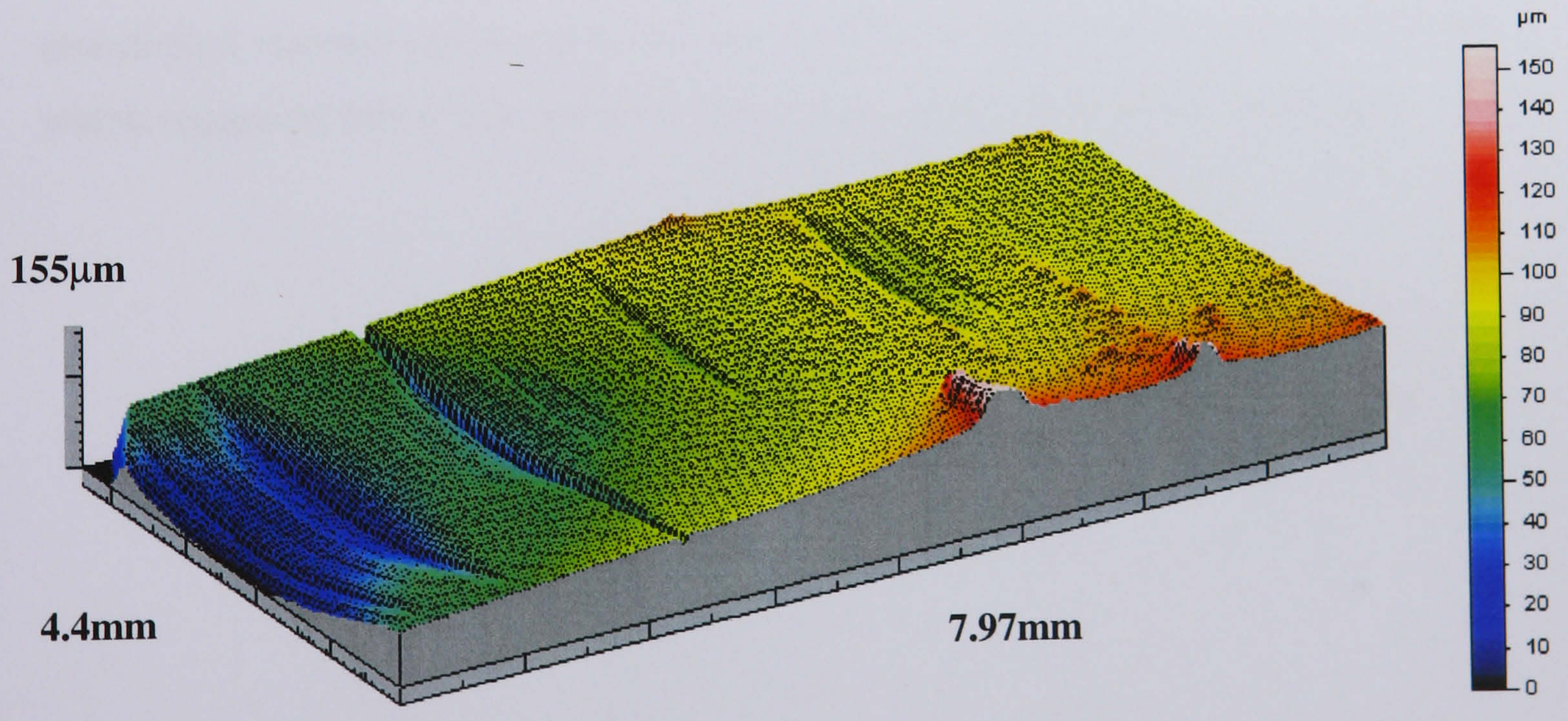

Figure 3.15 3D talysurf image of the surface of a 0MRad UHMWPE pin run against a medium scratched counterface.

A 3D talysurf image of a 5MRad pin run on a medium scratched counterface is shown in Figure 3.16. The surface of this pin appeared to be quite smooth compared to the scratched surface of the 0MRad pin.

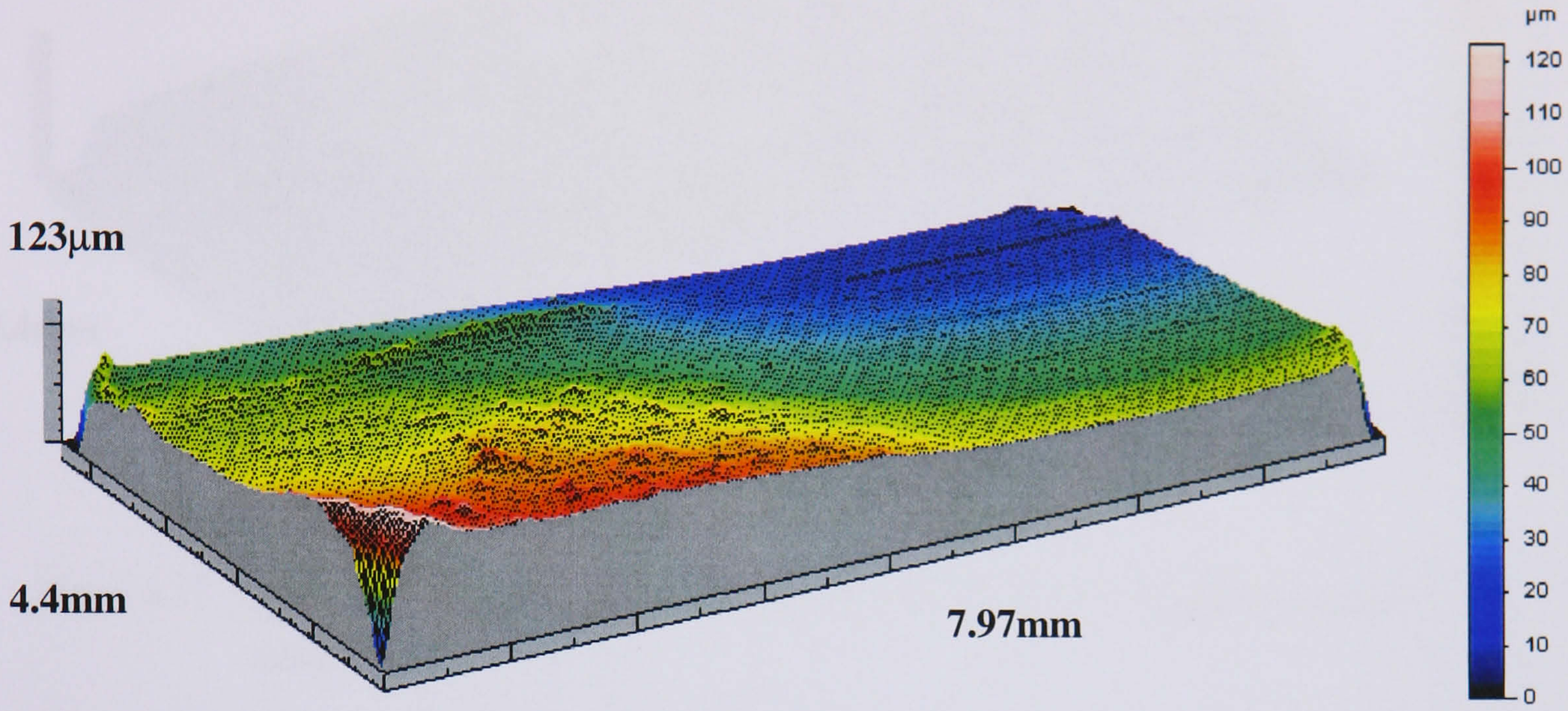

Figure 3.16 3D talysurf image of a 5MRad UHMWPE pin run against a medium scratched counterface.

The talysurf image of a 10MRad UHMWPE pin is shown in Figure 3.17. The surface of this pin was also smooth and did not have the scratches which were seen on the 0MRad pin. There appeared to be a difference in the surfaces of the crosslinked material compared to the noncrosslinked. There was a slope on this pin which suggested that it was not worn flat or was not flat when it was measured.

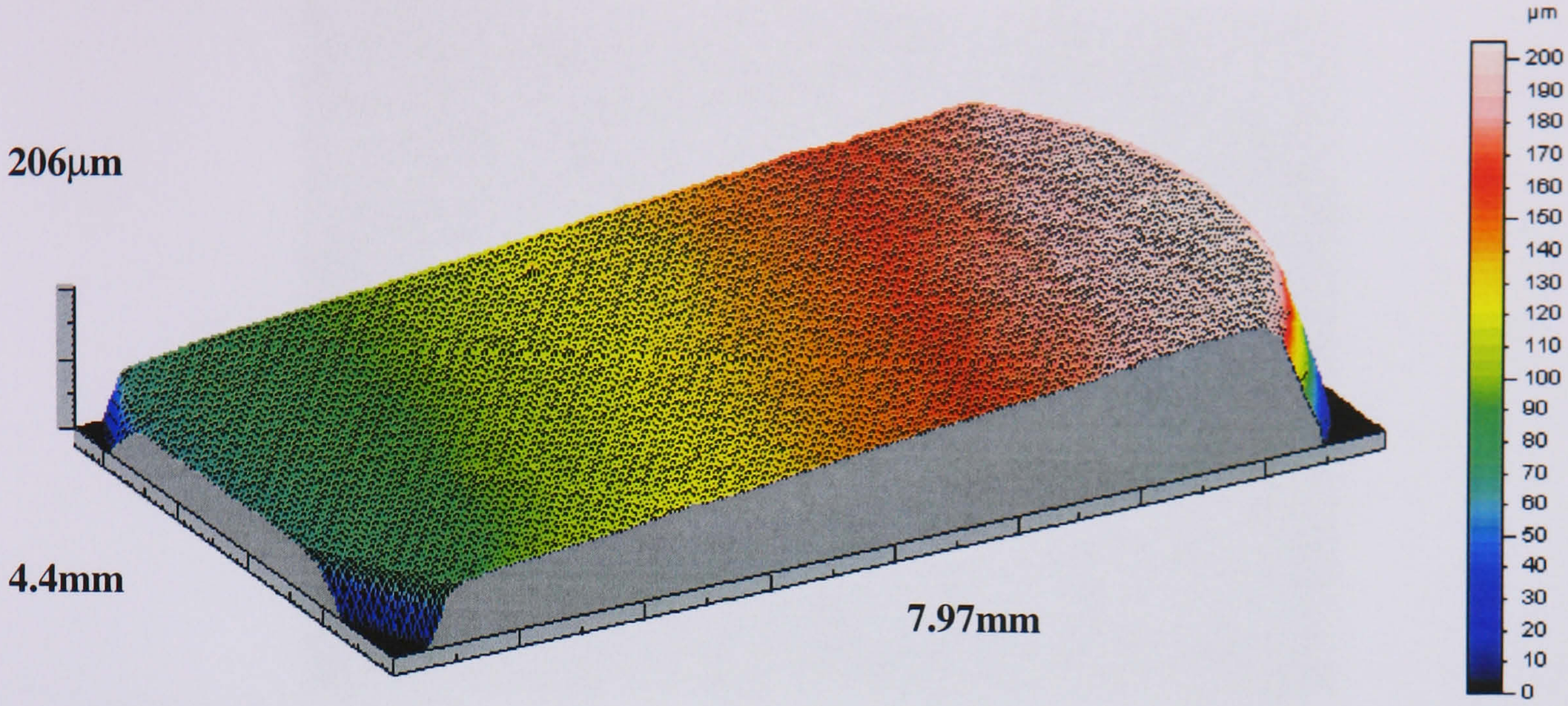

Figure 3.17 3D talysurf image of a 10MRad UHMWPE pin run against a medium scratched counterface.

SEM micrographs of small areas of the surfaces of the pins are shown in Figures 3.18-3.20. The micrograph of the 0MRad UHMWPE pin also showed areas of scratching as did the talysurf image (Figure 3.18). The scratches suggested that a more abrasive wear mechanism occurred. There were also areas of ripples which are associated with an adhesive wear mechanism.

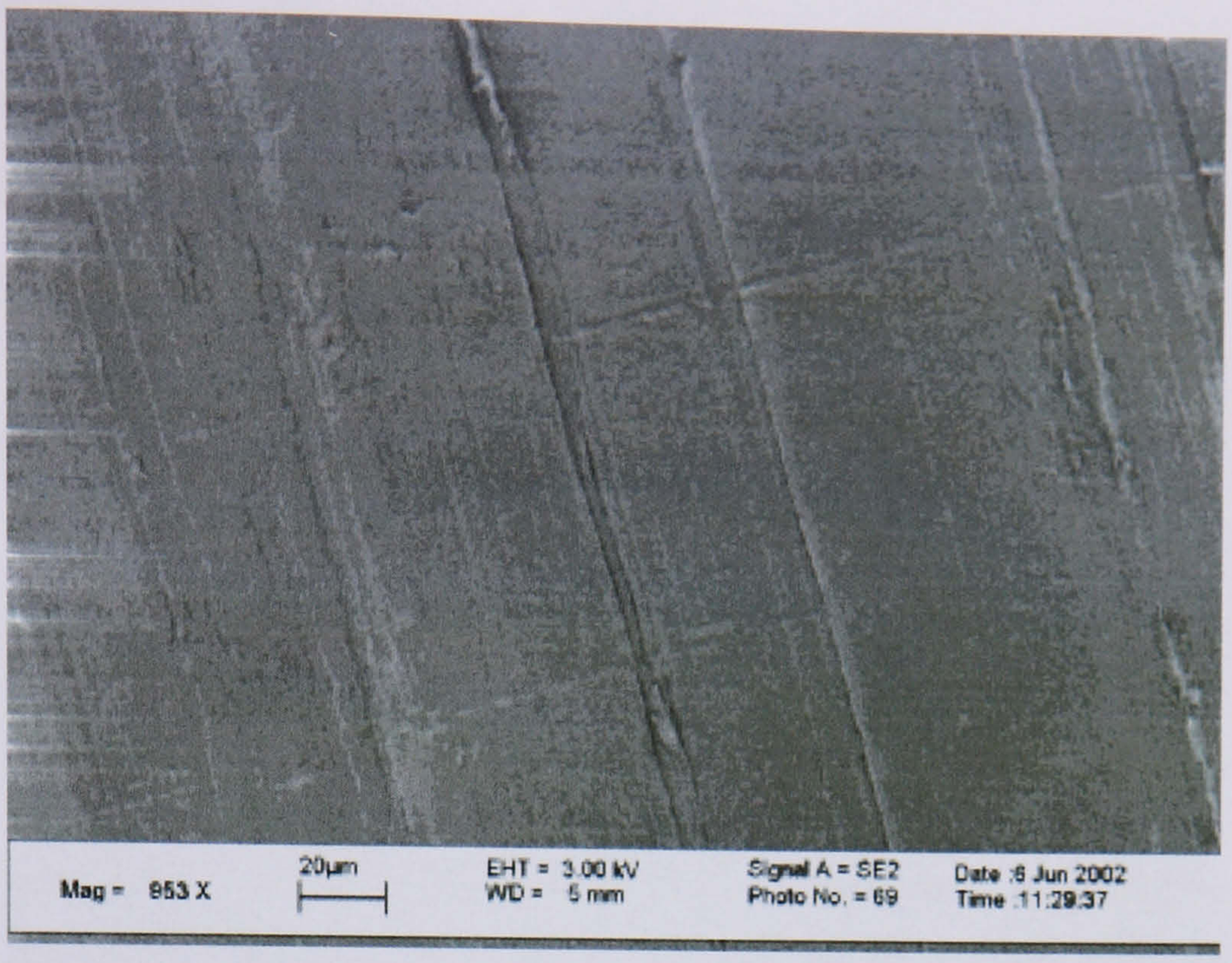

Figure 3.18 SEM micrograph of an area of a 0MRad UHMWPE pin run against a medium scratched counterface

A 5MRad UHMWPE pin tested against a medium scratched counterface is shown in Figure 3.19. This surface did not have the scratches which were seen on the 0MRad pin. There were large areas which looked like flakes and parts that had nearly detached from the surface and areas of reattachment which are associated with abrasive wear.

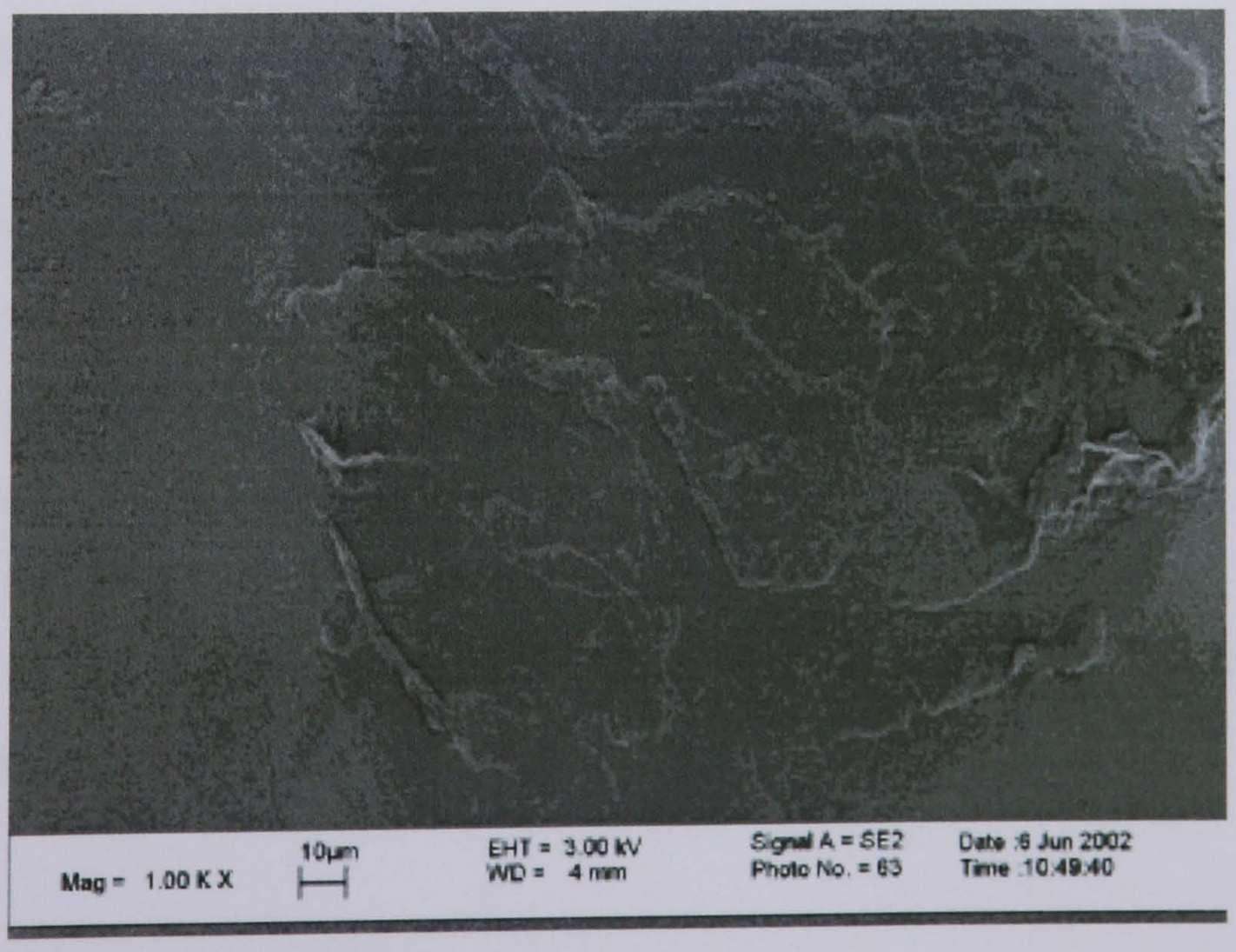

Figure 3.19 SEM micrograph of an area of a 5MRad UHMWPE pin run against a medium scratched counterface.

A SEM micrograph of the 10MRad material run against a medium scratched counterface is shown in Figure 3.20. This pin also did not appear to have the scratches which were clearly visible on the 0MRad material. The surface appeared quite smooth with just a ripple affect which is seen with an adhesive wear mechanism. The SEM images also showed there is a difference between the crosslinked and the noncrosslinked material.

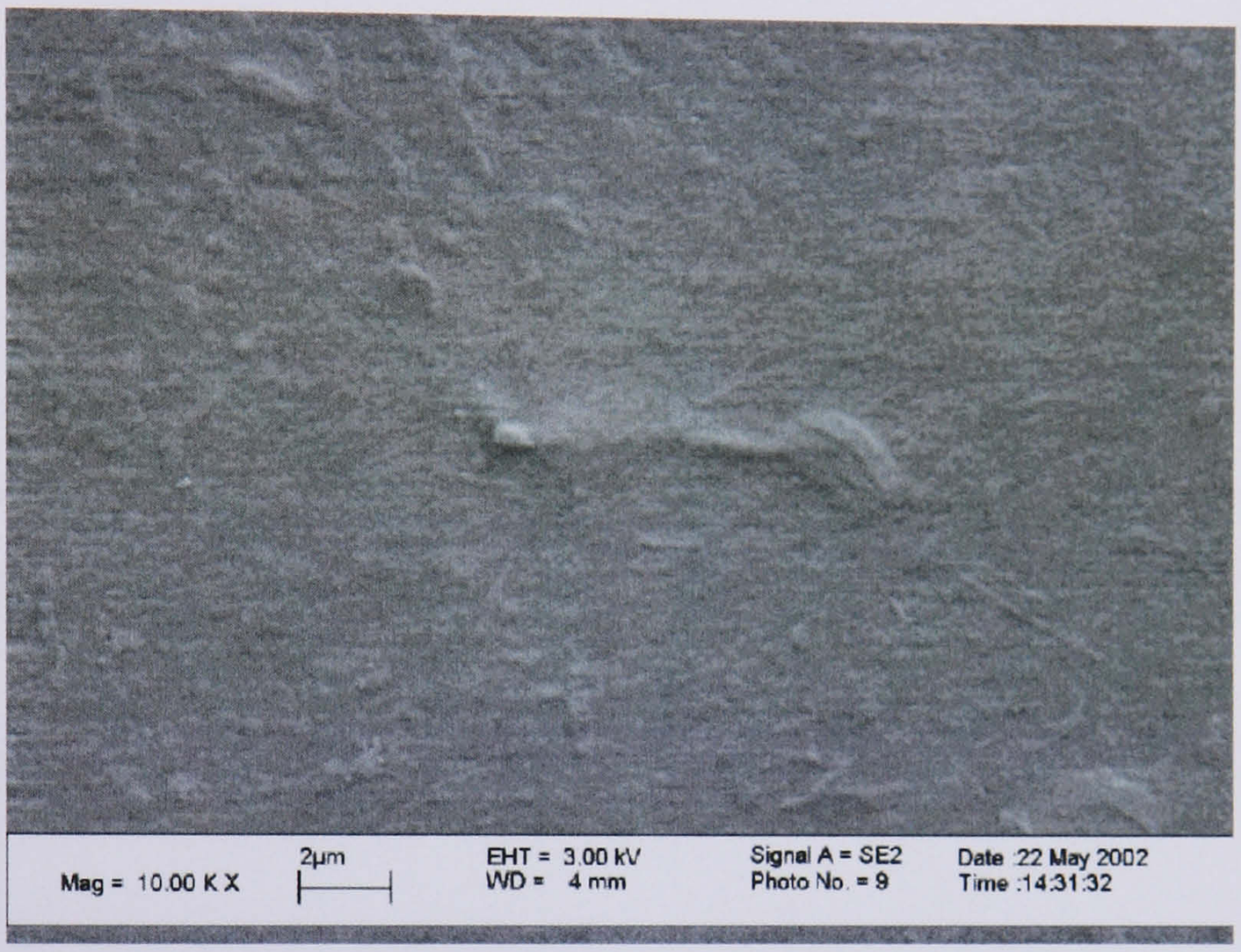

Figure 3.20 SEM micrograph of a 10MRad UHMWPE pin run against a medium scratched counterface.

3.3.4. Multidirectional High Scratched Pin on Plate Wear Tests.

The wear factors for the 0MRad, 5MRad and 10MRad UHMWPE pins in multidirectional pin on plate wear tests against a highly scratched counterface are shown in Figure 3.21 and Table 3.5. The highest wear factor for this test was again for the 5MRad material with 10MRad being the lowest. There was no significant difference between the 0MRad and 5MRad materials, but there was a significant difference with the 10MRad material when compared to the 0MRad and 5MRad materials ($p<0.05$; ANOVA).

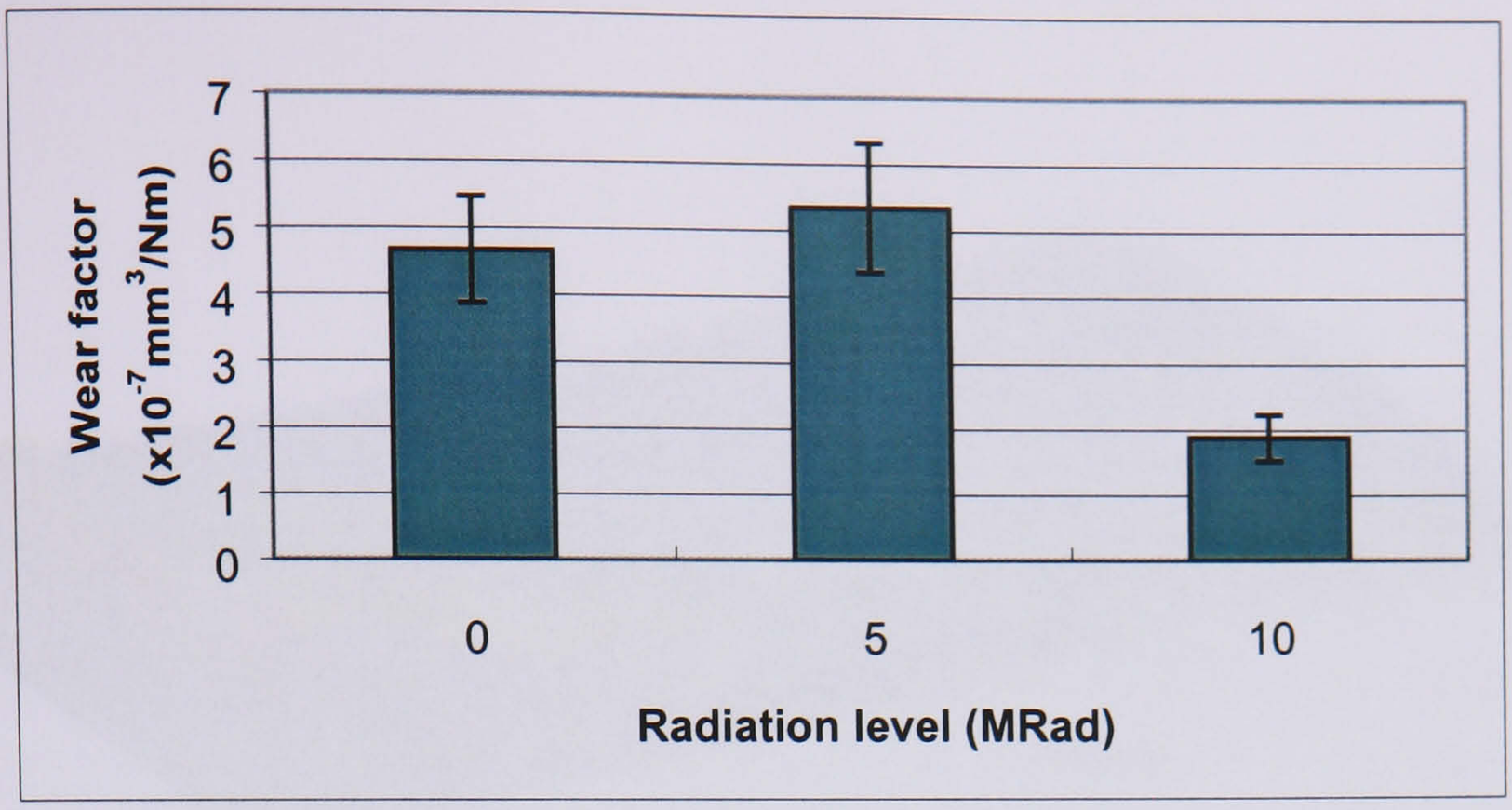

Figure 3.21 Average wear factors from six weeks on high scratched plates ± 95% confidence limits.

3D talysurf pictures of the surfaces of the pins after testing against a highly scratched counterface are shown in Figures 3.22-3.24. The surface of the 0MRad pin had many little peaks on it but there were no signs of any scratches (Figure 3.22).

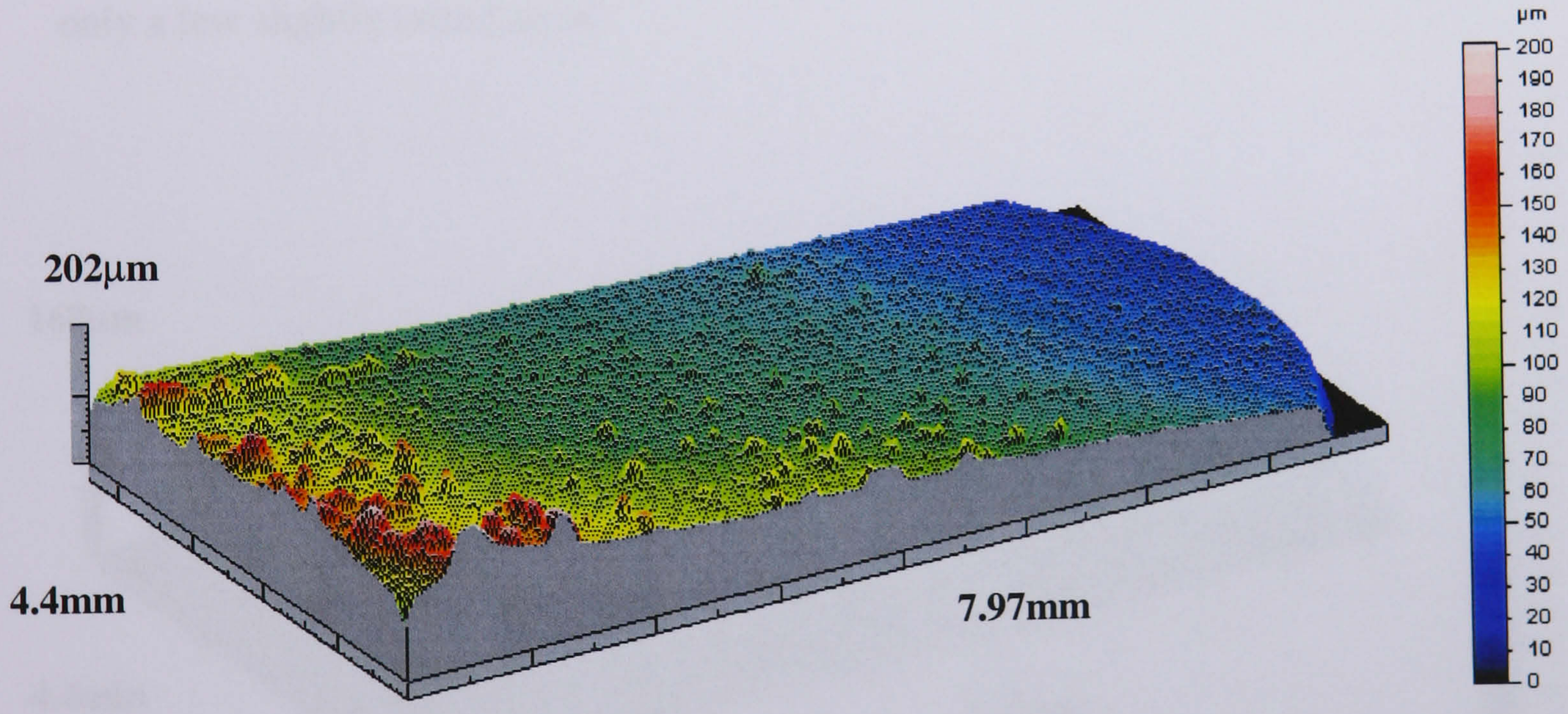

Figure 3.22 3D talysurf image of a 0MRad UHMWPE pin surface after testing against a highly scratched counterface.

A talysurf image of a 5MRad pin which had been worn against the same counterface as the 0MRad pin is shown in Figure 3.23. The surface had peaks at one end and was slightly higher but the rest of the surface was smooth with no signs of any scratches.

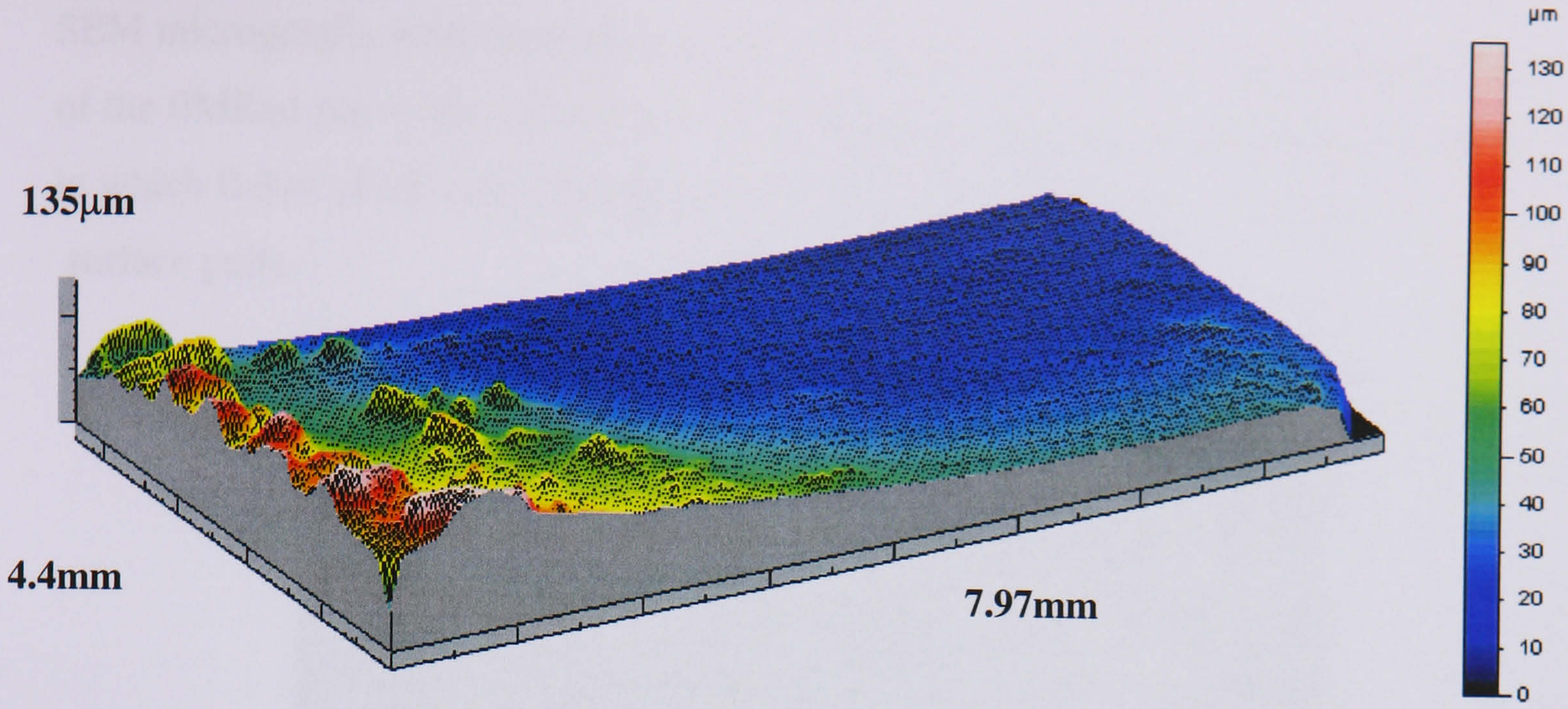

Figure 3.23 3D talysurf image of a 5MRad UHMWPE pin run against a highly scratched counterface.

The surface of the 10MRad pin again was quite flat with a slope across it suggesting it had not worn flat (Figure 3.24). There were no scratches or marks to be seen and only a few slightly raised areas.

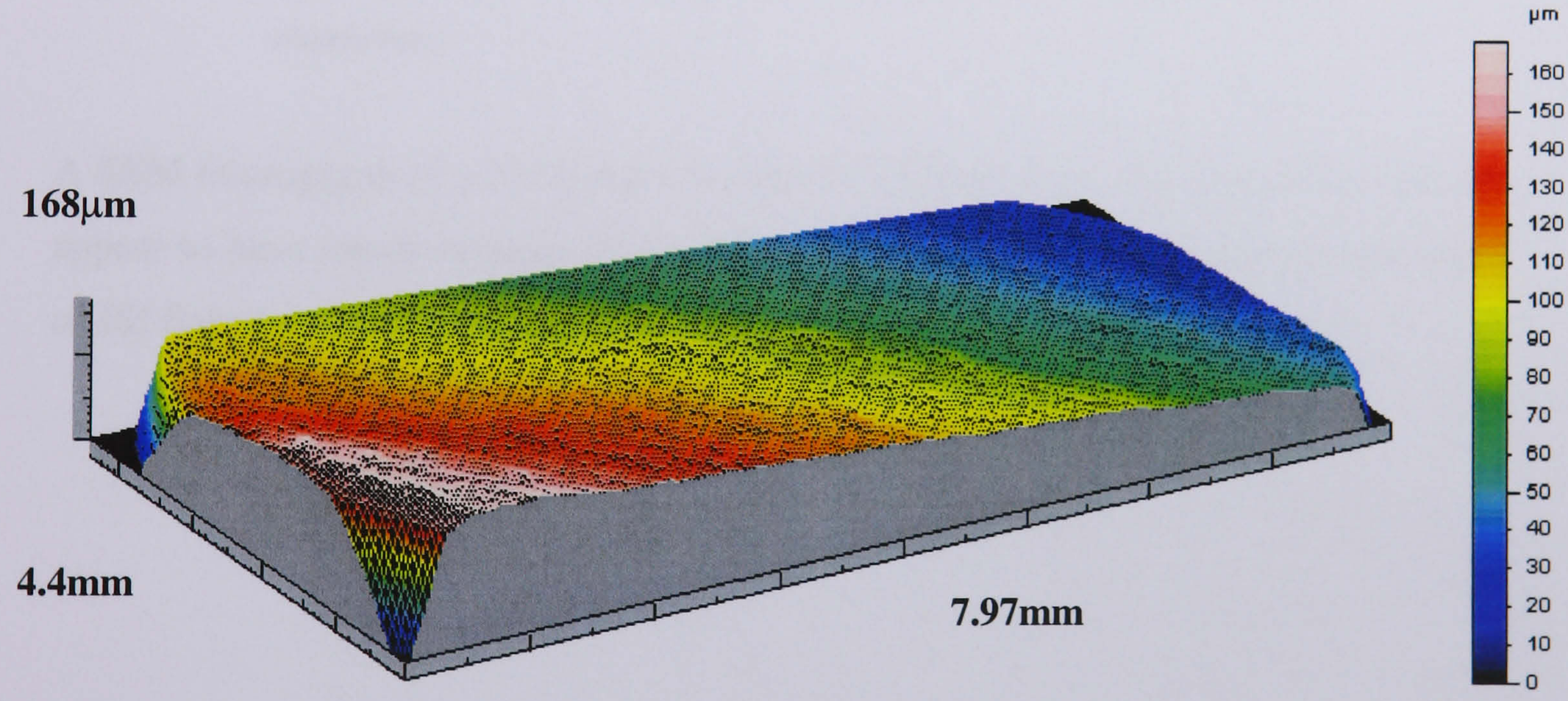

Figure 3.24 3D Talysurf image of a 10MRad UHMWPE pin run against a highly scratched counterface.

SEM micrographs were also taken of the pin surfaces. A small area from the surface of the 0MRad pin is shown in Figure 3.25. The area shown was damaged and areas in which flakes of PE were pulling away could be seen. There was evidence of surface pulls.

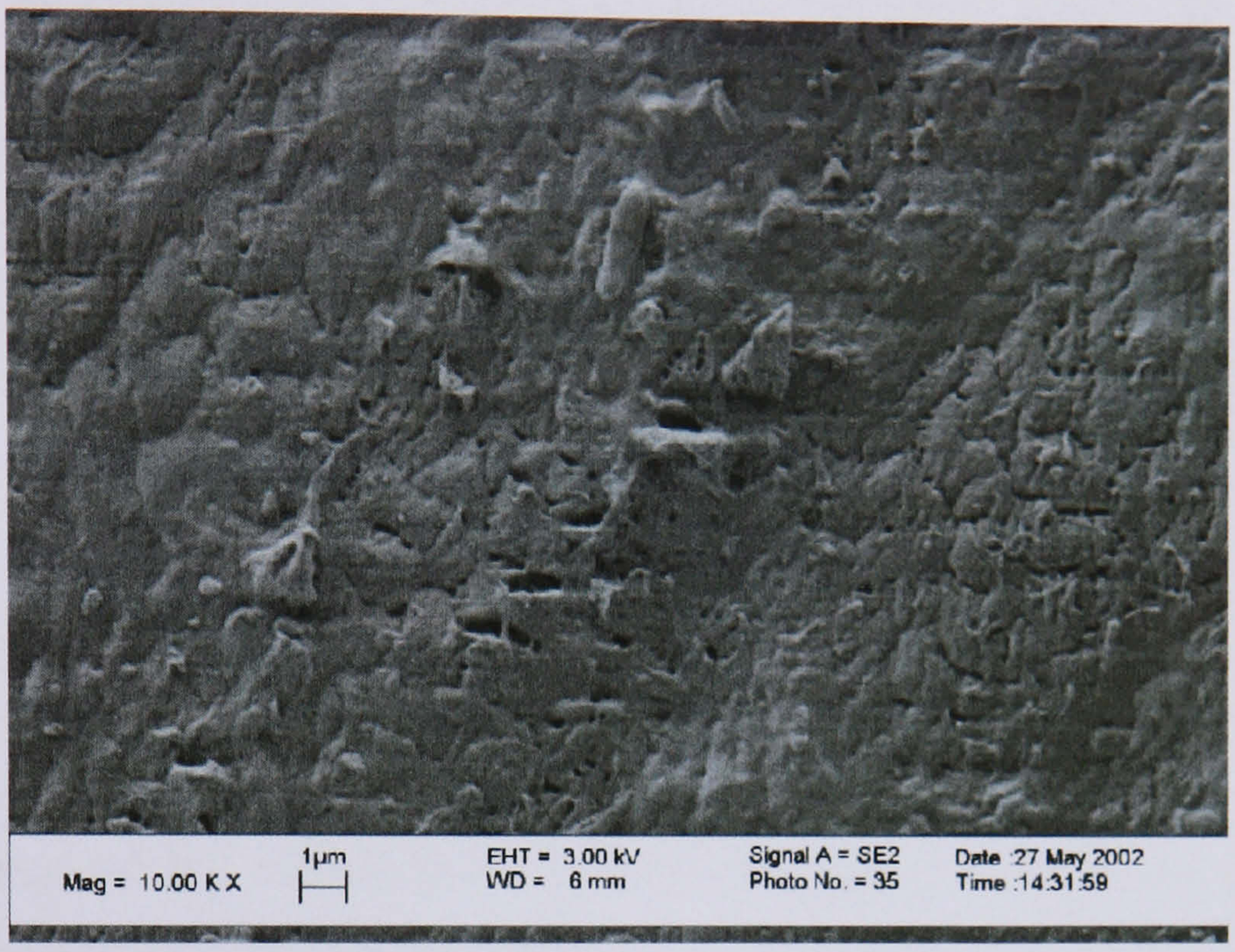

Figure 3.25 SEM micrograph of a 0MRad UHMWPE pin run against a highly scratched counterface.

A SEM micrograph of a 5MRad pin is shown in Figure 3.26. The pin surface did not appear to have much damage although there were scratches on the surface and signs of PE flakes.

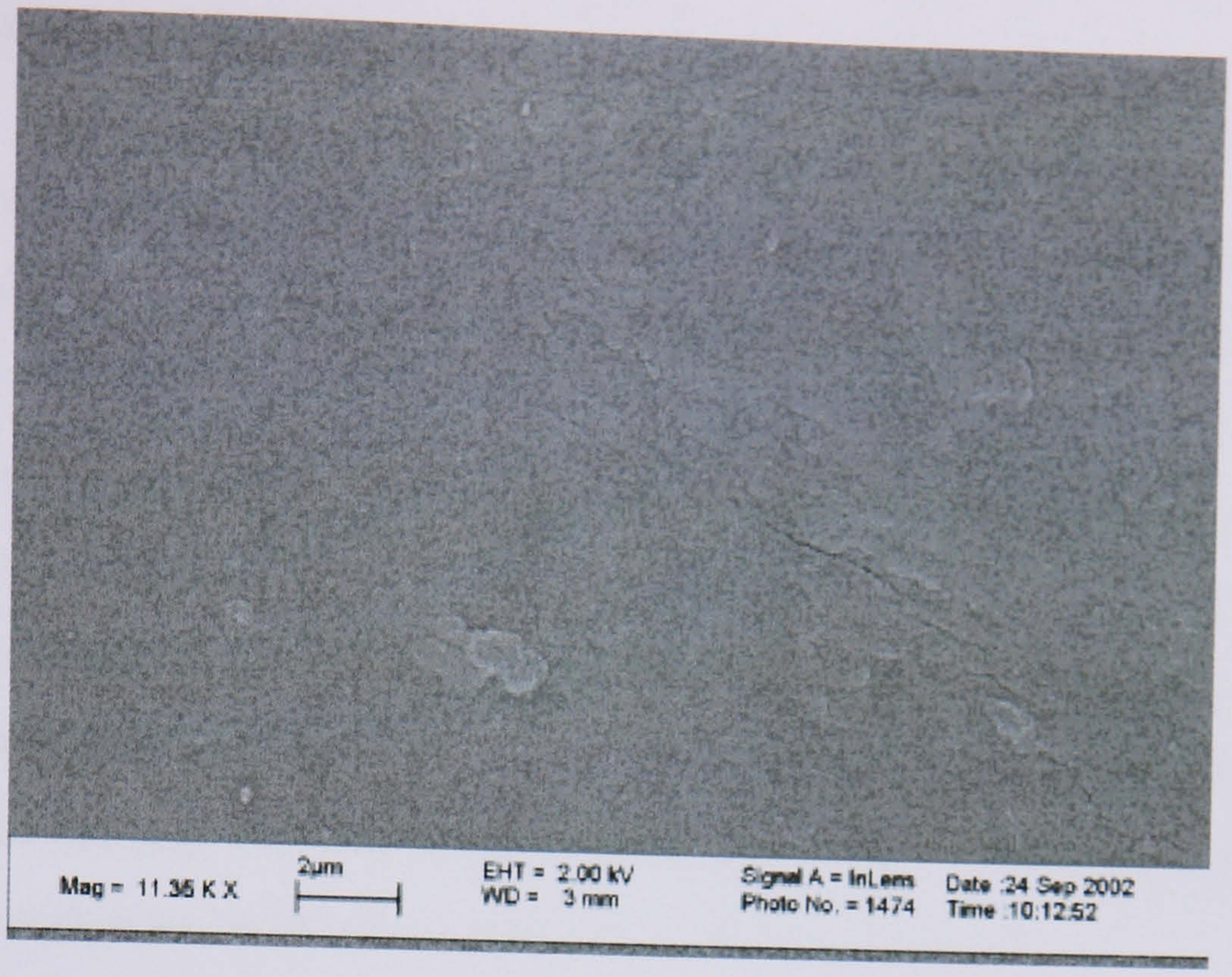

Figure 3.26 SEM micrograph of a 5MRad UHMWPE pin run against a highly scratched counterface.

An SEM image of the 10MRad pin against the highly scratched counterface is shown in Figure 3.27. The area had ripples and appeared to be pulling away from the surface of the pin.

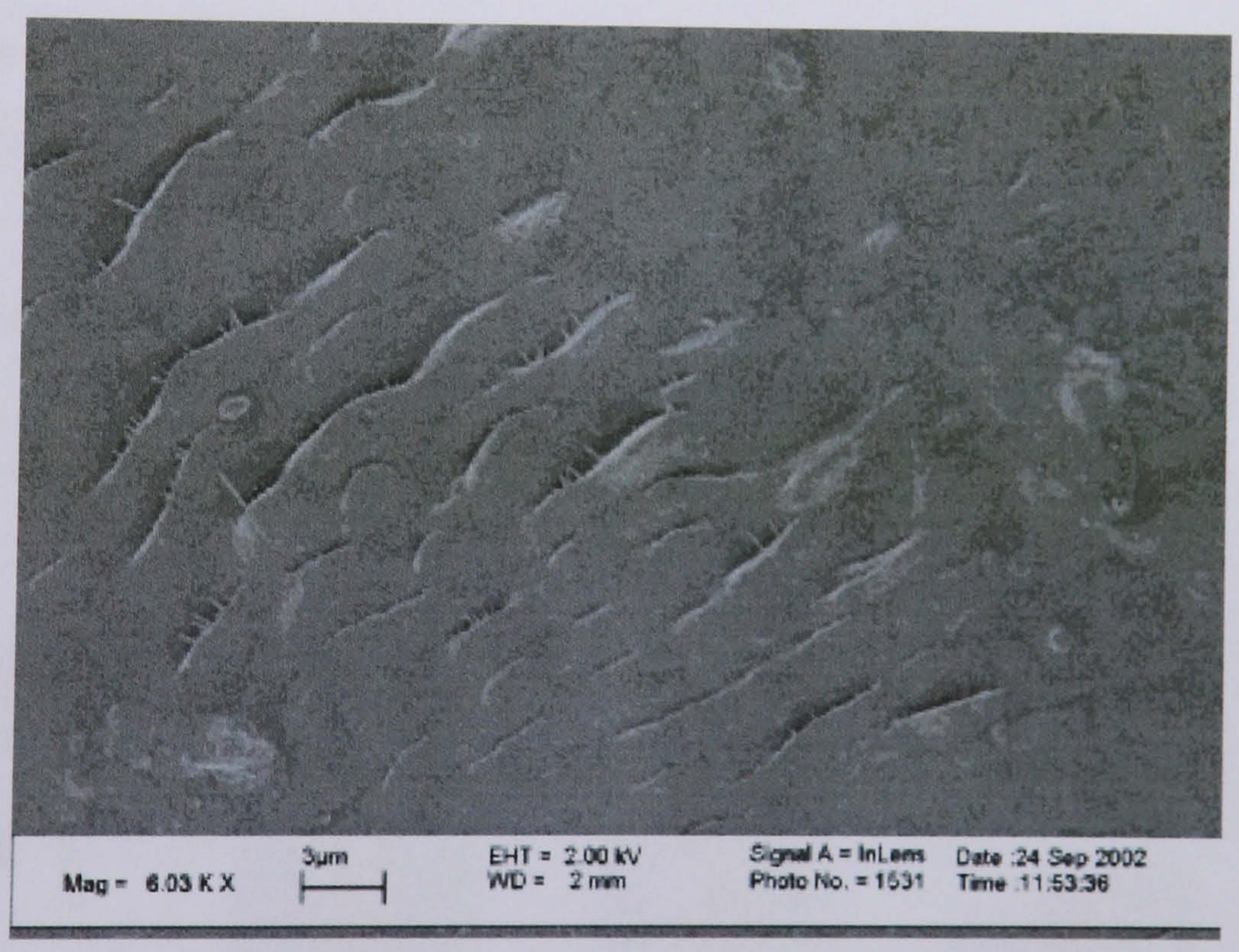

Figure 3.27 SEM micrograph of a 10MRad UHMWPE pin run against a highly scratched counterface.

3.3.5. Comparison of Wear Factors.

The mean wear factors from all the different counterface surfaces are shown in Table 3.5 and have been combined in Figure 3.28. These results show that for all the materials the wear factor increased as the scratch height increased. The high levels of crosslinking reduced wear by 64% on the medium scratched plates and by 60% on the highly scratched plates when compared to noncrosslinked material. The 5MRad material gave a slight but not significant increase in wear factors on the scratched plates when compared to the results from the noncrosslinked material. The results showed that the 10MRad material had a significantly lower wear factor than the other two materials on all of the surfaces ($p<0.05$; ANOVA).

Radiation level.	**Wear factor (mean ± 95% confidence intervals ($x10^{-7}$ mm^3/Nm))**		
	Smooth	**Medium**	**High**
0 MRad	2.16±0.43	3.05±0.88	4.67±0.8
5 MRad	1.8±0.3	3.31±0.51	5.35±0.98
10 MRad	0.58±0.21	1.1±0.36	1.88±0.35

Table 3.5 Average wear factors from all testing ± 95% confidence limits.

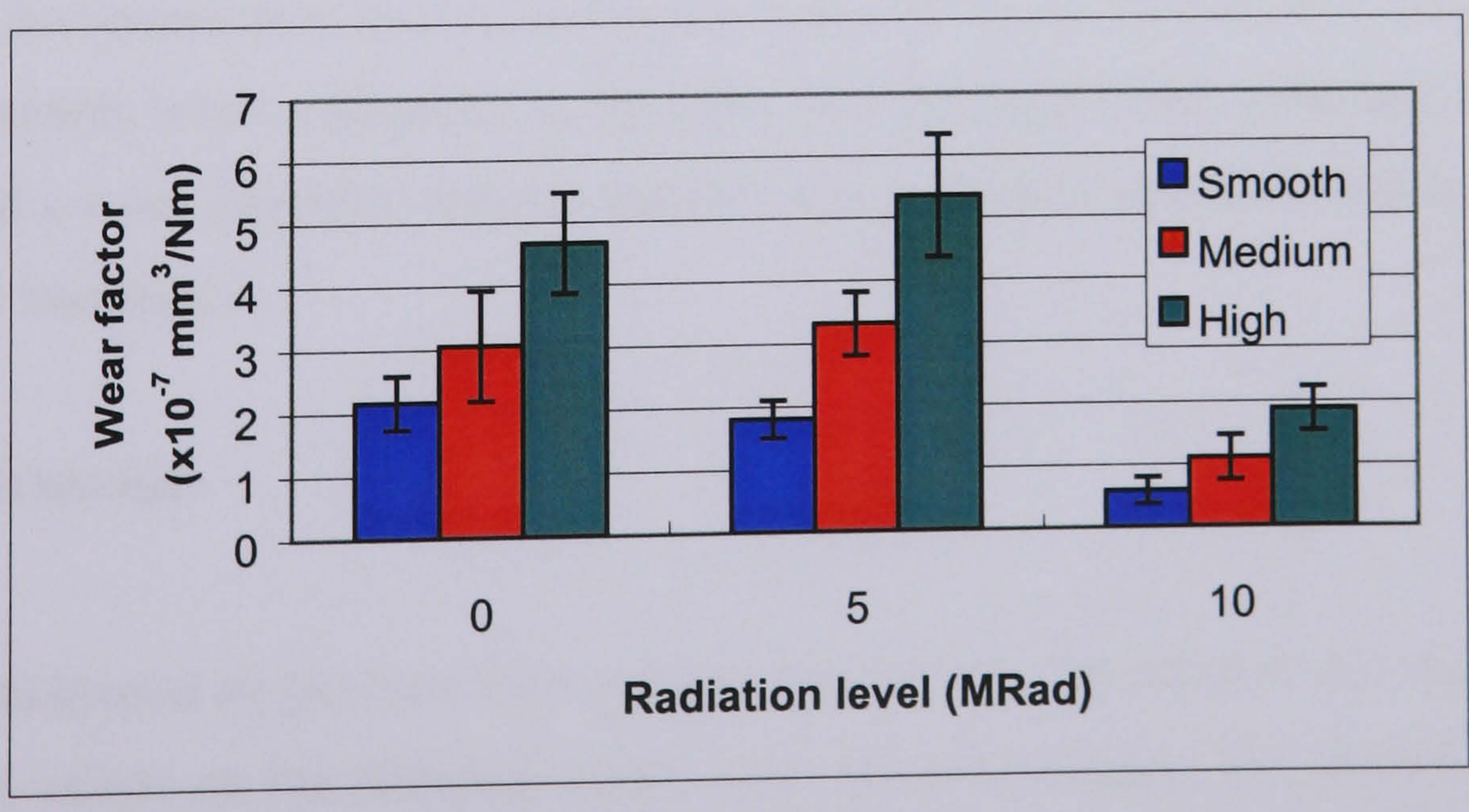

Figure 3.28 Comparison of wear factors with all three counterface conditions and radiation levels.

The percentage wear (by weight loss) of the materials against each counterface with respect to the non-crosslinked materials are shown in Figure 3.29. The reduction in wear observed with the highly crosslinked material could be clearly seen against all the counterfaces. The increase in wear with 5MRad material against scratched counterfaces was also seen.

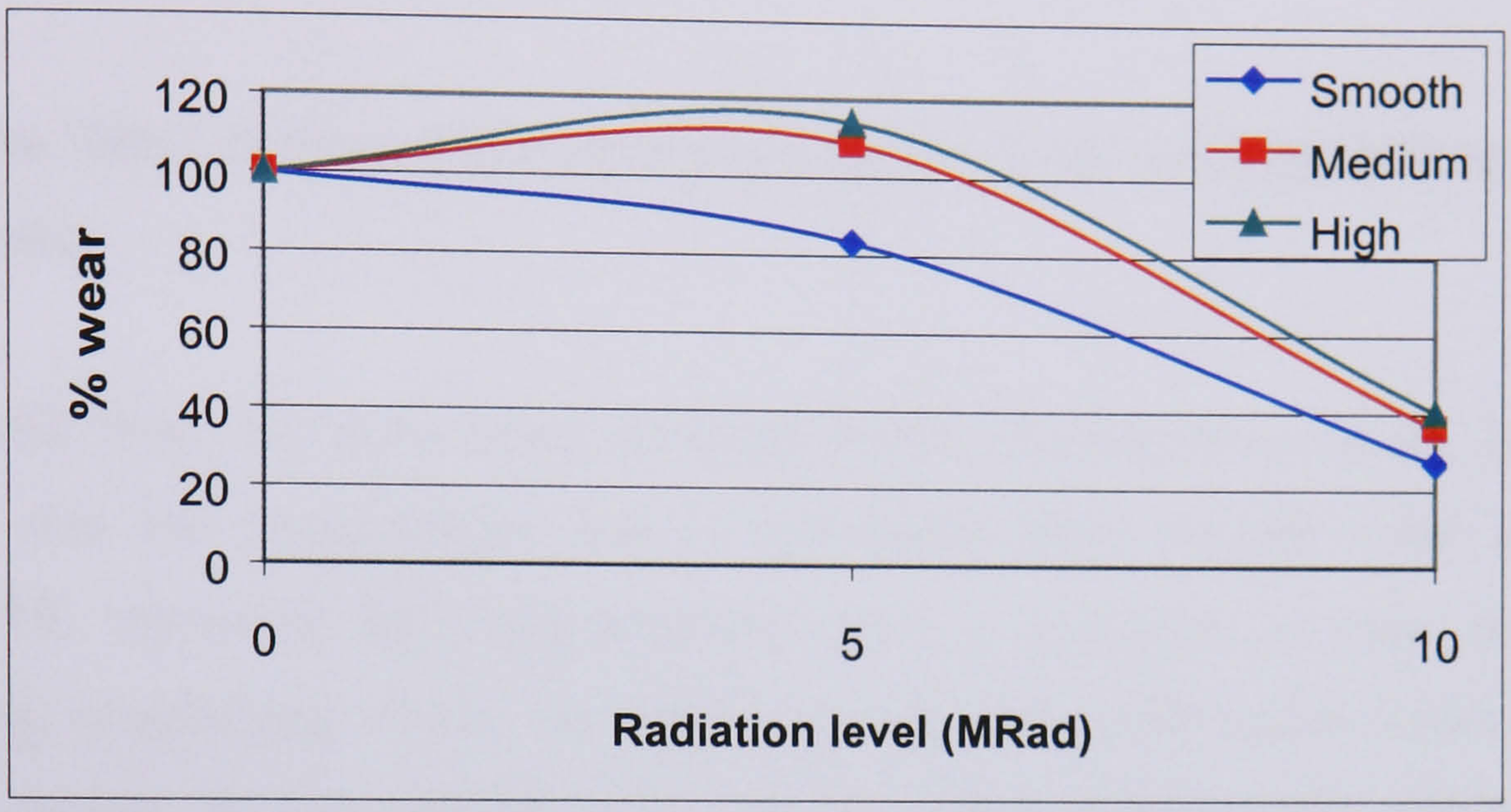

Figure 3.29 Percentage of wear of materials with 0MRad taken as 100%.

SEM micrographs and 3D talysurf images showed that the pins with the highest raised areas on talysurf images also showed the most damage on their surfaces in SEM images. Scratches could be seen on the surfaces which gave the highest wear factors which suggested that they were more damaged therefore giving rise to their increased wear factor. The 10MRad material appeared to have the smoothest surface with all the counterface conditions and this was evident by reduced wear factors and wear volumes when compared to the other two materials. The scratched surfaces produced a more damaged surface and this was consistent with wear moving to an abrasive mechanism.

3.4 Discussion.

The method used to generate the scratches was found to be reliable and repeatable, as the scratches on the different plates were all quite similar. The scratches were shown to be comparable to those seen on explants which had previously been examined by Barbour *et al.* (1999). The high scratches were equivalent to the largest

scratches observed on explants whereas the medium scratches were comparable to less extreme conditions. The measurements taken after testing showed that the scratches all had a slightly lower peak height when compared to before testing. This could have been due to wear of the peaks during testing, or could just have been caused by a variation in the position of the scratch measured, after testing had been completed.

3.4.1. The Effect of Serum Concentrations on the Wear of UHMWPE in Pin on Plate Tests.

The results from the study using different serum concentrations as the lubricant showed that the concentration had a significant effect on the wear rates of UHMWPE. Although both concentrations gave a reduction in wear rate with increasing crosslinking levels, the reduction with 95% (v/v) serum concentration was far greater. This was mainly due to the noncrosslinked material, which gave a significantly higher wear factor at 95% (v/v) serum concentrations compared to 25% (v/v) serum concentrations. The crosslinked materials both showed little difference and no significant difference in wear rates across the two different serum concentrations.

The reduction in wear with crosslinking of the UHMWPE seen with the 95% (v/v) serum concentrations gave a similar pattern to the data presented by McKellop *et al.* (1999) who also used high serum concentrations. At 25% (v/v) serum concentrations the reduction in wear rate was less and similar to that reported by Endo *et al.* (2000) who also used 25% (v/v) serum concentrations.

Using a lubricant containing protein has been shown to be very important in reproducing clinically relevant wear rates. However it has also been shown to be important to use protein concentrations that are within the *in vivo* range. The *in vivo* range is approximately 5mg/ml – 25mg/ml protein (Wang *et al* 1999). The 95% (v/v) serum concentration had protein levels above this concentration, whereas the 25% (v/v) serum concentration was at the lower end of the physiologically relevant range.

The wear factors recorded with the higher serum concentration were surprising, since the results might have been expected to be lower than those tested in 25% (v/v) serum concentrations. It is known that proteins within serum can act as a boundary lubricant, this is because proteins adsorb onto the surface and help to stop adhesive wear. Therefore with the 95% (v/v) serum containing more proteins it was expected that this would help to protect the surface to a greater extent than the 25% (v/v) serum and would produce lower wear rates. As this obviously was not the case some other mechanism must have been involved. This mechanism could have been protein precipitation.

After testing the serum was more opaque than at the start. This was probably due to protein precipitation. Excessive protein precipitation can reduce the boundary lubricating properties of the lubricant and artificially increase the friction and wear rates (Lu *et al.*, 1997). As all the results at the higher protein concentration were above what was expected this could have occurred, especially as protein precipitation is accelerated by the high temperatures generated during testing. With the lower serum concentration there are less proteins in the lubricant and therefore this is not as much of a problem.

The surfaces of all the pins after testing, appeared to have a rippled surface which showed that adhesive wear was the main mechanism involved. Rippling has been seen in explants by Jasty *et al.* (1997). The 3D talysurf images of the pins worn in 95% (v/v) serum all appeared to be smoother than the pins worn in 25% (v/v) serum. This could have been due to reattachment of polyethylene onto the surface of the pins at 25% (v/v) serum concentration which made the surface appear rougher.

The 95% (v/v) serum concentration had protein levels which were above what is present *in vivo*. Therefore the rest of the tests were run in 25% (v/v) serum which contained more clinically relevant levels of proteins.

3.4.2. Multidirectional Smooth Pin on Plate Wear Test.

The results from the smooth counterface experiments showed that the wear factor decreased as the crosslinking level increased. Previous studies, such as those by

Marrs *et al.* (1999) and Endo *et al.* (2000), have also shown a reduction in wear with crosslinked UHMWPE against smooth counterfaces. The reduction in wear rates is thought to be due to the effect of orientational hardening and softening. During unidirectional motion orientational hardening occurs. This means that the molecules orientate themselves with the direction of sliding resulting in a material which is strong in the direction of motion but weaker perpendicular to it. The frictional force remains in a constant direction, and therefore the direction of motion and also the direction in which the molecules are aligned remains constant. In multidirectional motion the frictional force constantly changes direction with respect to the polymer surface. This means that the frictional force is sometimes parallel to the direction of orientational softening and sometimes parallel to orientational hardening. Crosslinking reduces the amount of orientational hardening and softening, as it retards chain mobility and provides resistance to the cross shear forces (Pooley *et al.*, 1972; Wang *et al.*, 1997). Crosslinking also results in more C-C bonds between molecules which makes it harder to split them. The more crosslinking in the material, the more bonds that are present. This means that there is less orientational hardening and softening, which is why a reduction in wear rate was seen as the crosslinking levels increased.

Against a smooth counterface the main wear mechanism involved is an adhesive wear mechanism. This is when parts of the UHMWPE surface are removed after many interactions of the harder counterface asperity. The UHMWPE eventually breaks off due to fatigue. In this situation the mechanism is likely to be microadhesive wear which is when surface rupture of the polyethylene occurs rather than subsurface rupture. With subsurface rupture more damage would have been seen on the surfaces of the polymer pins.

3.4.3. Multidirectional Medium and High Scratched Pin on Plate Wear Tests.

When worn against scratched counterfaces there was a significant increase in wear factors for all the materials. However the 10MRad material had a significantly lower wear factor than the other two materials. Between the 0MRad and 5MRad materials there was no significant difference between the wear factors.

On scratched counterfaces an abrasive wear mechanism is more likely to occur. This means that orientational hardening is less able to happen, as the molecules are removed by a single asperity interaction. Other factors therefore become more important. The scratches on the counterface plough into the softer polymer surface causing particles to generate. Wear particles can be removed by one movement and therefore the wear rate increases. The higher scratches create more of a stress concentration when they cut into the polymer and are more likely to cause wear debris generation than the medium scratches.

The crosslinks still gave more protection against the scratches than the non-crosslinked material which is shown by its significantly lower wear factor. The links in the material provide resistance to the scratches and prevent particles breaking away as easily. As the 5MRad material contains fewer crosslinks they do not provide the same protection and this means it has a much higher wear factor than the highly crosslinked material.

3.5. Conclusion.

The largest reduction in wear rate produced by crosslinking was found with high concentrations of bovine serum and these results were consistent with those previously reported for similar serum concentrations (McKellop *et al.*, 1999). At lower concentrations of serum, as defined by the ISO standard, the reduction in wear produced by crosslinking was less. This difference may be due to a more adhesive wear mechanism occurring with the lower serum concentration.

Damage to the counterface increased the wear rate for all the materials as the wear moved to a more abrasive mechanism. Minakawa *et al.* (1998) have shown that ceramic has a much higher resistant to accidental damage then metal. This means that it would be an advantage to use crosslinked PE against damage resistance ceramic femoral heads.

This study has shown that the reduction in wear produced by crosslinking was critically dependent on the protein concentration of the lubricant and counterface

roughness. These factors need to be taken into account when predicting the functional biological activity and osteolytic potential that can be achieved with crosslinked polyethylene.

Chapter 4.

4. Pin on Plate Wear Studies with 20° Rotation under Three Different Counterface Conditions for Three Different Levels of Crosslinking.

4.1. Introduction.

In this study, a pin on plate rig was used to compare the wear rates of UHMWPE which had been irradiated at three different radiation levels. Lower levels of multidirectionality were applied, so that the kinematics in the rig were less multidirectional then those seen in a hip joint and were more comparable to those seen in a knee.

The aim of this study was to compare the effect of changes in counterface condition at a lower degree of rotation than the previous study for the same three levels of crosslinking.

4.2. Materials and Methods.

4.2.1 Materials.

The material studied was UHMWPE GUR 1050, which had been irradiated at three different levels as described in Chapter 2. The three materials were non-crosslinked – 0MRad, moderately crosslinked – 5MRad, and highly crosslinked – 10MRad. The pins were machined to have a flat wear surface with a diameter of 8mm. They were soaked in de-ionised water for at least four weeks before testing. The counterface surface was high nitrogen stainless steel. Three counterfaces were used during testing. These were a smooth surface, and two scratched surfaces. The height and FWHM were compared with scratches measured on explants by Barbour *et al.* (1999).

4.2.2. Method for Pin on Plate Tests.

The experiments were all carried out on a multidirectional pin on plate machine which has previously been described in Chapter 2. Tests were carried out at ±20° rotation. This gave lower levels of cross shear frictional energy than the previous study. The tests investigated the effect that the counterface roughness had on the wear rates. Scratches were achieved as described in Chapter 2. For the tests two different scratch heights were used. These were a medium scratch with an average Rp of 0.46μm and a high scratch with an average Rp of 1.4μm. Different loads were used to attain the two scratch heights. A load of 2.8N was used for the high scratches and 1.5N for medium scratches. They were applied at 5mm intervals along the length of the wear track. The smooth plates had an average Ra of 0.01μm. The average surface roughness and peak height of the scratches on the plates before testing are shown in Table 4.1.

Plate surface	**Plate number.**					
	1	**2**	**3**	**4**	**5**	**6**
Average surface roughness Ra of smooth plates (μm)	0.01	0.01	0.01	0.01	0.01	0.01
Average peak height of medium scratches (μm)	0.449	0.79	0.23	0.25	0.34	0.36
Average peak height of high scratches. (μm)	1.91	1.34	1.68	1.17	1.27	1.23

Table 4.1 Average surface roughness and scratch height before testing.

Two pins of each radiation level were run on smooth plates for three weeks and then this was repeated for a further three weeks with new pins. The whole method was further repeated with different pins against the scratched plates. During testing the pins were rotated across the plates to reduce the plate variability from affecting the

overall wear factors. For these experiments a 25% (v/v) serum concentration was used. For all the tests a stroke length of 10mm and a load of 160N was applied. Control pins from each radiation level were placed in the same lubricant as the wear pins in order to monitor moisture uptake during the test. The weight was either subtracted or added depending on whether the pins had absorbed or lost fluid. Wear factors were calculated (Chapter 2.) and analysed using one way ANOVA followed by calculation of the MSD using the T method.

4.3. Results.

The results of the peak height, and full width half maximum of the scratches on the counterface were compared to scratches seen on explants by Barbour *et al.* (1999). The results are shown in Figure 4.1. They showed that the peak height and FWHM of the scratches were comparable to those seen on explants. The high scratches resembled the severe scratches seen on explants while the medium scratches were comparable to smaller scratches observed *ex vivo*.

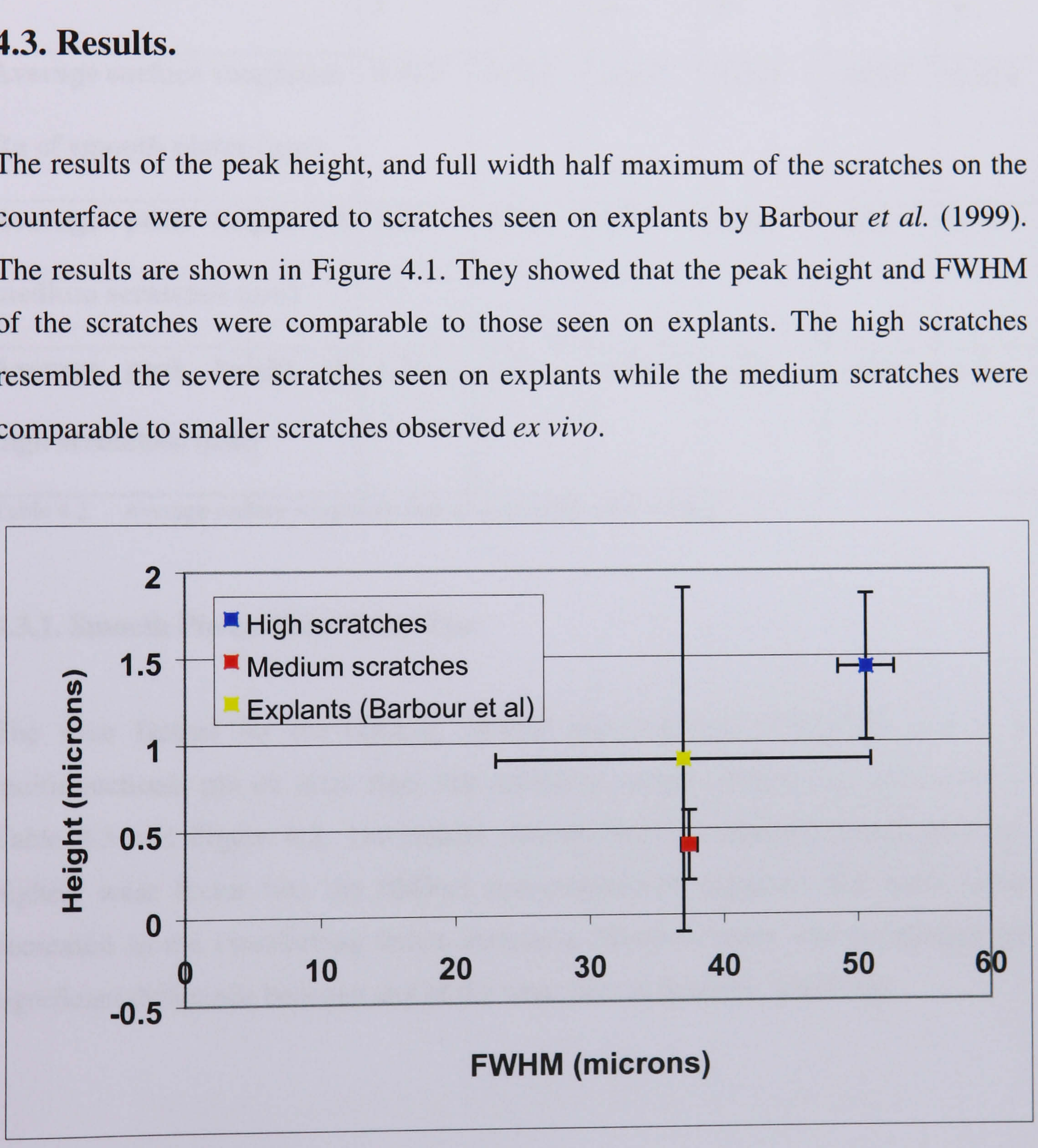

Figure 4.1 Comparison of FWHM against peak height for high and medium scratches with explants.

The average surface roughness and peak height after testing was completed are shown in Table 4.2. In all tests the plates had no significant change in their surface roughness after testing. The scratch heights differed in whether they had gained or lost height. This could have been due to a slightly different part of the scratch being measured after testing.

Plate surface	**Plate number**					
	1	**2**	**3**	**4**	**5**	**6**
Average surface roughness Ra of smooth plates (μm)	0.019	0.015	0.013	0.015	0.012	0.014
Average peak height of medium scratches (μm)	0.32	0.70	0.53	0.46	0.31	0.27
Average peak height of high scratches. (μm)	1.38	1.9	1.63	1.28	1.23	1.7

Table 4.2 Average surface roughness and scratch height after testing.

4.3.1. Smooth Pin on Plate Wear Test.

The wear factors for the 0MRad, 5MRad and 10MRad UHMWPE pins in a multidirectional pin on plate wear test against a smooth counterface are shown in Table 4.3 and Figure 4.2. The results showed that the material which gave the highest wear factor was the 0MRad non-crosslinked material. The wear factor decreased as the crosslinking levels increased. However there was no statistically significant difference between any of the wear factors ($p>0.05$; ANOVA).

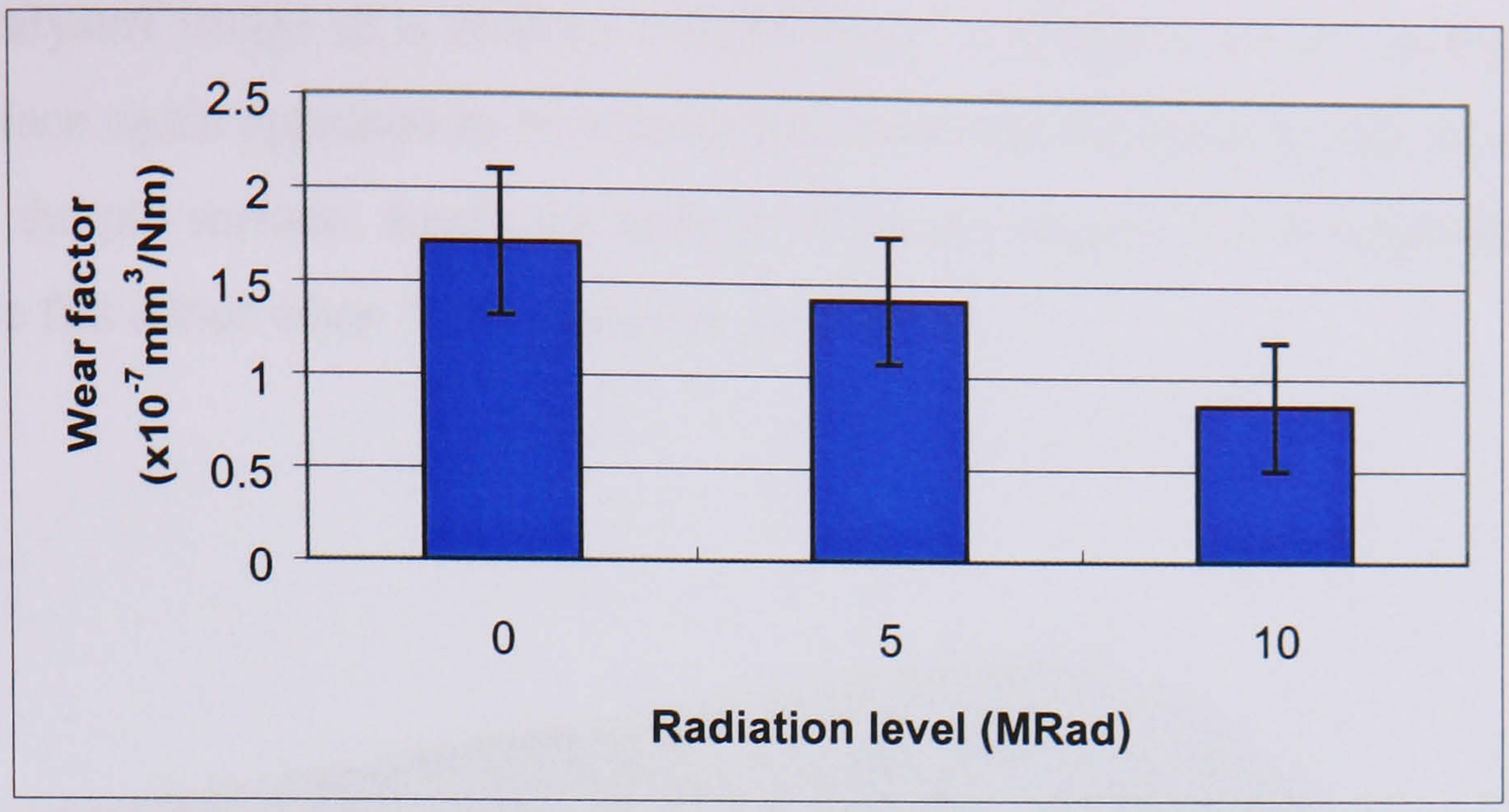

Figure 4.2 Average wear factors after six weeks on smooth plates ± 95% confidence limits.

A 3D talysurf image of a 0MRad UHMWPE pin surface is shown in Figure 4.3. The surface appeared to be smooth with only a few small raised areas. The surface of the pin sloped from one side to the other which suggested that the pin was not flat while it was being tested or it could have been due it not being laid flat during measurement. However, the difference in height of each side of the pin was very small.

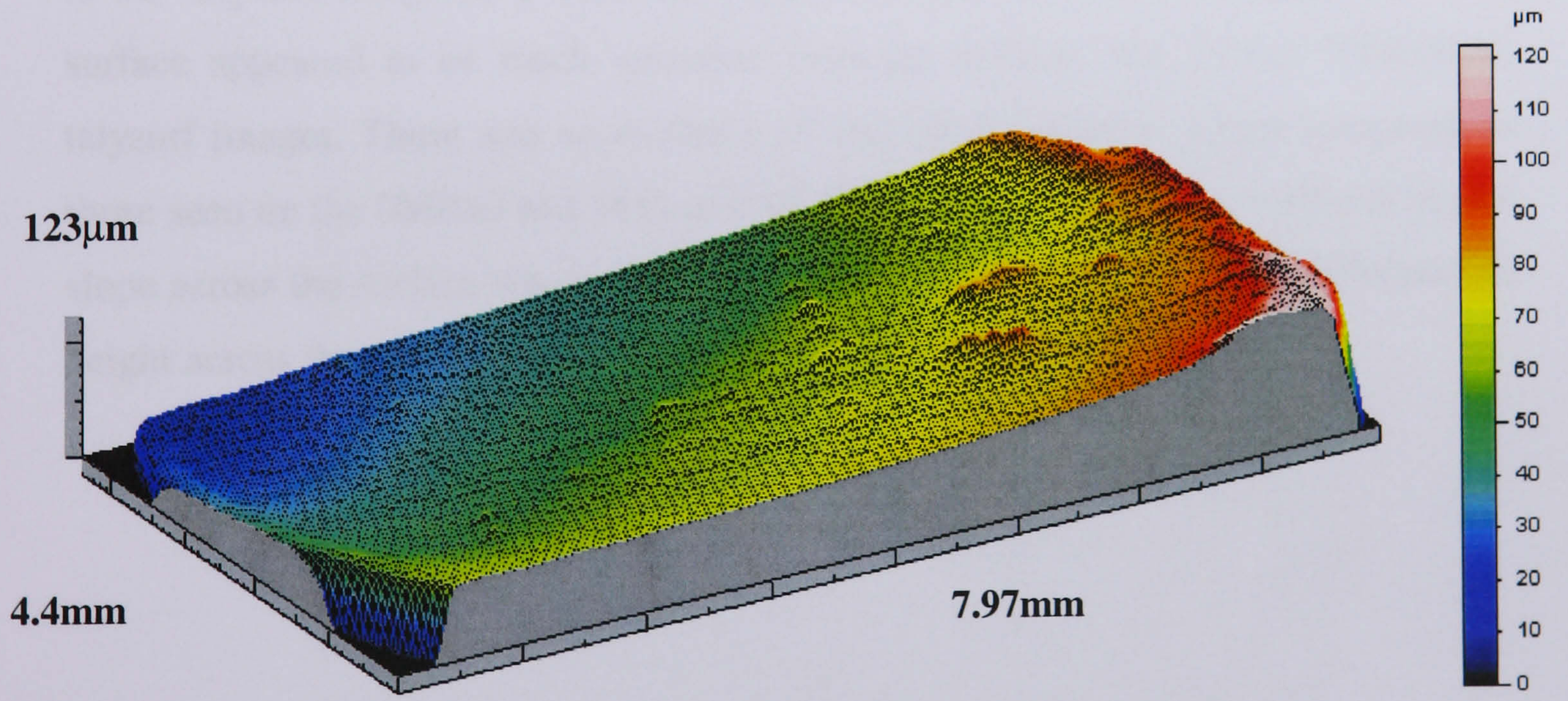

Figure 4.3 3D talysurf image of a 0MRad UHMWPE pin run against a smooth counterface.

A 3D talysurf image of a 5MRad UHMWPE pin surface is shown in Figure 4.4. The surface again appeared to be smooth but there was evidence of ridges near each edge of the pin surface. Again the surface of the pin sloped which suggested it was not quite flat either when it was tested or measured.

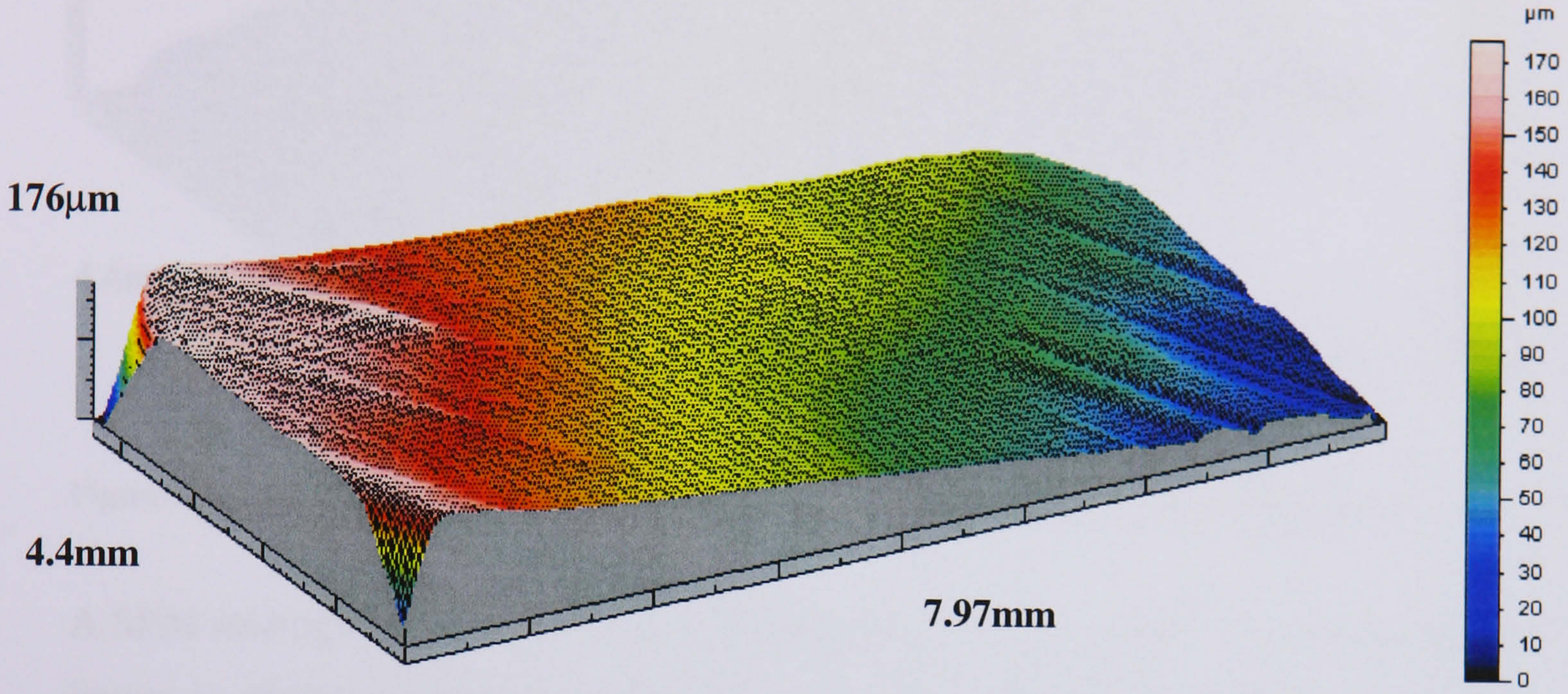

Figure 4.4 3D talysurf image of a 5MRad UHMWPE pin run against a smooth counterface.

A 3D talysurf image of a 10MRad UHMWPE pin is shown in Figure 4.5. This surface appeared to be much smoother than the 0MRad and 5MRad UHMWPE talysurf images. There was no evidence of any raised areas or bumps compared to those seen on the 0MRad and 5MRad UHMWPE images. It did however still have a slope across the surface which was seen on the other pins although the difference in height across the pin was smaller than for the 0MRad and 5MRad pins.

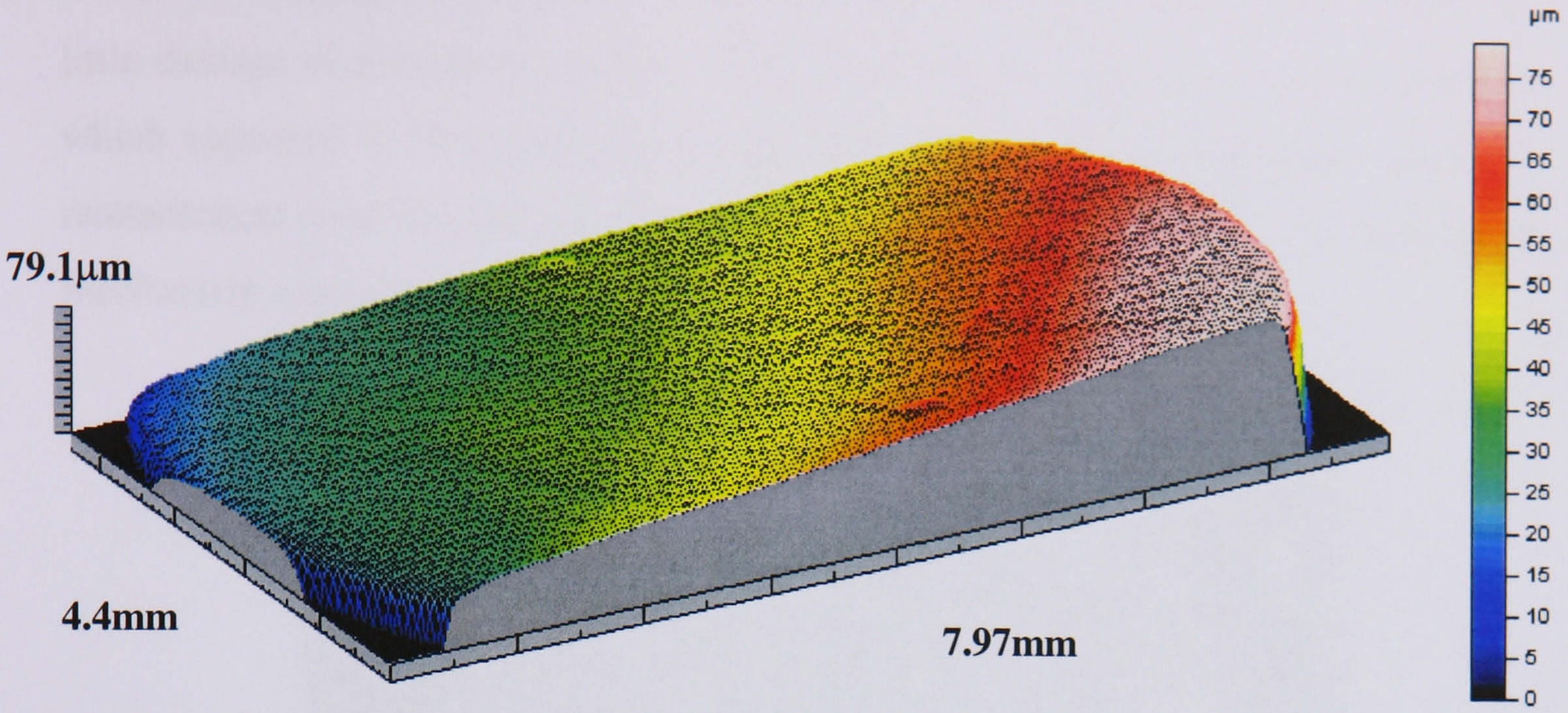

Figure 4.5 3D talysurf image of a 10MRad UHMWPE pin run against a smooth counterface.

A SEM micrograph of the 0MRad UHMWPE pin which is shown in the 3D talysurf image is shown in Figure 4.6. There were signs of some small particles on the surface. These could have been about to come away from the surface or could have reattached. There was also an indication of ripples across the surface. This was not unexpected since ripples are a sign of adhesive wear which is the wear mechanism which predominates on a smooth surface.

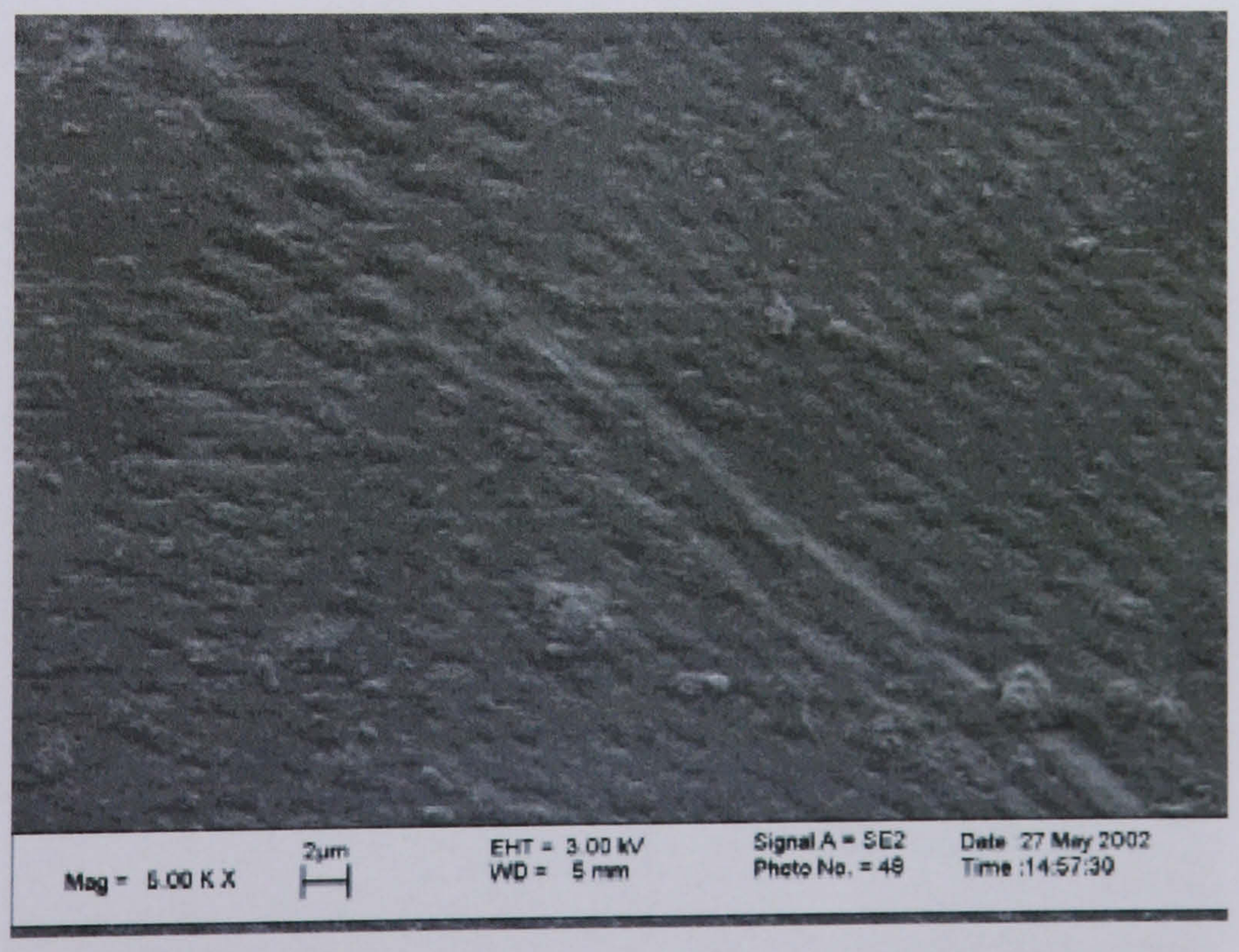

Figure 4.6 SEM micrograph of a 0MRad UHMWPE pin run against a smooth counterface.

A SEM micrograph of a 5MRad UHMWPE pin is shown in Figure 4.7. There was little damage visible on the surface of the pin although some areas showed particles which appeared to be coming away from the surface. These could also have been reattachment onto the surface. The signs of ripples indicated that an adhesive wear mechanism was occurring.

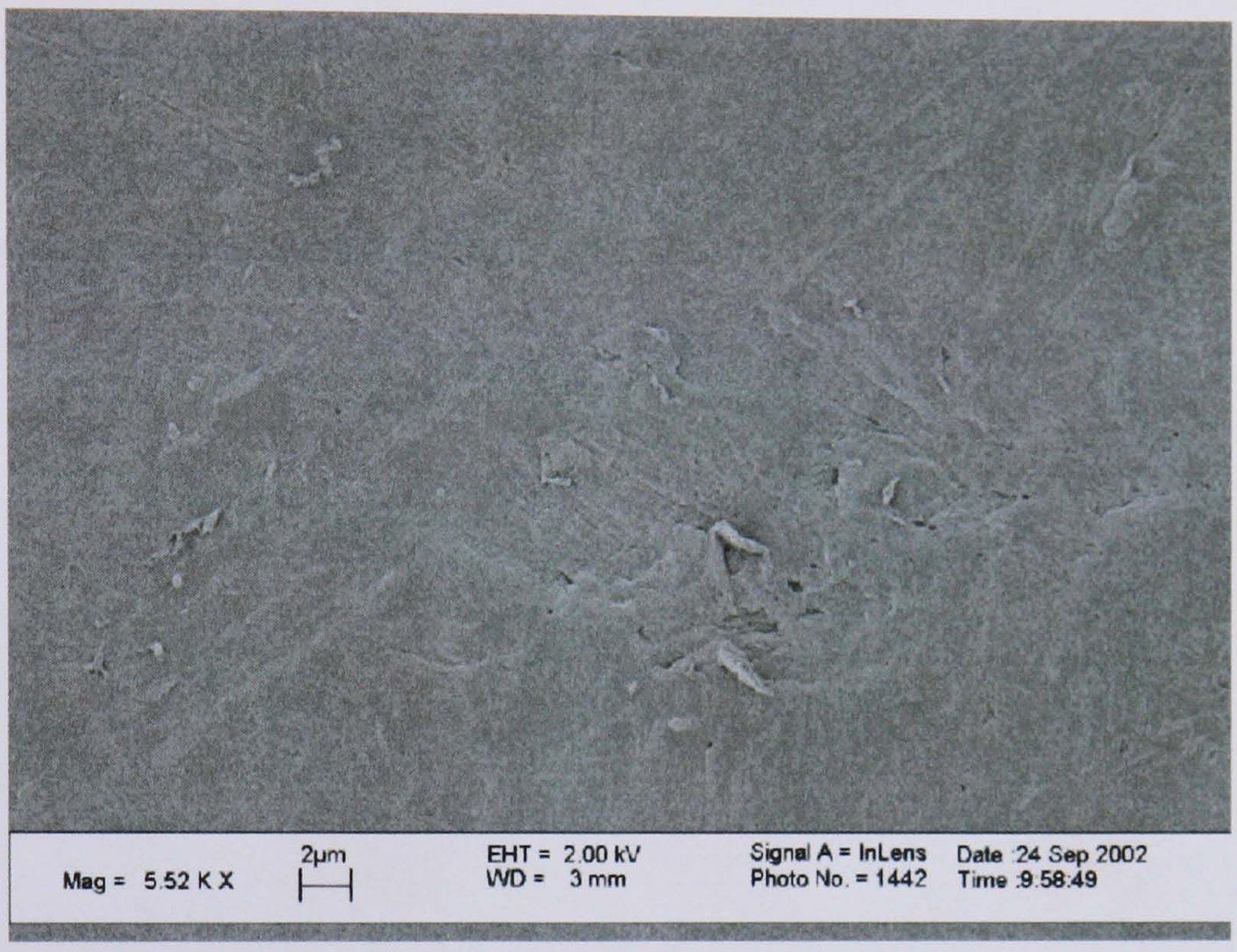

Figure 4.7 SEM micrograph of a 5MRad UHMWPE pin run against a smooth counterface.

A SEM micrograph of a 10MRad UHMWPE pin is shown in Figure 4.8. This again did not appear to have much damage on the surface. Small particles were visible which could have been detaching from the surface.

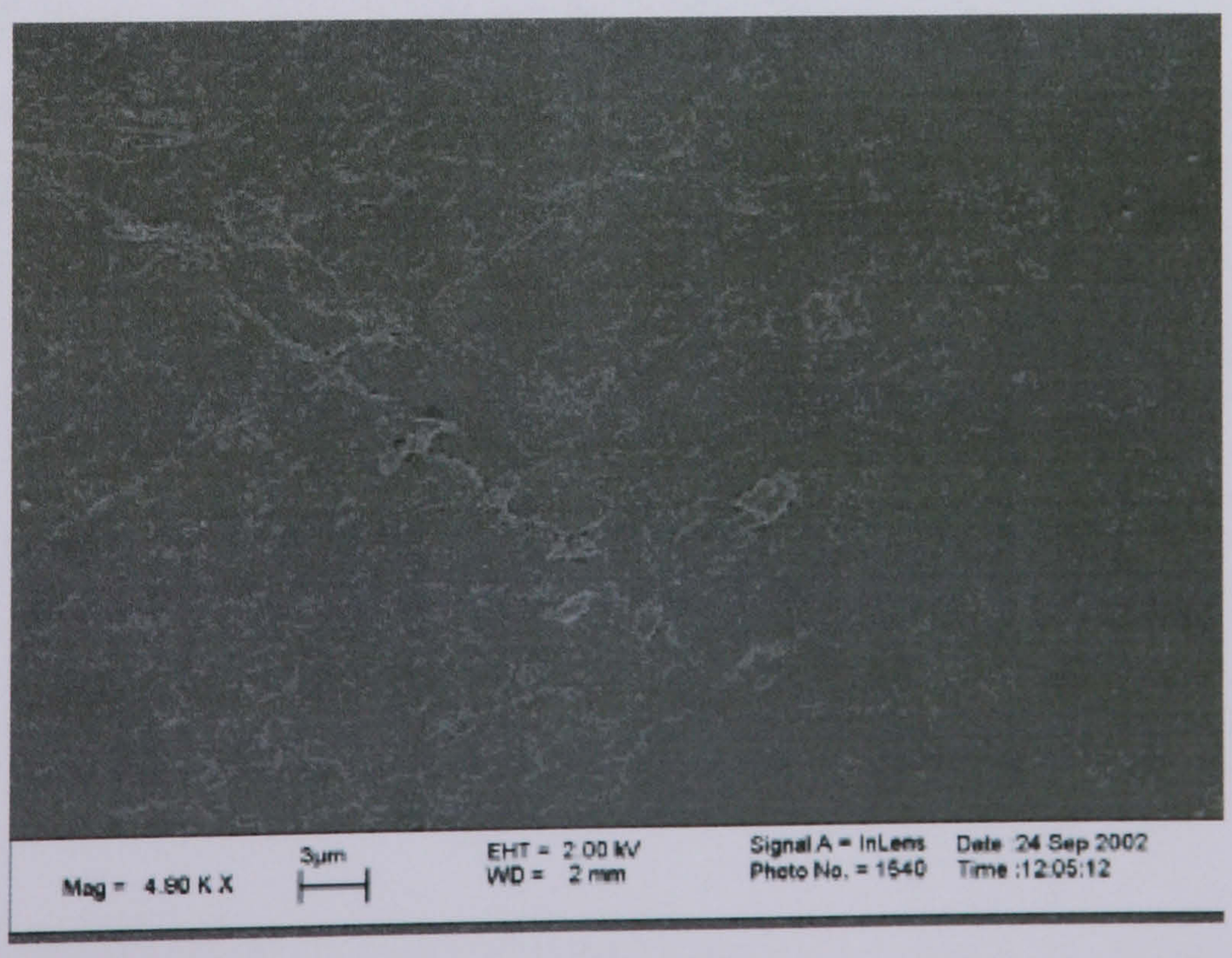

Figure 4.8 SEM micrograph of 10MRad UHMWPE pin run against a smooth counterface.

4.3.2. Medium Scratched Pin on Plate Wear Tests.

The wear factors for the 0MRad, 5MRad and 10MRad UHMWPE pins in a multidirectional pin on plate test against a medium scratched counterface are shown in Figure 4.9 and Table 4.3. The results showed that there was no significant difference between the wear factors of the 0MRad and 5MRad materials. The 10MRad crosslinked material had a much lower wear rate than the other two materials. This difference was shown to be statistically significantly different for both materials ($p<0.05$; ANOVA).

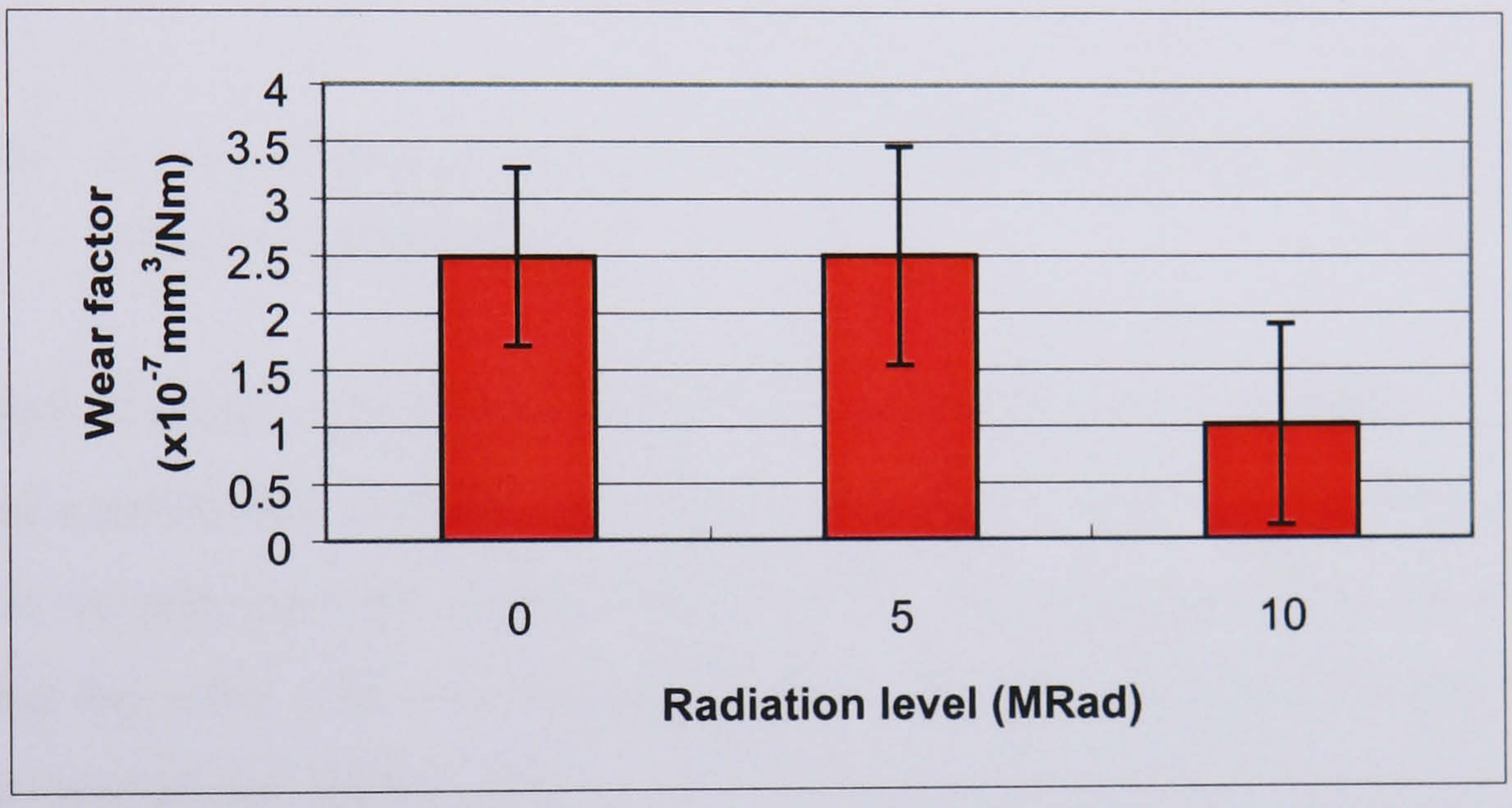

Figure 4.9 Average wear factors from six weeks on medium scratched plates ± 95% confidence limits.

A 3D talysurf image of the surface of one of the 0MRad pins which was tested is shown in Figure 4.10. The surface of the pin was sloped suggesting it was not totally flat either when tested or measured. There were a few peaks in the surface but not much sign of any other damage.

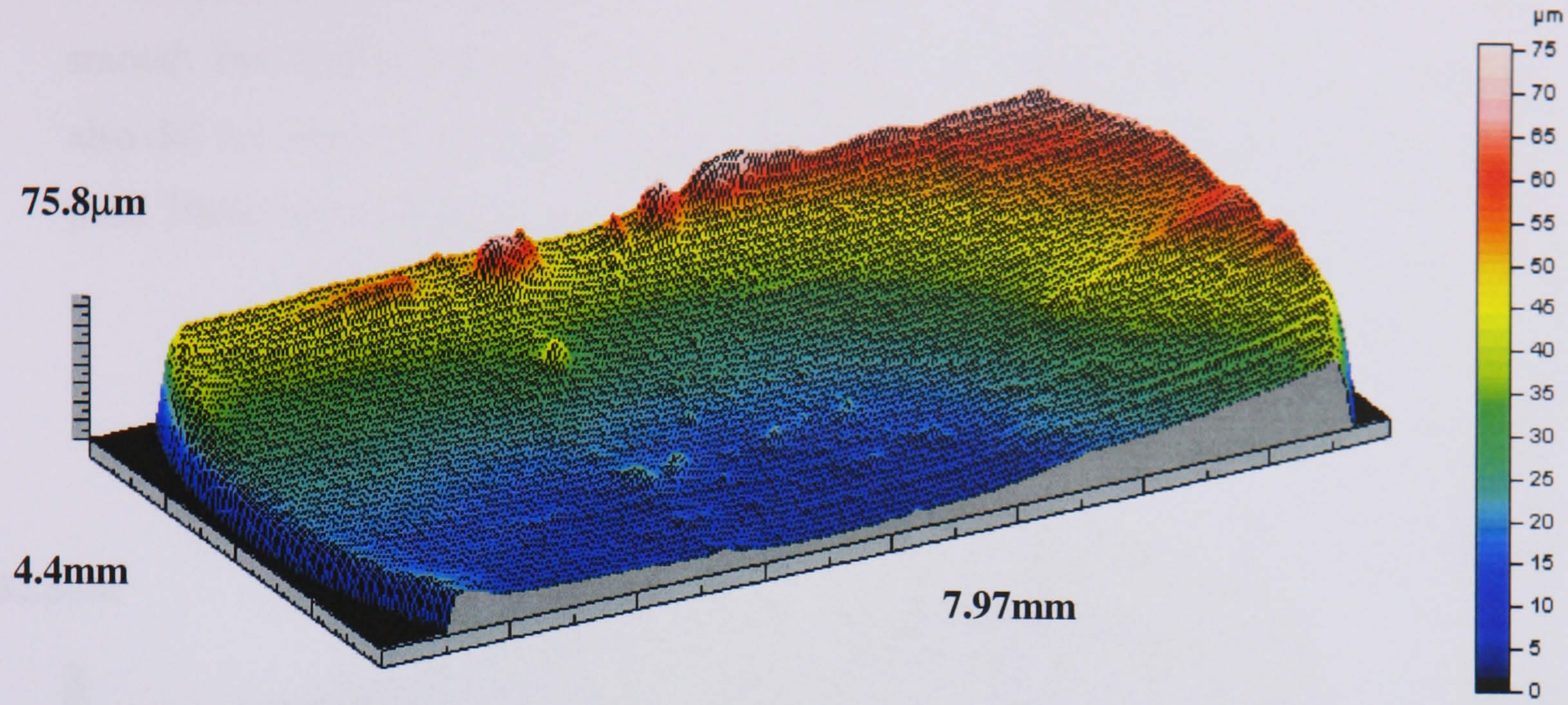

Figure 4.10 3D talysurf image of the surface of a 0MRad UHMWPE pin run against a medium scratched counterface.

A 3D talysurf image of a 5MRad UHMWPE pin which was tested against a medium scratched counterface is shown in Figure 4.11. The surface of this pin was also sloped as the previous pin surfaces were. At one end of the pin there were signs of ridges but the other end was much smoother. The damage to the surface was less than that seen on the 0MRad pin.

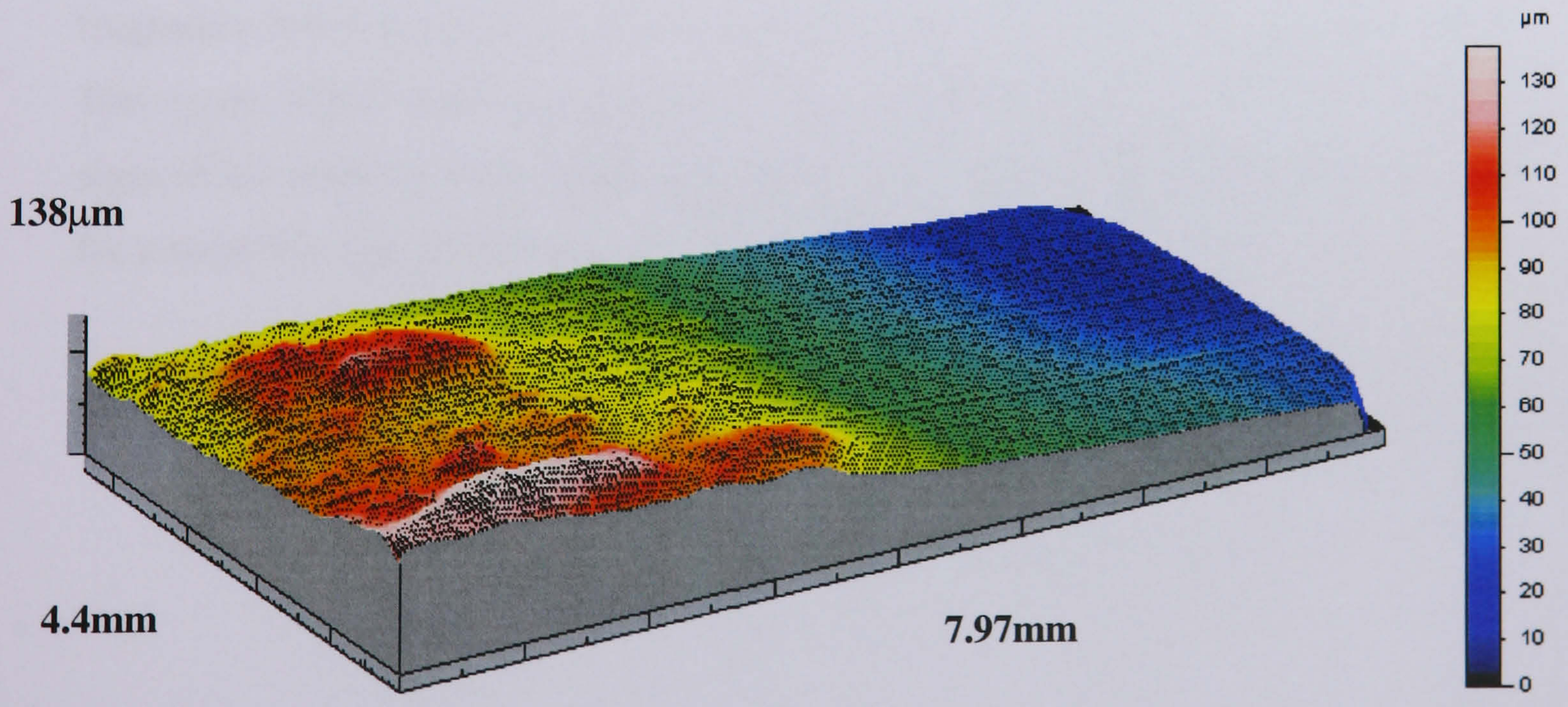

Figure 4.11 3D talysurf image of the surface of a 5MRad UHMWPE pin run against a medium scratched counterface.

A 10MRad UHMWPE pin is shown in Figure 4.12. The surface of this pin was smooth but sloped although not to the same extent as the previous two pins. The pin also did not have the raised areas and signs of damage which were seen on the other pins. There was a slight scratch at one end but this was very shallow.

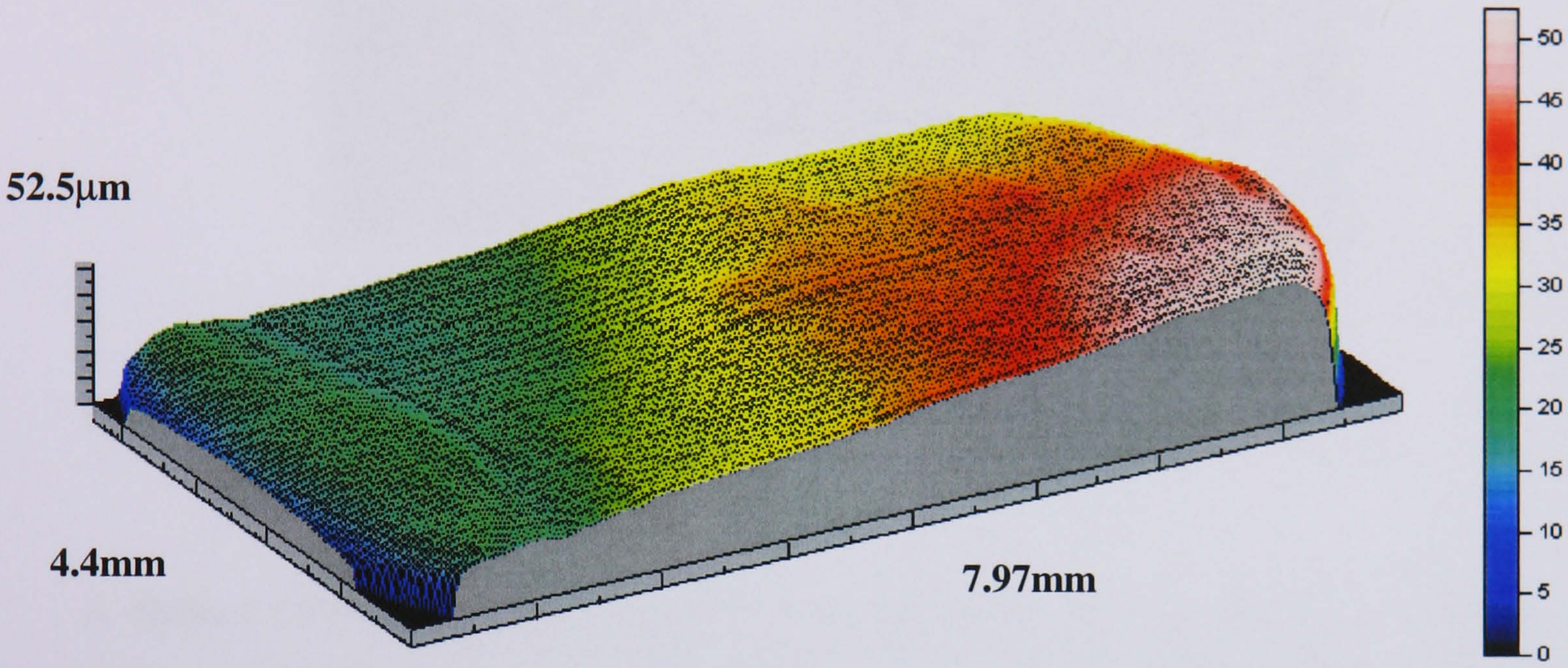

Figure 4.12 3D talysurf image of a 10MRad UHMWPE pin run against a medium scratched counterface.

SEM micrographs of small areas of the surfaces of the pins are shown in Figures 4.13-4.15. The 0MRad UHMWPE pin had a large area of ripples and also some fragments which could have been particles which were detaching from the surface. The ripple effect could be related to an adhesive wear mechanism. There were no signs of an abrasive wear mechanism taking place which would have been expected for a scratched test (Figure 4.13).

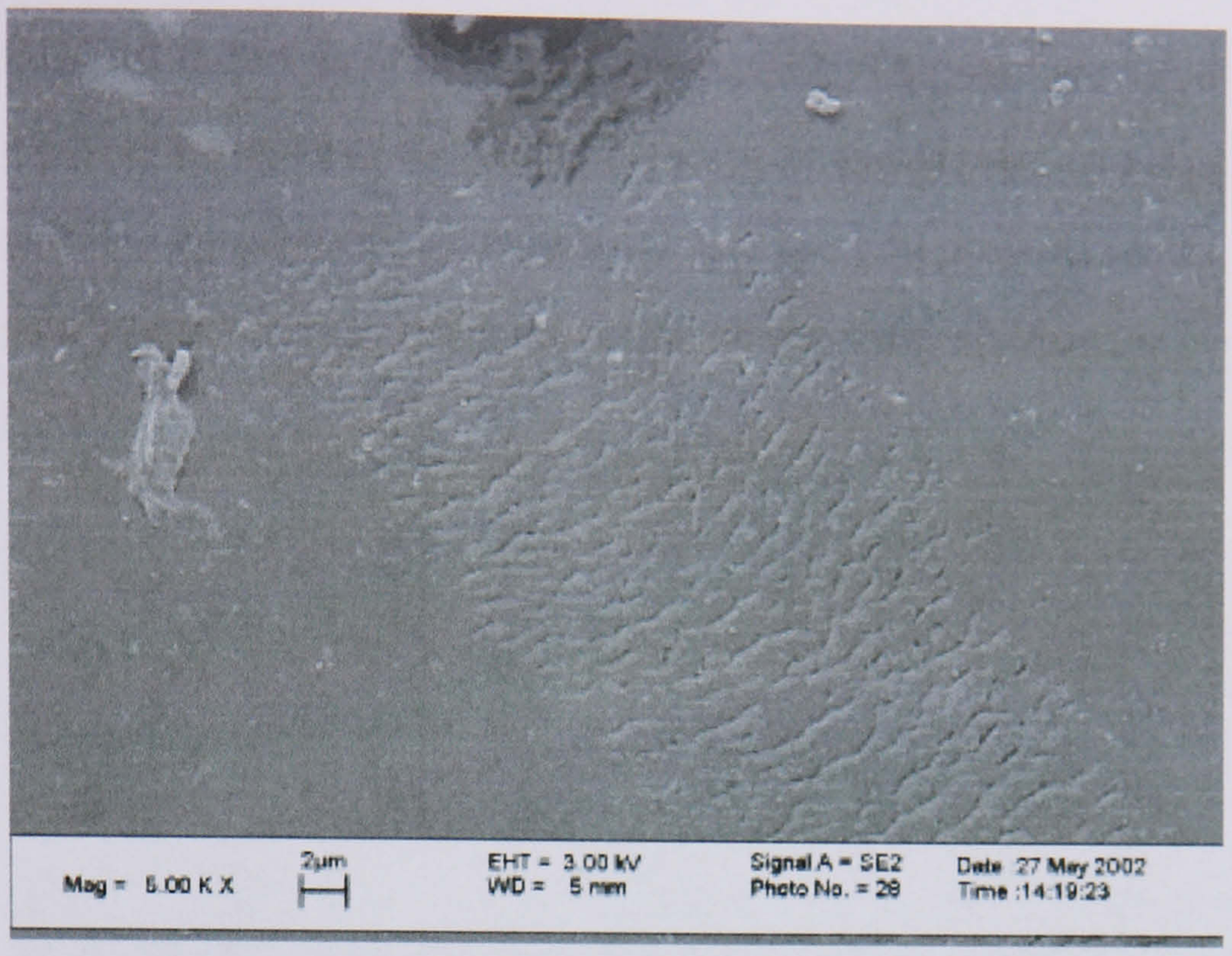

Figure 4.13 SEM micrograph of an area of a 0MRad UHMWPE pin run against a medium scratched counterface.

A 5MRad UHMWPE pin tested against medium scratched counterface is shown in Figure 4.14. This surface did not have the ripples which were seen on the 0MRad pin. There were large areas which looked like flakes that were either about to come off the surface or could have reattached to the surface. These wear mechanisms are associated with an adhesive wear process.

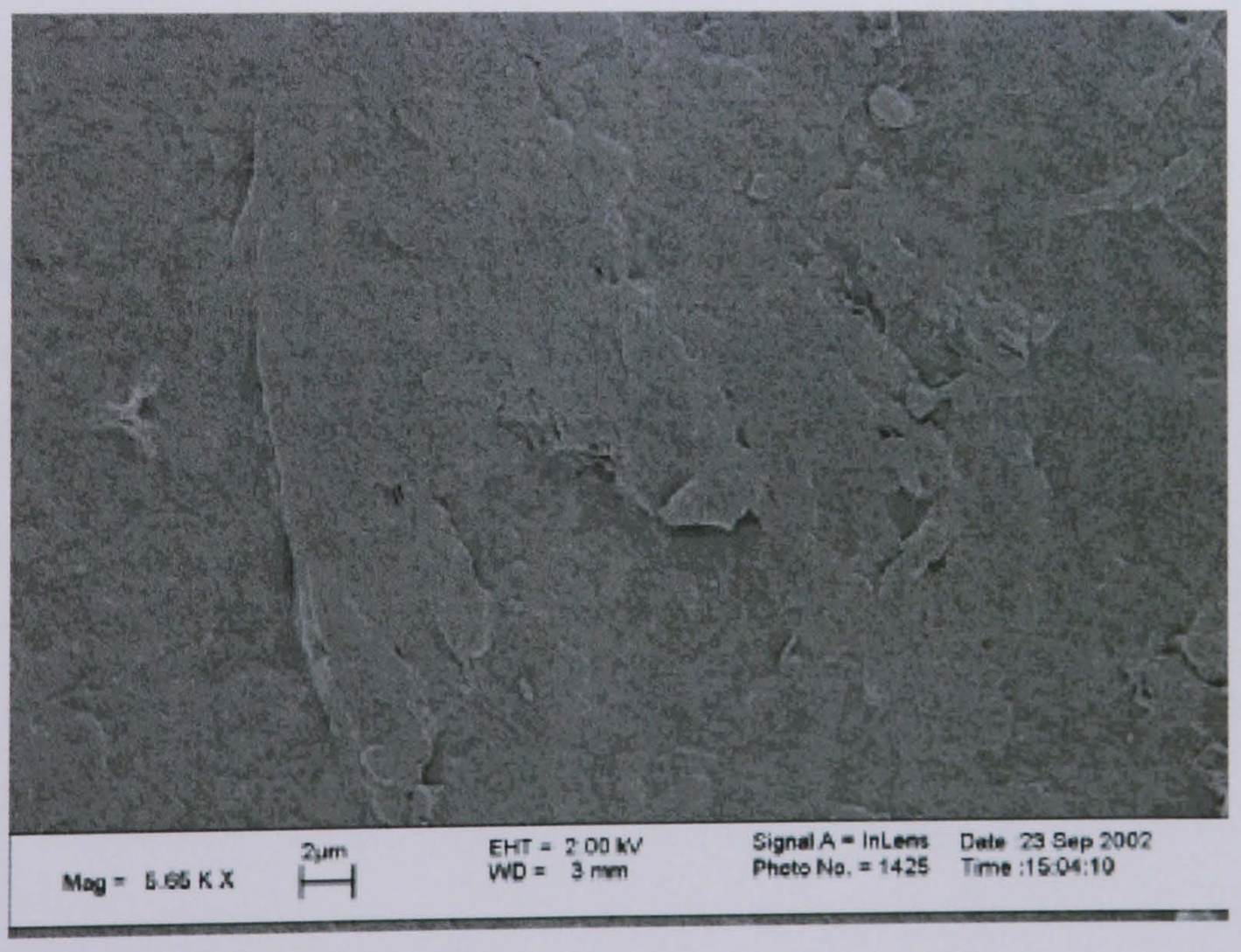

Figure 4.14 SEM micrograph of an area of a 5MRad UHMWPE pin run against a medium scratched counterface.

A SEM micrograph of the 10MRad material tested against a medium scratched counterface is shown in Figure 4.15. This pin also did not have the ripples which were clearly visible on the 0MRad material. The surface appeared quite smooth but contained a few areas of damage which could be where material had been removed from the surface.

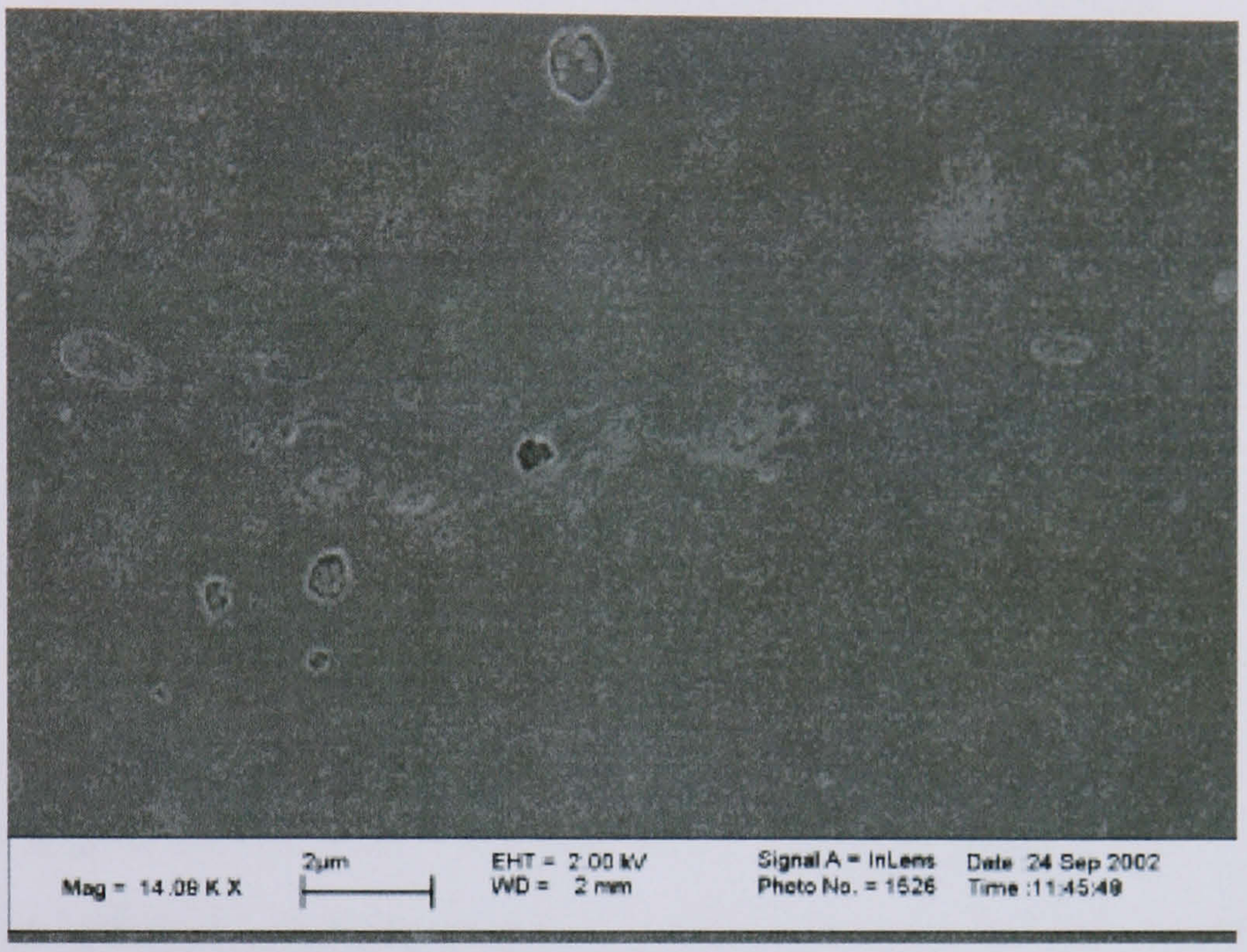

Figure 4.15 SEM micrograph of a 10MRad UHMWPE pin run against a medium scratched counterface.

4.3.3. Multidirectional High Scratched Pin on Plate Wear Tests.

The wear factors for the 0MRad, 5MRad and 10MRad UHMWPE pins in multidirectional pin on plate wear tests against a highly scratched counterface are shown in Figure 4.16 and Table 4.3. The results showed that the highest wear factor for this test was for the noncrosslinked material. The 5MRad UHMWPE had a slightly lower wear factor but the difference was not significantly different. The 10MRad material had an even lower wear factor and this difference was statistically significantly different to both the other materials.

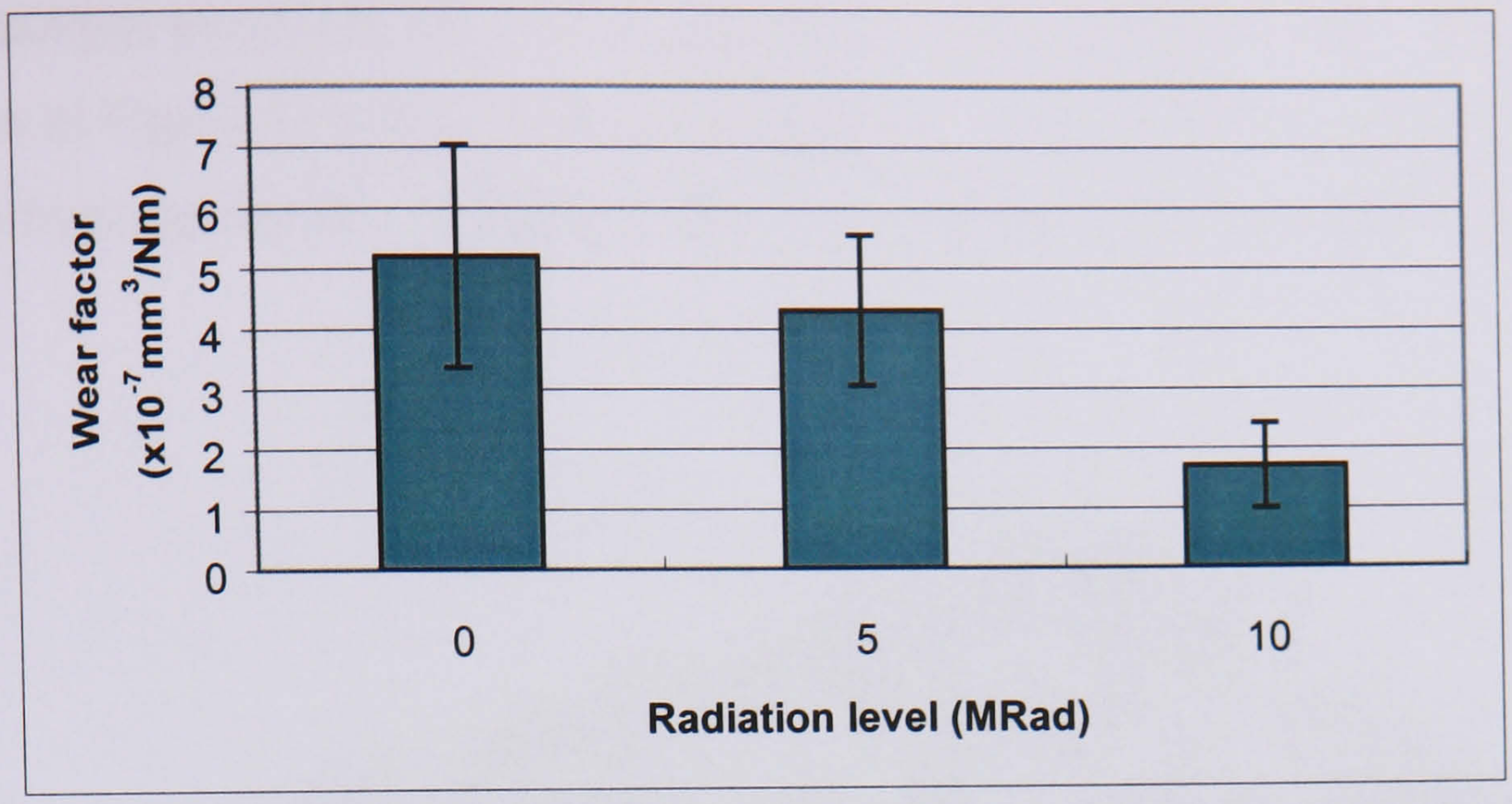

Figure 4.16 Average wear factors from six weeks on high scratched plates ± 95% confidence limits.

3D talysurf images of the surfaces of the pins after testing against a highly scratched counterface are shown in Figures 4.17-4.19. The 0MRad UHMWPE pin surface had a raised area at one edge which went steeply down to the rest of the surface. The rest of the surface appeared to be smooth with only two little peaks visible. The surface did not have a gradual gradient across it as was seen on a lot of the other pin surfaces (Figure 4.14).

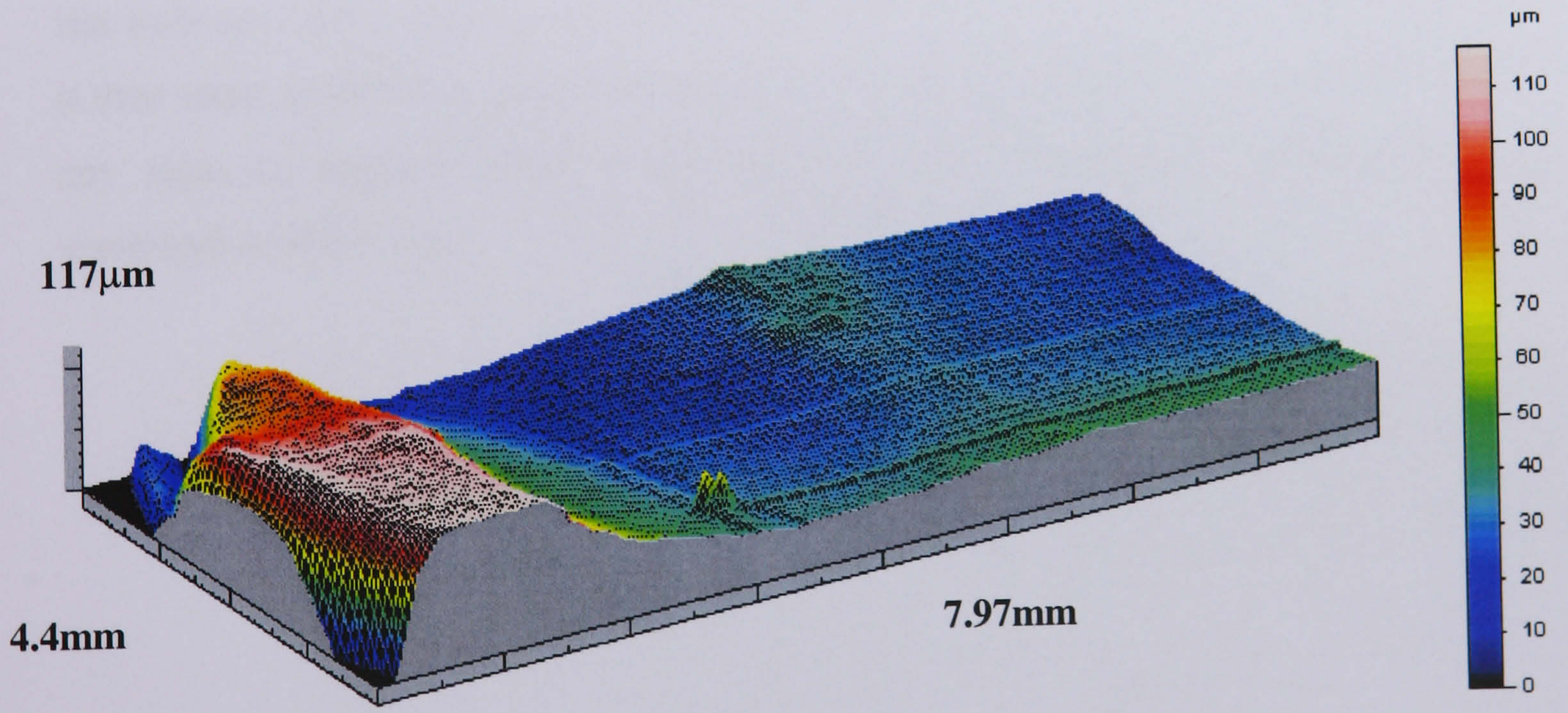

Figure 4.17 3D talysurf image of a 0MRad UHMWPE pin surface run against a highly scratched counterface.

A 5MRad pin which has been worn against the same counterface as the 0MRad pin is shown in Figure 4.18. The surface appeared to be smooth with no visible signs of damage from the testing. The surface did have a bigger slope than most of the other pins.

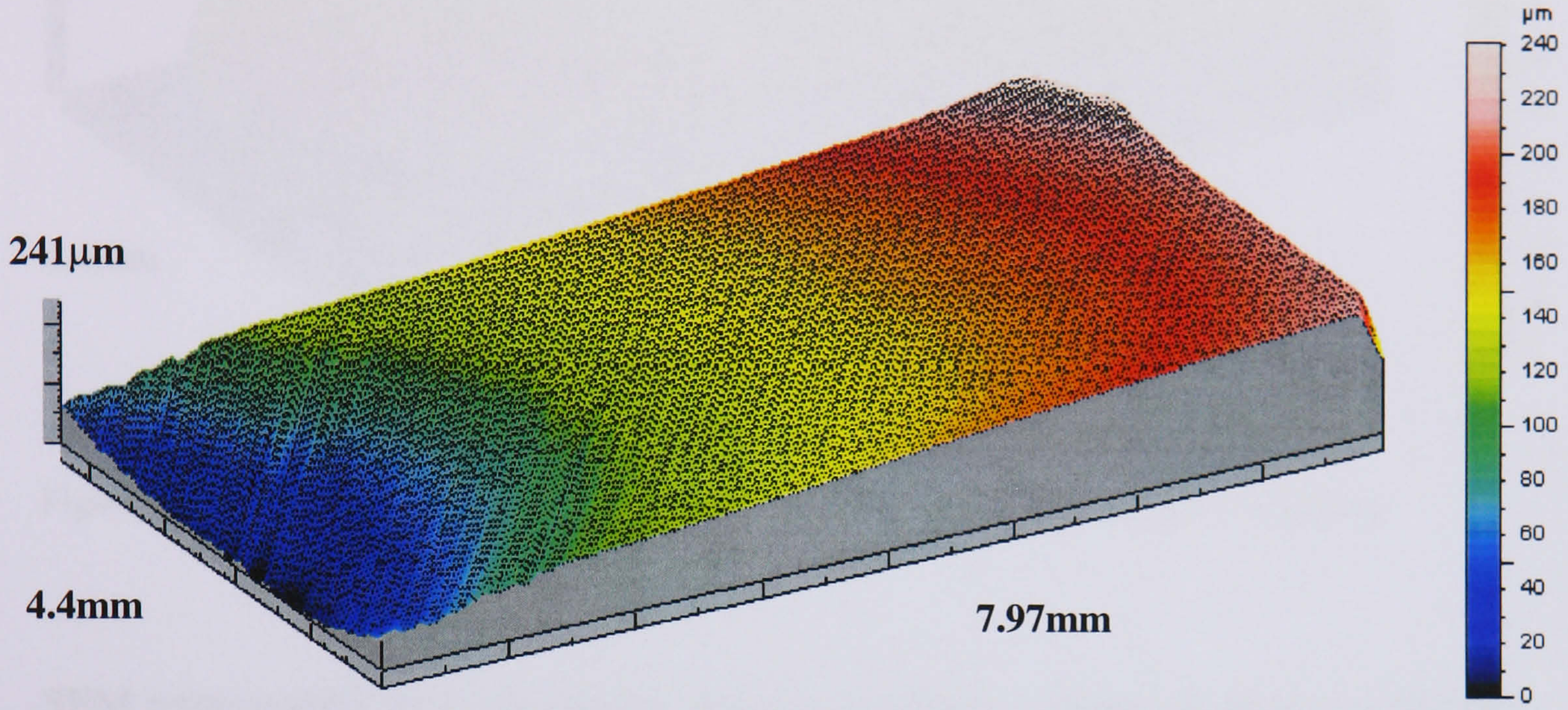

Figure 4.18 3D talysurf image of a 5MRad UHMWPE pin run against a highly scratched counterface.

A 10MRad UHMWPE pin surface is shown in Figure 4.19. This surface again was flat with no visible signs of damage. This surface had much less of a gradient across it than most of the other pins. This pin and the 5MRad UHMWPE pin did not have any signs of damage which were expected after being worn against a highly scratched counterface.

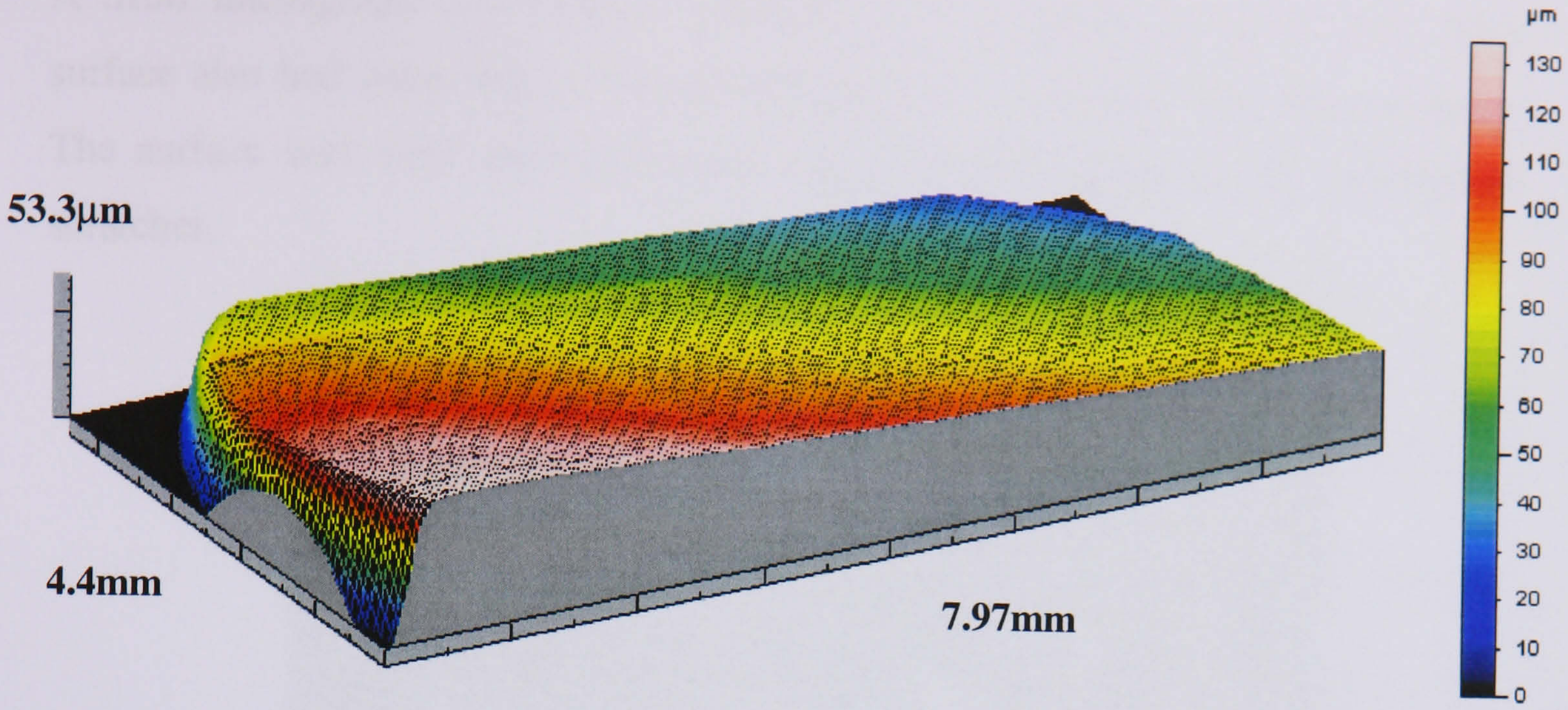

Figure 4.19 3D talysurf image of a 10MRad UHMWPE pin run against a highly scratched counterface.

SEM micrographs were also taken of the pin surfaces. These are shown in Figures 4.20-4.22. Figure 4.20 is an SEM micrograph of a small area from the surface of the 0MRad UHMWPE pin. The area shown had a great amount of damage and areas where flakes of UHMWPE appeared to be pulling away. There was evidence of surface pulls which are associated with adhesive wear.

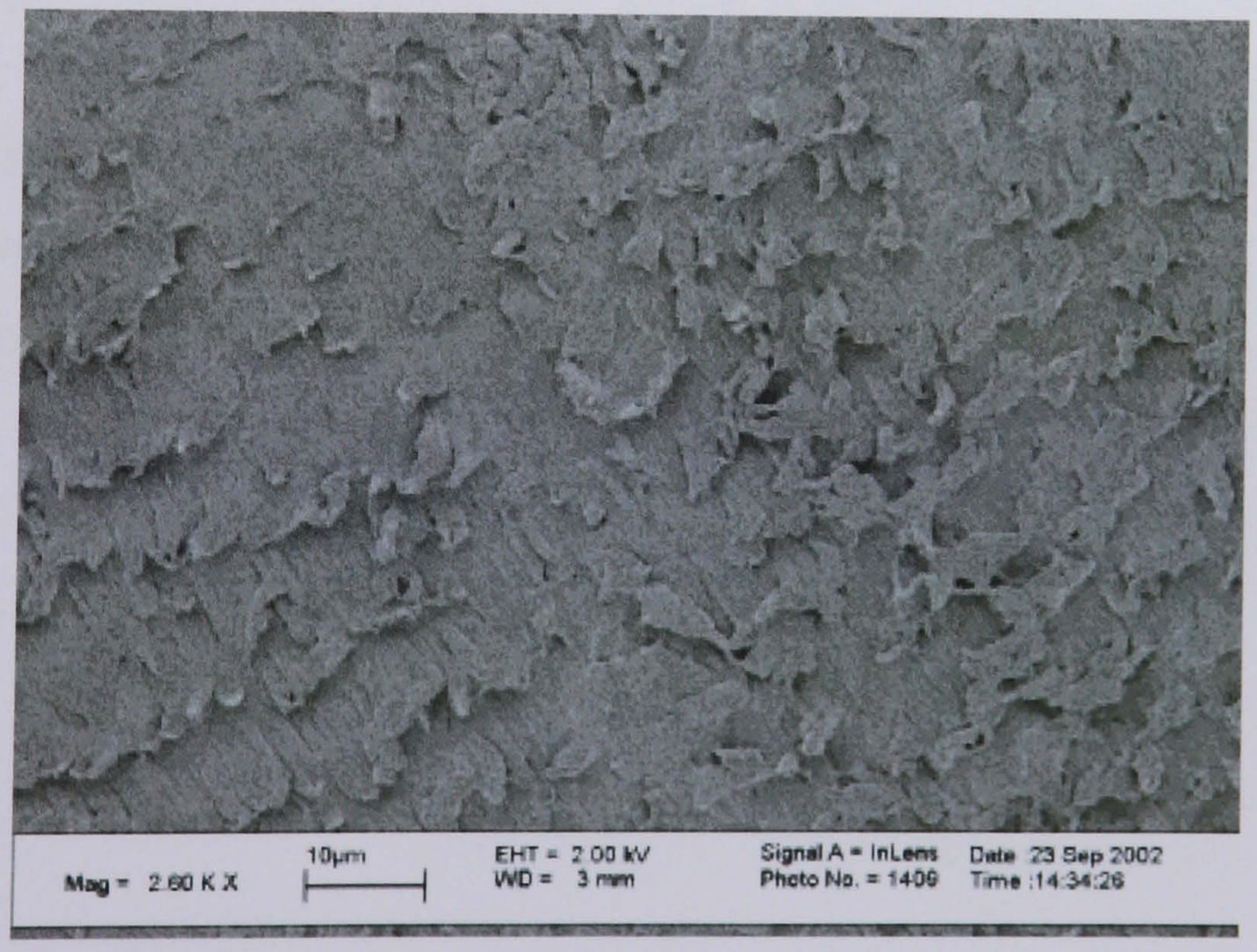

Figure 4.20 SEM micrograph of a 0MRad UHMWPE pin run against a highly scratched counterface.

A SEM micrograph of a 5MRad UHMWPE pin is shown in Figure 4.21. This surface also had areas which showed surface pulls associated with abrasive wear. The surface was quite damaged which was probably caused by the counterface scratches.

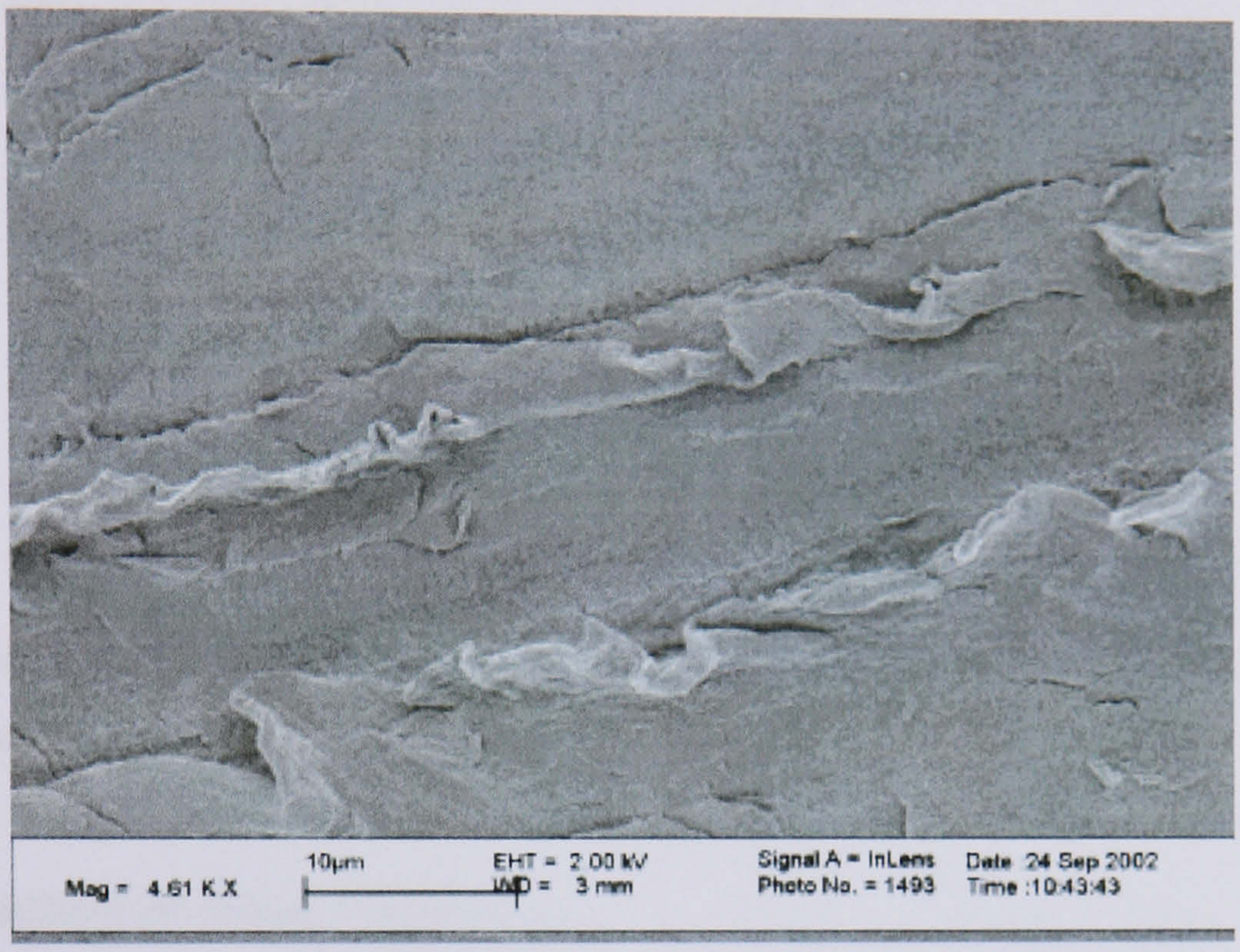

Figure 4.21 SEM micrograph of a 5MRad UHMWPE pin run against a highly scratched counterface.

A 10MRad pin after testing against the highly scratched counterface is shown in Figure 4.22. The area appeared to be smooth and showed few signs of damage. There was evidence of particles on the surface which could have been about to be detached or reattached to the surface. The lack of damage was also reflected in the 3D talysurf image.

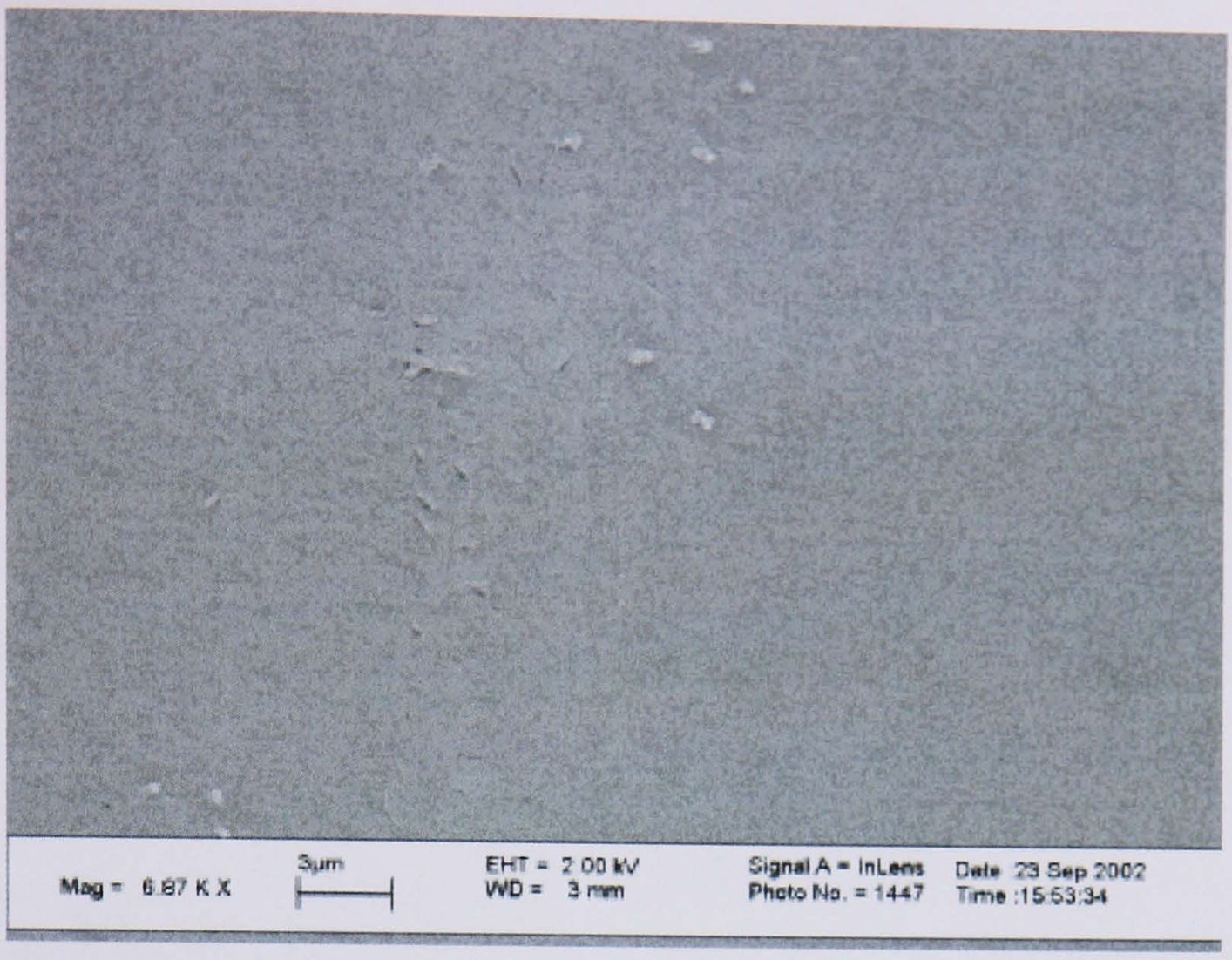

Figure 4.22 SEM micrograph of a 10MRad UHMWPE pin run against a highly scratched counterface.

4.3.4. Comparison of Wear Factors.

The mean wear factors from all the different counterface surfaces are shown in Table 4.3 and combined together in Figure 4.23. These results show that for all the materials the wear factors increased as the scratch height increased. The high levels of crosslinking reduced wear on the smooth, medium scratched plates and on the highly scratched plates when compared to noncrosslinked material. With the medium counterface there was very little difference between the wear factors of the 0MRad and the 5MRad materials. Between these two materials there was no statistically significant difference under any of the counterface conditions. The results showed that the highly crosslinked 10MRad material gave the lowest wear factors with all of the test conditions, with the results being statistically significantly different with both of the scratched counterfaces ($p>0.05$; ANOVA).

Radiation level.	**Wear factor (mean ± 95% confidence intervals (x10^{-7} mm^3/Nm))**		
	Smooth	**Medium**	**High**
0 MRad	1.71±0.39	2.49±0.78	5.2±1.84
5 MRad	1.41±0.34	2.5±0.96	4.3±1.25
10 MRad	0.85±0.35	1.01±0.89	1.71±0.71

Table 4.3 Average wear factors from all testing ± 95% confidence limits.

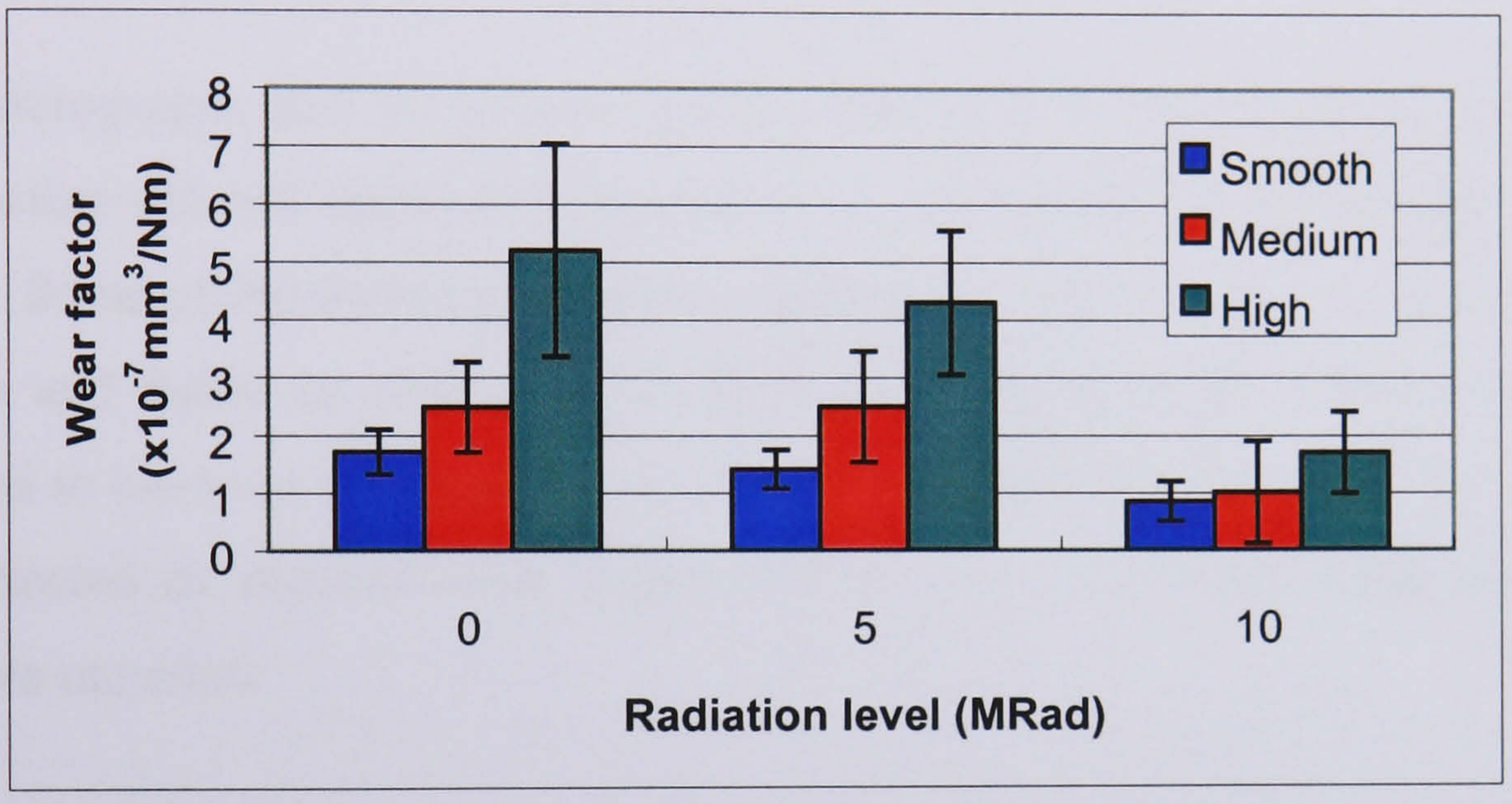

Figure 4.23 Comparison of wear factors with all three counterface conditions and radiation levels.

The percentage wear of the materials against each counterface with respect to the non-crosslinked materials are shown in Figure 4.24. The reduction in wear observed with the highly crosslinked material could be clearly seen against all the counterfaces. The results also showed the only slight reduction in wear seen with 5MRad UHMWPE.

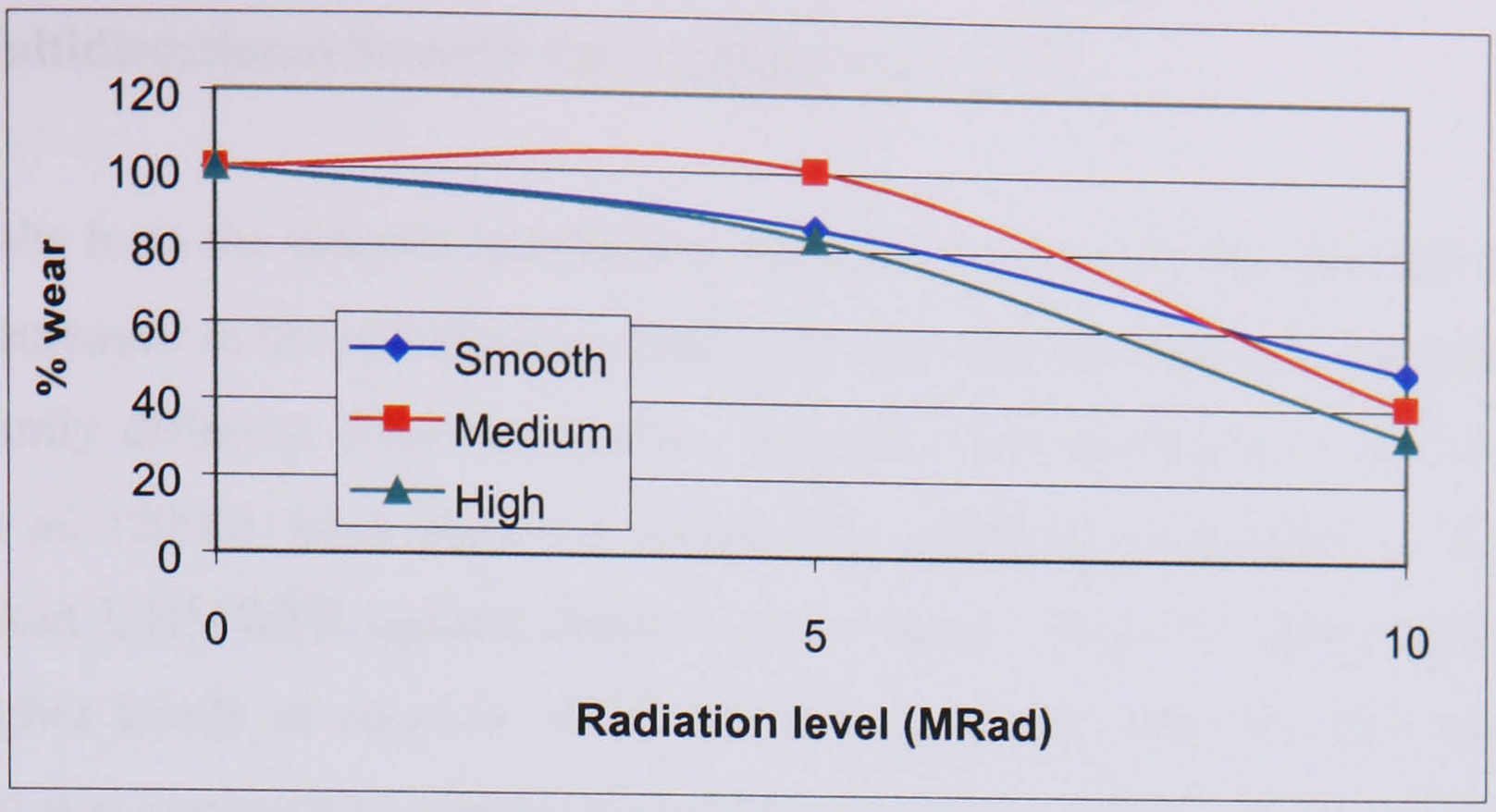

Figure 4.24 Percentage of wear of materials with 0MRad taken as 100%.

SEM micrographs and 3D talysurf images showed that the pins with the highest wear factors did not necessarily also have the most evidence of damage on their surface. Some of the surfaces from the scratched counterfaces did show more signs of pulls and flakes on their surfaces, but not all of them. The 10MRad material appeared to have the smoothest surface with all the counterface conditions and this was reflected by reduced wear factors and wear volumes when compared to the other two materials.

4.4 Discussion.

The method used to generate scratches was the same as in Chapter 3. The method was repeatable and generated scratches which were equivalent to those seen on explants by Barbour *et al.* (1999). The high scratches corresponded to the largest scratches observed on explants whereas the medium scratches were comparable to less severe conditions. The measurements taken after testing showed that the scratches varied in whether they had lost or gained height during testing. This could have been due to a variation in the part of the scratch measured, after testing had been completed. A lower peak height after testing was expected due to damage caused during testing.

4.4.1. Multidirectional Smooth Pin on Plate Wear Test.

The results from the smooth counterface experiments showed that although the wear factor decreased as the crosslinking level increased, the decrease was not statistically significantly different. Previous studies, such as those by Marrs *et al.* (1999) and Endo *et al.* (2000), have shown a statistically significant reduction in wear with crosslinked UHMWPE against smooth counterfaces. However these studies both used higher levels of rotation which could be a reason why the difference they observed was statistically significantly different and the difference in this study was not. The small reduction seen with the crosslinking was again thought to be due to orientational hardening as was described in Chapter 2. During unidirectional motion, orientational hardening occurs. Orientational hardening results in the molecules in the material orientating themselves in the direction of sliding and therefore becoming stronger in this direction but weaker perpendicular to it. In multidirectional motion the frictional force constantly changes direction with respect to the polymer surface. This means that the molecules cannot orientate in any particular direction, and therefore the material does not have a much weaker direction. Orientational hardening can still occur during multidirectional motion but not to the same extent as in unidirectional motion. Crosslinking reduces the amount of orientational hardening and softening, as it retards chain mobility and provides resistance to the cross shear forces. Crosslinking also results in more C-C bonds between molecules which makes it harder to break bonds. The more crosslinking in the material, the more bonds that are present. This means that there is less orientational hardening and softening, which is why a reduction in wear rate was seen as the crosslinking levels increased.

The level of rotation in this test compared to the previous study meant that there was less cross shear frictional force on the surface of the pin. The wear rates against the cross shear frictional energy are shown in Figure 4.25. More orientational hardening was able to occur especially with the non-crosslinked pins which resulted in their lower wear factor compared to the ±60° rotation 0MRad pins. The crosslinks in the other two materials meant that the orientational hardening could not occur as easily but because of the reduced frictional force the wear factors were not significantly

different. Crosslinking the material meant it was more resistant to the cross shear force. The greater number of crosslinks in the 10MRad material meant it was more resistant and therefore gave a slightly lower wear rate at the higher cross shear frictional energy ratio. As the 5MRad materials did not contain the same number of crosslinks this did not have the same kind of effect.

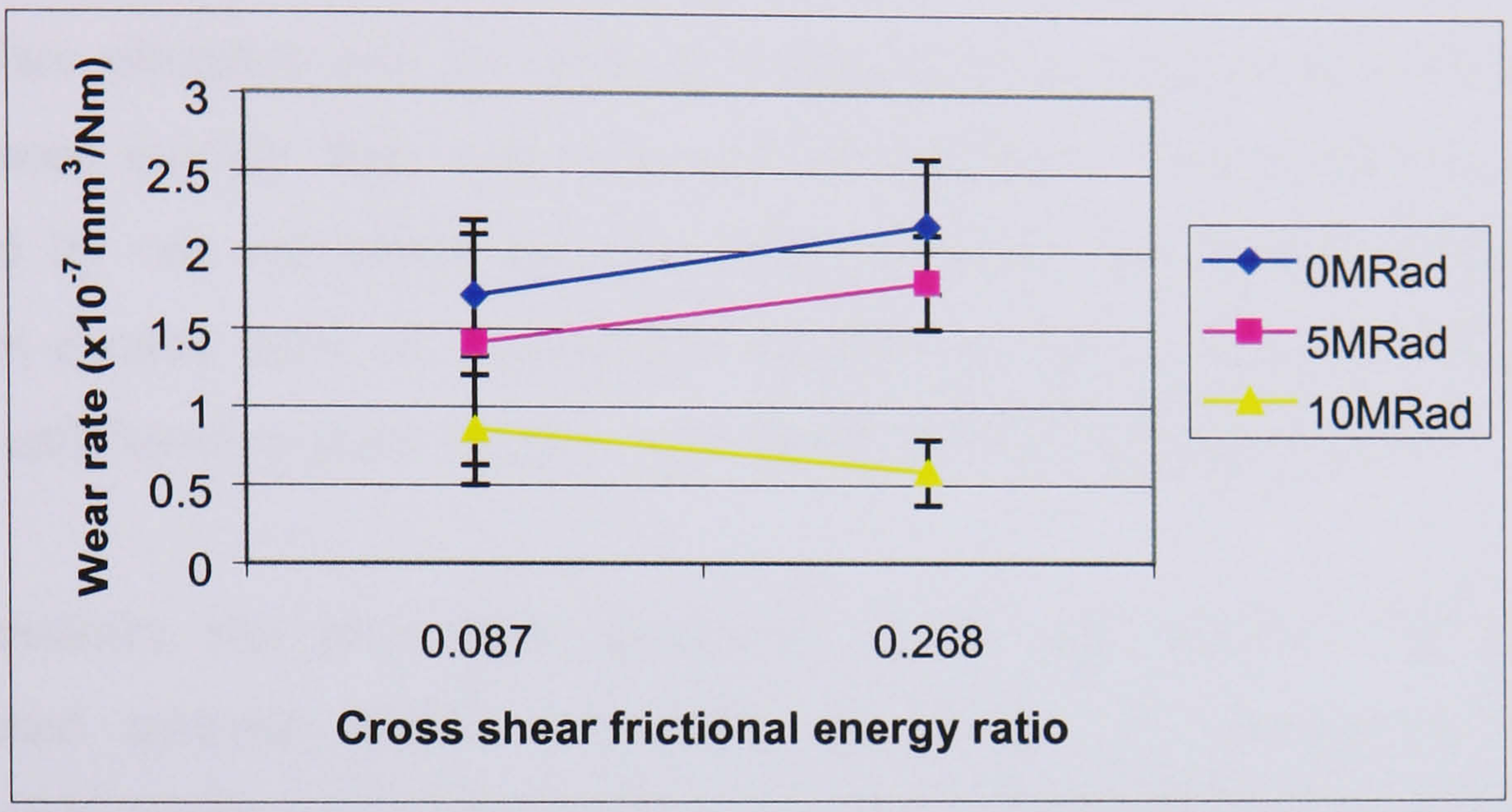

Figure 4.25 Cross shear frictional energy against wear rate for smooth counterfaces.

Against a smooth counterface the main wear mechanism involved was an adhesive wear process. This occurs when parts of the UHMWPE surface are removed after many interactions of the harder counterface asperity. The UHMWPE eventually breaks off due to fatigue. Microadhesive wear was thought to be the dominant wear mode as the damage appeared to be more on the surface than subsurface. Subsurface damage would have been more obvious on the pin surfaces.

4.4.2. Multidirectional Medium and High Scratched Pin on Plate Wear Tests.

When worn against both medium and highly scratched counterface conditions there was a significant increase in wear factors for all the materials. However the 10MRad material had a significantly lower wear factor than the other two materials. Between the 0MRad and 5MRad materials there was no significant difference between the wear factors.

The 3D talysurf images did not show a lot of damage to the surfaces of the pins, however, the SEM images did show more signs of wear.

On scratched counterfaces an abrasive wear mechanism was the main wear process which occurred. This means that orientational hardening was less able to happen, as the molecules were removed by a single asperity interaction. The scratches on the counterface ploughed into the softer polymer surface causing particles to generate much more quickly than with a smooth counterface. Wear particles could be removed by one movement and therefore the wear rate increased. The higher scratches created more of a stress concentration as they ran against the polymer surface and therefore gave a higher wear factor than the medium scratches.

The crosslinks still gave more protection against the scratches than the non-crosslinked material which was shown by the highly crosslinked materials significantly lower wear factor. The links in the material provided resistance to the scratches and prevented particles breaking away as easily. As the 5MRad material contained much fewer crosslinks they did not provide the same protection and this meant that it had a much higher wear factor than the 10MRad crosslinked material.

The wear factors are dependent on the amount of cross shear frictional energy that occurs during the test. If there is more multidirectionality there is more cross shear frictional energy and more strain is put onto the components being tested and therefore the wear rates increase.

The cross shear frictional energy against the wear rates are shown in Figures 4.26 and 4.27 for the medium scratches and the high scratches respectively. For both the counterface conditions the highly crosslinked UHMWPE gave much lower wear factors at each cross shear frictional energy level. The highly crosslinked material had a much lower difference in the wear rates between the two cross shear conditions as the crosslinks made the material more resistant to cross shear frictional energy. The level of cross shear frictional energy did not appear to have any significant effect on the wear of highly crosslinked UHMWPE.

The 0MRad and 5MRad UHMWPE did not show any significant difference in wear factors at either cross shear frictional energy level. This would suggest that the number of crosslinks in the 5MRad material were not large enough to overcome the effect of cross shear frictional energy. The results suggest that small levels of crosslinking do not give any improvement in resistance to cross shear frictional energy compared to non-crosslinked UHMWPE. The higher cross shear frictional energy did cause an increase in wear for the 0MRad and 5MRad UHMWPE compared to 10MRad UHMWPE on the medium scratched counterface. These materials are more effected by changes in cross shear frictional energy than highly crosslinked UHMWPE. This is because the non-crosslinked material does not have any cross links to provide resistance to cross shear and the amount of crosslinks in the 5MRad material is not high enough to give any a sufficient amount of resistance.

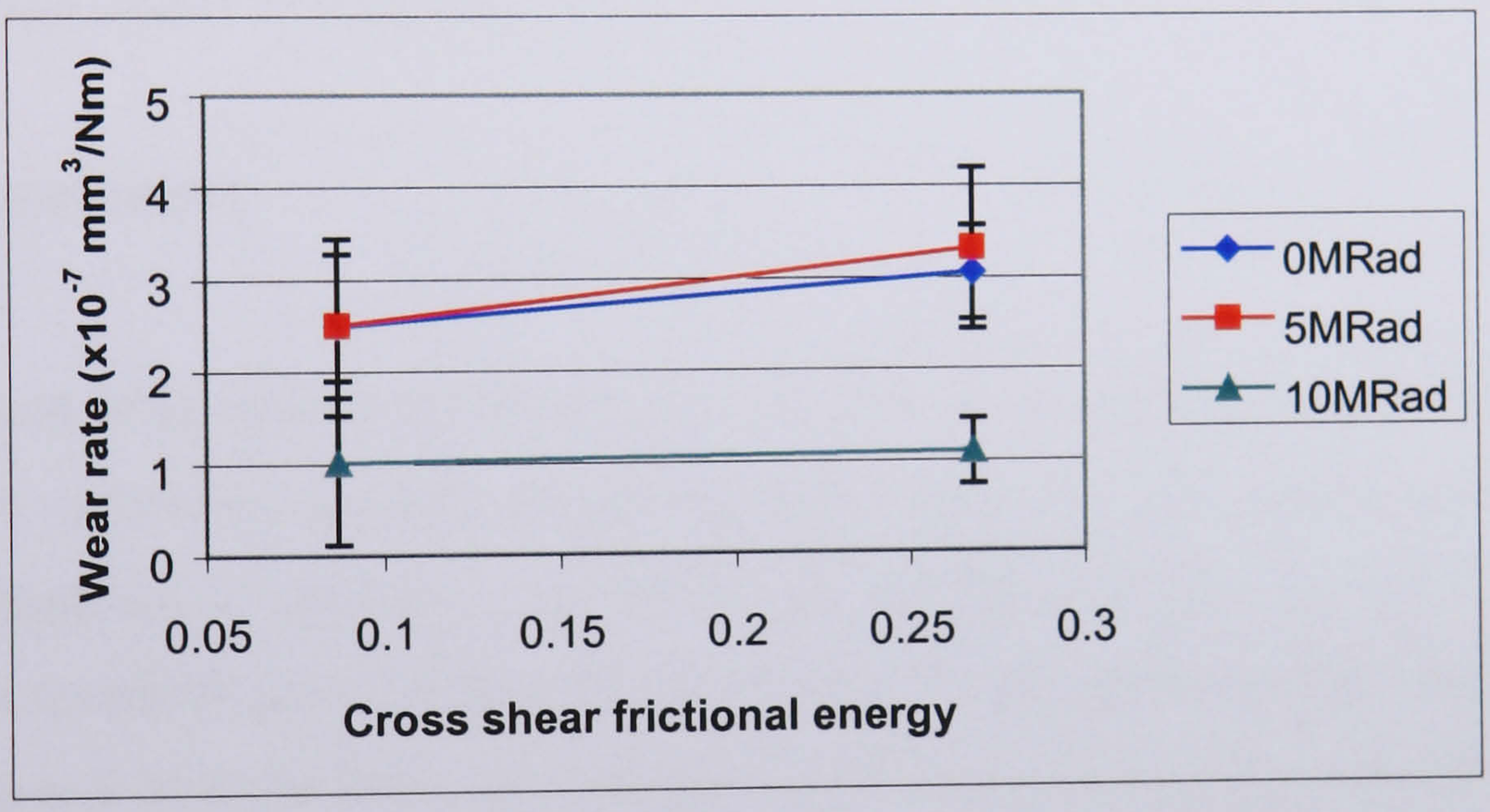

Figure 4.26 Cross shear frictional energy against wear rate for medium scratches.

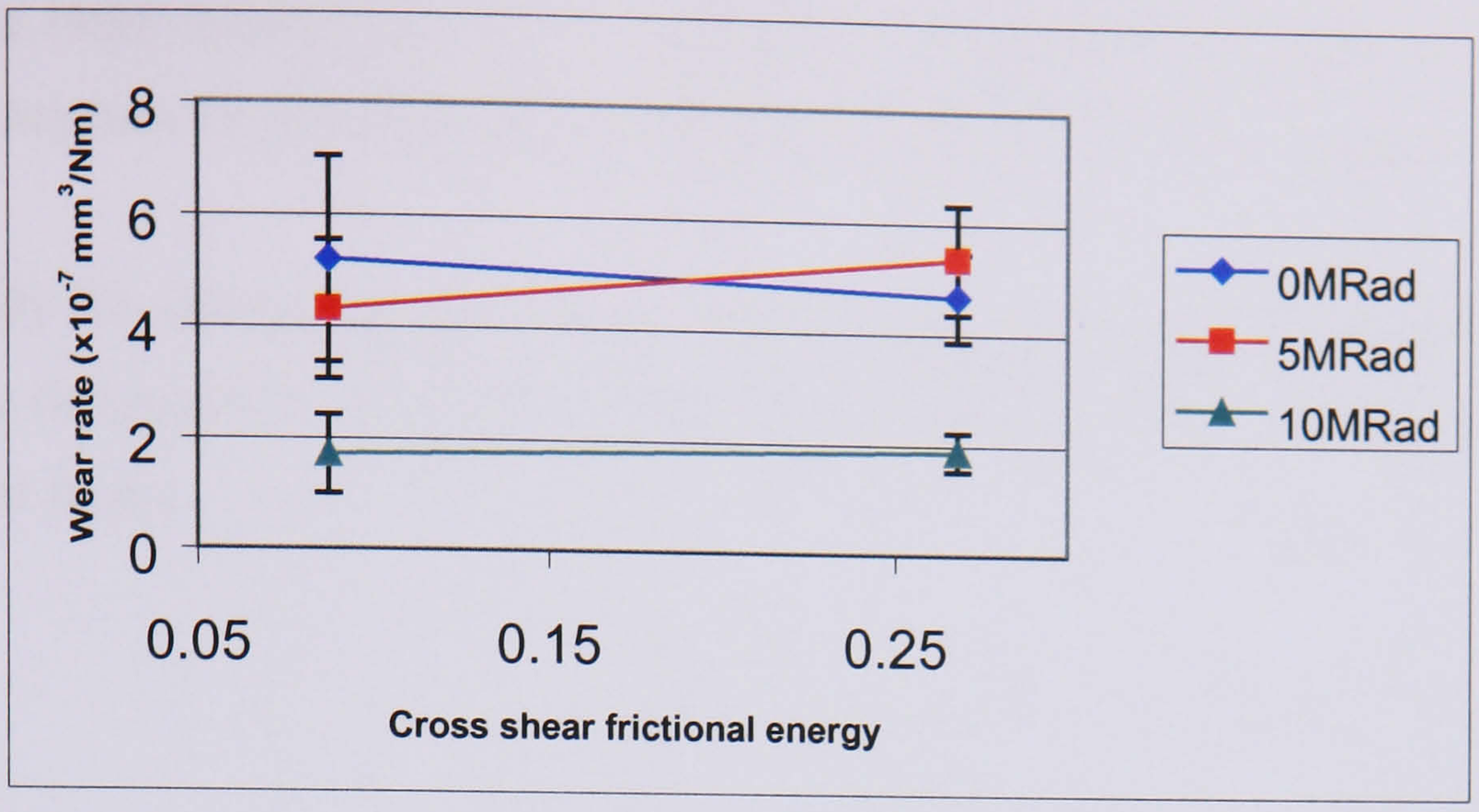

Figure 4.27 Cross shear frictional energy against wear rate for high scratches.

Any dependency of wear rate on cross shear energy seen on smooth surfaces was lost on high scratched surfaces.

4.5. Conclusion.

The pin on plate studies reported in this Chapter and Chapter 3 were carried out using two different kinematic conditions. These were ±60° and ±20° rotation. This was carried out to determine the effect that multidirectionality had on the three different levels of crosslinking. The results showed that generally the wear factors were lower with the lower levels of rotation. The result from the smooth counterface test at ±20° rotation showed that there was no significant difference between the wear factors for the three materials. At the higher rotation the highly crosslinked material had a significantly lower wear factor. The results from the higher rotation were consistent with results reported by Marrs *et al*. (1999) and Endo *et al*. (2000).

Damage to the counterface increased the wear rate for all the materials as the wear moved to a more abrasive mechanism. This means that it would be an advantage to use crosslinked UHMWPE against damage resistance ceramic femoral heads.

The 10MRad UHMWPE was found to be much more resistant to cross shear frictional energy than the other materials. This was because the crosslinks in the material made it more resistant to cross shear. The 5MRad UHMWPE did not show

the same improvement. The lower amount of crosslinks in this material did not provide any benefit when looking at different cross shear frictional energies.

This study has shown that that the reduction in wear produced by crosslinking was critically dependent on counterface roughness and that the level of rotation is also an important factor.

Chapter 5.

5. Wear Debris.

5.1. Introduction.

Wear debris induced osteolysis is one of the major causes of failure in long term total hip replacements. It has been shown that wear debris in certain size ranges is more reactive. The wear particles activate macrophages, which leads to the release of osteolytic cytokines, which then cause bone resorption. The critical size range is 0.1–1.0μm. A study by Matthews *et al.* (2000) also showed it is not only the size that is important but also the volumetric concentration in that size range. The aim of the experiments in this study was to see if different levels of radiation to UHMWPE gave rise to a material that generated different sizes and shapes of wear debris particles and to determine whether their specific and functional biological activities were different.

5.2. Materials and Methods.

5.2.1. Materials.

At the end of each pin on plate test, the lubricant was collected and frozen. Some of this was then used for the analyses described in this chapter. Lubricant was taken from the smooth tests at ±60° rotation for all three materials and from the highly scratched test conditions, again for all three materials. Wear debris from three samples of lubricant from each test condition was analysed.

5.2.2. Methods.

The debris was isolated using a multistage digestion process. The method has been described in detail in Chapter 2. After digestion the solutions were filtered through 1μm and 0.1μm polycarbonate filters. The filters were dried and randomly selected

areas were then placed onto SEM stubs for imaging. SEM images were taken at up to x50000 magnification. They were examined using low voltage (1-3kV) at high resolution. Three different areas from each filter were used. The percentage number and the percentage area of the particles was calculated using the equations in Chapter 2. A minimum of 500 particles were counted for each sample. The percentage area of the particles was then converted into a percentage volume assuming a constant thickness for the particles. The volumetric concentration C(r) as a function of particle size was derived.

This enabled the specific biological activity (SBA) to be calculated. The specific biological activity is defined as the relative biological activity of UHMWPE wear debris per unit volume. The biological activity function B(r) was calculated by Matthews *et al.* (2000). It was carried out by determining the biological activity function of sterile, endotoxin free, polyethylene wear debris which was generated *in vitro*, as a function of particle size. TNFα was used as the marker for biological activity as this has previously been shown to correlate with bone resorption (Green *et al.*, 2000). Three size ranges were examined. These were 0.1-1.0μm, 1.0-10μm and 10-100μm. It was found that the 0.1-1.0μm size range was the most reactive and this was given an arbitrary value of one (Fisher *et al.*, 2000). The larger size ranges were normalised with respect to the smallest size range. The biological activity B(r) values are shown in Figure 5.1 (Fisher *et al.*, 2000). The particles less than 0.1μm were not assigned a B(r) since at the time that these studies had been carried out, the nanometre size particles had not been observed. Assigning a biological activity value to the nanometre size particles has not been possible due to the number needed to get a large enough volume to be able to perform the experiments. It was therefore assumed that they had the same reactivity as the 0.1-1μm size range. In practice this may not be the case, and they may be less reactive, but as yet this is not known and therefore the worse case scenario was used.

The SBA was calculated by determination of the integrated product of the biological activity function per unit value and the volumetric concentration function for each size range of the wear particles (equation 5.1). The results were added together to estimate the SBA. The SBA has a high value when the majority of the mass of the

debris is mainly in the small size range, but if the debris is large the SBA will be small. This is shown schematically in Figure 5.2.

$$\mathrm{SBA} = \sum_{0.1}^{100} C(r)\ x\ B(r) \qquad (5.1)$$

Figure 5.1 Biological activity as a function of particle size. (Adapted from Fisher *et al.*, 2000).

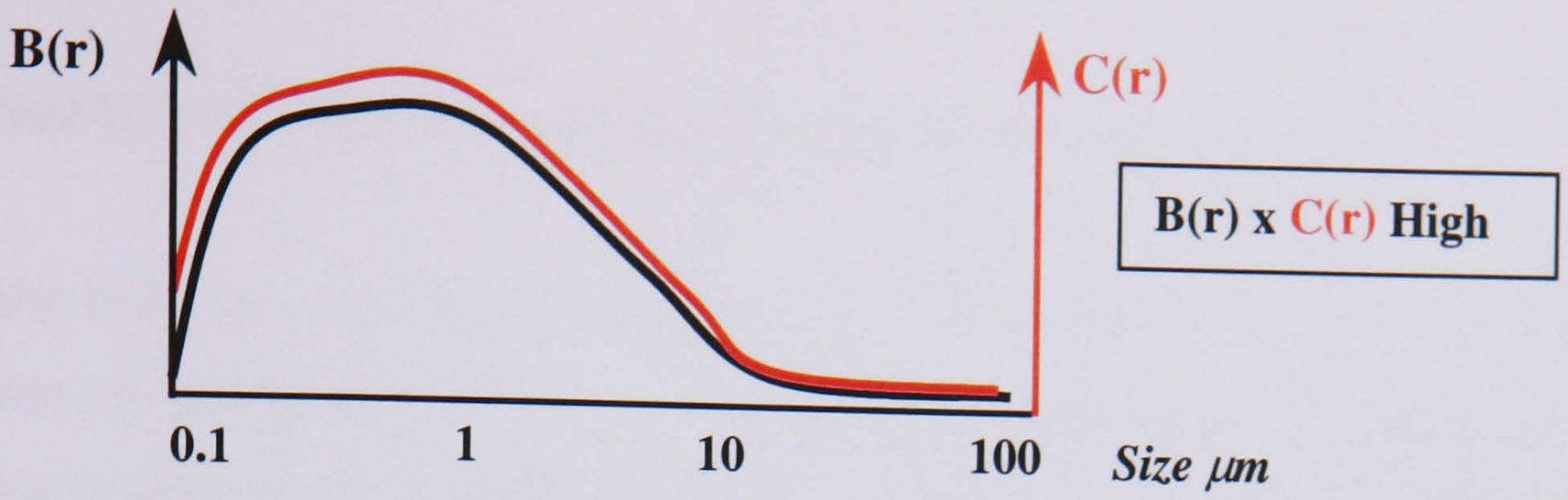

(a)

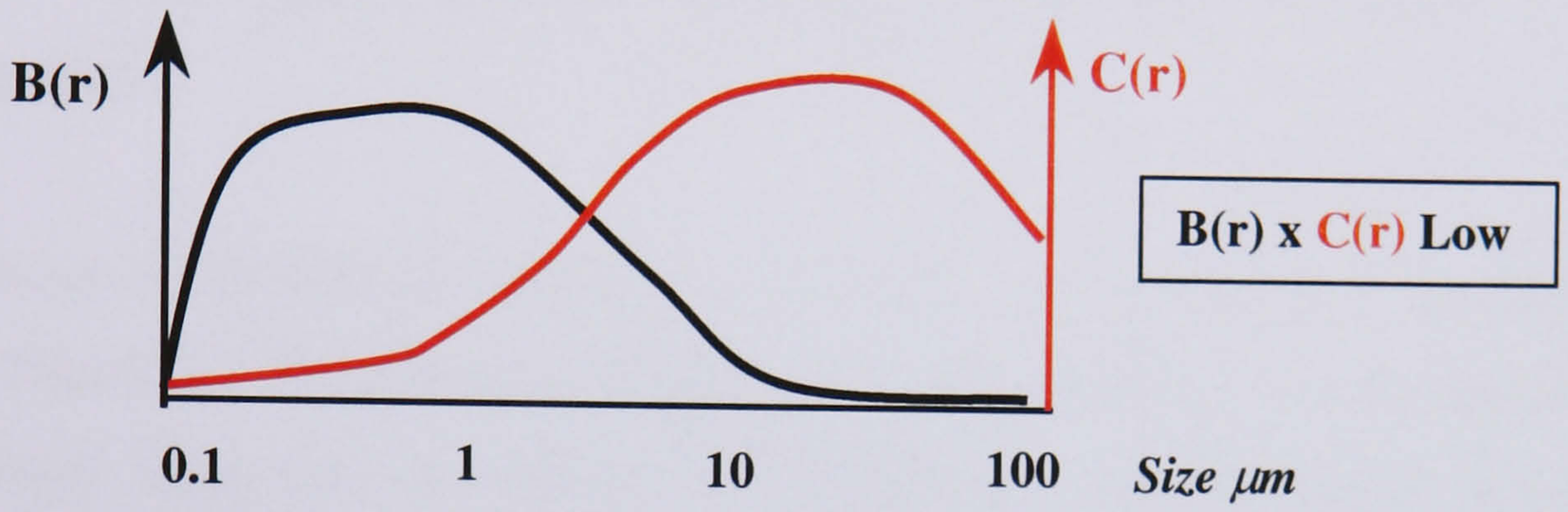

(b)

Figure 5.2 How the SBA is affected by the volume of wear debris in different size ranges. (a) a high SBA value. (b) a low SBA value.

Once the SBA had been calculated the functional biological activity (FBA) was obtained. This is the product of the volumetric wear rate V ($mm^3/10^6$ cycles) and the SBA (equation 5.2).

$$FBA = V \; x \; SBA \qquad (5.2)$$

5.2.3. Statistical Analysis.

Before statistical anaylsis could be done the data had to be transformed as the results were percentages. Once the data was transformed, means, standard deviations and then 95% confidence limits were calculated. One way ANOVA was also carried out on the transformed data. Statistical significance was judged using the MSD method. The data was back transformed into percentages for the graphs.

5.3 Results.

5.3.1. Wear Debris Generated Against a Smooth Counterface.

The results from the analysis of the wear debris from the tests against a smooth counterface are shown in Figures 5.3 –5.12. A typical SEM image for each of the filter sizes is shown and then the quantitative results for each material. The data shows the mean for the three samples analysed ± 95% confidence limits. The 95% confidence limits were calculated following arcsine transformations of the percentage data.

A SEM image of the 0MRad UHMWPE wear debris filtered through a 1μm filter is shown in Figure 5.3. The debris on the filter was mainly small and it all appeared to be very round. There was no evidence of any fibrils on any of the images and there were very few particles greater than 10μm in length.

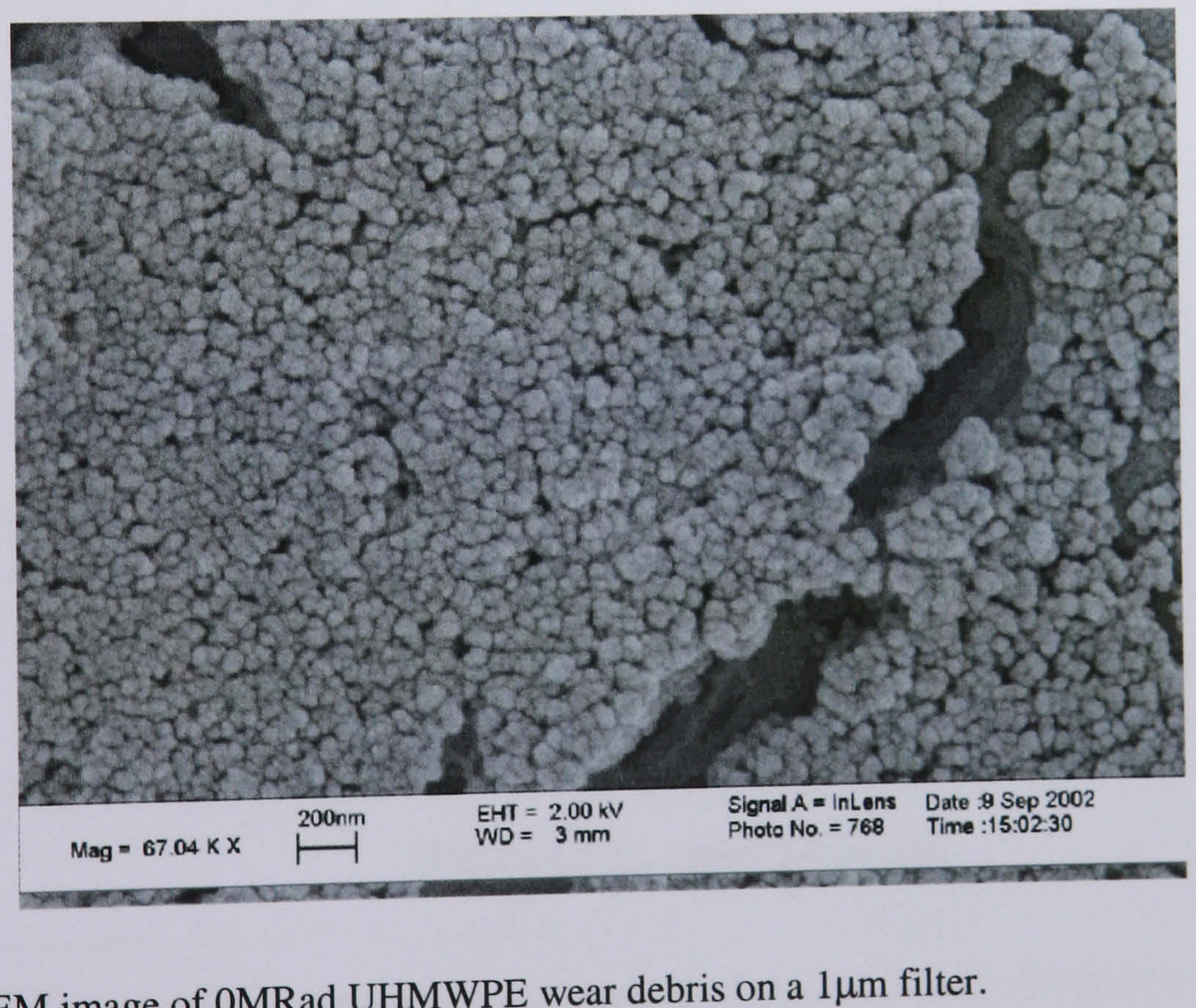

Figure 5.3 SEM image of 0MRad UHMWPE wear debris on a 1μm filter.

A SEM image of the 0MRad UHMWPE wear debris on a 0.1μm filter is shown in Figure 5.4. The 0.1μm filters contained very few particles. The occasional particle seen on the filter was small with no particles above 10μm being found. The majority of the particles were found on the 1μm filter.

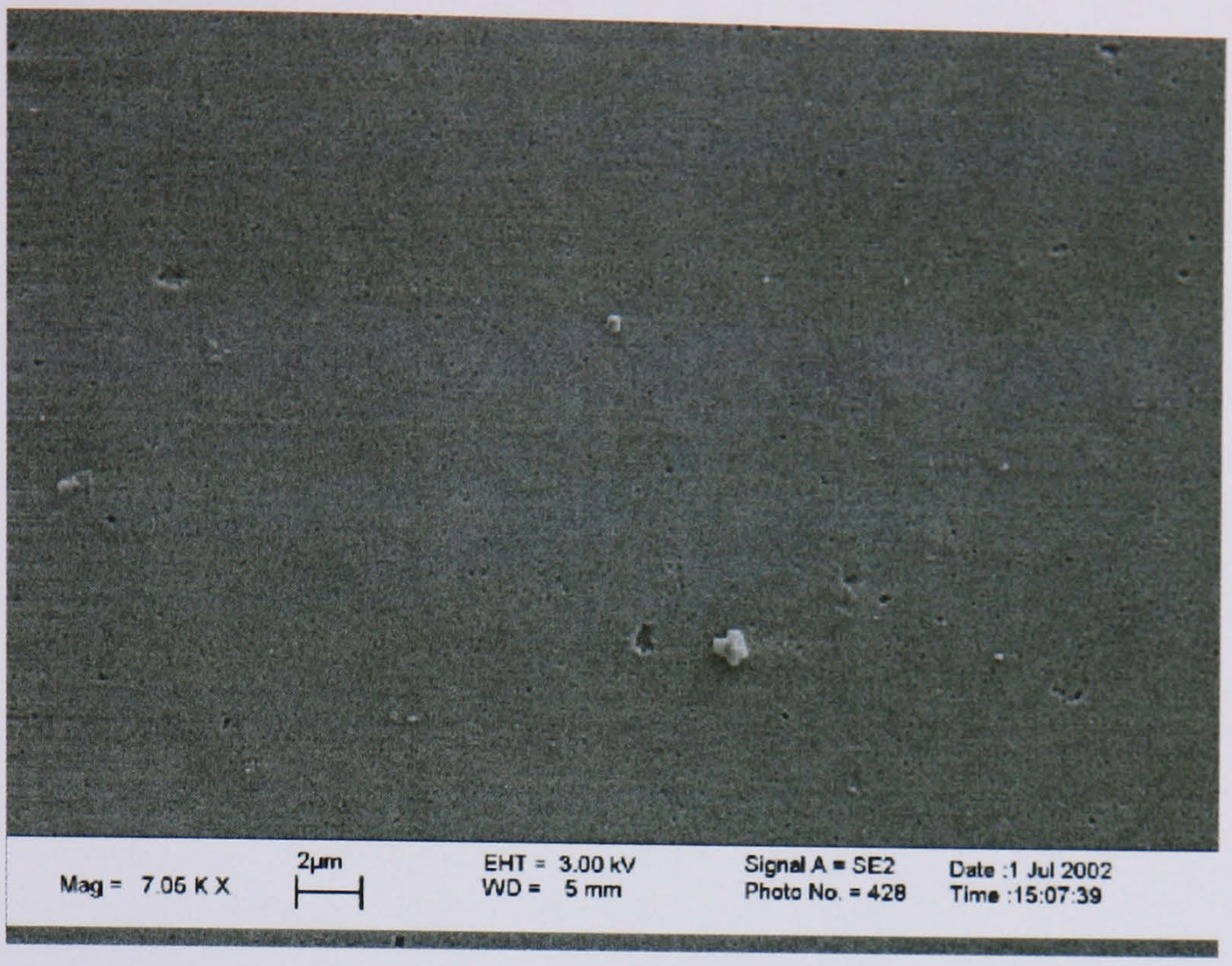

Figure 5.4 SEM image of 0MRad UHMWPE wear debris on a 0.1µm filter.

The percentage number of particles as a function of size in each size range for the 0MRad UHMWPE wear debris is shown in Figure 5.5. The results showed that the majority of the particles were less than 0.1µm. There were also many particles in the 0.1-1.0µm size range but very few particles larger than this.

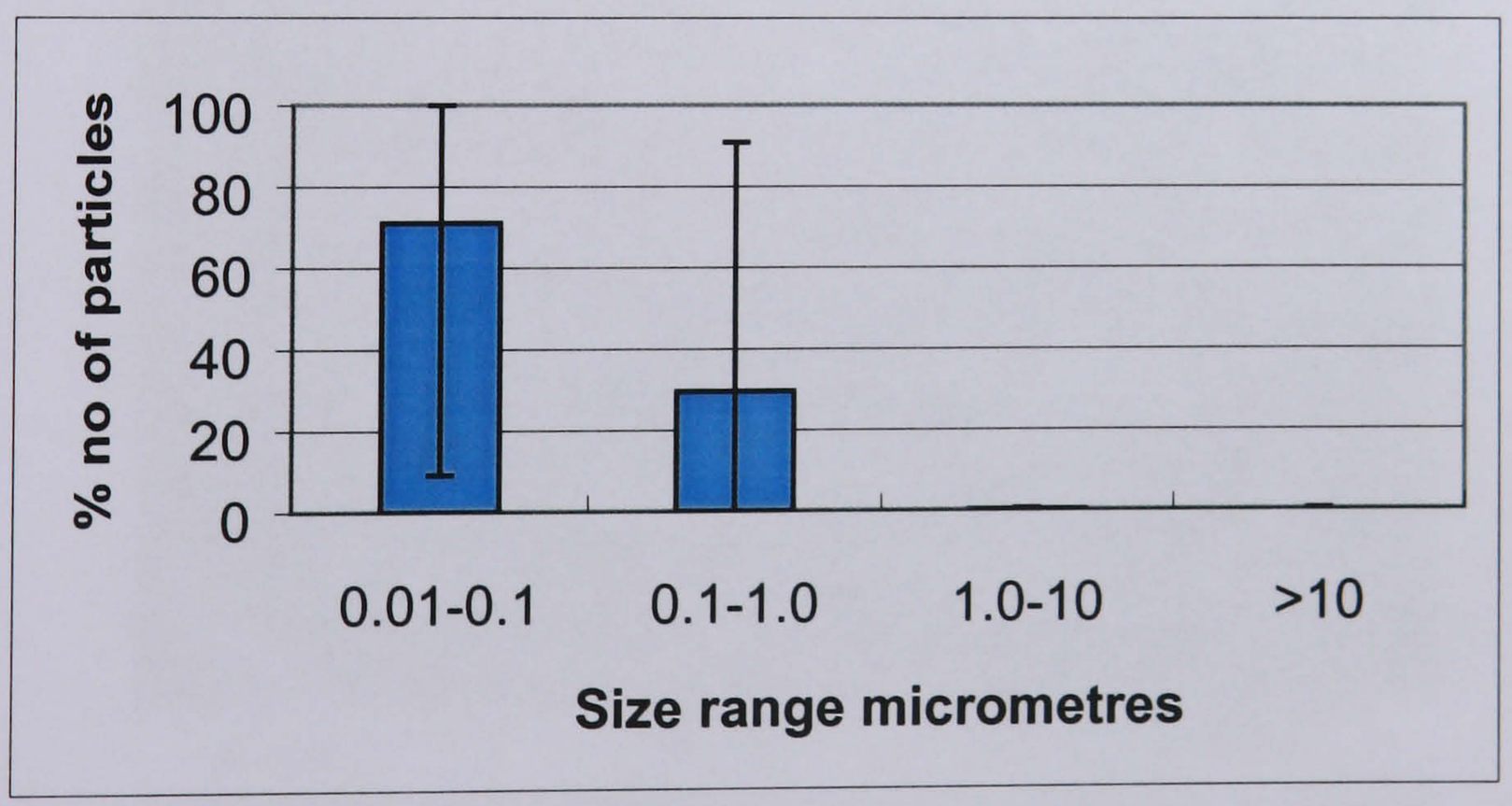

Figure 5.5 Percentage number of particles as a function of size for 0MRad UHMWPE wear debris.

The percentage area as a function of size of the 0MRad UHMWPE wear particles is shown in Figure 5.6. The majority of the area of the particles was in the 0.1-1.0µm size range. Although the majority of the number of particles were in the 0.01-0.1µm

size range this did not affect the area distribution because of the extremely small size of the particles.

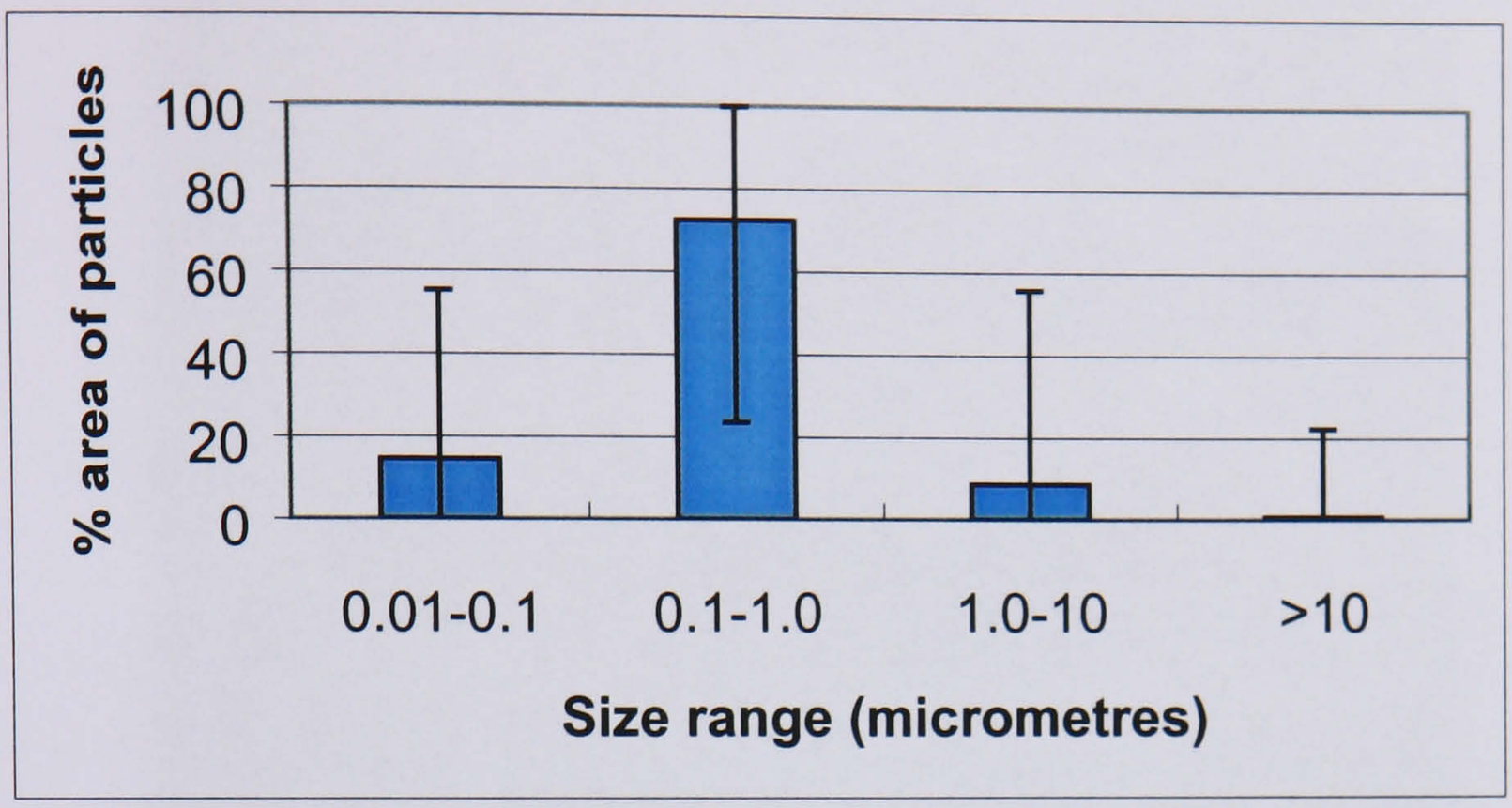

Figure 5.6 Percentage area of particles as a function of size for the 0MRad UHMWPE wear debris.

A SEM image of 5MRad UHMWPE wear debris on a 1μm filter is shown in Figure 5.7. The debris appeared to be very similar to the 0MRad debris with the majority being small and round. Again there were very few larger particles and no fibrils.

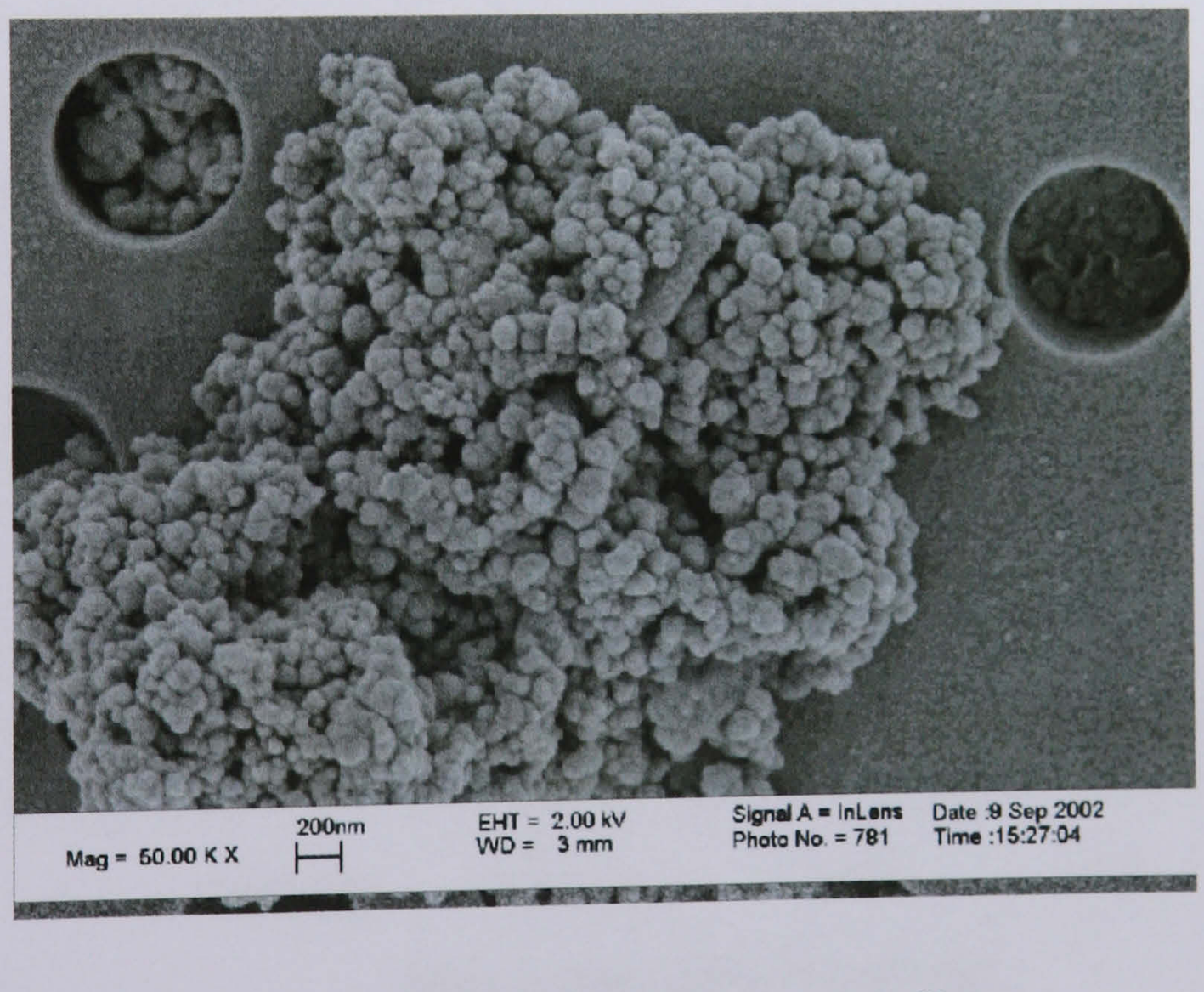

Figure 5.7 SEM image of 5MRad UHMWPE wear debris on a 1μm filter.

A SEM image of the 5MRad UHMWPE wear debris on a 0.1μm filter is shown in Figure 5.8. There were very few particles to be seen on this filter and any particles

which were seen were small and round. As observed for the 0MRad UHMWPE wear debris, the majority of the debris was on the 1μm filter.

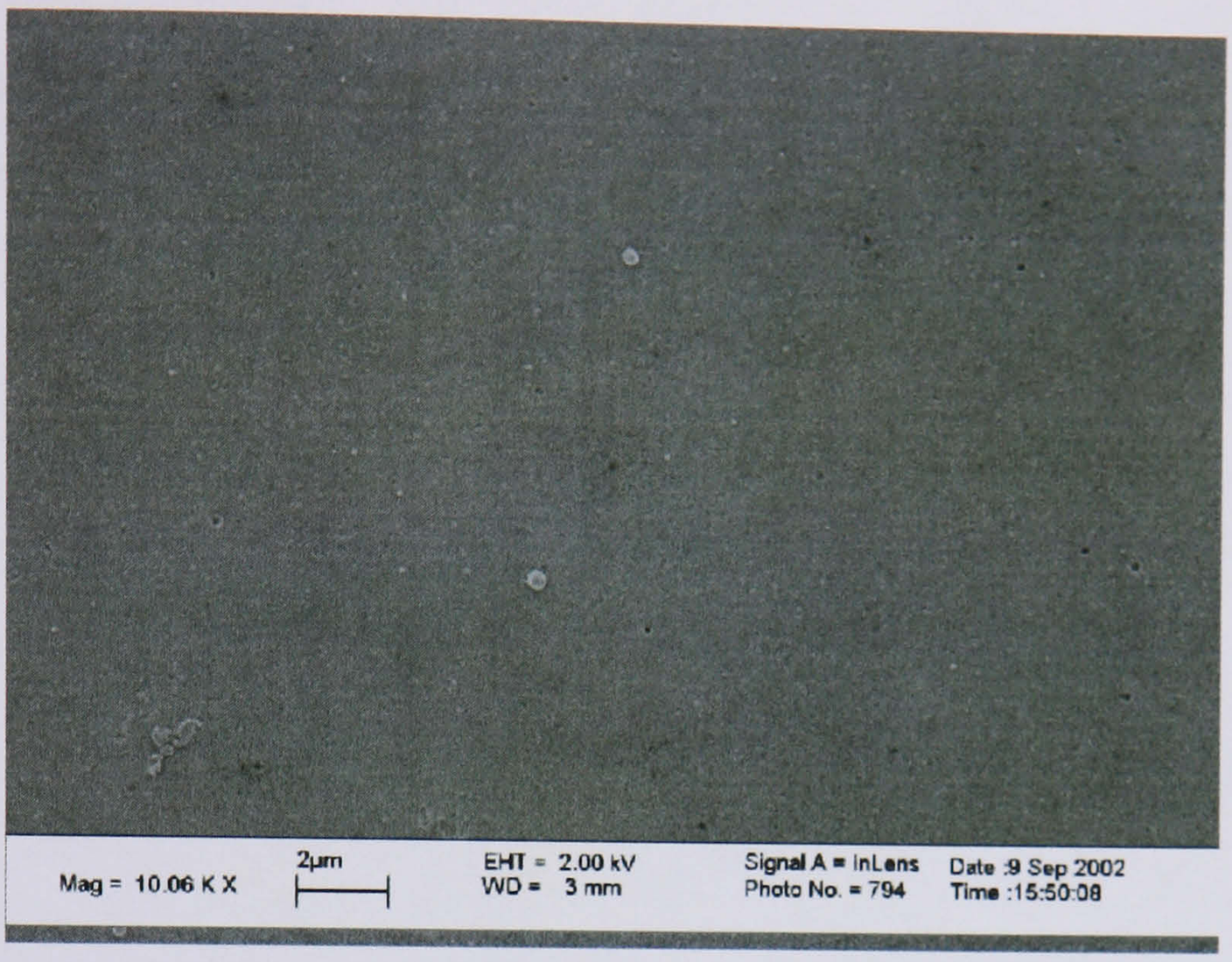

Figure 5.8 SEM image of 5MRad UHMWPE wear debris on a 0.1μm filter.

The percentage number of particles in each size range for the 5MRad UHMWPE wear debris is shown in Figure 5.9. The majority of the particles were in the 0.01-0.1μm size range. As with the 0MRad debris, hardly any larger particles were found. Although there were slightly more particles in the 0.1-1.0μm size range.

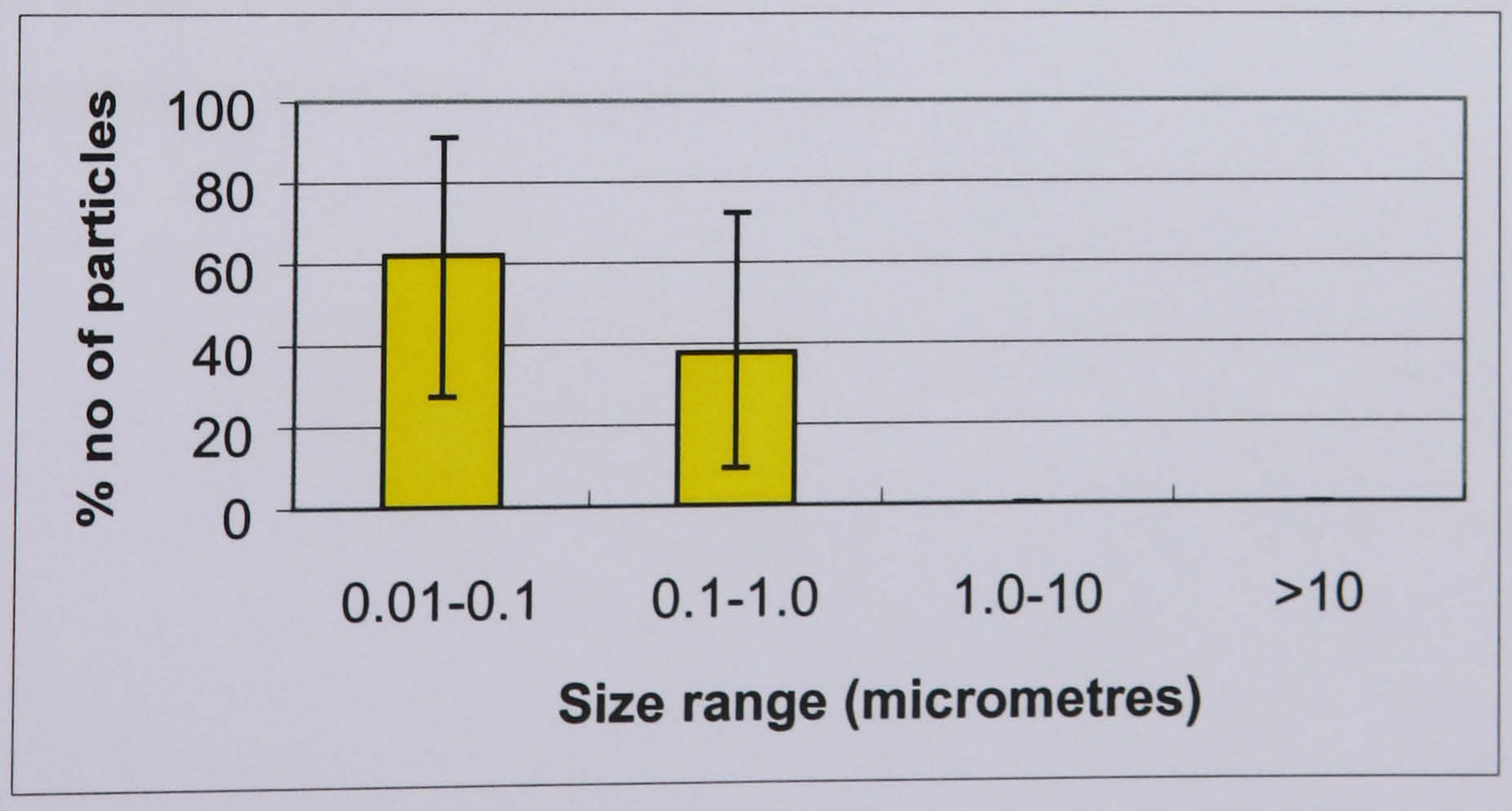

Figure 5.9 Percentage number of particles in different size ranges for 5MRad UHMWPE wear debris.

The percentage area of the particles in the different size ranges are shown in Figure 5.10. The majority of the area of the particles was in the 0.1-1.0μm size range, which is the most reactive size range. This was the same as for the 0MRad debris. The percentage area in the 0.01-0.1μm and 1-10μm size range was about the same. There was also a small amount of wear debris in the largest size range but this probably only represented one or two particles.

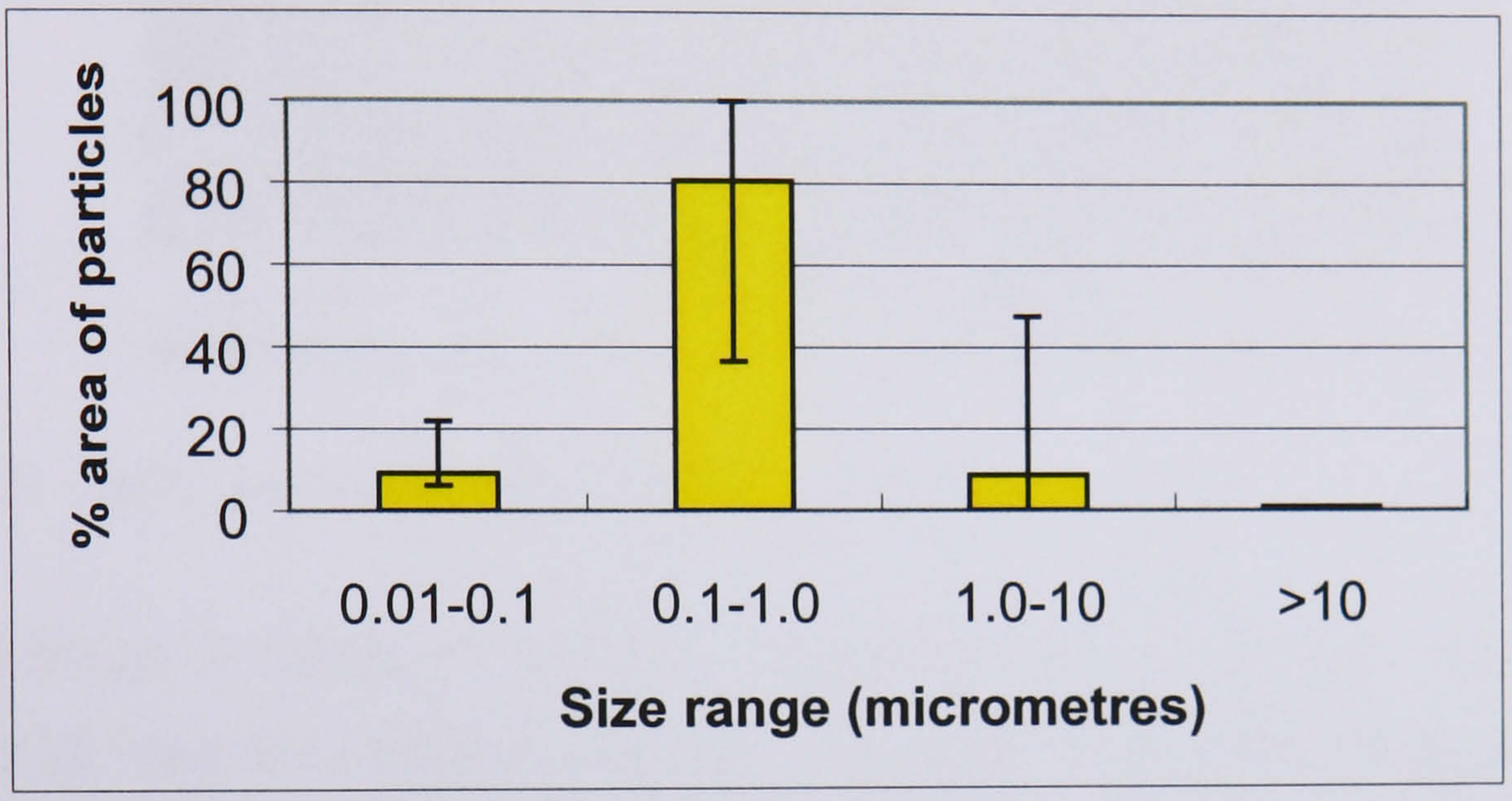

Figure 5.10 Percentage area of particles in different size ranges for 5MRad UHMWPE wear debris.

A SEM image of 10MRad UHMWPE wear debris on a 1μm filter is shown in Figure 5.11. The debris appeared to be very similar to the 0MRad and 5MRad UHMWPE wear debris described previously. The particles were all small and round. Very few particles above 1μm were observed.

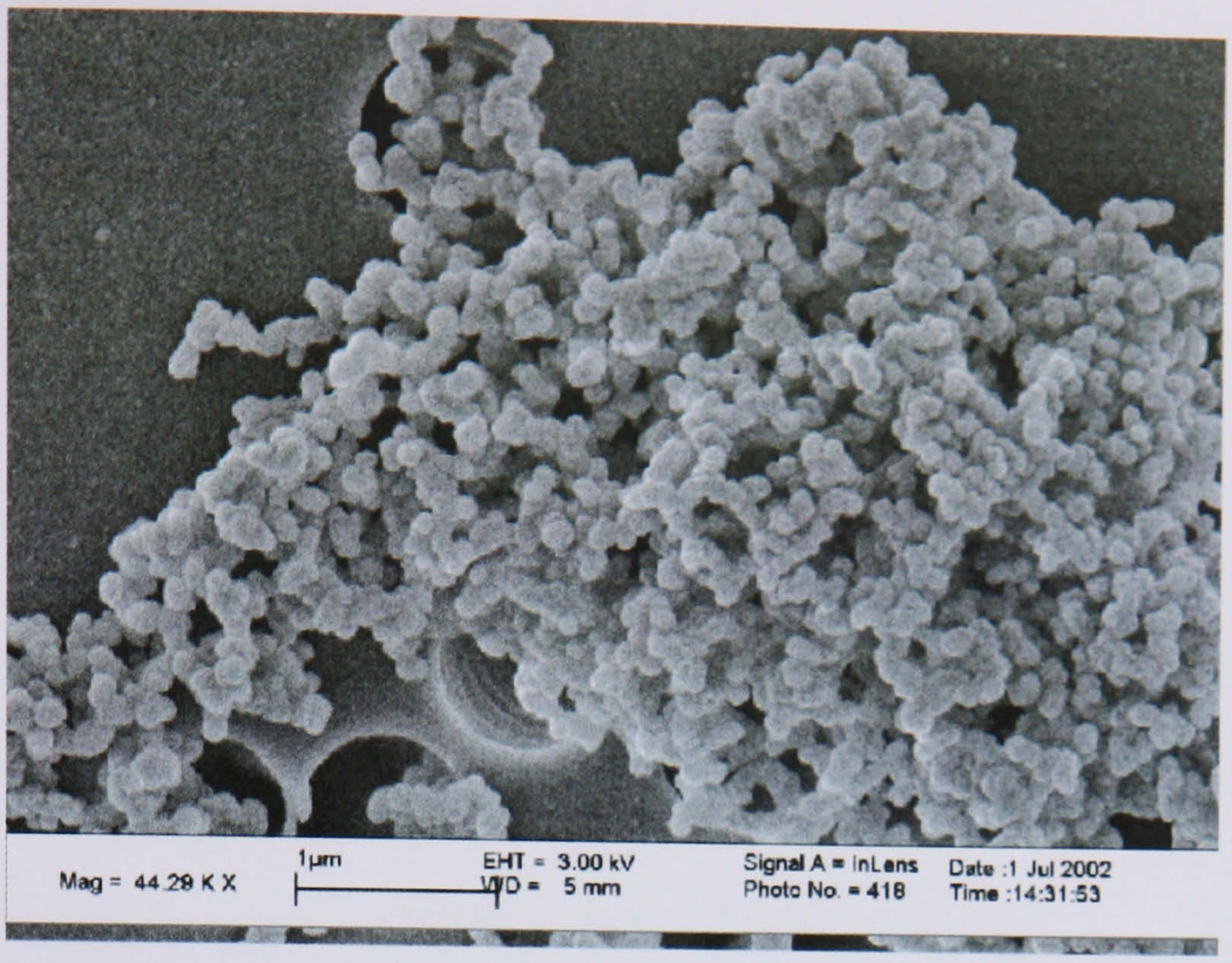

Figure 5.11 SEM image of 10MRad UHMWPE wear debris on a 1µm filter.

A SEM image of 10MRad UHMWPE wear debris on a 0.1µm filter is shown in Figure 5.12. Very few particles were seen on this filter as observed for the other two materials. The particles that were visible were all small.

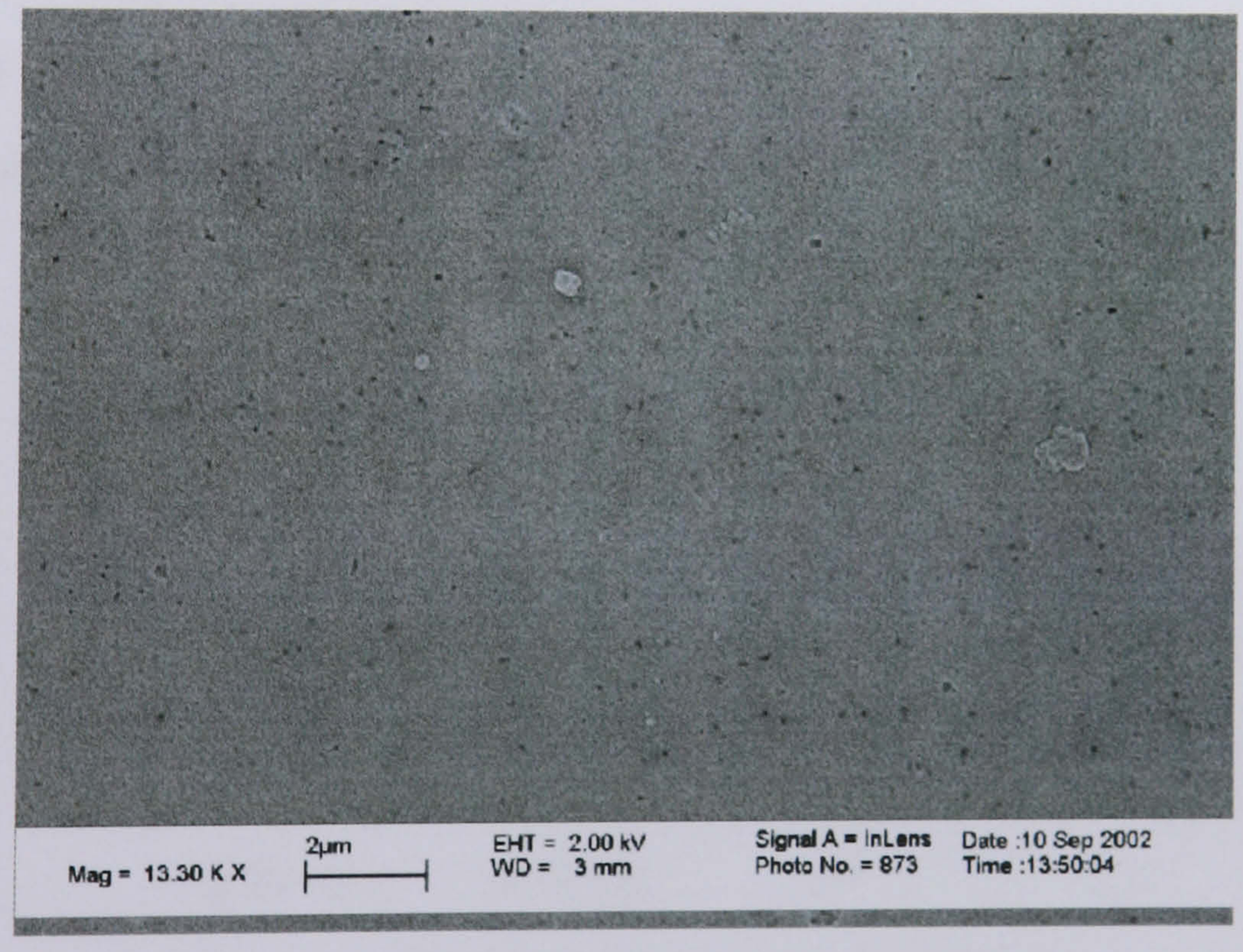

Figure 5.12 SEM image of 10MRad UHMWPE wear debris on a 0.1µm filter.

The percentage number of particles in each size range from the 10MRad UHMWPE wear debris is shown in Figure 5.13. Most of the particles were in the 0.01-0.1µm

size range although there were many in the 0.1-1.0μm size range. There were few particles above 1μm in size.

Figure 5.13 Percentage number of particles as a function of size for 10MRad UHMWPE wear debris.

The percentage area in the different size ranges of the 10MRad UHMWPE wear debris is shown in Figure 5.14. The majority of the area of the particles was in the 0.1-1.0μm size range and again this was the same as for the previous materials. The percentage of the area in the 0.01-0.1μm and 1.0-10.0μm size range was very small. The percentage are above 10μm was negligible.

Figure 5.14 Percentage area of particles as a function of size for 10MRad UHMWPE wear debris.

5.3.2. Wear Debris Generated Against a Scratched Counterface.

The following figures are the results of the analysis of the wear debris from the scratched wear tests. As with the previous results a typical SEM image is shown for each filter size for each material and then two graphs which represent the percentage number and the percentage area in different size ranges of the particles generated by each material. The graphs show the mean ± 95% confidence limits. The 95% confidence limits were calculated following arcsine transformation of the percentage data.

A SEM image of the 0MRad UHMWPE wear debris on a 1μm filter is shown in Figure 5.15. This wear debris was generated under scratched counterface conditions. The debris appeared to be more dispersed than the debris generated under smooth counterface conditions, and it was not as clumped together. The debris was again generally very small and round. More larger particles were observed than in the smooth tests.

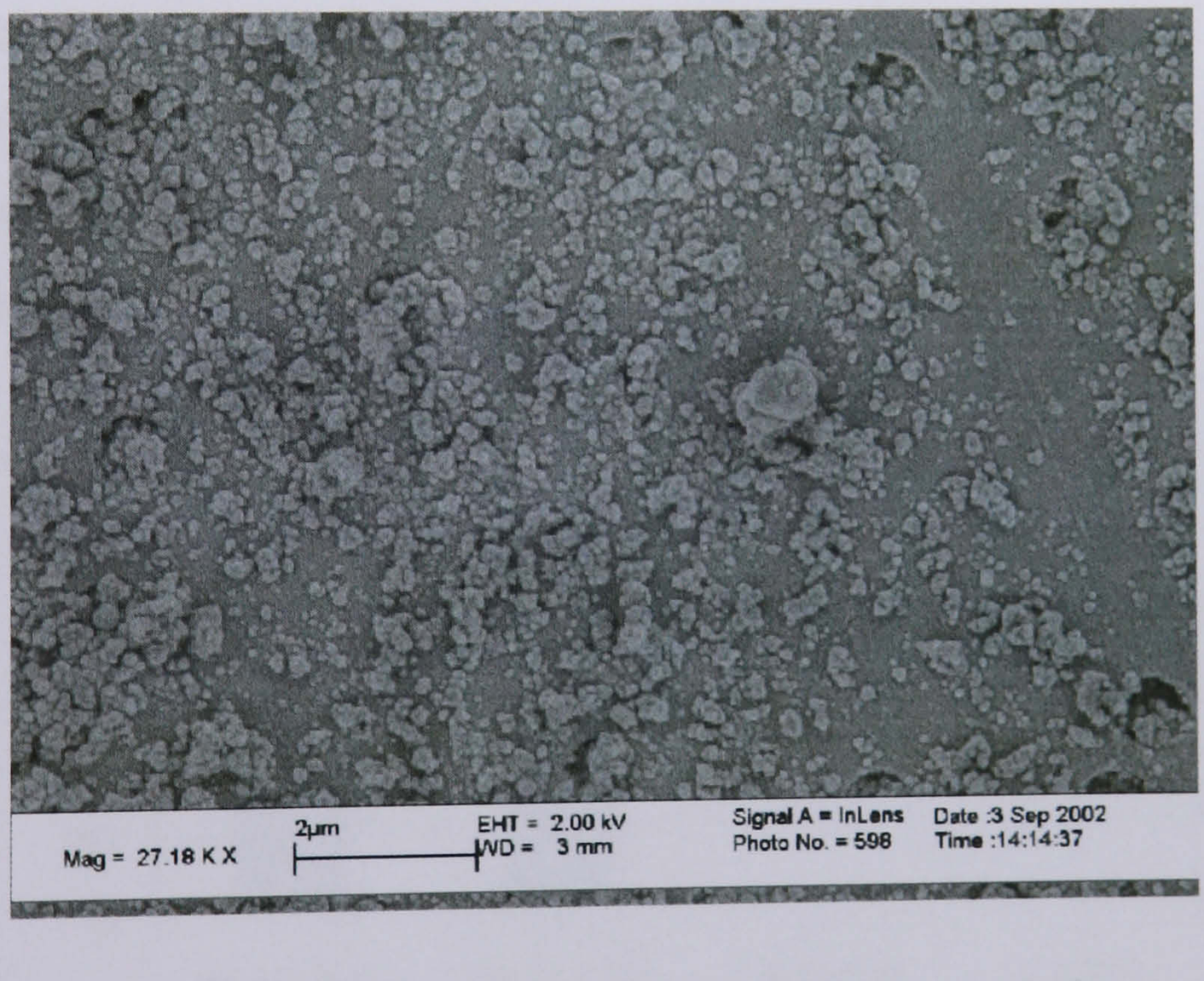

Figure 5.15 SEM image of 0MRad UHMWPE wear debris from a scratched wear test on a 1μm filter.

An SEM image of 0MRad UHMWPE wear debris from a 0.1μm filter is shown in Figure 5.16. This was again debris generated under scratched counterface conditions. In keeping with all the previous samples there was little debris on the

0.1μm filter. The debris seen was very small and round with no large particles visible on this filter.

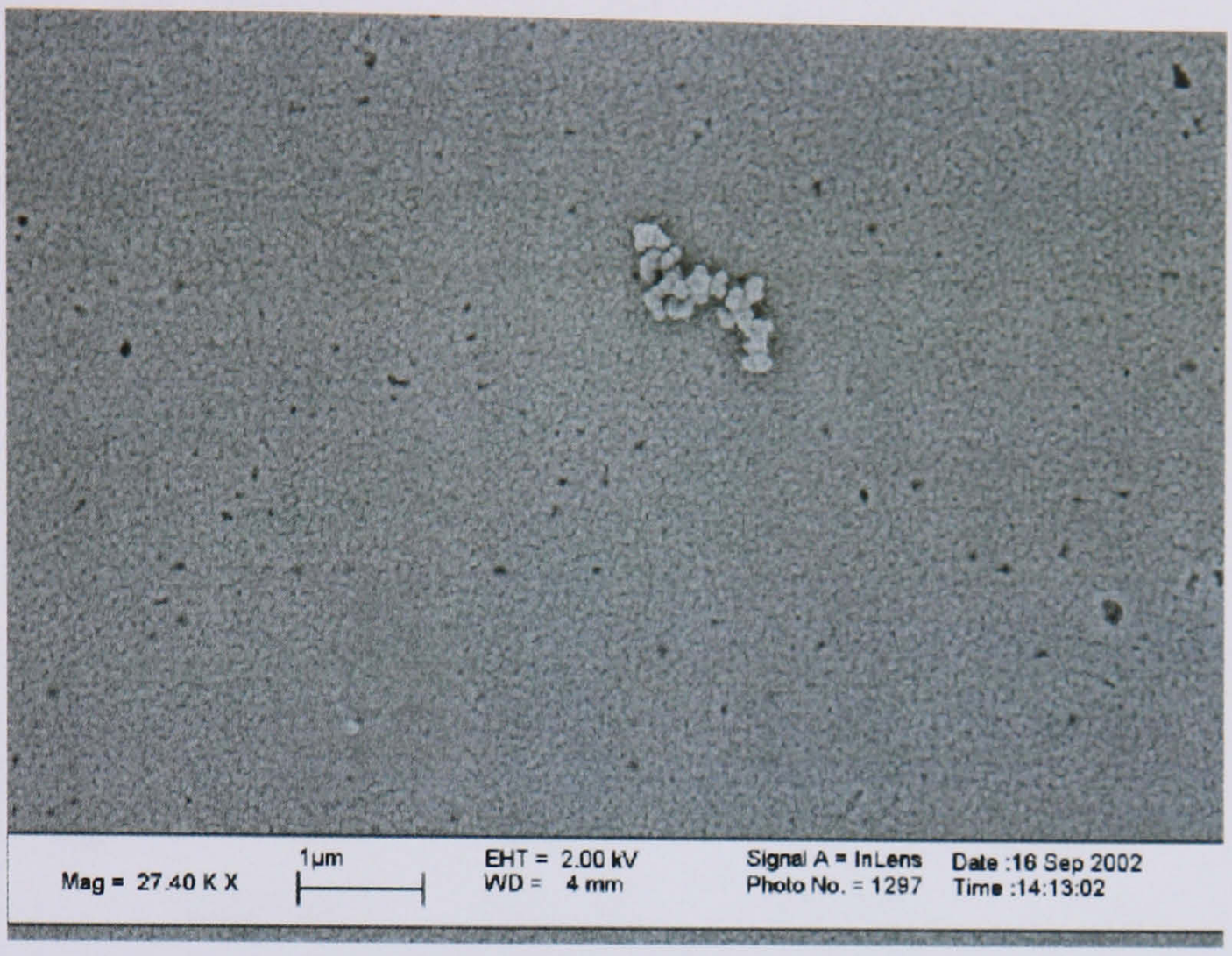

Figure 5.16 SEM image of 0MRad UHMWPE wear debris from a scratched wear test on a 0.1μm filter.

The percentage number of particles in the different size ranges for the 0MRad UHMWPE wear debris is shown in Figure 5.17. The numbers of particles in the 0.01μm-0.1μm and the 0.1-1.0μm were similar with very few particles in the other two size ranges.

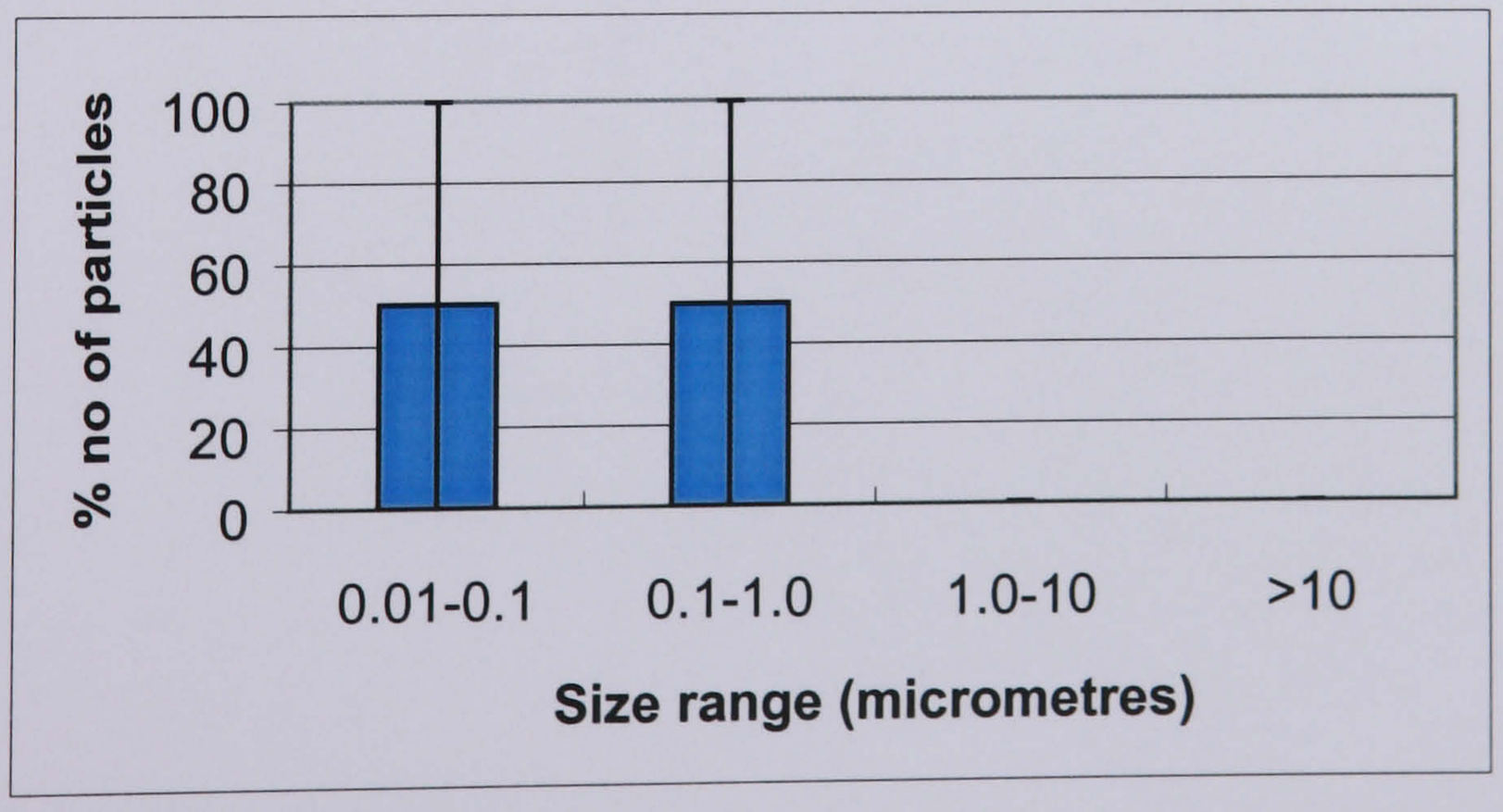

Figure 5.17 Percentage number of particles as a function of size from 0MRad UHMWPE wear debris.

The percentage area of particles as a function of size for the 0MRad UHMWPE wear debris is shown in Figure 5.18. The main area of the particles was in the 0.1-1.0μm size range. The percentage of the area in each of the other size ranges was similar. The area in the >10μm size range was greater than the area recorded for the smooth wear debris. Larger particles were therefore generated in the scratched test.

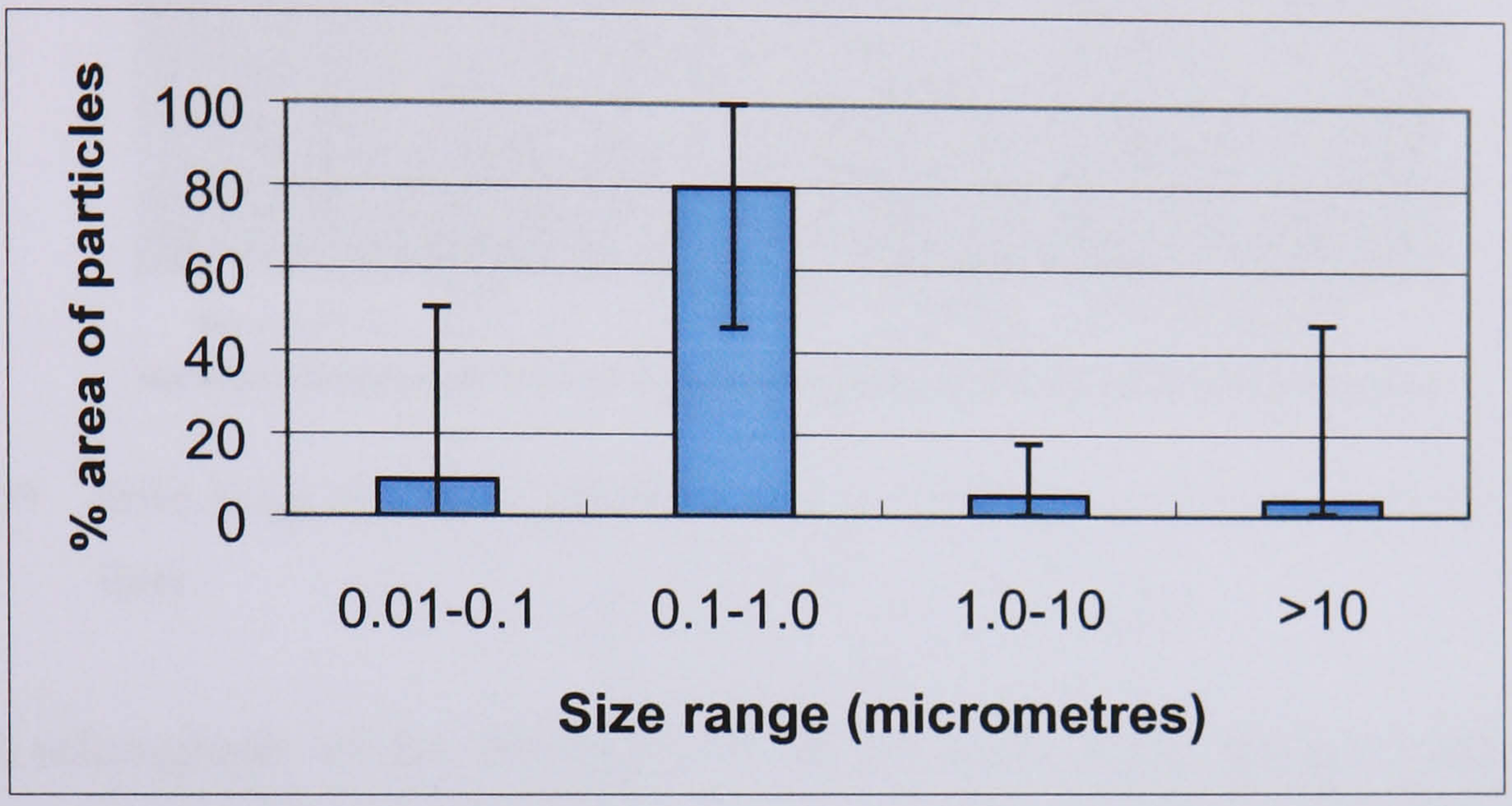

Figure 5.18 Percentage area of particles as a function of size for the 0MRad UHMWPE wear debris.

A SEM micrograph of the 5MRad UHMWPE wear debris seen on a 1μm filter is shown in Figure 5.19. The debris was again small and round with very few larger particles being observed. The debris appeared to be slightly less clumped together than the debris isolated from the smooth test.

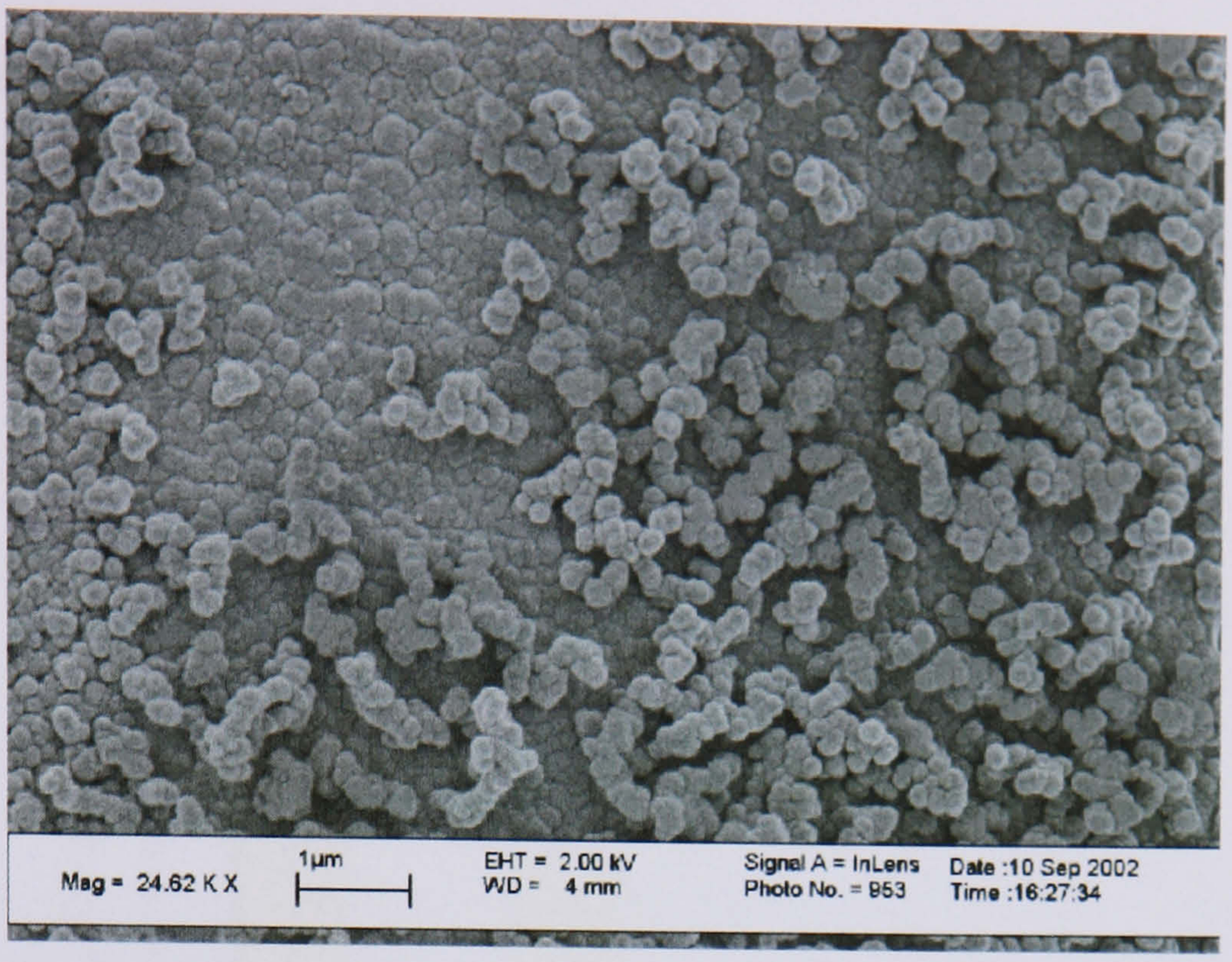

Figure 5.19 SEM image of 5MRad UHMWPE wear debris from a scratched wear test on a 1µm filter.

A SEM micrograph of the 5MRad UHMWPE wear debris on a 0.1µm filter is shown in Figure 5.20. There were very few particles to be found on filters of this size with most of the debris being on the 1µm filter. The particles that were seen were all very small.

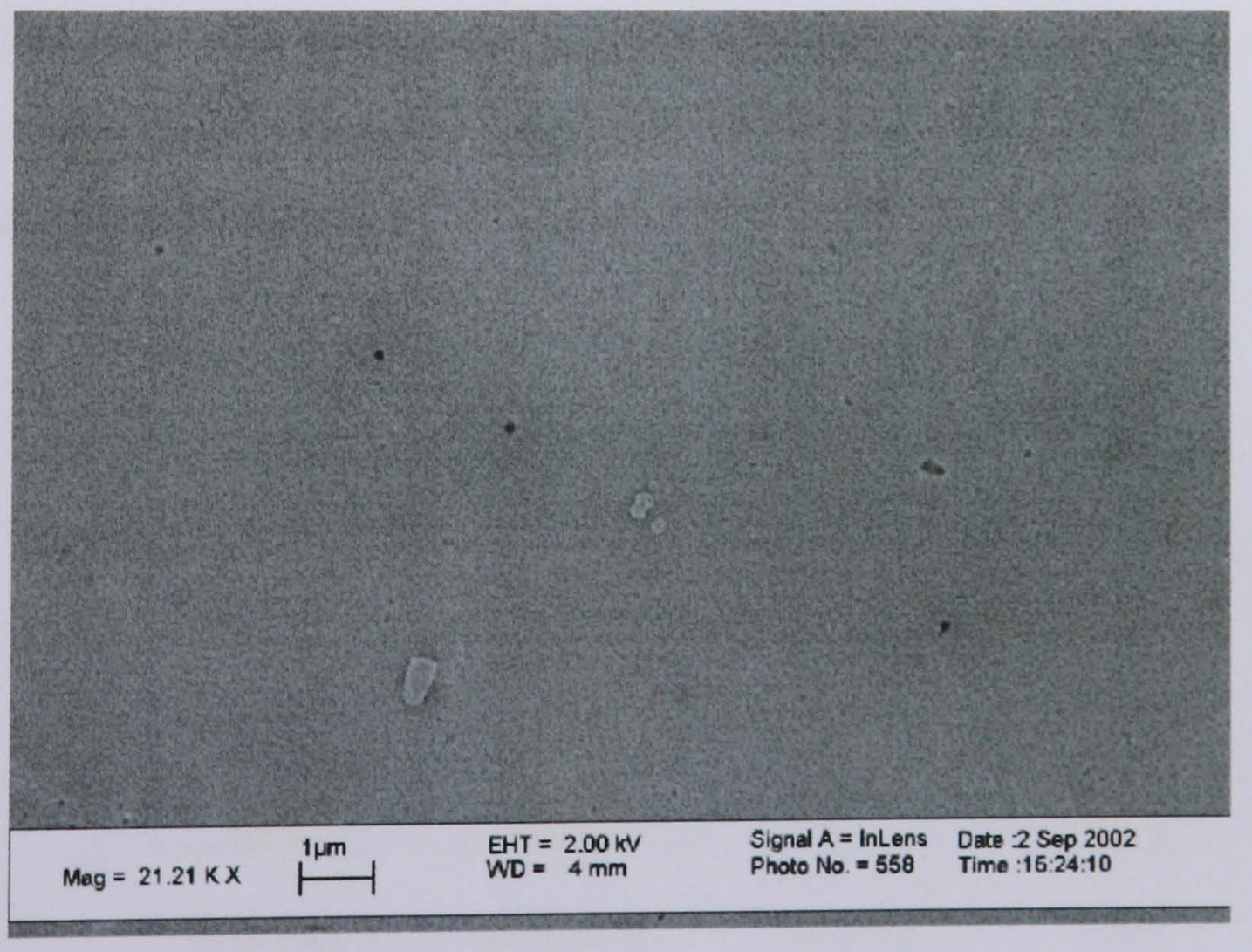

Figure 5.20 SEM image of 5MRad UHMWPE wear debris from a scratched wear test on a 0.1µm filter.

The percentage numbers of particles in each size range is shown in Figure 5.21. The results showed that the greatest number of particles were in the smallest size range. There were also many particles in the 0.1-1.0μm size range but very few in the size ranges above this.

Figure 5.21 Percentage number of particles as a function of size for the 5MRad UHMWPE wear debris.

The percentage area of the particles as a function of size for the 5MRad UHMWPE wear debris is shown in Figure 5.22. The majority of the area was in the 0.1-1.0μm size range. The smallest and largest size ranges had similar areas. The percentage area in the >10μm size range was increased compared to the amount generated against the smooth counterface.

Figure 5.22 Percentage area as a function of size of particles from 5MRad UHMWPE wear debris.

A 1μm filter SEM micrograph is shown in Figure 5.23. The debris is from the 10MRad UHMWPE material. As with all the previous images the debris appeared small and round and there were not many larger particles.

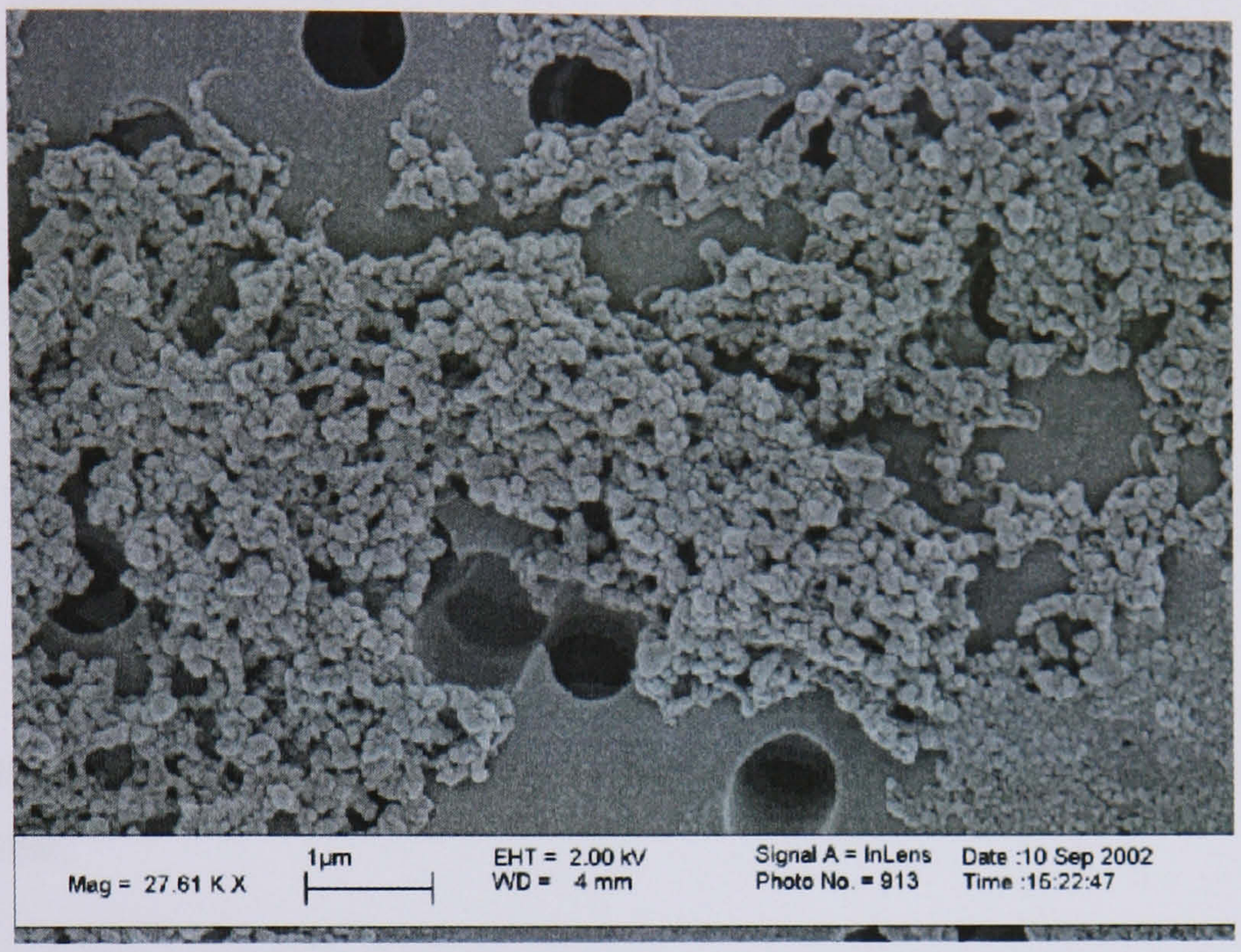

Figure 5.23 SEM image of 10MRad UHMWPE wear debris from a scratched wear test on a 1μm filter.

A SEM micrograph of the 10MRad UHMWPE wear debris on a 0.1μm filter is shown in Figure 5.24. There was little wear debris on this filter and any debris that was there was small.

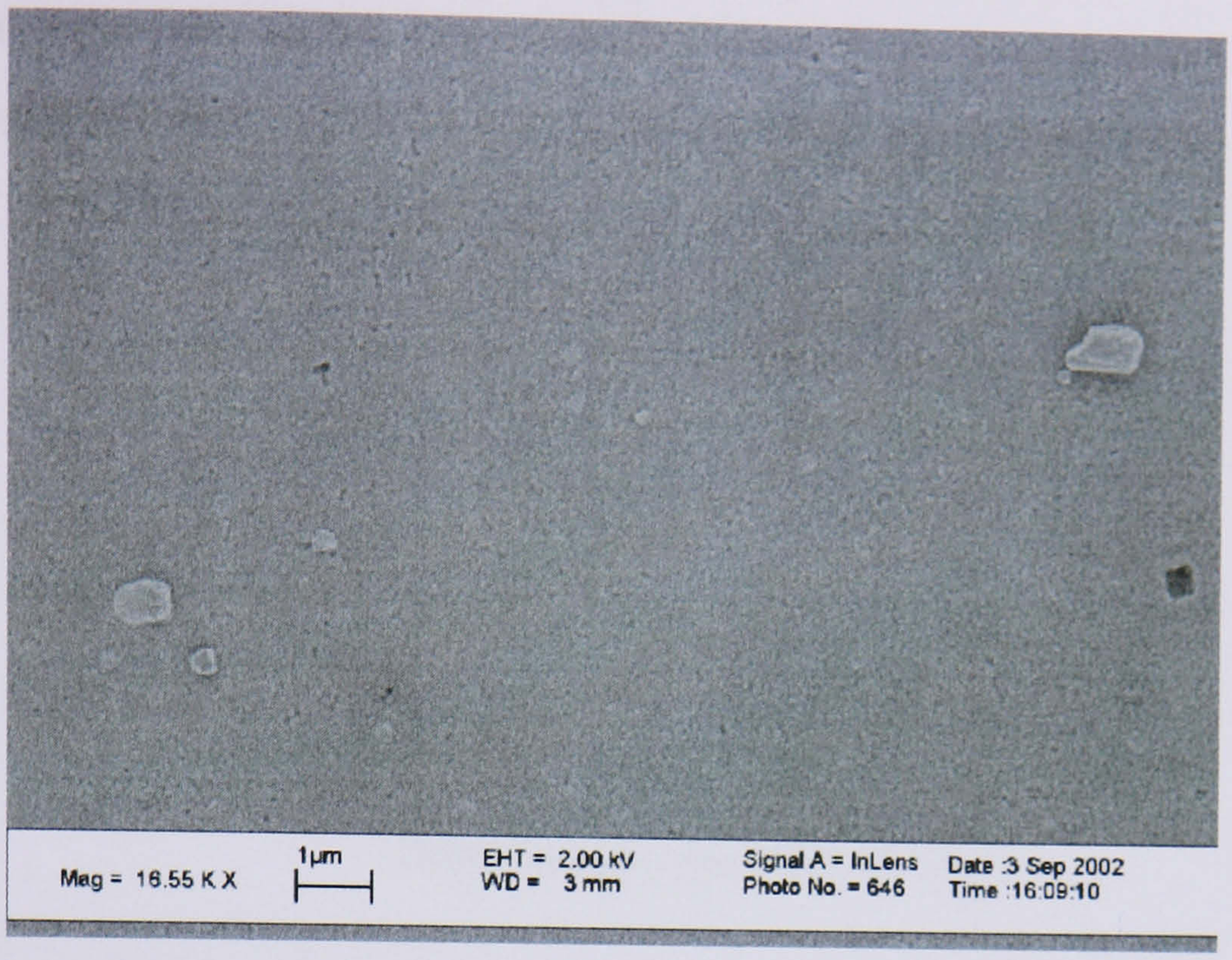

Figure 5.24 SEM image of 10MRad UHMWPE wear debris from a scratched wear test on a 0.1µm filter.

The percentage numbers of particles as a function of particle size is shown in Figure 5.25. Most of the particles were found to be less than 0.1µm, although there were still several particles in the 0.1-1.0µm size range. There were very few particles above this size range.

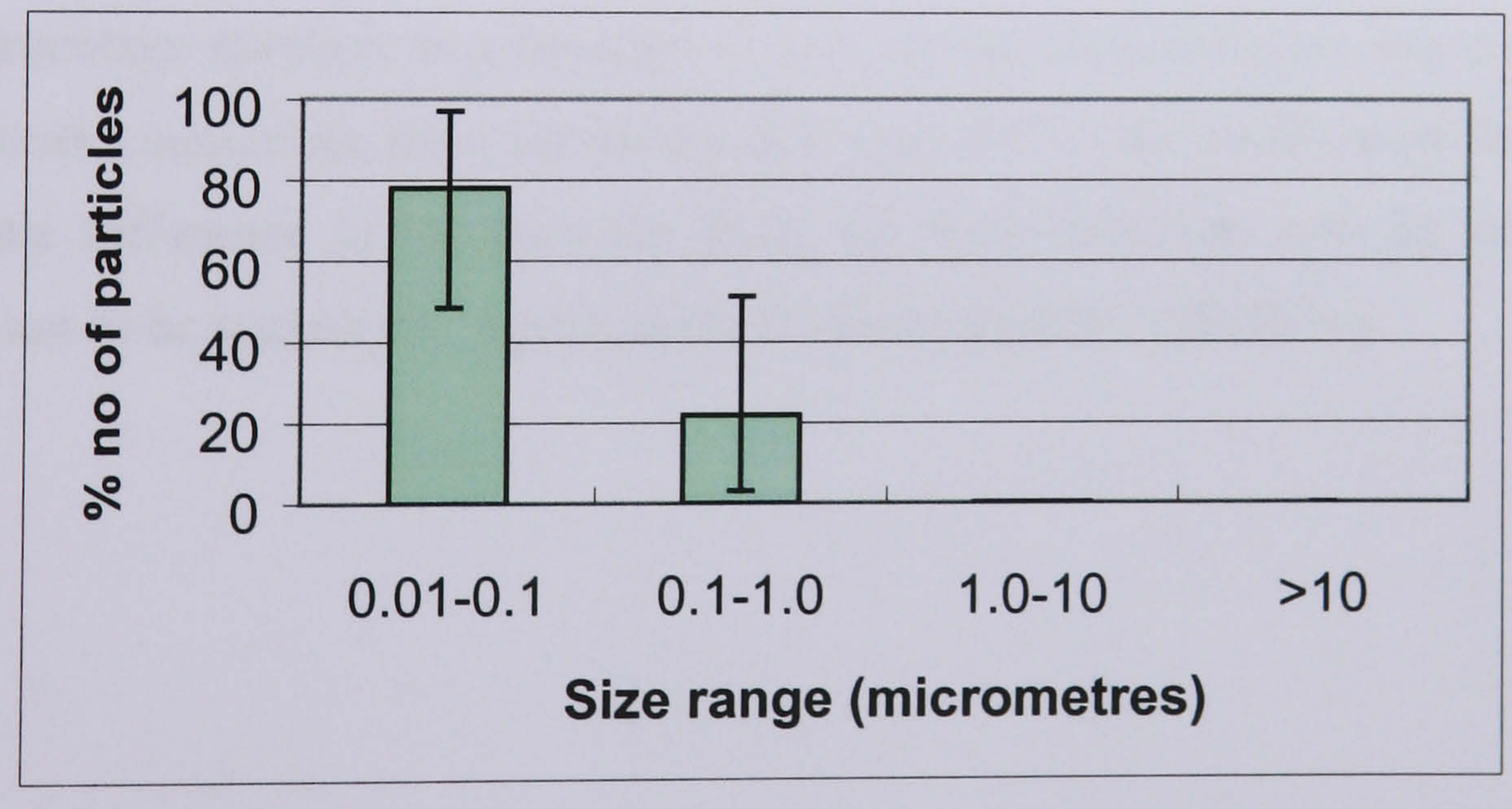

Figure 5.25 Percentage number of particles as a function of size for the 10MRad UHMWPE wear debris.

The percentage area as a function of particle size for the 10MRad UHMWPE wear particles is shown in Figure 5.26. The majority of the area of the particles was in the 0.1-1.0µm size range. As with the other wear debris from the scratched counterfaces

there were more particles above 10μm compared to the debris generated against the smooth counterface.

Figure 5.26 Percentage area as a function of size of particles from 10MRad UHMWPE wear debris.

5.3.3. Comparison of Wear Debris.

The percentage number and the percentage area of particles in the different size ranges for the 0MRad, 5MRad and 10MRad UHMWPE wear debris were combined in single figures for comparison (Figures 5.27-5.32).

The percentage numbers as a function of size for the three different materials from the smooth counterface tests are shown in Figure 5.27. The results show that there was little difference in the particles from the three materials and the data were shown not to be statistically significantly different ($p>0.05$; ANOVA).

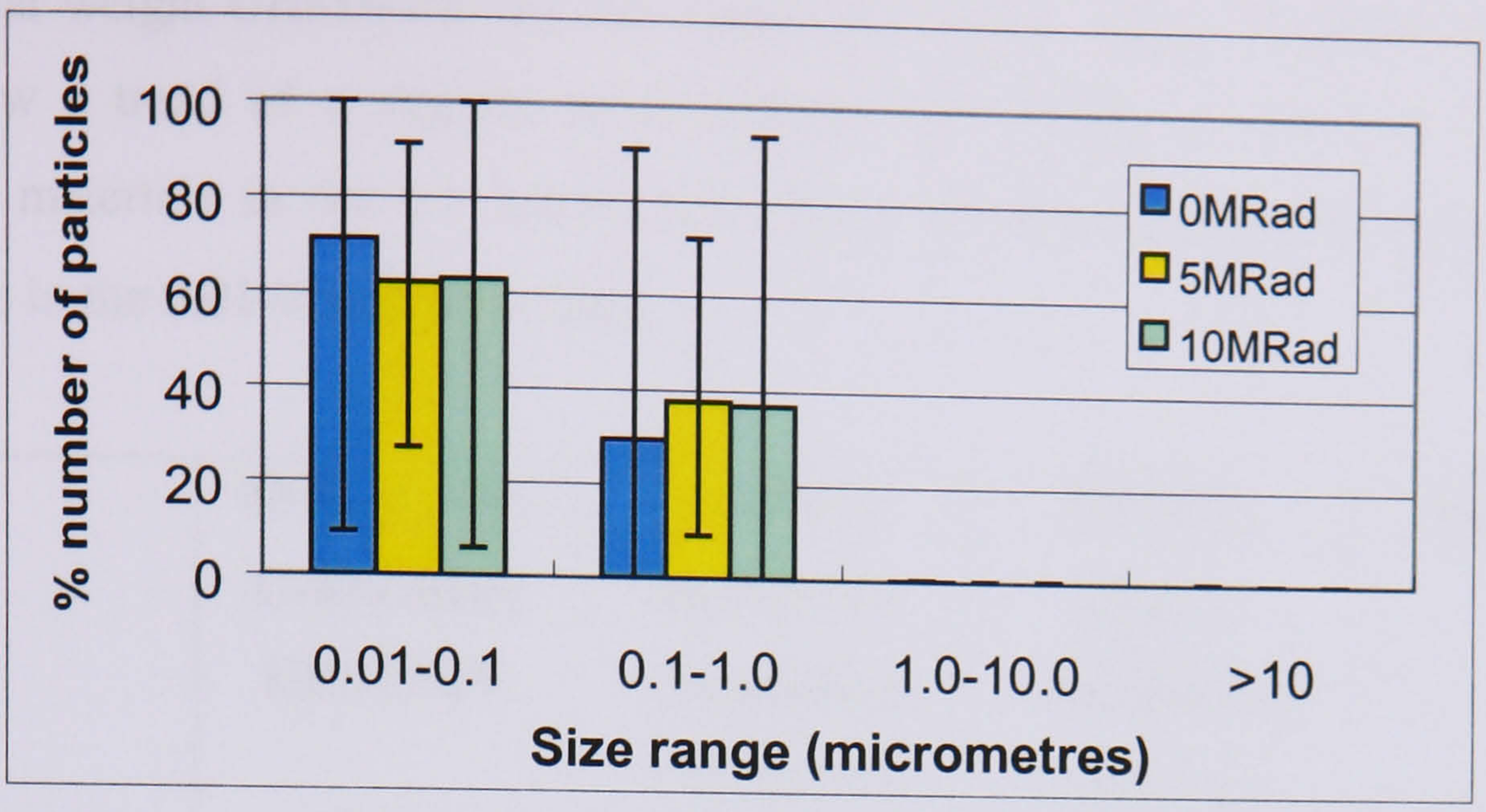

Figure 5.27 Percentage number of particles in each size range from all materials against a smooth counterface.

The percentage area of particles in the different size ranges of the three materials from the smooth counterface tests are shown in Figure 5.28. There was no difference in the particles from the three materials and the results were again found to be not statistically significantly different ($p>0.05$; ANOVA).

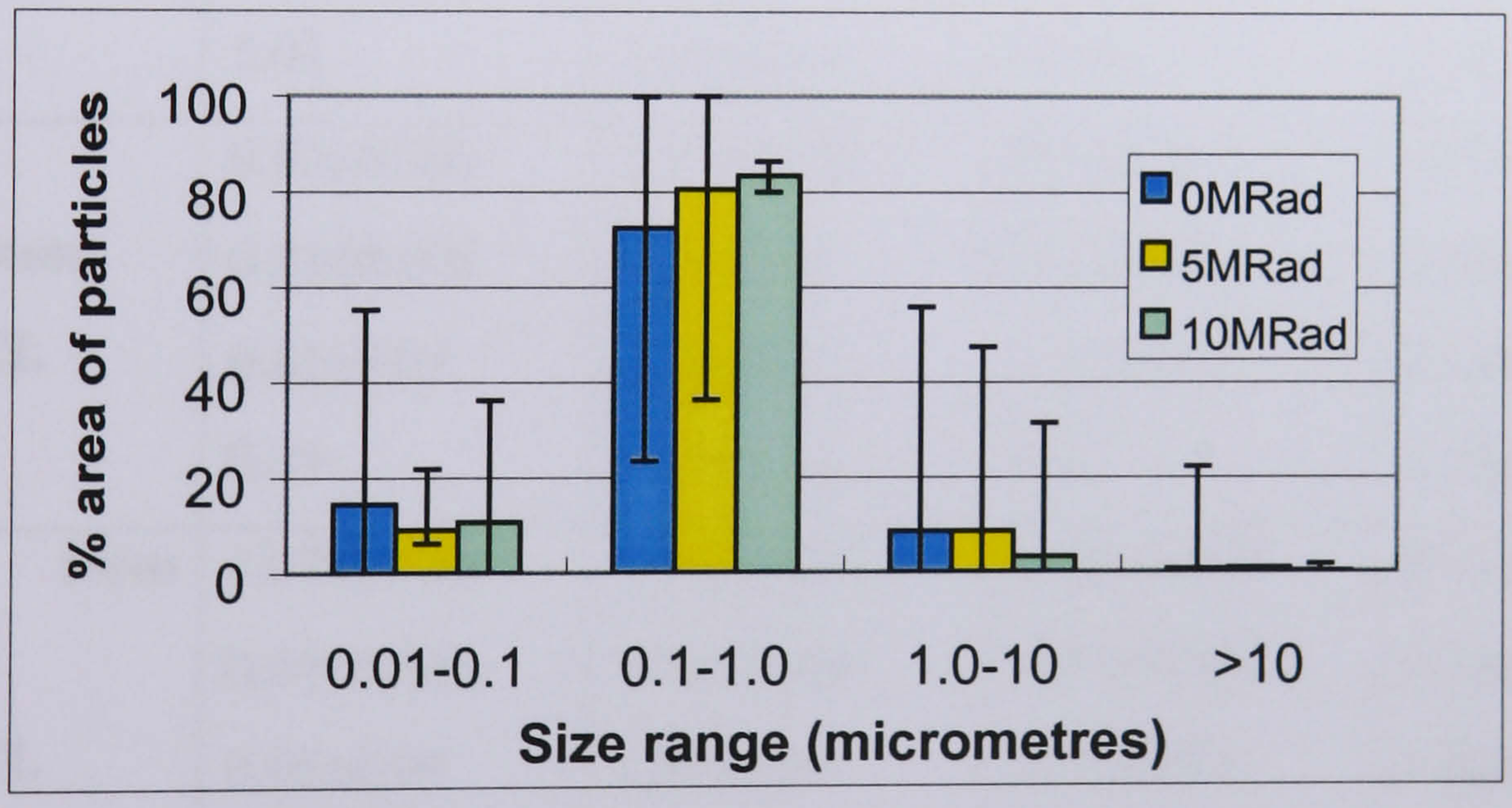

Figure 5.28 Percentage area of particles in each size range from all materials against a smooth counterface.

The wear debris characteristics are summarised in Table 5.1. The results showed that there was no significant difference in any of the parameters used to measure the particles across the three materials. Previous studies (Yamamoto *et al.*, 2001; Endo *et al.*, 2002) have shown that crosslinked UHWMPE produces smaller particles but this was not reflected in the results seen in this study. These studies looked at lower

molecular weight UHMWPE and this could have been a factor. However this study did show a trend of a slightly lower number and volume of particles from the 0MRad materials in the 0.1-1.0μm size range. No previous studies have shown particles in the 0.01-0.1μm size range.

	0MRad Non-Crosslinked UHMWPE	**5MRad Moderately Crosslinked UHMWPE**	**10MRad Highly Crosslinked UHMWPE**	**Size range**
Mean equivalent circle diameter ±95% CL	0.06±0.001 0.22±0.007 1.57±0.21 6.17	0.08±0.03 0.27±0.009 2.32±0.33 21.70±8.09	0.07±0.001 0.24±0.008 1.75±0.33 22.8	0.01μm-0.1μm 0.1μm-1.0μm 1.0μm-10μm >10μm
Mean aspect ratio ±95% CL	1.36±0.012 1.41±0.02 1.63±0.38 5.02	1.31±0.01 1.40±0.02 1.45±0.73 2.51±0.80	1.35±0.02 1.46±0.03 1.45±0.11 1.54	0.01μm-0.1μm 0.1μm-1.0μm 1.0μm-10μm >10μm
Mean Roundness ±95% CL	0.90±0.006 0.83±0.006 0.81±0.03 0.29	0.92±0.008 0.86±0.01 0.84±0.03 0.53±0.12	0.92±0.04 0.81±0.01 0.82±0.05 0.73	0.01μm-0.1μm 0.1μm-1.0μm 1.0μm-10μm >10μm
Mean form factor ±95% CL	1.07±0.005 0.99±0.006 0.95±0.04 0.43	1.10±0.005 1.01±0.006 1.04±0.03 0.71±0.14	1.69±0.006 0.97±0.006 1.00±0.04 0.79	0.01μm-0.1μm 0.1μm-1.0μm 1.0μm-10μm >10μm
Mean elongation. ±95% CL	1.28±0.008 1.27±0.01 1.29±0.06 3.11	1.24±0.01 1.27±0.01 1.35±0.06 2.27±0.66	1.27±0.014 1.29±0.01 1.35±0.09 1.12	0.01μm-0.1μm 0.1μm-1.0μm 1.0μm-10μm >10μm

Table 5.1 Size and morphology of wear debris from 0Mrad, 5MRad and 10MRad UHMWPE generated under smooth counterface conditions.

The percentage number of particles in the different size ranges for all three materials generated against a scratched counterface is shown in Figure 5.29. The results showed some differences between the particles from the three materials but this was not found to be statistically significantly different ($p>0.05$; ANOVA).

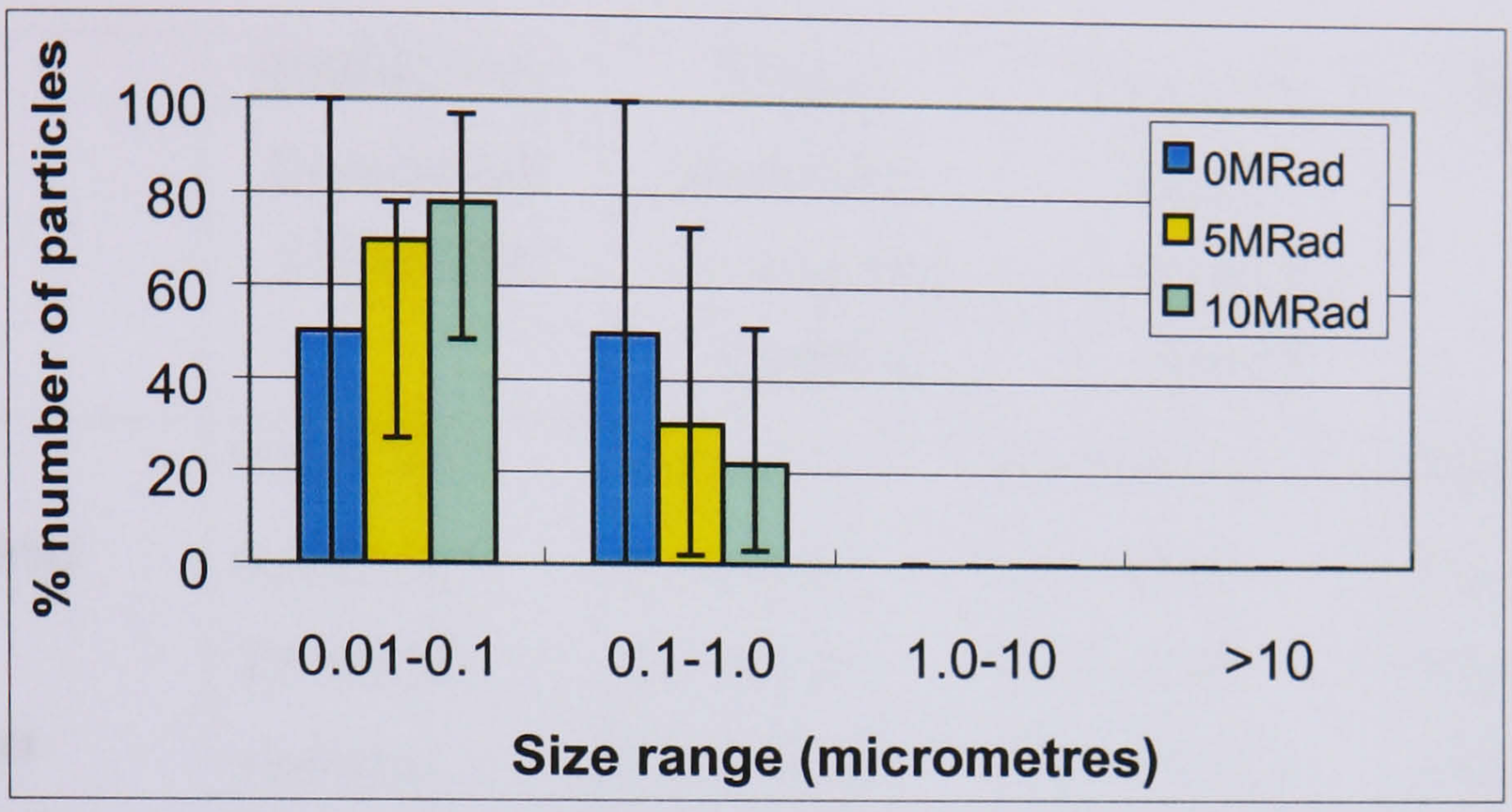

Figure 5.29 Percentage number of particles in the different size ranges from all materials against scratched counterfaces.

The percentage area of particles in the different size ranges from the three materials from a scratched counterface test is shown in Figure 5.30. There was a small variation in the particles results but again this was not found to be statistically significantly different. There was a greater area of particles in the >10μm size range compared to the smooth counterface study.

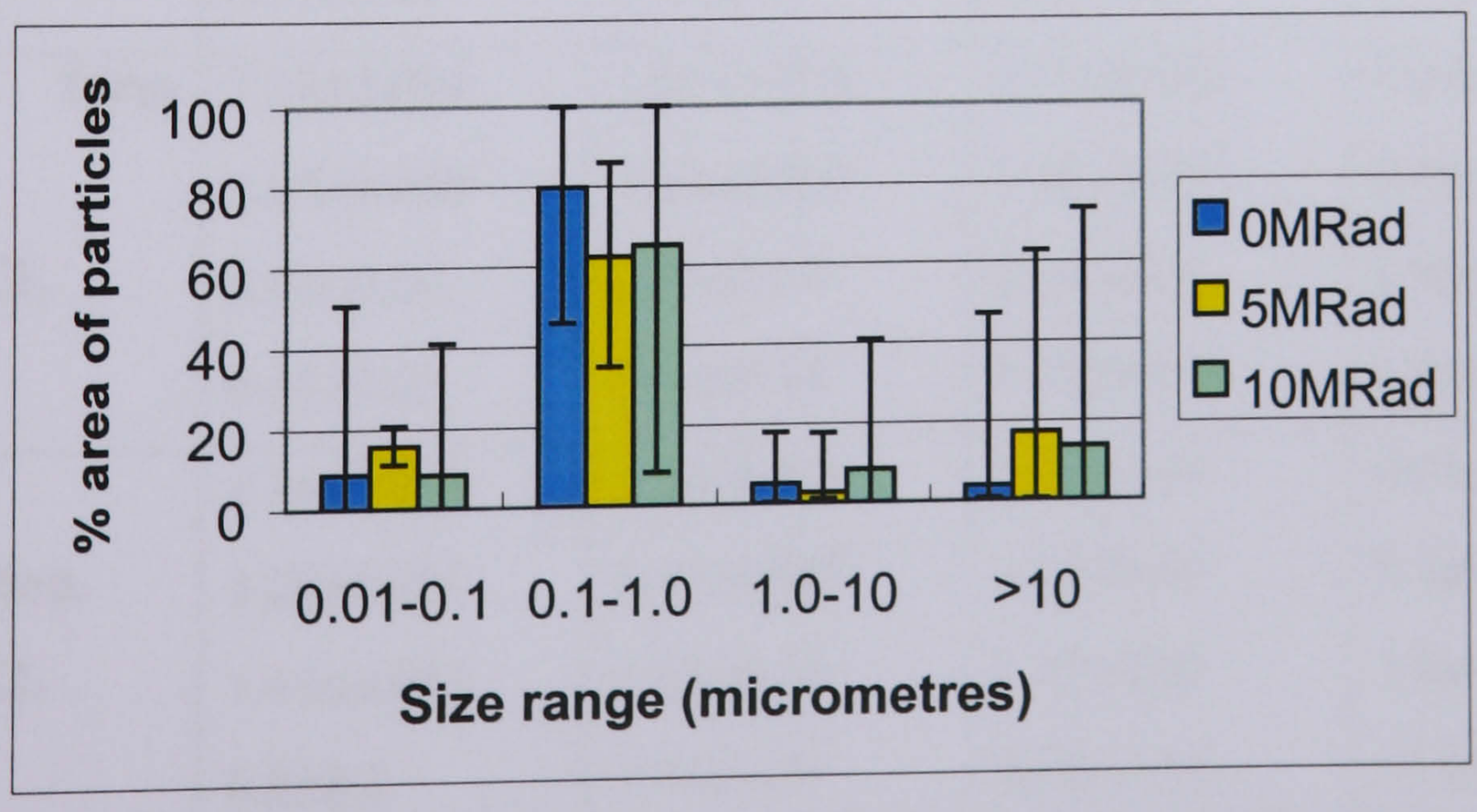

Figure 5.30 Percentage area of particles in the different size ranges from all materials against scratched counterfaces.

The particle characteristics of the wear debris generated in the scratched counterface are shown in Table 5.2. The results showed that there was no statistically significant difference in the sizes of the debris from the three materials. The crosslinked material did not generate smaller particles than the non crosslinked material.

	0MRad Non-Crosslinked UHMWPE	**5MRad Moderately Crosslinked UHMWPE**	**10MRad Highly Crosslinked UHMWPE**	**Size range**
Mean equivalent circle diameter ±95%CL	0.07±0.001 0.23±0.005 2.57±0.56 18.9±5.6	0.07±0.001 0.20±0.004 2.15±0.36 33.8±19.31	0.07±0.001 0.31±0.01 2.20±0.15 34.16±13.05	0.01μm-0.1μm 0.1μm-1.0μm 1.0μm-10μm >10μm
Mean aspect ratio ±95%CL	1.3±0.009 1.35±0.008 1.57±0.12 3.77±2.24	1.31±0.009 1.36±0.009 1.77±0.16 3.71±1.04	1.31±0.009 1.35±0.01 1.60±0.06 2.42±0.46	0.01μm-0.1μm 0.1μm-1.0μm 1.0μm-10μm >10μm
Mean Roundness ±95%CL	0.92±0.02 0.87±0.004 0.77±0.06 0.51±0.13	1.20±0.20 0.87±0.004 0.73±0.05 0.4±0.14	0.92±0.007 0.89±0.01 0.78±0.02 0.56±0.06	0.01μm-0.1μm 0.1μm-1.0μm 1.0μm-10μm >10μm
Mean form factor ±95%CL	1.08±0.004 1.05±0.003 0.94±0.06 0.65±0.13	1.08±0.003 1.05±0.003 0.93±0.04 0.54±0.14	1.09±0.004 1.06±0.005 0.98±0.01 0.71±0.078	0.01μm-0.1μm 0.1μm-1.0μm 1.0μm-10μm >10μm
Mean elongation. ±95%CL	1.24±0.009 1.28±0.007 1.45±0.097 6.0±8.2	1.25±0.008 1.27±0.007 1.63±0.14 3.31±1.29	1.25±0.01 1.28±0.01 1.45±0.05 2.08±0.45	0.01μm-0.1μm 0.1μm-1.0μm 1.0μm-10μm >10μm

Table 5.2 Size and morphology of wear debris from 0MRad, 5MRad and 10MRad UHMWPE generated under scratched counterface conditions.

5.3.4. Volumes of Particles.

The volume of debris found in each size range is shown in Figure 5.31. The results showed that the 10MRad UHMWPE wear debris had a lower wear volume of particles in the 0.1-1.0μm size range than the other two materials, although because of the variation between samples this was not significantly different.

Figure 5.31 Volume of wear particles in the different size ranges from the smooth pin on plate study.

The volume of debris in the different size ranges from the scratched pin on plate test is shown in Figure 5.32. The volumes were much higher than for the smooth tests because of the increased wear. Again the 10MRad UHMWPE wear debris had a lower wear volume then the other two materials in the 0.1-1.0μm size range. There was little difference in the volume for the other two materials apart from a slight increase in the volume of larger particles with the 5MRad UHMWPE wear debris.

Figure 5.32 Volume of wear particles in the different size ranges from the scratched pin on plate study.

5.3.5. Specific and Functional Biological Activity.

After the percentage area of each of the particles had been calculated the SBA was calculated for each of the materials. The results showed that there was little difference in the SBA of any of the materials. The scratched SBA was slightly lower with the crosslinked materials but the difference was not significant ($p>0.05$; ANOVA).

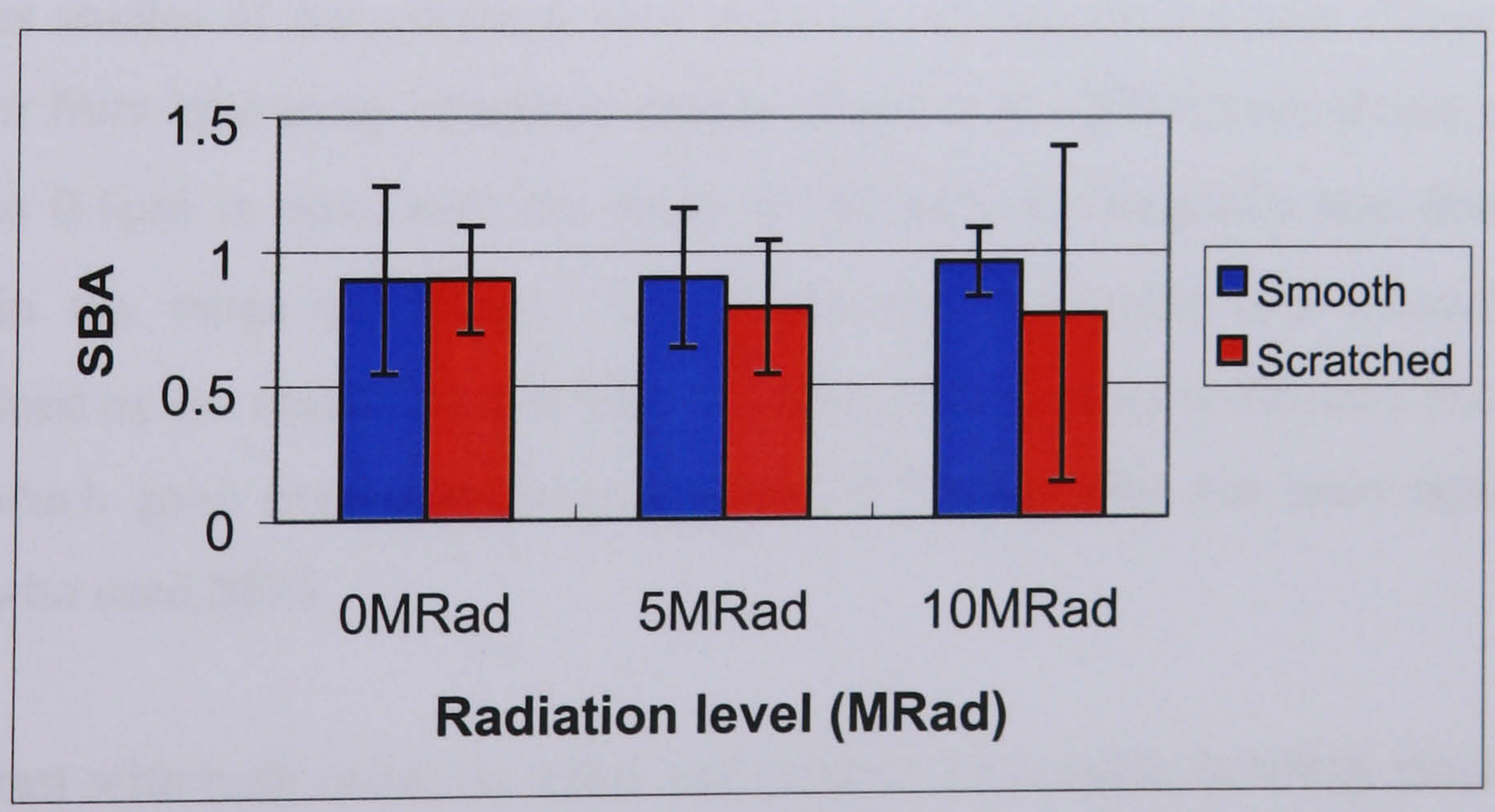

Figure 5.33 SBA of wear debris.

After the SBA's were calculated, the FBA's for each material were then obtained. These results showed that the scratched debris gave a much higher FBA than the smooth debris for all three materials. The 10MRad highly crosslinked materials gave

the lowest FBA on both smooth and scratched counterfaces. There was not any difference in the FBA of the 0MRad and 5MRad UHMWPE wear debris with both of the counterface conditions. The FBA in this study was calculated from a wear volume per million cycles from a pin on plate test. This resulted in much lower values than those previously reported by Fisher *et al.* (2001) who used simulator studies to calculate their FBA.

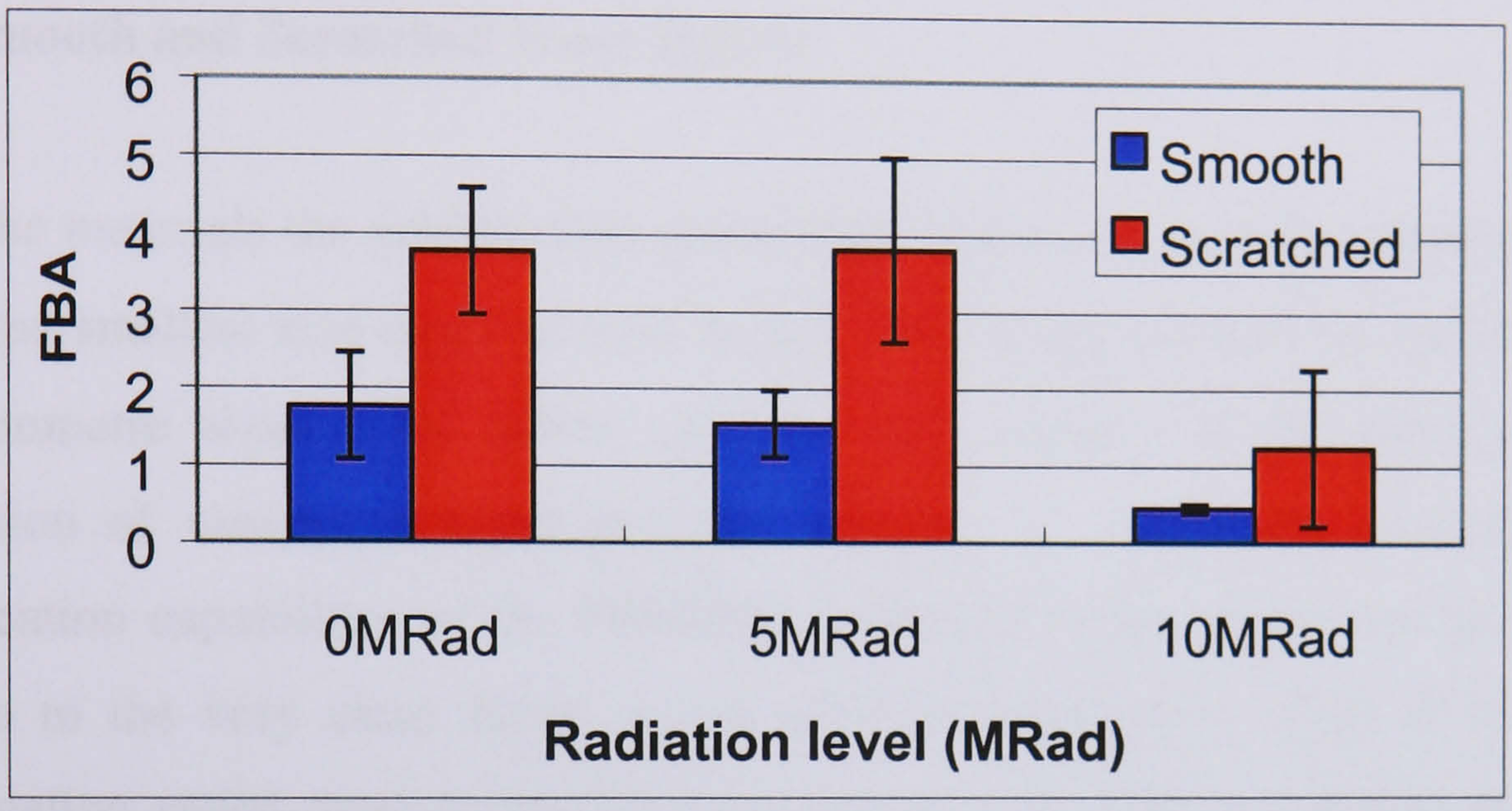

Figure 5.34 FBA of wear debris.

5.4 Discussion.

Previous studies of polyethylene wear debris from explanted tissues (Tipper *et al.*, 2000) or from laboratory simulator studies (Endo *et al.*, 2002) have shown particles down to 0.1μm in size, with the mode of the particle frequency size distribution being in the range 0.1-1.0μm. The lowest size detectable and measured was determined by the resolution and magnification of the scanning electron microscope used, which gave maximum magnification of ??????. This has been reported by others who used SEM.

In contrast with both metal on metal and ceramic on ceramic bearings much higher resolution transmission electron microscopy has been used to detect these more electron dense particles down to 10nm in size. Transmission electron microscopy is not appropriate for detection and imaging of polyethylene particles.

In the early stages of this study conventional SEM was used and particle distribution down to 100nm were recorded. However during the course of the project a new field emission gun scanning electron microscope became available and this allowed high resolution imaging of polyethylene particles down to 10nm in size. The result was the detection for the first time of large numbers of polyethylene particles in the size range 10-100nm.

5.4.1. Smooth and Scratched Wear Debris.

For all the materials the predominant percentage number of the wear debris particles was in the smallest size range of 0.01-0.1μm. This study showed for the first time that nanometre sized wear debris particles were present in the lubricant. The observation of nanometre sized particles was due to the higher resolution and magnification capabilities of the FEGSEM compared to the SEM used previously and also to the very clean filters which were produced as a result of the faster centrifugation speed used during the isolation process. This meant that the small particles were not obscured by proteins and bacteria on the filters. Nanometre sized particles were seen in the debris generated against both the smooth and scratched counterfaces.

When the percentage area was calculated the predominant size range was the 0.1-1.0μm size range. This shift in the predominant size range between the percentage number and the percentage area of particles was due to the very small size of particles in the smallest size range. Although there were a lot less particles in the larger size range their greater size meant that overall they had a much greater area.
The analysis of the wear debris generated against the scratched counterface showed that more particles were found in the largest size range (>10μm). This was due to a different wear mechanism generating the particles. An abrasive wear mechanism meant that larger particles were generated even with the crosslinked material. Less molecular orientation was produced and molecules of UHMWPE were removed by a single asperity interaction.

5.4.2. Volumes of Particles.

The results from the volume of debris generated against both the smooth and scratched counterface showed that the 10MRad UHMWPE wear debris gave a lower volume in most of the size ranges, although because of the high variation in the samples only the 0.1-1.0μm was significantly different. This reduction in volume was because of the lower wear factors of the crosslinked material. Even though the percentage areas of the particles did not show any significant difference the volume of particles was reduced with the highly crosslinked material.

The debris generated against the scratched counterface had higher wear volumes than the debris generated against the smooth counterfaces. Again this was because of the higher wear factors seen when the materials where tested against a scratched counterface.

The significant reduction in the 0.1-1.0μm size range with the highly crosslinked UHMWPE in both the smooth and scratched UHMWPE wear debris was a very important observation. This size range is the most biologically active so the lower volume of particles that are in this size range, the less likely there is to be a reaction to them, as it is not only the size that is important but also the volume.

5.4.3. Specific and Functional Biological Activity.

The SBA for all the materials was approximately equal. The 10MRad UHMWPE smooth wear debris had a slightly higher SBA but this was not significantly different. There was no significant difference between any of the SBA values. The lack of any significant difference was not surprising when looking at the percentage areas of particles seen as they were very similar for all the materials. However when the FBA was calculated for the highly crosslinked material it had a significantly lower value than the other two materials on both the smooth and scratched counterfaces due to the reduced wear factors found with highly crosslinked material. There was no significant difference between the 0MRad and 5MRad UHMWPE wear debris FBA values from the smooth and scratched counterface. However the

difference between the 0MRad UHWMPE wear debris FBA values from the smooth and scratched surfaces was statistically significantly different. The same was true for the 5MRad UHMWPE wear debris. Previous studies looking at wear debris particles from highly crosslinked UHMWPE have reported seeing smaller particles with the highly crosslinked material compared to non-crosslinked UHMWPE in tests carried out against smooth counterfaces (Scott *et al.*, 2001). Most of these studies have used debris taken from simulator studies and this could be a factor. Previous studies have also looked at lower molecular weight polyethylene such as GUR 1020 UHMWPE.

A study by Endo *et al.* (2001) found that non-irradiated GUR 1120 produced more of the larger particles. This was also seen in a study by Ingram *et al.* (2002) who found larger particles with the lower molecular weight polyethylene. They showed that GUR 1050 wear debris was more reactive than GUR 1120 wear debris due to more smaller particles present in the GUR 1050. Endo *et al.* (2001) found smaller particles in crosslinked GUR 1120 UHMWPE compared to noncrosslinked UHMWPE wear debris. Crosslinking has less effect at the higher molecular weight because of the smaller particles found in the noncrosslinked UHMWPE. The present study and the study by Ingram *et al.* (2002) would suggest that the molecular weight of the polyethylene has more of an impact on its biological activity than the radiation level and amount of crosslinking. The results show that the higher molecular weight UHMWPE has more smaller particles. As the nonirradiated UHMWPE 1050 has smaller particles the effect of crosslinking is less.

The reduction in the FBA value for the 10MRad material was due to its much lower wear factor as seen in the wear tests. As the wear factors for the 0MRad and 5MRad materials were similar, the lack of difference in the FBA values were not unexpected.

5.4.4 Nanometre Particles.

This study has shown the presence of nanometre sized particles for the first time. At present little is known about the biological reaction to nanometre sized particles *in vivo*. A recent study by Galvin *et al.* (2004) has found nanometre sized particles

present in hip and knee simulator debris, although the PE used was a different molecular weight to the PE used throughout this thesis.

Nanometre sized particles have been widely reported in literature on ceramic and metal prostheses. These are observed using a transmission electron microscope which is not suitable for looking at UHMWPE particles. A study by Hatton *et al.* (2003) found that clinically relevant ceramic wear particles (bimodal size distribution 5-20nm and 0.2->10μm) needed a higher volume to stimulate TNFα production compared to uniform 0.5μm ceramic particles. They postulated that this was because there was less volume of particles in the most biologically active size range in the clinically relevant debris. This suggests that nanometre sized particles are either less reactive than those in the 0.1-1.0μm size range or that a far greater volume is needed for them to activate macrophages. Although ceramic particles do not react in completely the same way as PE particles (they are thought to be less reactive) their most biologically active size range is the same. At present the biological activity of polyethylene particles in the size range 10-100nm has not been directly studied. This needs to be the focus of future studies. However it is clear from the graphs of particle area as a function of size that only a small percentage volume of debris (even though this comprises the largest number of particles) is in the size range 10-100nm. This small percentage volume is unlikely to play a major role in the osteolytic cascade unless they are much more reactive than particles in the size range 0.1-1.0μm, which at present we do not think is the case. A further consideration for the small 10-100nm size particles is their transport within the body. Particles of this size may be taken up by cells by mechanisms other than phagocytosis and they may be distributed more widely in the body. Again this requires further research.

5.5 Conclusion.

Although the percentage areas and numbers in the different size ranges of the materials showed no difference between the materials, when the FBA's were calculated a difference was seen. The highly crosslinked material was found to have a much lower FBA than the other two materials. The FBA values for the debris

generated against a smooth counterface were also statistically significantly lower than the results from the scratched surfaces. This was due to their lower wear factors and wear volumes. This study showed that the 10MRad material was the optimal in terms of its FBA value and wear factors. This study also showed for the first time the presence of nanometre sized wear debris particles.

Chapter 6.

6. Discussion and Conclusions.

6.1. Introduction.

Total hip arthroplasty is one of the most successful surgical procedures of recent times. However wear debris induced osteolysis remains a problem. UHMWPE wear particles have been shown to be a major cause of long term failure of total hip replacements. *In vitro* studies have shown that not only is the size of the wear debris particles important in initiating a osteolytic reaction but the volume of particles is also important.

It was postulated at the start of these research studies that although crosslinked UHMWPE reduced the wear of the materials, the resulting size of the particles produced would be smaller and more biologically active than non-crosslinked UHMWPE particles.

The aim of this study was to investigate the effect of different serum concentrations, different kinematics and counterface roughness on the wear rate of UHMWPE crosslinked at three different levels and also to investigate the wear debris produced. This chapter is a final discussion and conclusion of the results presented throughout this thesis.

6.2. Discussion of Results.

Multidirectional reciprocating pin on plate tests were used to determine the wear rates of UHMWPE with three different levels of crosslinking. In Chapter 3 the materials were examined using a high degree of multidirectionality against different counterface conditions. The effect of serum concentration against smooth counterfaces was also studied. In Chapter 4 the materials were examined at a lower level of multidirectionality against similar counterfaces to those in Chapter 3.

6.2.1. The Effect of Serum Concentration on the Wear of UHMWPE in Pin on Plate Tests.

The results from the study using different serum concentrations in the lubricant, showed that the concentration had a significant effect on the wear rate of UHMWPE. They showed that the serum concentration had the greatest effect on non-crosslinked UHMWPE. The wear factors with the high serum concentration were significantly higher than the results with the low serum concentration. The crosslinked materials both had no significant difference in their wear factors with the different serum concentrations.

The results with the high serum concentration gave a similar pattern to data presented by McKellop *et al.* (1999). They found that the wear of crosslinked UHMWPE was greatly reduced compared to non-crosslinked. They also used high concentrations of serum. The results obtained with the 25% (v/v) serum concentration were similar to those reported by Endo *et al.* (2000) who also used a lower serum concentration.

The serum concentration of the lubricant used during testing has been shown to be important in producing clinically relevant wear rates. The high serum concentration used in this study was considered to be too high and above the physiologically relevant range and therefore the lower serum concentration was used for the subsequent studies.

6.2.2. Effect of Kinematics on the Wear of UHMWPE in Pin on Plate Tests.

The pin on plate studies reported in this thesis were carried out using two different kinematic conditions. These were ±60° and ±20° rotation. This was carried out to determine the effect that multidirectionality had on the three different levels of crosslinking. The results showed that generally the wear factors were lower with the lower levels of rotation. The result from the smooth counterface test at ±20° rotation showed that there was no significant difference between the wear factors for the three materials. At the higher rotation the highly crosslinked material had a significantly lower wear factor. The results from the higher rotation were consistent with results reported by Marrs *et al.* (1999) and Endo *et al.* (2000).

The level of cross shear was examined to determine the effect that this had. The higher rotation gave a higher level of cross shear due to the higher multidirectionality. The lower levels of cross shear in the ±20° rotation experiments meant that more orientational hardening could occur with the non-crosslinked UHMWPE which was why its wear rate was reduced. The levels of crosslinking in the other two materials meant that orientational hardening could not occur as easily, however because the frictional force was reduced the wear rates were not significantly different.

Against the scratched counterfaces the highly crosslinked UHMWPE gave significantly lower wear factors for each of the kinematic conditions. The reduction in the wear rates between the two different cross shear frictional energy levels was less for the highly crosslinked UHMWPE than for the other two materials. This was because the crosslinks provided resistance against cross shear frictional energy. There was no significant difference in wear factors for the 0MRad and 5MRad UHMWPE at either kinematic level. This suggested that the extent of crosslinks in the 5MRad material were not high enough to reduce the effect of cross shear frictional energy.

6.2.3. Effect of Counterface Roughness of the Wear of UHMWPE in Pin on Plate Tests.

The results from the pin on plate tests against different counterfaces showed that the scratched plates increased the wear rate of the three materials. The increase in wear was significant for all the materials, however the highly crosslinked material had a significantly lower wear rate than the 0MRad and 5MRad UHMWPE's.

The results from the smooth counterface tests were consistent with the results of Marrs *et al.* (1999) and Endo *et al.* (2000). Both of these studies showed a decrease in wear with crosslinked UHMWPE. The reduction in wear rate was thought to be due to orientational hardening. Crosslinking reduces the amount of orientational hardening that can occur and provides more resistance to cross shear frictional energy which is an advantage against multidirectional motion (Wang *et al.*, 1997).

The crosslinks in the material also provided resistance to the scratches and resulted in the lower wear factor for the highly crosslinked material against the scratched counterface compared to the noncrosslinked material. Orientational hardening was thought to have less effect against the scratched counterface as the molecules were removed more easily and often by just a single interaction with a scratch.

The wear mechanism also changed according to the counterface surface. Against a smooth counterface the main wear mechanism involved was an adhesive micro-polishing one. This occurs when it takes many interactions to remove a particle from the surface. The surfaces of the pins showed ripples and polished areas which are characteristic of these mechanisms. On the scratched counterfaces an abrasive mechanism was more likely to occur. This meant that the particles were removed by very few interactions. The higher scratches generated more of a stress concentration when they cut into the polymer, than the medium scratches and therefore gave higher wear factors.

6.2.4. Wear Debris from Smooth and Scratched Wear Tests.

The wear debris from the pin on plate tests was analysed in Chapter 5. Debris was taken from smooth and scratched tests at ±60° rotation. The results from the analysis showed that there was no significant difference between the materials on the smooth and scratched counterfaces. The lack of significant difference was partly due to the high variation between samples which could have been reduced if more samples had been studied.

The percentage number of particles in different size ranges showed that for all the materials the predominant size range was the 0.01-0.1μm. This study showed for the first time that nanometre sized wear particles were present in the test lubricant. The nanometre sized particles were observed in debris from both the smooth and scratched tests.

The results from the percentage area of the particles in different size ranges showed that for all the materials on both the smooth and scratched counterfaces the predominant size range was 0.1-1.0μm. This is the most biologically active size range. The shift in the predominant size range between the percentage number and percentage area of particles was due to the very small size of the particles in the smallest range. The greater size of the particles in the 0.1-1.0μm size range meant that they had a much larger area and also a larger volume.

The results for the wear debris from the scratched tests showed that more particles could be found in the largest size range. This was because of the different wear mechanism generating the particles.

6.2.5. Volume of Particles.

The volume of the wear debris particles was also determined for each material in Chapter 5. The results showed that the highly crosslinked material had a lower overall volume than the other two materials. The reduction was due to the lower wear factor obtained with the highly crosslinked material.

The debris from the scratched tests gave higher volumes than the debris from the smooth tests because of the higher wear factor seen with the scratched tests. The overall pattern of the results was similar for the debris from both types of tests.

The only size range that showed any significant difference was the 0.1-1.0μm size range. As this size range is the most biologically active the reduction seen with the 10MRad UHMWPE crosslinked material was very important. The volume of debris in this size range was significantly lower for debris from both the smooth and scratched tests.

6.2.6. Specific and Functional Biological Activity.

When the percentage area of the particles in the different size ranges had been calculated, the specific and functional biological activity was calculated for all the materials from the smooth and scratched tests. It was calculated using the method of Fisher *et al.* (2001). The results showed that the SBA for all the materials was not significantly different. This was predicted from the very similar percentage areas in different size ranges that were seen for all the materials.

The FBA which takes into account the wear volume of the materials did show a significant difference. The highly crosslinked material had a significantly smaller FBA value in the results from both the smooth and scratched debris. This was due to the reduced wear factor of the highly crosslinked materials. The 0MRad and 5MRad UHMWPE did not have a significant difference in their FBA values. However they did have a significant difference when comparing the results from the smooth and scratched tests. Again this was due to the increased wear volumes found with the scratched tests. A previous study by Ingram *et al.* (2002) found that UHMWPE 1050 was more reactive because of the smaller particles found compared to lower molecular weight UHMWPE. The study carried out for this thesis and the one by Ingram *et al.* (2002) would suggest that molecular weight is more important than the crosslinking level when considering wear debris particles and their osteolytic potential.

6.2.7. Effect of Crosslinking on the Wear of UHMWPE.

This study has looked at the wear of different levels of crosslinking under two different kinematic conditions and three different counterface surfaces. The results have shown that the 10MRad highly crosslinked UHMWPE had the best performance in terms of wear factors and biological activity of the wear debris. The moderately crosslinked 5MRad UHMWPE did not appear to have any benefits above the non-crosslinked UHMWPE. The results suggested that the low levels of crosslinks found in the 5MRad UHMWPE did not benefit the material and were not sufficient to overcome the slight reduction in mechanical properties caused by the crosslinking process.

The results have disproved some of the theories of the wear of crosslinked UHMWPE. There was no significant difference in the size and number of particles from any of the materials. This was unexpected as highly crosslinked UHMWPE was thought to produce smaller particles than non-crosslinked UHMWPE. The wear rate of the 5MRad UHMWPE were also unexpected as this was also thought to produce lower wear rates than non-crosslinked UHMWPE.

6.2.8. Shortcomings.

The method used for isolation and analysis of the wear debris involved procedures in which errors could have occurred. The very small UHMWPE particles were difficult to rinse off the equipment e.g. the filtration units. This meant that there could have been some cross contamination of filters. Carrying over any particles from one set of samples to another could not only provide an inaccurate distribution, but could also limit the ability to differentiate between the different samples and materials. Although the units were carefully washed each time they were used, it was difficult to determine how many particles remained in the equipment after each use.

The analysis of the debris was also very subjective. The particles were assumed to have a constant thickness which was almost certainly not the case. This does not

effect the percentage area calculation but does effect the volumes of particles. However this was the only assumption that could be applied at the time.

6.2.9. Future Work.

This work has compared for the first time the wear factors and osteolytic potential of UHMWPE GUR 1050 at three different levels of crosslinking. The presence of nanometre sized UHMWPE particles were seen for the first time. The work now needs to be continued to examine the wear rates of highly crosslinked UHMWPE in a simulator study and also to analyse the debris to determine whether the results are comparable to pin on plate studies and to determine whether nanometre sized UHMWPE particles are produced in simulator studies.

Further work should also be carried out on lower molecular weight UHMWPE's to examine if the molecular weight has more of an effect on the wear particles than the crosslinking levels. This would involve simulator studies and debris characterisation.

The biological activity of nanometre sized UHMWPE particles needs to be investigated, as when the experiments were carried out to determine the biological activity of UHMWPE nanometre sized particles had not been observed. The biological activity could also be compared to nanometre sized metal and ceramic particles.

The discovery of nanometre size polyethylene wear particles (size range 0.01-0.1μm) for the first time raises questions about their distribution and transport within the body. Further studies of debris retrieved from explant tissues are needed using high resolution FEGSEM to investigate the distribution of nanometre size polyethylene debris in the body and also examine how they are taken up by different cell types. Tissue studies need to include remote tissues and organs as well as periprosthetic tissue to determine the transport.

6.3. Final Conclusions.

- The largest reduction in wear rate produced by crosslinking was found with a high concentration of bovine serum in the lubricant and these results were consistent with those previously reported for similar serum concentrations (McKellop *et al.*, 1999). At lower concentrations of serum, as defined by the ISO standard, the reduction in wear produced by crosslinking was less. This difference may have been due to a more adhesive wear mechanism occurring with the lower serum concentration.

- Damage to the counterface increased the wear rate for all the materials as the wear moved to a more abrasive mechanism. This indicated that it would be an advantage to use crosslinked PE against damage resistance ceramic femoral heads.

- The 10MRad UHMWPE was found to be much more resistant to cross shear frictional energy than the other materials. This was because the crosslinks in the material make it more resistant to cross shear. The 5MRad UHMWPE did not show the same improvement. The lower levels of crosslinks in this material did not provide any benefit when looking at different cross shear frictional energies.

- High resolution FEGSEM revealed the presence of nanometre size UHMWPE wear particles for the first time. Particles in the size range 0.01-0.1μm were the most frequent for all materials and conditions.

- Although the percentage areas and numbers of particles in different size ranges showed no difference between the materials, when the FBA's were calculated a difference was seen. The highly crosslinked material was found to have a much lower FBA than the other two materials. The FBA values for the debris from smooth counterface tests were also statistically significantly lower than the results from the scratched surfaces. This was due to their lower wear factors and wear volumes. This study has shown that the 10MRad material is superior in

terms of its FBA value and wear factor. This study also showed for the first time the presence of nanometre sized wear debris particles.

References.

Amstutz H.C., Campbell P., Kossovsky N. & Clarke I.C. (1992). Mechanism and clinical significance of wear debris-induced osteolysis. *Clinical Orthopaedics and Related Research.* **276**, 7-18.

Atkinson J.R., Dowling J.M. & Cicek R.Z. (1980). Materials for internal prostheses: the present position and possible future developments. *Biomaterials.* **1**, 89-96.

Atkinson J.R., Dowson D., Wroblewski B.M. & Isaac G.H. (1985). Laboratory wear tests and clinical observations of femoral heads in acetabular cups. *Wear.* **104**, 225-244.

Barbour P.S.M., Stone M.H. & Fisher J. (1999). A study of the wear resistance of three types of clinically applied UHMWPE for total replacement hip prostheses. *Biomaterials.* **20**, 2101-2106.

Barbour P.S.M., Stone M.H. & Fisher J. (1999). A hip joint simulator study using simplified loading and motion cycles generating physiological wear paths and rates. *Proceedings of the Institution of Mechanical Engineers.* **213**H, 455-467.

Barbour P.S.M., Stone M.H., Fisher J. (1999). Third body wear test methods for total hip morphologies. *In*: *DTI CAM Project*, Accelerated test methods to predict the durability of materials and surface treatments employed for total hip replacements. Task **3.7**.

Bell J., Besong A.A., Tipper J.L., Ingham E., Wroblewski P.M., Stone M.H. & Fisher J. (2000). Influence of gelatin and bovine serum lubricants on ultra high molecular weight polyethylene wear debris generated in *in vitro* simulations. *Proceedings of the Institution of Mechanical Engineers.* **214**H, 513-518.

Bennett D., Orr J.F., Beverland D.E. & Baker R. (2002). The influence of shape and sliding of femoral head movement loci on the wear of acetabular cups in total hip

arthroplasty. *Proceedings of the Institution of Mechanical Engineers.* **216**H, 393-402.

Besong A.A., Hailey J.L., Ingham E., Stone M., Wroblewski B.M. & Fisher J. (1997). A study of the combined effects of shelf ageing following irradiation in air and counterface roughness on the wear of UHMWPE. *Bio-Medical Materials and Engineering.* **7**, 59-65.

Besong A.A., Tipper J.L., Ingham E., Stone M.H., Wroblewski B.M. & Fisher J. (1998). Quantitative comparison of wear debris from UHMWPE that has and has not been sterilised by gamma irradiation. *Journal of Bone and Joint Surgery.* **80**, 340-344.

Besong A.A., Tipper J.L., Stone M.H., Ingham E. & Fisher J. (1999). The influence of joint kinematics on the number and morphology of polyethylene wear particles in models of hip and knee prostheses. *In: International Conference on Knee Replacement*, London 22-24 April 1999. IMechE, 70-73.

Campbell P., Ma S., Yeom B., McKellop H., Schmalzreid T.P. & Amstutz H.C. (1995). Isolation of predominantly submicron-sized UHMWPE wear particles from periprosthetic tissues. *Journal of Biomedical Materials Research.* **29**, p127-131.

Cooper J.R., Dowson D. & Fisher J. (1993). Macroscopic and microscopic wear mechanisms in ultra high molecular weight polyethylene. *Wear.* **162-164**, 378-383.

Dowson D., Taheri S. & Wallbridge N.C. (1987). The role of counterface imperfections in the wear of polyethylene. *Wear.* **119**, 277-293.

Dowson D. (1991). Wear particles: From the cradle to the grave. *Tribology Series 21*. Amsterdam; New York. Elsevier.

Edidin A.A., Pruitt L., Jewett C.H., Crane D.J., Roberts D. & Kurtz S.M. (1999). Plasticity induced damage layer is a precursor to wear in radiation cross linked UHMWPE acetabular components for total hip replacement. *Journal of Arthroplasty* **14** (5), 616-627.

Endo M.M., Barbour P.S.M., Barton D.C., Wroblewski B.M., Fisher J., Tipper J.L., Ingham E. & Stone M.H. (1999). A comparison of the wear and debris generation of GUR 1120 (compression moulded) and GUR 4150HP (ram extruded) Ultra High Molecular Weight Polyethylene. *Bio-Medical Materials and Engineering*. **9**, 113-124.

Endo M.M., Barbour P.S.M., Barton D.C., Tipper J.L., Ingham E., Stone M.H. & Fisher J. (2000). Comparative wear and debris generation of crosslinked and non-crosslinked ultra high molecular weight polyethylene under three different femoral counterface conditions. *In*: *6th World Biomaterials Congress Transactions*. **836**.

Endo E.E., Barbour P.S.M., Barton D.C., Fisher J., Ingham E. & Stone M. (2001). Comparative wear and wear debris under three different counterface conditions of crosslinked and non-crosslinked ultra high molecular weight polyethylene. *Bio-Medical Materials and Engineering*. **11**, 23-35.

Endo MM., Tipper J.L., Barton D.C., Stone M.H., Ingham E. & Fisher J. (2002) Comparison of wear, wear debris and functional biological activity of crosslinked and non-crosslinked polyethylenes in hip prostheses. *Proceedings of the Institution of Mechanical Engineers*. **216**H, 111-122.

Essner A., Polieni V.K., Schmidig G., Wang A., Stark C., Dumbleton J.J. (1997). Long-term wear simulation of stabilised UHMWPE acetabular cups. *In: Transactions of 43rd Orthopaedic Research Society Meeting*. **784**.

Fisher J. & Dowson D. (1991). Tribology of artificial joints. *Proceedings of the Institution of Mechanical Engineers*. **205**H, 73-39.

Fisher J. (1994). Wear of ultra high molecular weight polyethylene in total artificial joints. *Current Orthopaedics.* **8**, 164-167.

Fisher J., Bell J., Barbour P.S.M., Tipper J.L., Matthews J.B., Stone M.H. & Ingham E. (2001). A novel method for the prediction of functional biological activity of polyethylene wear debris. *Proceedings of the Institution of Mechanical Engineers.* **215**H, 127-132.

Galvin A.L., Tipper J.L., McEwen H.M.J., Williams S., Stone M.H., Ingham E. & Fisher J. (2004). Nanometre size polyethylene particles from hip and knee simulator studies. *Proceedings of the 50th annual meeting of the Orthopaedic Research Society.* **1505.**

Green T.R., Fisher J., Stone M., Wroblewski B.M. & Ingham E. (1998). Polyethylene particles of a "critical size" are necessary for the induction of cytokines by macrophages *in vitro*. *Biomaterials.* **19**, 2297-2302.

Green T.R., Fisher J., Matthews J.B., Stone M. & Ingham E. (2000). Effect of size and dose on bone resorption activity of macrophages by *in vitro* clinically relevant ultra high molecular weight polyethylene particles. *Journal of Biomedical Materials Research (Applied Biomaterials).* **53**, 490-497.

Goodman S., Per Aspenberg S., Yong Song L., Knoblich G. Huie P.& Regula D. (1995). Tissue ingrowth and differentiation in the bone-harvest chamber in the presence of cobalt-chromium-alloy and high-density-polyethylene particles. *Journal of Bone and Joint Surgery.* **77**A, 1025-1035.

Hailey J.L., Ingham E., Stone M., Wroblewski B.M. & Fisher J. (1996). Ultra high molecular weight polyethylene wear debris generated in vivo and in laboratory tests; the influence of counterface roughness. *Proceedings of the Institution of Mechanical Engineers.* **210**H, 3-10.

Ingham E., Green T.R. Matthews J.B. Stone M.H. & Fisher J. (1999). Influence of TNFα in polyethylene particle stimulated macrophage bone resorption. *In: Proceedings of the 45th annual meeting of the Orthopaedic Research Society*. **899**.

Ingham E & Fisher J. (2000). Biological reactions to wear debris in total joint replacement. *Proceedings of the Institution of Mechanical Engineers*. **214**H, 21-37.

Ingram J., Matthews J.B., Tipper J., Stone M., Fisher J. & Ingham E. (2002). Comparison of the biological activity of grade GUR 1120 and GUR 415HP UHMWPE wear debris. *Bio-Medical Materials and Engineering*. **12**, 177-188.

Jasty M., Goetz D.D., Bragdon C.R., Lee K.R., Hanson A.E., Elder J.R. & Harris W. (1997). Wear of poylethylene acetabular components in total hip arthroplasty. An analaysis of one hundred and twenty eight components retrieved at autopsy or revision operations. *Journal of Bone and Joint Surgery*. **79**A (3), 349-358.

Jin Z.M., Dowson D. & Fisher F. (1992). The effect of porosity of articular cartilage on the lubrication of a normal hip joint. *Proceedings of the Institution of Mechanical Engineers*. **206**H, 117-124.

Jin Z.M., Dowson D. & Fisher J. (1993). Fluid film lubrication in natural hip joints. *Tribology series 25. Thin films in Tribology*. Amsterdam: Elsevier, 545-555.

Kontinnen Y.T., Xu J.W., Patiala H., Imai S., Wais V., Li T.F., Goodman S.B., Nordsletten L. & Santavira S. (1997). Cytokines in aseptic loosening of total hip replacements. *Current orthopaedics*. **11**, 40-47.

Kurtz S.M., Pruitt L.A., Jewett C.W., Foulds J.R. & Edidin A.A. (1999). Radiation and chemical crosslinking promote strain hardening behaviour and molecular alignment in ultra high molecular weight polyethylene during multi-axial loading conditions. *Biomaterials*. **20**, 1449-1462.

Kurtz S.M., Muratoglu O.K., Evans M. & Edidin A.A. (1999). Advances in the processing, sterilisation, and crosslinking of ultra-high molecular weight polyethylene for total joint arthroplasty. *Biomaterials.* **20**, 1659-1688.

Lu Z. & McKellop H. (1997). Frictional heating of bearing materials tested in a hip joint wear simulator. *Proceedings of the Institution of Mechanical Engineers.* **211**H, 101-108.

MacConaill M.A. (1932). The function of intra-articular fibrocartilage, with special references to the knee and inferior radio-ulnar joints. *Journal of Anatomy.* **66,** 210-227.

Marrs H., Barton D.C., Jones R.A., Ward I.M. & Fisher J. (1999). Comparative wear under four different tribological conditions of acetylene enhanced cross-linked ultra high molecular weight polyethylene. *Journal of Materials Science: Materials in Medicine.* **10**, 333-342.

Matthews J.B., Besong A.A., Green T.R., Stone M.H, Wroblewski B.M., Fisher J & Ingham E. (2000). Evalution of the responses of primary human peripheral blood mononuclear phagocytes to challenge with i*n vitro* generated clinically relevant UHMWPE particles of known size and dose. *Journal of Biomedical Materials Research.* **52**, 296-307.

McKellop H.A., Campbell P., Park S.H., Schmalzried T.P., Grigoris P., Amstutz H.C. & Sarmiento A. (1995). The origin of submicron polyethelene wear debris in total hip arthroplasty. *Clinical Orthopaedics and Related Research.* **311**, 3-20.

McKellop H., Shen F.W., DiMaio W. & Lancaster J.G. (1999). Wear of gamma-crosslinked polyethylene acetabular cups against roughened femoral balls. *Clinical Orthopaedics and Related Research.* **369**, 73-82.

Minakawa H., Stone M.H., Wroblewski B.M., Lancaster J.G., Ingham E. & Fisher J. (1998). Quantification of third-body damage and its effect on UHMWPE wear with different types of femoral head. *Journal of Bone and Joint Surgery*. **80B** no5 894-899.

Morrey B.F. (1991). Joint Replacement Arthroplasty. New York. Churchill Livingstone.

Muratoglu O.K., Biggs S.A., Bragdon C.R., O'Connor D.O., Merrill E.W., Premnath V., Jasty M. & Harris W.H. (1997). Long term stability of radiation and peroxide cross-linked UHMWPE. *In: Transactions of the 23rd Society of Biomaterials Meeting*. **20**:49.

Muratoglu O.K., Bragdon C.R., O'Connor D.O., Jasty M, Harris W.H., Gul R. & McGarry F. (1999). Unified wear model for highly crosslinked ultra-high molecular weight polyethylene's (UHMWPE). *Biomaterials*. **20**, 1463-1470.

Murtagolu O.K., Bragdon C.R., O'Connor D.O., Skehan H., Delaney J., Jasty M. & Harris W.H. (2000). The comparison of the wear behaviour of four different types of crosslinked acetabular components. *In: 6th World Biomaterials Congress Transactions*. **865**.

Parry S.A., Sutherland C.J., Miller G., Gilden J. & Joyce M.E. (1995). Synovial fluid IL-6 levels in failed total joint arthroplasty with osteolysis. *In*: *Proceedings of the 41st annual meeting of the Orthopaedic Research Society*. 216.

Pastalanga N., Field D. & Soames R. (2002). Anatomy and Human movement. 4th edition. Oxford: Butterworth Heinemann.

Paul J.P. (1967). Forces transmitted by joints in human body. *Proceedings of the Institution of Mechanical Engineers*. **181**(3J) 8-21.

Pooley C.M. & Tabor D. (1972). Friction and molecular structure: the behaviour of some thermoplastics. *Proceedings of the Royal Society of London A*. **329,** 251-271.

Revell P.A., Al-Saffar N. & Kobayashi A. (1997). Biological reaction to debris in relation to joint prosthesis. *Proceedings of the Institution of Mechanical Engineers.* **211**H, 187-197.

Rose M.R., Ries M.D., Paul I.L., Crugnola A.M. & Ellis E. (1984). On the true wear of ultra high molecular weight polyethylene in the total knee prosthesis. *Journal of Biomedical Materials Research.* **18**, 207-224.

Savio J.A., Overcamp L.M. & Black J. (1994). Review Paper: Size and shape of biomaterial wear debris. *Clinical materials.* **15**, 101-147.

Scott M., Widding K., Ries M. & Shanbhag A. (2001). Wear particle analyses of conventional and crosslinked UHMWPE tested in an anatomic simulator. *In: Proceedings of the 47th annual meeting of the Orthopaedic Research Society.* **1**.

Shen F.W., McKellop H.A. & Salovey R. (1996). Irradiation of chemically crosslinked ultrahigh molecular weight polyethylene. *Journal of Polymer Science; Part B, Polymer Physics.* **24**, 1063-1077.

Tipper J.L., Ingham E., Hailey J.L., Besong A.A, Wroblewski B.M., Stone M.H. & Fisher J. (2000). Quantitative analysis of polyethylene wear debris, wear rate and head damage in retrieved charnley hip prostheses. *Journal of Materials Science: Materials in Medicine.* **11**(2) 117-124

Wang A., Stark S. & Dumbleton J.H. (1996). Mechanistic and morphological origins of ultra high molecular weight polyethylene wear debris in total joint replacement prostheses. *Proceedings of the Institution of Mechanical Engineers.* **210**H, 141-156.

Wang A., Polineni V.K., Essner A., Sun D.C., Stark C., Dumbleton J.H. (1997). Effect of radiation dosage on the wear of stabilised UHMWPE evaluated by hip and knee simulators. *In: Transaction of the 23rd Society of Biomaterials Meeting.* **20**, 394.

Wang A., Sun D.C. Yau S.S., Edwards B., Sokol M., Essner A., Polineni V.K., Stark C. & Dumbleton J.H. (1997). Orientation softening in the deformation and wear of ultra high molecular weight polyethylene. *Wear*. **203-204**, 230-241.

Wang A., Essner A., Polineni V.K., Stark C. & Dumbleton J.H. (1998). Lubrication and wear of ultra high molecular weight polyethylene in total joint replacements. *Tribology International*. **31**(1-3), 17-33.

Wang A., Essner A., Stark C. & Dumbleton J.H. (1999). A biaxial line-contact wear machine for the evaluation of implant bearing materials for total knee joint replacement. *Wear*. **225-229**, 701-707.

Willert H.G. & Semlitsch M. (1977). Reactions of the articular capsule to wear products of artificial joint prostheses. *Journal of Biomedical Materials Research*. **11**, 157-164.

Yamamoto K., Williams P., Good V., Clarke I.C., Masaoka T., Imakiire & Oonishi H. (2000). Wear-mode and morphology of extensively cross-linked polyethylene cup surface and wear debris. *In: 6th World biomaterials congress transactions*. **485**.

Yamamoto K., Clarke I.C., Masaoka T., Oonishi H., Williams P.A., Good V.A. & Imakiire A. (2001) Microwear phenomena of ultra high molecular weight polyethylene cups and debris morphology related to gamma radiation dose in simulator study. *Journal of Biomedical Materials Research*. **56**(1). 65-73.